AD-A062 888 CALSPAN ADVANCED TECHNOLOGY CENTER BUFFALO NY F/G 4/2
AEROSOL CHARACTERISTICS OF THE MARINE BOUNDARY LAYER OF THE NOR--ETC(U)
OCT 78 E J MACK, R J ANDERSON, C K AKERS N00019-78-C-0179
UNCLASSIFIED CALSPAN-6232-M-1 NL

1 OF 3
ADA
062888

CALSPAN ADVANCED TECHNOLOGY CENTER

6 AEROSOL CHARACTERISTICS OF THE MARINE BOUNDARY LAYER OF THE NORTH ATLANTIC AND MEDITERRANEAN DURING MAY-JUNE 1977.

by

10 E.J. Mack, R.J. Anderson, C.K. Akers, T.A. Niziol

Calspan Report No. 6232-M-1

12 225 p.

15 Contract No. N00019-78-C-0179

11 October 1978

Project Sea Fog
Sixth Annual Summary Report

9 Annual summary rept. no. 6,

Prepared for:

DEPARTMENT OF THE NAVY
NAVAL AIR SYSTEMS COMMAND
WASHINGTON, D.C. 20361
CODE: AIR-370C

14 CALSPAN-6232-M-1

APPROVED FOR PUBLIC RELEASE:
DISTRIBUTION UNLIMITED

A DIVISION OF CALSPAN CORPORATION
an Arvin Company P.O. Box 400 Buffalo, New York 14225

JDC

TABLE OF CONTENTS

TABLE OF CONTENTS (Cont.)

ABSTRACT

During May and early June 1977, Calspan participated in a Transatlantic-Mediterranean research expedition (NRL Cruise 77-16-04) aboard the USNS HAYES to investigate atmospheric marine boundary layer phenomena. Calspan's objective was the acquisition of data describing the magnitudes and spatial variations of a variety of aerosol and meteorological parameters in the lowest 20 m. Continuous or hourly observations of visibility, scattering coefficient, total particle concentration, aerosol size spectra (0.01 to >3.0 μm diameter), relative humidity, air and sea surface temperatures, and winds were obtained throughout the cruise. At less regular intervals, measurements of cloud condensation nuclei and aqueous sea spray aerosols and collections of aerosols for chemical analyses were also obtained. These data were used to describe differences between the clean marine air of the mid-Atlantic and the modified-continental air of the Mediterranean observed during the cruise and data previously acquired in the Eastern Pacific. In addition, complete aerosol spectra (0.01 μm to >20.0 μm diameter) were utilized to compute extinction as functions index of refraction, wavelength and changes in relative humidity.

LIST OF FIGURES

LIST OF FIGURES (Cont.)

LIST OF FIGURES (Cont.)

LIST OF FIGURES (Cont.)

LIST OF TABLES

ACKNOWLEDGMENTS

The authors are indebted to both past and present personnel (U. Katz, W. Rogers, J. Hanley, and G. Zigrossi) of the Environmental Sciences Department of Calspan, who participated in the preparation, data acquisition, and data reduction phases of this effort. Special thanks are due to Mr. R. Pilié for his many helpful discussions during preparation of this manuscript. The text was typed by Mrs. Marilyn Handley.

We would also like to express our appreciation to Dr. L. H. Ruhnke and personnel of the Naval Research Laboratory for the many courtesies afforded us during the cruise.

In particular, we gratefully acknowledge the assistance of J. L. Durham (and his staff) of the Atmospheric Chemistry and Physics Division of the Environmental Protection Agency's National Research Center at Research Triangle Park, North Carolina, in providing wavelength-dispersive X-ray fluorescence analyses of some of our aerosol samples.

Section 1
INTRODUCTION AND SUMMARY

For the past six years under sponsorship of the Naval Air Systems Command (NASC), Calspan Corporation in cooperation with the Naval Postgraduate School (NPS), the Naval Research Laboratory (NRL), and the Naval Avionics Center (NAC) has been conducting an investigation of the evolutionary processes and physical properties of marine fog and marine boundary-layer aerosols. During the first four years, attention was focused on determination of the formation mechanisms and physical and chemical characteristics of marine fogs occurring off the coasts of California and Nova Scotia. Last year the scope of Calspan's effort was expanded to include investigation of evolutionary processes which control compositional and physical characteristics of marine boundary layer aerosols. Results of these efforts are summarized in References 1-9.

This year, under Contract No. N00019-78-C-0179 from NASC, Calspan continued its contribution to the Navy's marine boundary layer physics program with a combined marine aerosol/fog investigation involving two separate Tasks. Task 1 encompassed analysis and interpretation of marine boundary layer aerosol data previously acquired by Calspan (Ref. 8) under Contract No. N00173-77-C-0126 from NRL, during the NRL-sponsored Transatlantic-Mediterranean Cruise of May-June 1977. The scope of Calspan's participation in the Cruise was initially limited to the acquisition of data describing the physical and chemical characteristics of the aerosol, as well as the pertinent basic meteorological parameters, in the lower atmospheric marine boundary layer. Results of the analyses and interpretation of these data, performed as Task 1 under the current contract, are presented within this report.

As Task 2, Calspan in collaboration with NPS, the Naval Ocean Systems Center (NOSC), NRL and NAC participated in CEWCOM-78 to obtain data describing marine fogs and marine boundary layer characteristics off the coast of California in the vicinity of San Nicolas Island (SNI). Calspan's primary objective during the CEWCOM-78 field effort of May 1978 was to acquire data

from aboard the NPS R/V ACANIA with which to assess the representativeness of SNI of clean (natural) marine boundary layer conditions. Under the scope of the contract, these data were to be provided only in reduced, "data-volume" format. Results of this effort are reported in a separate volume (Ref. 10).

The objective of Calspan's participation in NRL Cruise 77-16-04 was to acquire data with which to describe the aerosol and optical properties of the marine boundary layer of the North Atlantic and the Mediterranean. Data were acquired from aboard the USNS HAYES during the period 15 May to 7 June 1977 while en route from Virginia to Athens, Greece via the Grand Banks and the Strait of Gibraltar. Ship's track for the cruise is shown in Figure 1. (The dates shown on the cruise track, as well as all times referred to in this report, are GMT.)

Calspan instrumentation deployed aboard the HAYES is listed in Table 1 along with information on parameters measured, range of variables, frequency of measurements and measurement heights above the sea surface. The locations of the various instruments on the ship are depicted schematically in Figure 2. The first five items in Table 1 were installed in a shelter which formed the lower half of a small tower erected atop the flying bridge. In order to minimize the risk of contamination, the sample air for the various particle monitors was aspirated through a 5 cm diameter (ID), 2.5 m long tube extending to 2 m forward of and 2 m above the flying bridge. (Flow rate was such that aerosol residence within the tube was 2 sec.) Fog sampling equipment (items 6, 7 and 8) was mounted on top of the tower to minimize the ship's thermal influence when the wind direction was within the forward quadrant. A second drop sampler was positioned on the tip of one of the bows (depending on wind direction) for collecting sea spray droplets as close to the water surface as possible while escaping any spray generated by the ship. Continuous temperature recordings were obtained at four levels, the lowest being the sea surface. An armored sea surface temperature probe was towed between the bows to obtain temperature measurements of the approximate top 10 centimeters of the water surface. Continuous humidity measurements were obtained at two levels with lithium chloride based dewpoint sensors while manual psychrometry provided calibration and backup measurements. The primary purpose of the wind

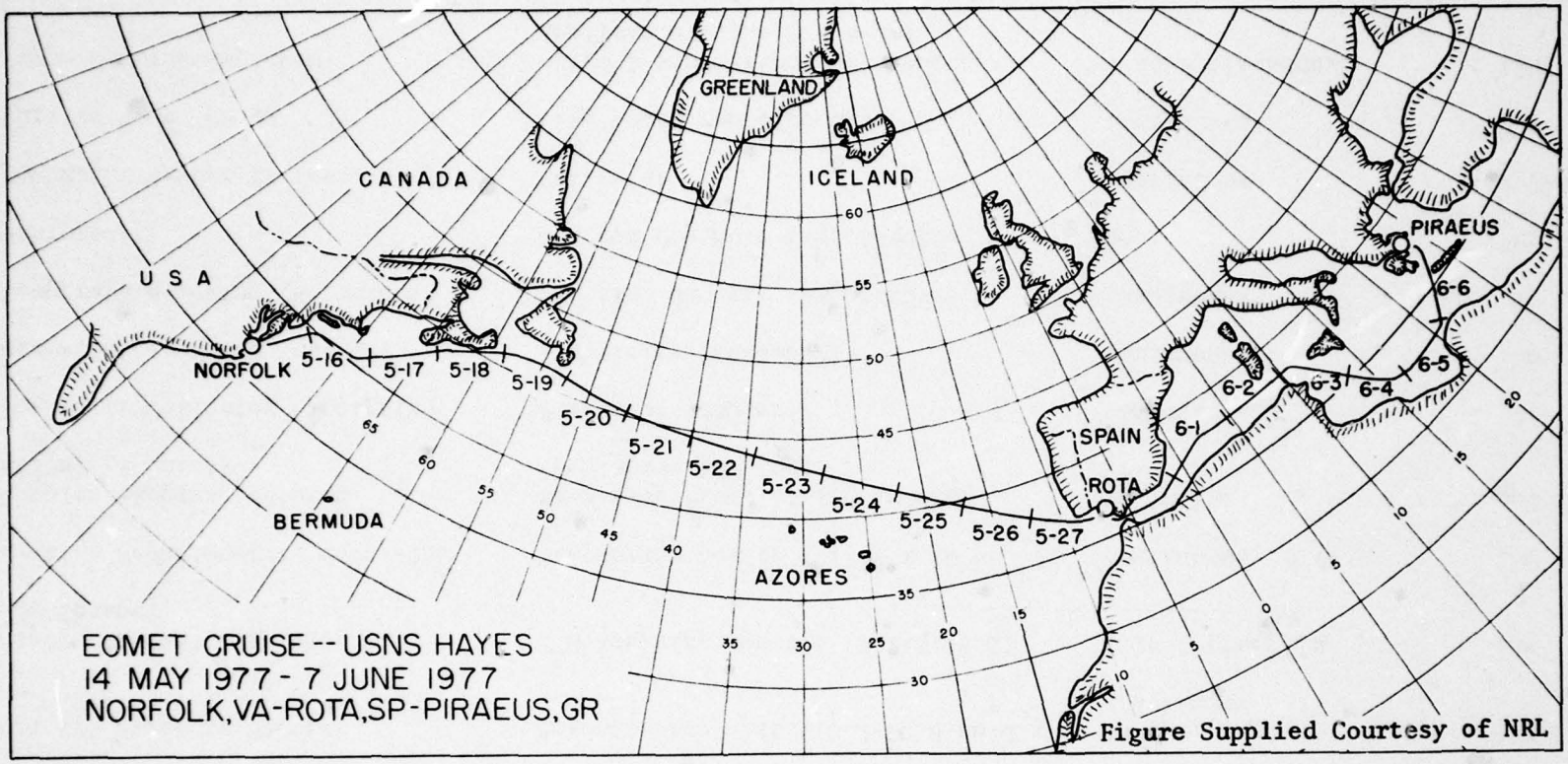

Figure 1: Track of the USNS HAYES During NRL Cruise 77-16-04

Table 1

CALSPAN INSTRUMENTATION INSTALLED ON THE USNS HAYES
NORTH ATLANTIC/MEDITERRANEAN EOMET CRUISE--MAY-JUNE 1977

INSTRUMENT	PARAMETER	RECORD	HEIGHT ABOVE SEA SURFACE
Gardner Small Particle Detector	Aerosol conc. (>.0025 μm dia)	hourly	15m
Thermo Systems Model 3030 Electrical Aerosol Analyzer	Aerosol Size Dist. (0.003-1.0 μm dia)	hourly; occ'n'ly more frequently	15m
Royco Model 225 Particle Counter	Aerosol size dist. (0.3-10.0 μm dia)	10 min. avg. continuous	15m
Calspan Static Thermal Gradient Diffusion Chamber	CCN Activity Spectra (0.2-3.0% S)	2 to 7 times/day	15m
MRI Integrating Nephelometer, Mod. 2050	Scattering Coeff. ($.1^{-40} \times 10^{-4} m^{-1}$)	continuous	15m
Calspan Droplet Sampler (gelatin replication) (2 units)	Drop size dist. (3-100 μm dia) (Sea spray and fog)	variable	9m and 17m
Calspan Fog Water Collector (impaction)	Fog water samples	variable	17m
EG&G Forward Scatter Meter, Mod 107	Visibility (60-6000m)	continuous	17m
Foxboro Temperature System (4 sensors)	Sea sfc. and air temperatures	continuous	sea sfc, 9, 15,27m
Sling Psychrometer	Wet and dry bulb temperatures	hourly	17m;3m
Foxboro Dew Point System (2 sensors)	Dew point	continuous	15m,27m
Beckman-Whitley Wind System	Wind Speed and direction	continuous	27m
Battelle-type Cascade Impactor	Aerosol separation for chemical analysis by size (>0.5 μm)	1 to 4 times/day	15m
Hi-Vol Aerosol Samplers (3 systems)	Chemical analysis of bulk aerosol samples on 2 diff. filter types: teflon and quartz	daily	17m

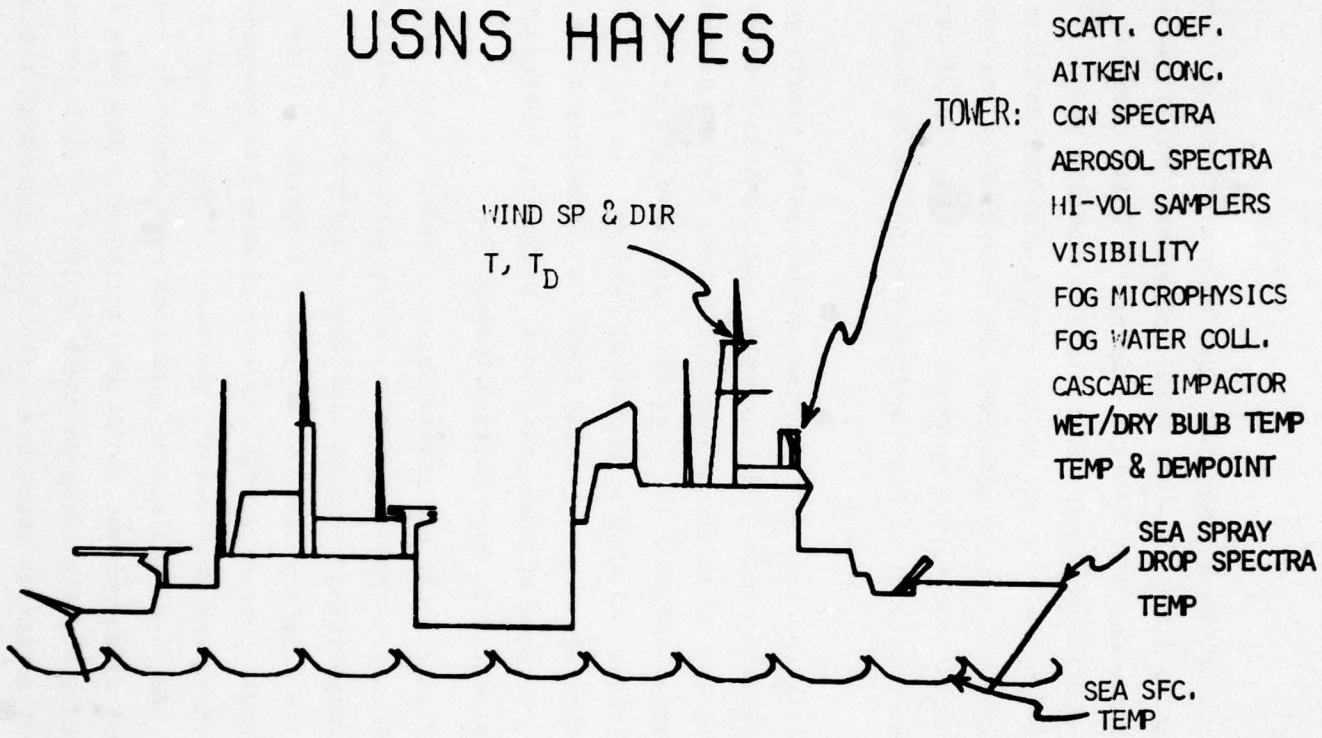

Figure 2: Deployment of Calspan Instrumentation on the USNS HAYES During NRL Cruise 77-16-04

instrumentation mounted on the antenna mast was the convenient detection of potentially contaminating (ship-related) wind conditions. While the last two items in Table 1 provided bulk aerosol samples for later chemical analysis, the cascade impactor samples were most suitable for combined scanning electron microscopy and energy dispersive x-ray analysis of individual particles, whereas the bulk filter samples were partly earmarked for wet chemical analyses and partly designed for atomic absorption spectroscopy or x-ray fluorescence analysis. Detailed descriptions of this instrumentation may be found elsewhere (e.g., Ref. 1-4).

During the cruise, logs were maintained comprising hourly values of all the parameters measured except CCN, sea spray and chemical samples which were obtained at irregular intervals and which required further processing to arrive at quantitative values. The logs also contained hourly observations of weather, sky conditions and ship's (magnetic) heading. In total, the logs comprised approximately 400 successful hourly observations and were reported in Ref. 8. Portions of these data logs, including subsequently reduced data, are reproduced in Appendices A through H.

Analyses of visibility and scattering coefficient data, aerosol size spectra, and supersaturation activity spectra, along with detailed analyses of individual particle composition revealed significant differences in the aerosol character of the marine boundary layer at different locations. Clean, though not necessarily 'natural', marine conditions were observed in the mid-Atlantic. A modified-marine airmass was observed off the coast of North America; and distinctly different modified-continental airmasses were observed, respectively, off the Atlantic coast of Europe and in the Mediterranean. The data show that the airmasses observed along the European coast to 1200 km offshore and in the Mediterranean were not of marine character. The data from which these conclusions are derived are presented and discussed in detail in Section 2 of this report.

During the cruise, complete aerosol size spectra (0.01μm to ∿20.0μm diameter) were acquired by combining the data obtained with three different instruments: an EAA, a Royco and a Calspan droplet sampler. Extinction (visibility) calculated from these spectra showed good agreement with measured values. The calculations showed that >90% of observed extinction was due to aerosols in the size range 0.2 to 20.μm diameter. The complete aerosol spectra were also used to compute extinction as functions of index of refraction, wavelength (ignoring absorption), and, through particle growth-theory, changes in relative humidity. These exercises are presented and described in Section 3.

Section 2

CHARACTERISTICS OF THE MARINE BOUNDARY LAYERS OF THE NORTH ATLANTIC AND MEDITERRANEAN

Calspan participated in the Transatlantic-Mediterranean cruise of May-June 1977 with the objective of providing descriptions of the magnitudes and spatial variations of a variety of aerosol and meteorological parameters in the lowest 20m of the marine boundary layer. During the cruise, Calspan obtained continuous or hourly observations of visibility, scattering coefficient, total particle concentration, aerosol size spectra (0.01 to >3.0μm), winds, temperature and relative humidity. At less regular intervals, measurements of cloud condensation nuclei (CCN) and sea spray aerosols and collections of aerosols for chemical analyses were also obtained. The data are presented and discussed within this section. (All times referred to in this report are GMT.)

2.1 Cruise Scenario and General Meteorological Conditions

The HAYES departed Virginia on 15 May 1977, passing through the mouth of Chesapeake Bay at ∿0500 GMT, and headed in a general northeasterly direction. Turning eastward, the ship cruised along the coast of Nova Scotia at ∿60 km offshore, passing the southeastern coast of Newfoundland by 2200 GMT on 19 May. The ship arrived in port at Rota, Spain at ∿0800 GMT on 28 May and, after a 3 day lay-over, departed Rota at 1930 GMT on 30 May. After passing through the Strait of Gibraltar at ∿0200 on 31 May, the ship cruised eastward through the Mediterranean approximately paralleling the African coast at about 150 km offshore, finally docking at Piraeus, Greece (near Athens) at ∿0800, 7 June. The general cruise track is depicted in Figure 1.

2.11 Winds

Winds observed during the cruise are plotted in Figures 3a and b and 4a and b. These data were generated from Calspan hourly observations of relative winds and ship's magnetic heading, assuming a ship's speed of 6m sec^{-1}. (Ship's-speed data computed by NRL from satellite navigation data, show

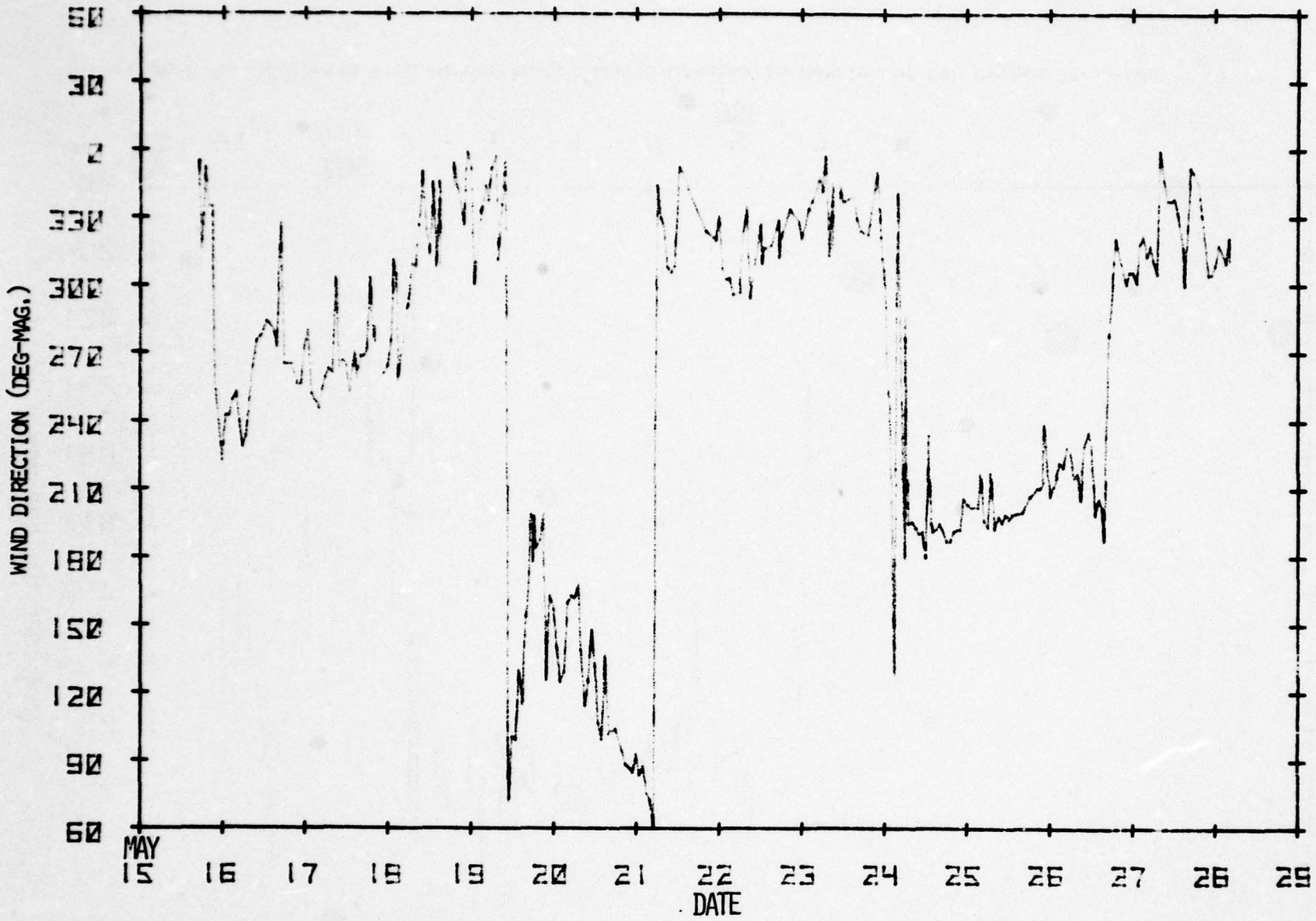

Figure 3a: Computed Wind Direction for the Atlantic Portion of NRL Cruise 77-16-04

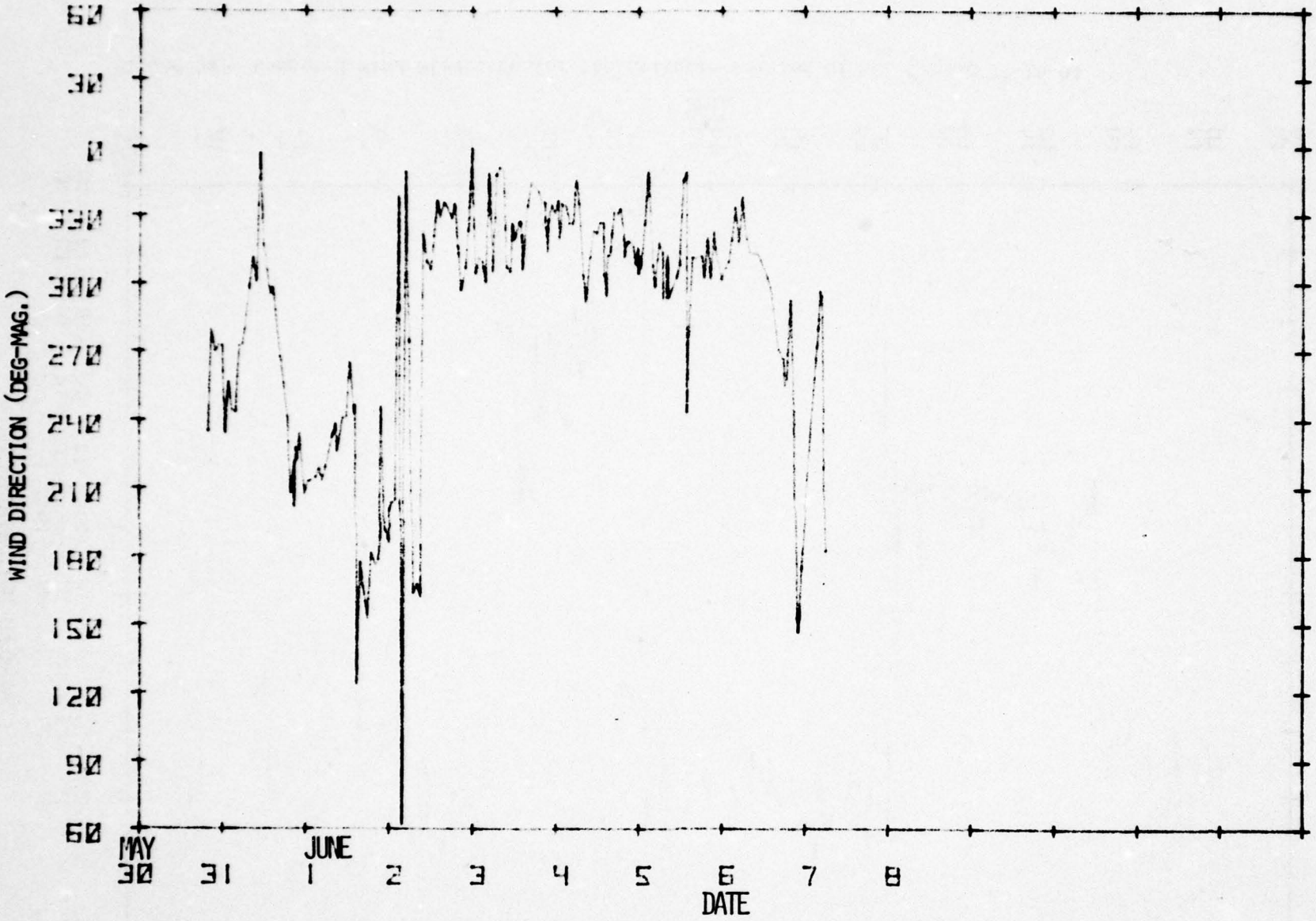

Figure 3b: Computed Wind Direction for the Mediterranean Portion of NRL Cruise 77-16-04

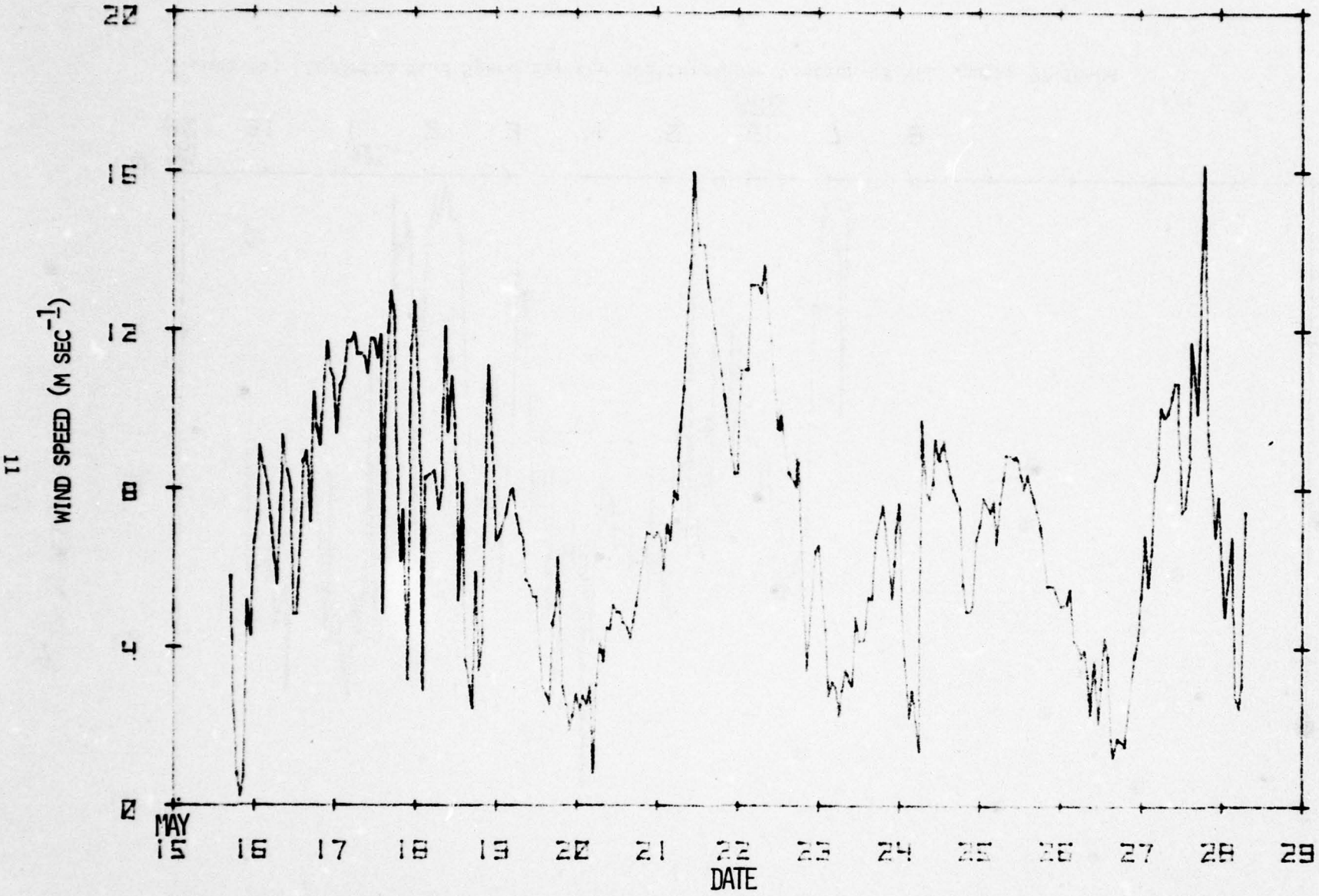

Figure 4a: Computed Wind Speed for the Atlantic Portion of NRL Cruise 77-16-04

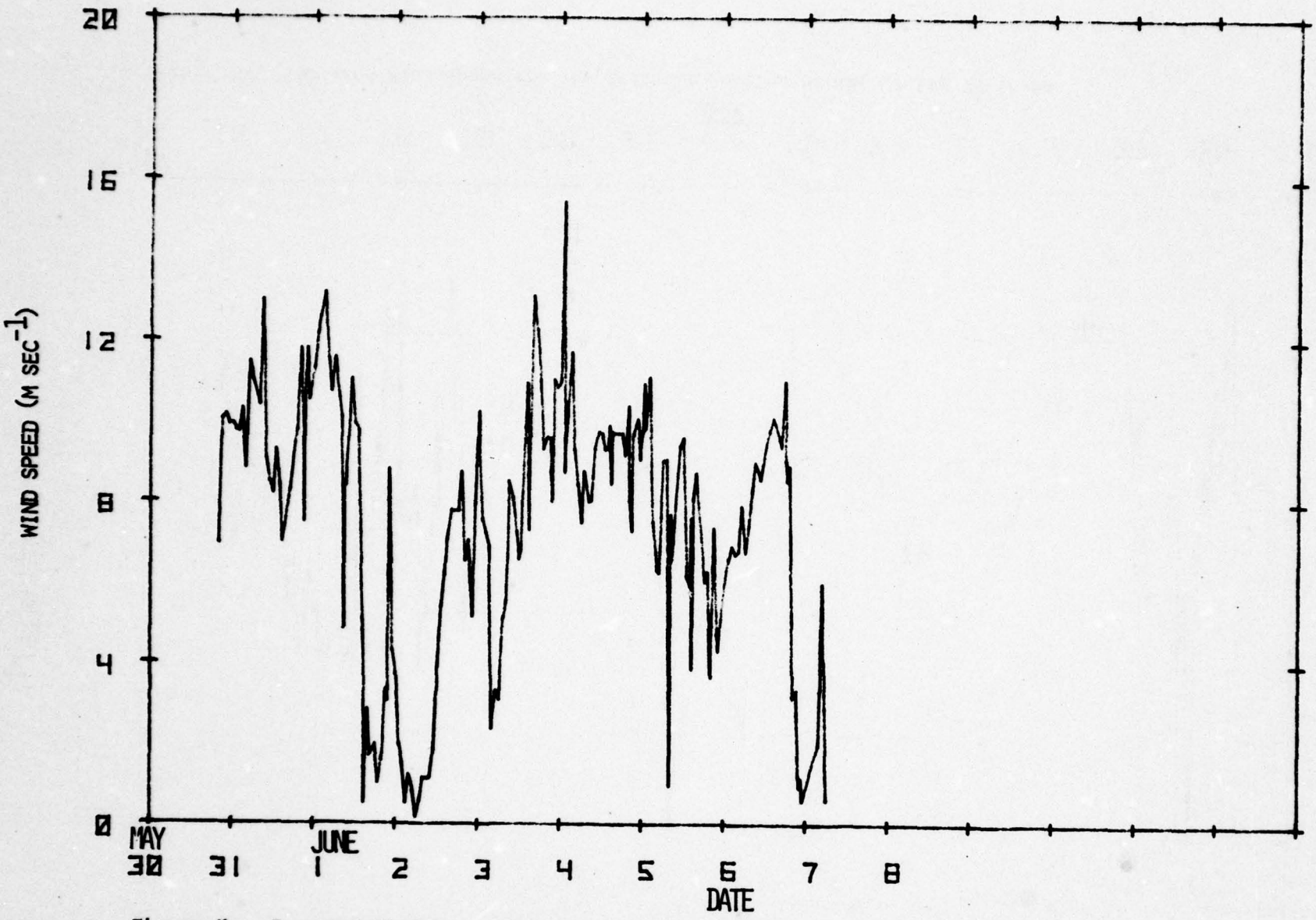

Figure 4b: Computed Wind Speed for the Mediterranean Portion of NRL Cruise 77-16-04

6m sec^{-1} to be a reasonable average for ship's speed.) These data are not intended to provide an absolute measure of wind direction and speed, but rather to indicate the general direction and short-term fetch of air sampled during the cruise. Numerical values of these data are tabulated in Appendix A.

Along the North American coast, winds were westerly to northerly offshore at 4-12 m sec^{-1} through the period ending mid-day on 19 May. On 19 May, winds shifted to south-southeasterly and then gradually backed to northwesterly by early on 21 May. In the mid-Atlantic, winds remained northwesterly before shifting abruptly to south-southwesterly early on 24 May. Winds shifted back to northwesterly late on 26 May and remained from that direction until data acquisition was terminated near Rota. In the western Mediterranean, winds were southerly to westerly until a wind shift early on 2 June brought northwesterly winds through the duration of the cruise. The observed wind shifts appeared to be associated with frontal passages.

2.12 Visibility Characteristics

Visibility and scattering coefficient were monitored continuously throughout the cruise with an MRI Nephelometer. At times, following winds prevented the acquisition of data uncontaminated by ship's heat and exhaust emissions; during extended periods of such conditions, the ship was frequently turned into the wind to allow for brief intervals of data collection. Visibility, scattering coefficient, and total particle (Aitken nuclei) concentration data obtained at hourly intervals (where possible) are shown for the Atlantic and Mediterranean portions of the expedition in Figures 5a and 5b, respectively. A log of the numerical values of these data is provided in Appendix B.

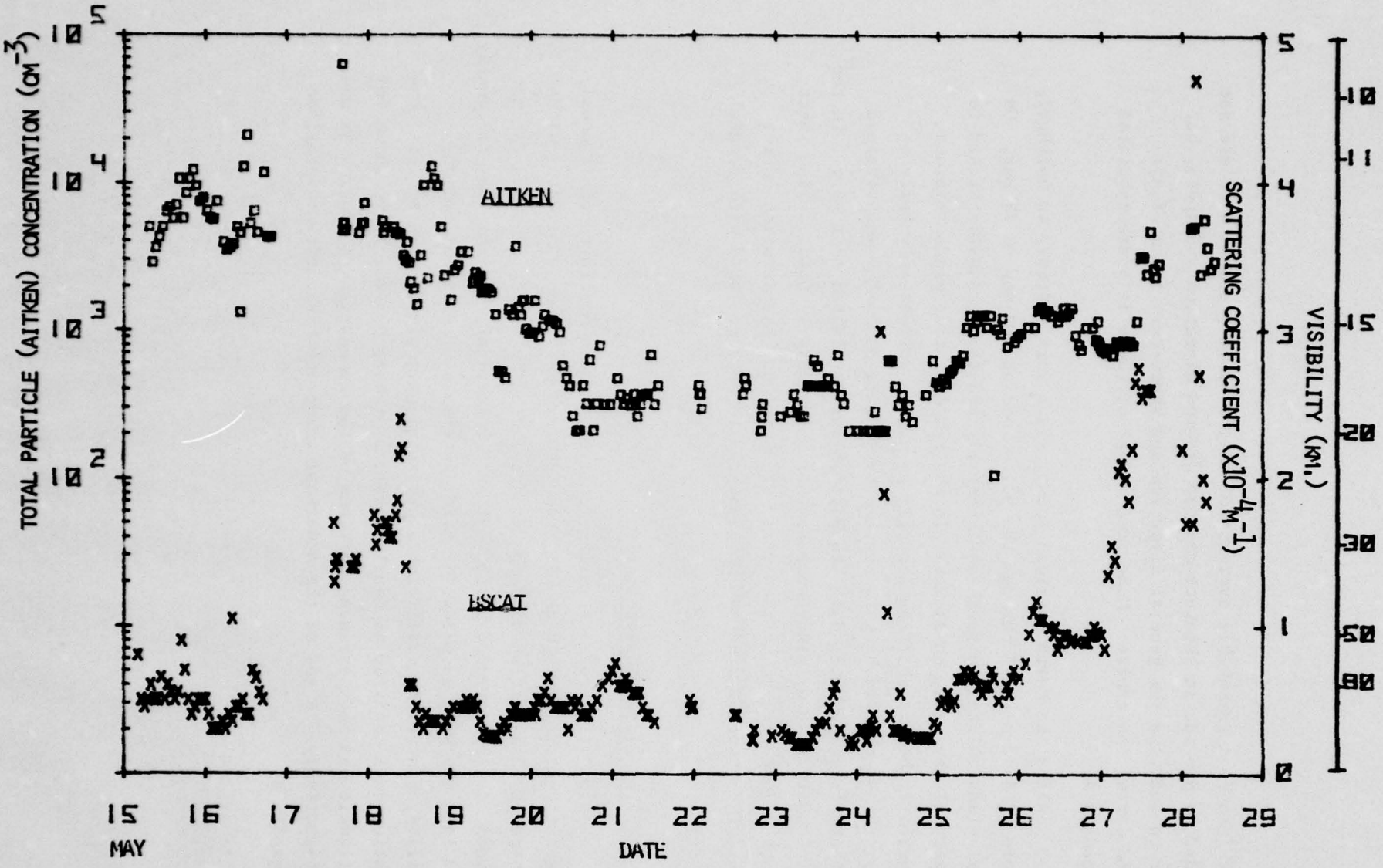

Figure 5a: Visibility, Bscat and Total Particle Concentration for the Atlantic Portion of NRL Cruise 77-16-04

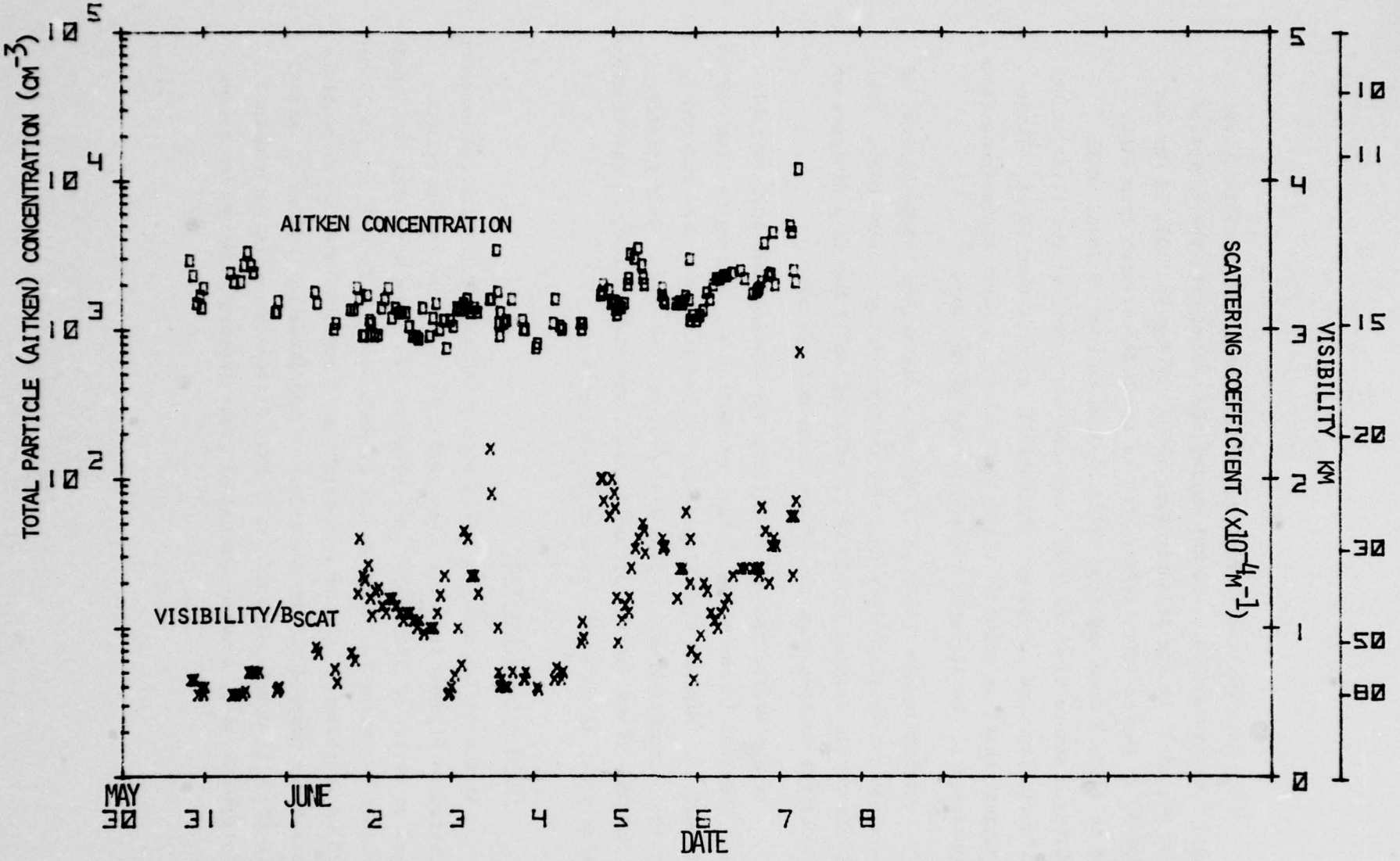

Figure 5b: Visibility, Bscat and Total Particle Concentration for the Mediterranean Portion of NRL Cruise 77-16-04

The data plotted in Figures 5a and b show that visibility was generally unlimited (i.e., >50 km) during the cruise with the exception of four periods: in the Atlantic from ∿0000, 17 May to 1100, 18 May and from 0300, 26 May to 0800, 28 May; and in the Mediterranean from 2100, 1 June to 1400, 3 June and from ∿1400, 4 June to 0600, 7 June. With increasing distance from the North American Continent, visibilities in the mid-Atlantic improved to values substantially greater than 80 km. These data suggest that, in terms of visibility, clean, natural marine conditions were observed in the Atlantic between 19 and 25 May 1978.

Beginning about 0100 on 25 May at a distance of ∿1200 km west of the European coast, visibility degraded with proximity to the coast. Visibility ultimately dropped to ∿10 km by 1200 GMT on 27 May at a distance of ∿30 km off the southwestern tip of the Iberian Peninsula.

In the Mediterranean, visibility was considerably more variable than was observed in the mid-Atlantic, exhibiting values ranging from < 80 km down to ∿25 km. Minimum visibilities in the Mediterranean were observed during the nocturnal hours of 2-3, 3-4, 4-5, and 6-7 June. Only briefly, on 31 May and on the latter half of 3 June, were visibilities in the Mediterranean as great as those observed in mid-Atlantic.

2.13 Total Aerosol Loading

Aitken nuclei data, obtained with a Gardner Small Particle Detector and plotted in Figures 5a and b, show that total particle concentration remained at levels of 5000-10000 cm^{-3} offshore along the North American coastline before beginning to decrease east of Nova Scotia. By 0800 GMT on 20 May at ∿270 km southeast of the southeastern tip of Newfoundland, total particle concentrations dropped nearly two orders of magnitude to < 500 cm^{-3}. Across the mid-Atlantic until ∿0100 GMT on 25 May, Aitken concentration remained between 200-500 cm^{-3}, a value typical of clean (natural) marine air masses

observed elsewhere (e.g., Ref. 9). Thereafter, particle concentration increased to and leveled off at ∿1000 cm^{-3}, remaining at that level to within ∿30 km of the Iberian Peninsula. In the Mediterranean, total particle concentration generally remained between values of 1000-3000 cm^{-3}, with the lowest values occurring in the time period from ∿2 to 5 June.

It should be noted that, except for a period on 25 May when particle concentration increased simultaneously with a decrease in visibility, very little correlation was observed in either the Atlantic or Mediterranean between fluctuations of total particle concentration and 'clear air' visibility. For example, comparison of the Aitken nucleus concentration and visibility data in Figure 5a shows that, while visibility improved dramatically to mid-Atlantic values on 18 May, total particle concentration did not reach mid-Atlantic values until two days later on 20 May. The apparent lack of correlation between visibility and total aerosol concentration represents a departure from relationships observed by these authors in the marine boundary layer off the coast of California (e.g., Ref. 9 and 10).

2.14 Air Temperature, Relative Humidity and Sea Surface Temperature

Dry-bulb and wet-bulb temperature data obtained at the flying bridge level (17m above the surface) by manual psychrometry techniques are shown for the respective portions of the cruise in Figures 6a and b. Relative humidity values computed from these data are shown in Figures 7a and b. (Records of mixing ratio, air temperature at 3 heights above the sea surface, and sea surface temperature data may be found in Appendix C.)

The data plotted in Figure 7 show that in addition to general trends, considerable variation in relative humidity, almost on a diurnal basis, was observed during the cruise. Average relative humidity increased from ∿70% on 15 May to nearly 90% by 21 May, before dropping abruptly to values averaging

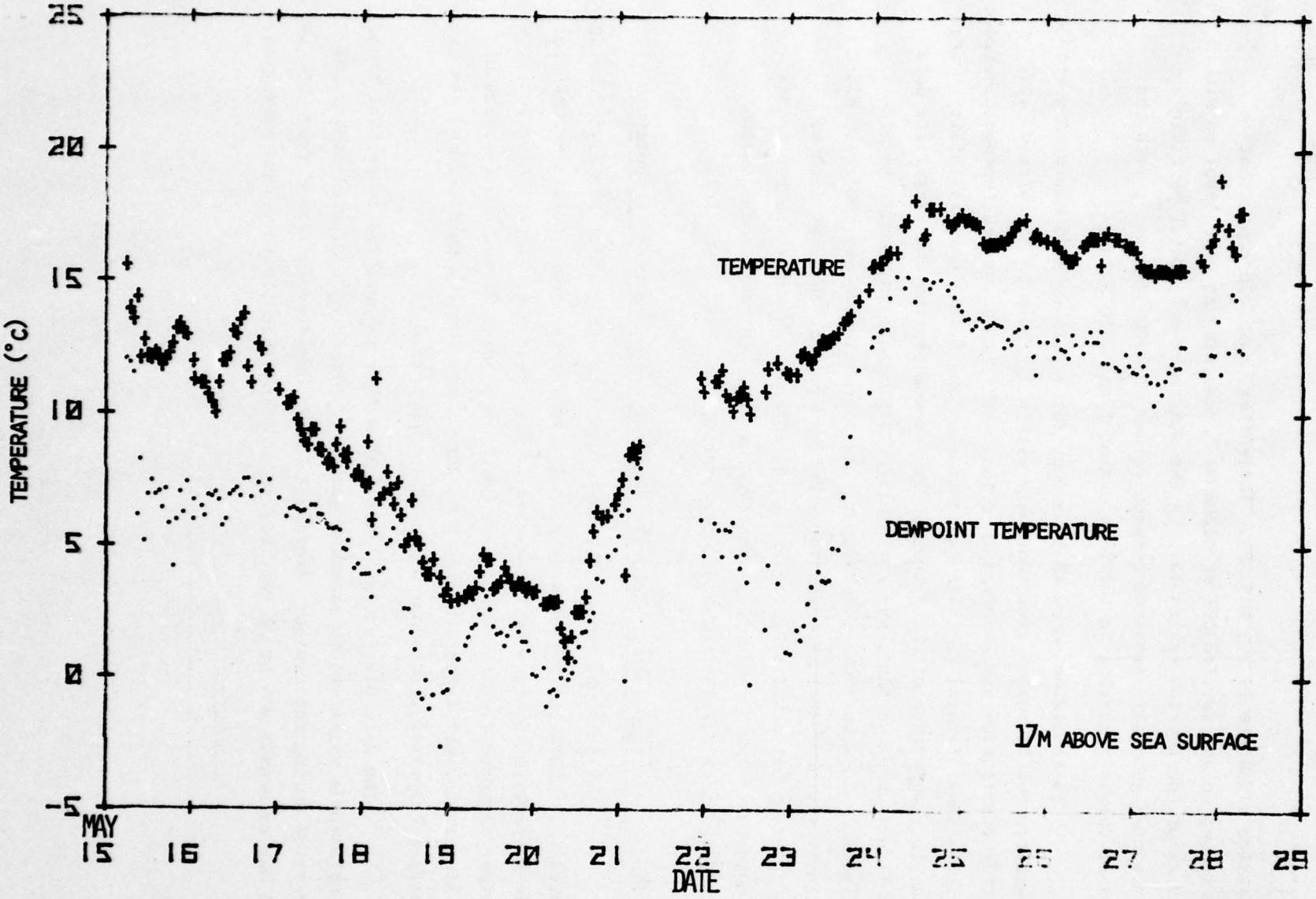

Figure 6a: Temperature and Dewpoint as Functions of Time for the Atlantic Portion of NRL Cruise 77-16-04

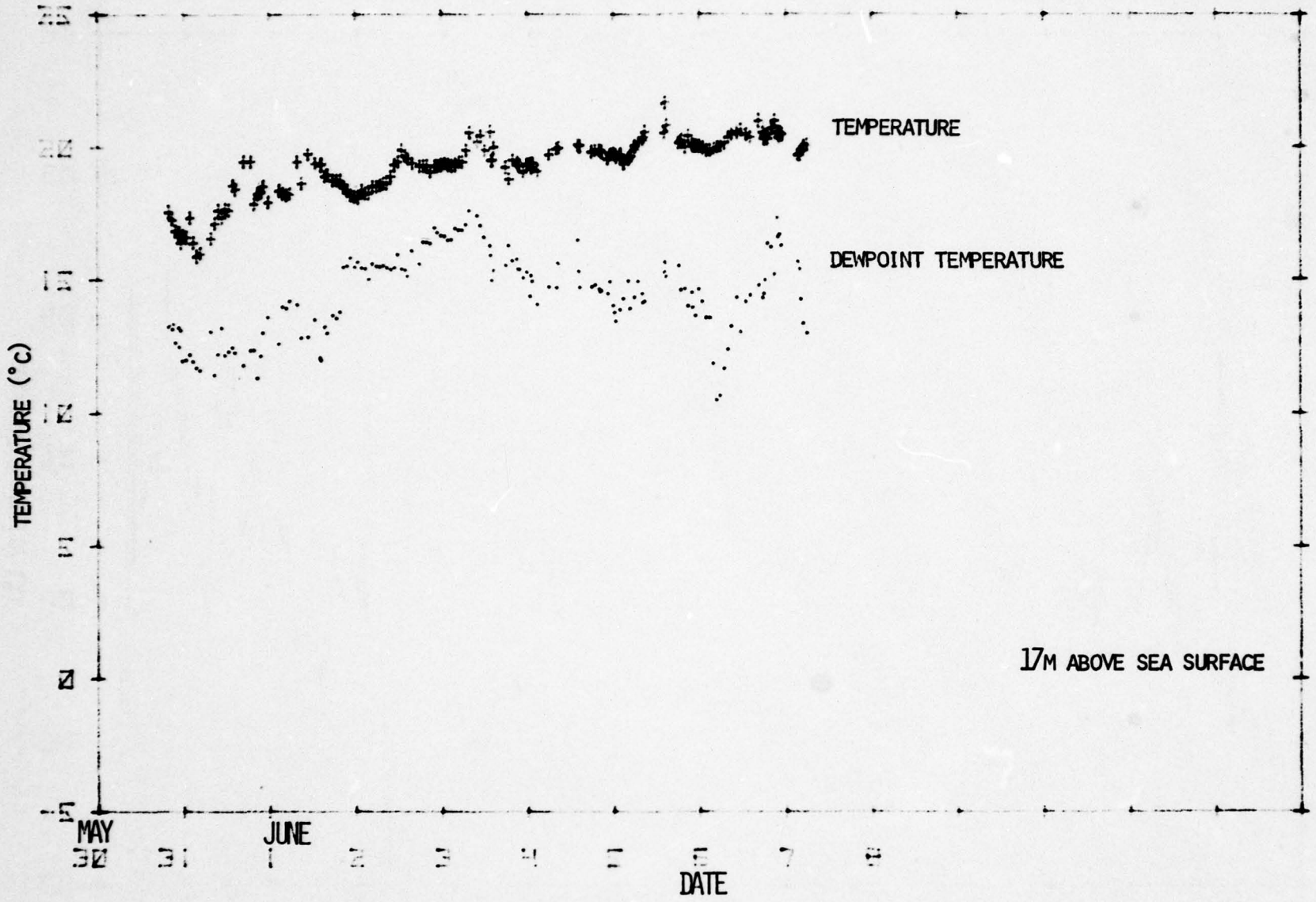

Figure 6b: Temperature and Dewpoint as Functions of Time for the Mediterranean Portion of NRL Cruise 77-16-04

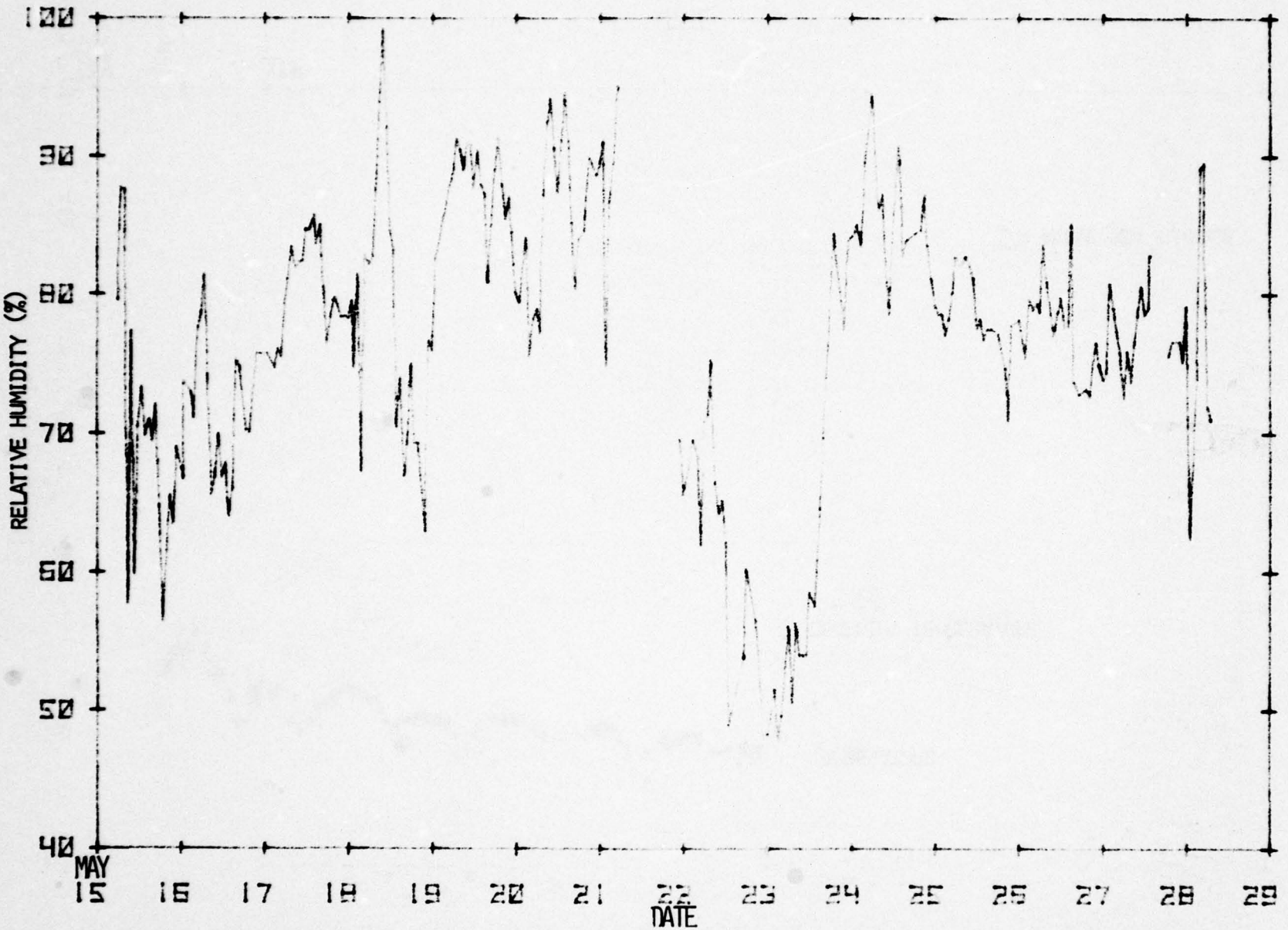

Figure 7a: Relative Humidity as a Function of Time During the Atlantic Portion of NRL Cruise 77-16-04

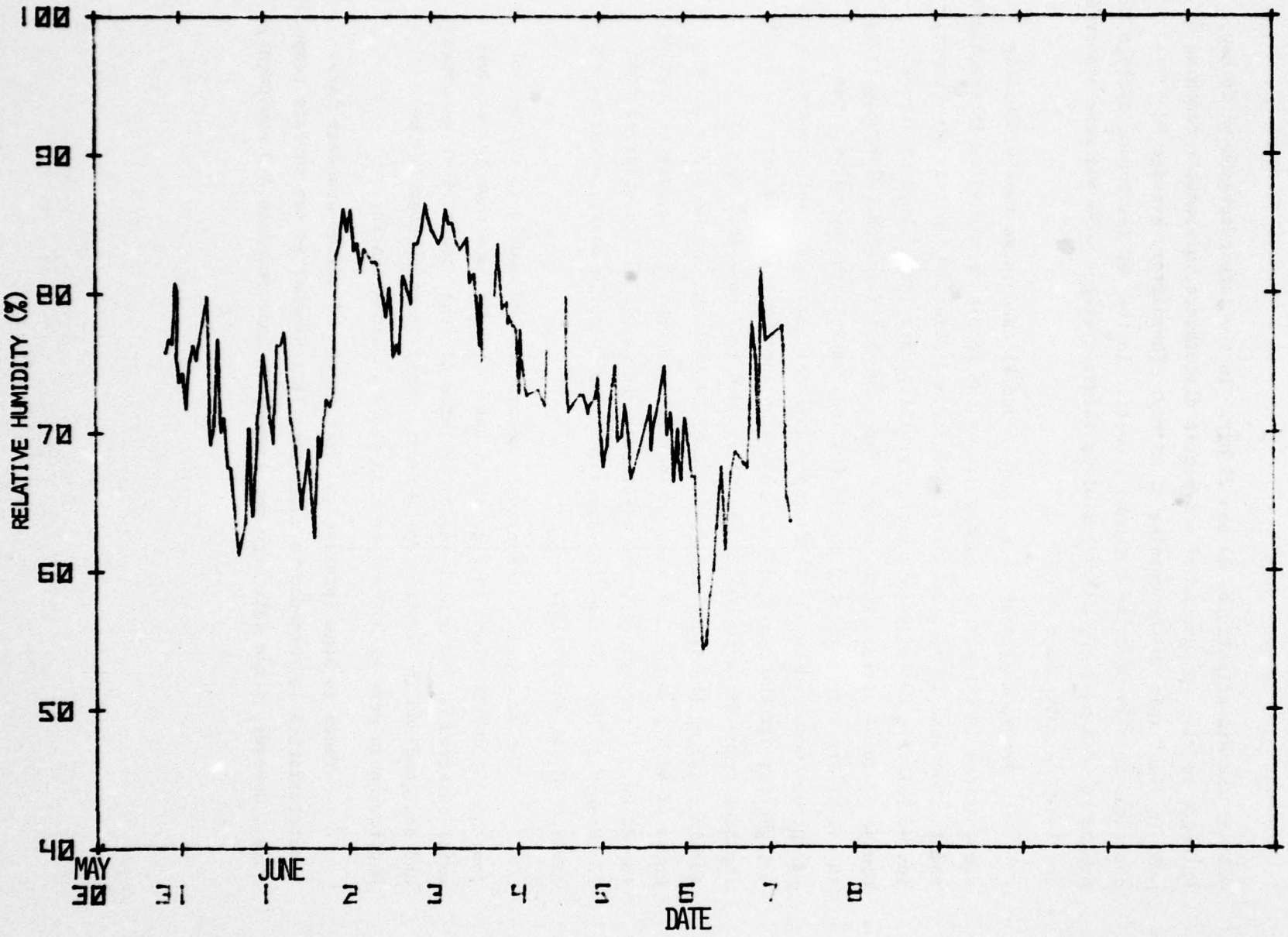

Figure 7b: Relative Humidity as a Function of Time During the Mediterranean Portion of NRL Cruise 77-16-04

∿55% in the mid-Atlantic on 22 and 23 May. In the late afternoon on 23 May, RH began to rise in advance of a synoptic disturbance, ultimately reaching ∿95% in light rain on the morning of 24 May. Thereafter, average RH decreased to ∿77% near the Portuguese coast. In the Mediterranean, average RH peaked at ∿84% on 2 and 3 June; minimum values averaged ∿65% and were observed on 31 May, 1 June and 6 June.

Previous studies (e.g., Ref. 6 and 9) have shown that visibility fluctuations in the marine boundary layer can result from complex interactions and fluctuations of both relative humidity and aerosol populations. Comparison of relative humidity data with visibility data (see Figure 5) for NRL Cruise 77-16-04 reveals that, except for a few brief instances, fluctuations in visibility were unrelated to fluctuations in relative humidity. The exceptions occurred on the following occasions: after a brief encounter with a light fog off the coast of Nova Scotia on the morning of 18 May, visibility improved from < 15 km to >80 km and RH dropped from near 100% to < 70% by evening; during the light rain episode of 24 May; and on the early morning hours of both 2 and 3 June when RH increased to ∿86% and visibility degraded to < 30 km. Interestingly, the major decrease in visibility observed from 25 through 27 May, as the ship approached the European coast, occurred while average RH was decreasing.

The sea surface temperature record for the cruise is reproduced from hourly observations in Figures 8a and b. These data show the coldest water observed on the cruise was encountered off the coasts of Nova Scotia and Newfoundland in the Labrador Current. Water temperatures in the Mediterranean were ∿2-3°C warmer than those in mid-Atlantic.

There is some interest in fluctuations of marine boundary layer characteristics in response to variations (patchiness) in sea surface temperature. However, since data were not logged via fast response A-D equipment,

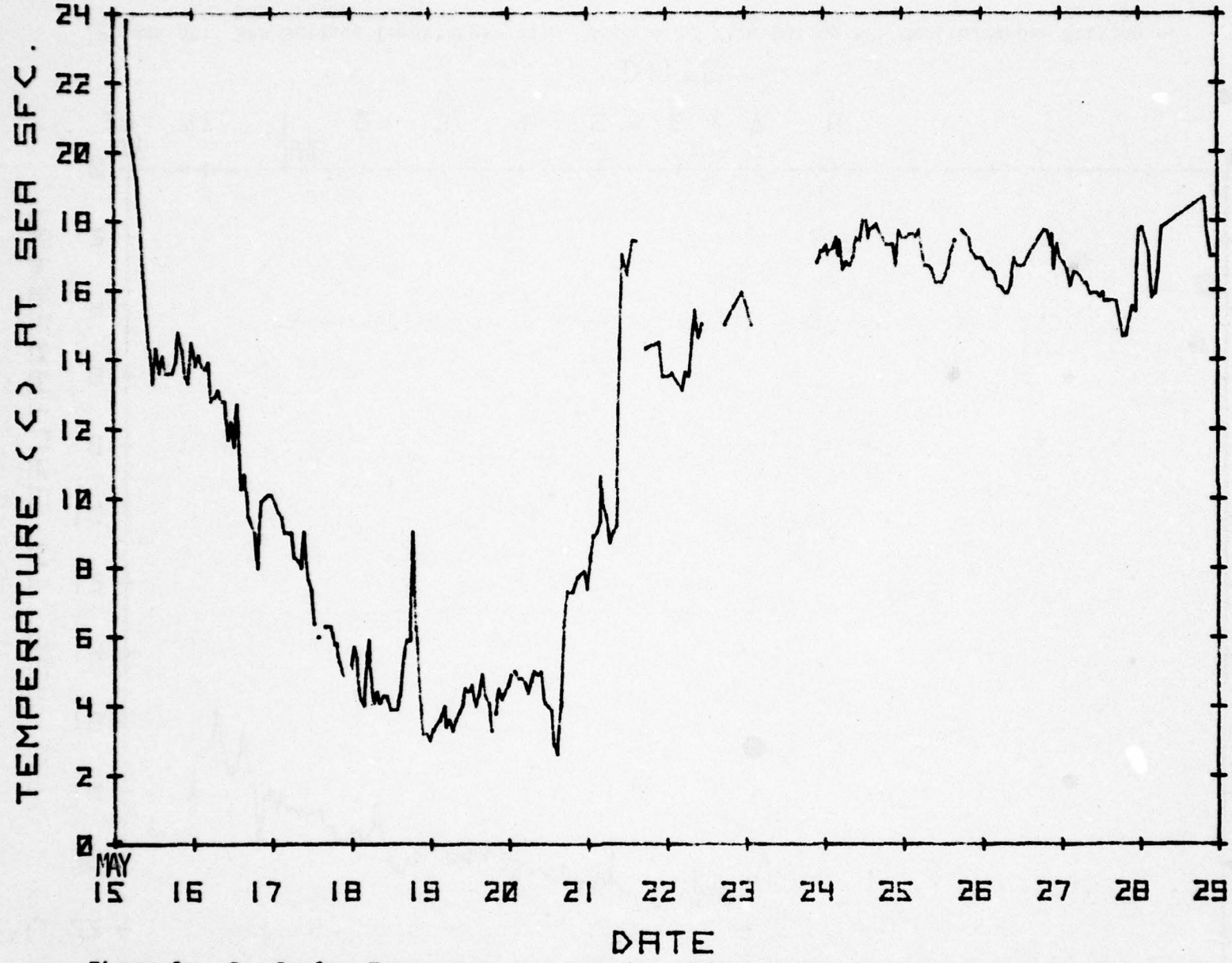

Figure 8a: Sea Surface Temperature as a Function of Time During the Atlantic Portion of NRL Cruise 77-16-04

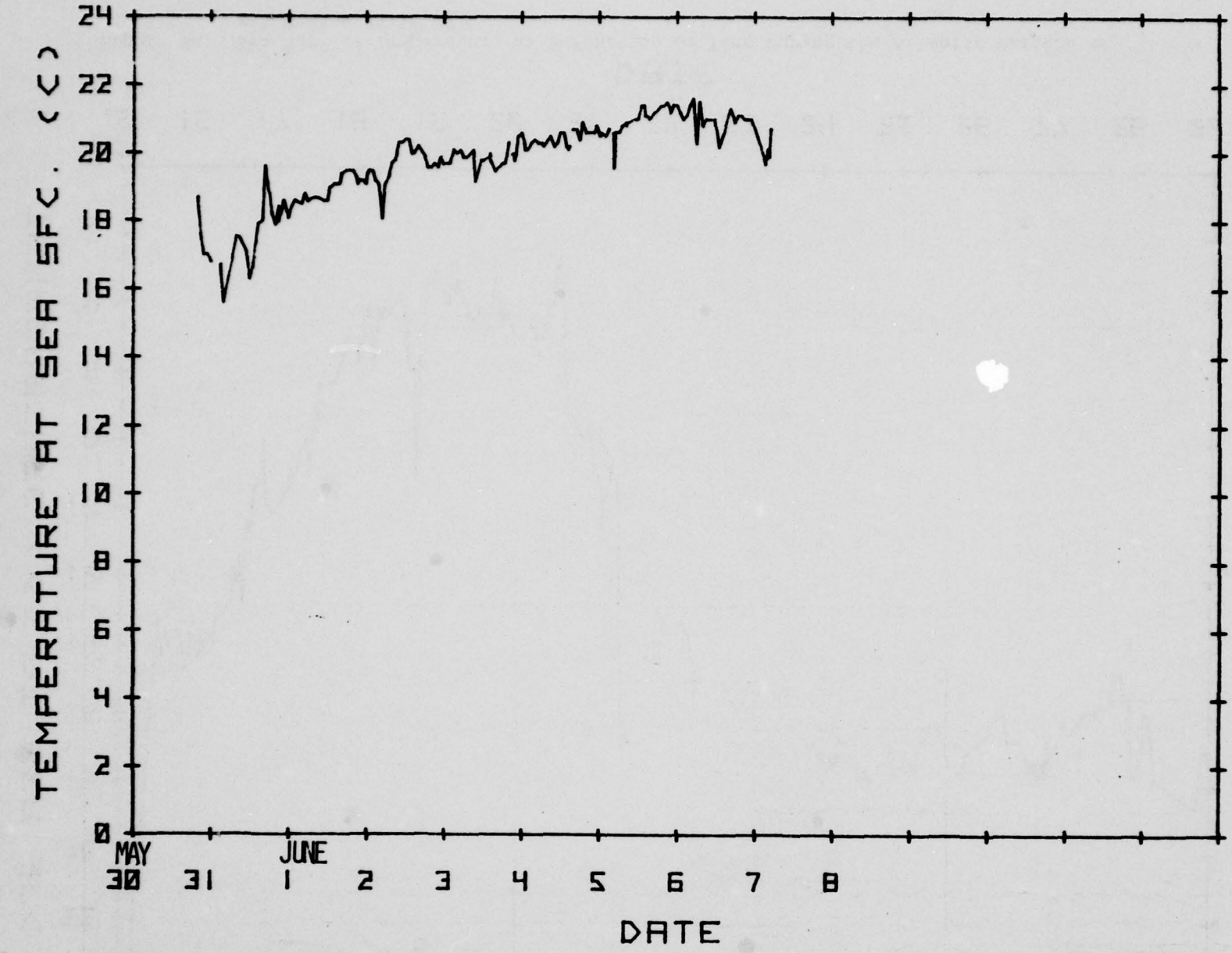

Figure 8b: Sea Surface Temperature as a Function of Time During the Mediterranean Portion of NRL Cruise 77-16-04

it is not possible to provide a complete power spectrum for sea surface temperature fluctuation. Instead, the hourly records were searched for sea surface temperature changes of $\pm$ 0.3-0.49°C, 0.5-0.99, 1.0-1.49, 1.5-1.99, 2.0-2.49 and 2.5-2.99°C over the period of an hour--or, at a mean ship speed of 6m sec^{-1}, a spatial resolution of ∿20 km. A minimum variation of 0.3°C was chosen to avoid uncertainties associated with sampling and strip-chart-reading errors. The data were summed for three portions of the cruise (along the North American Coast and in the Labrador Current from 16-21 May, in the mid-Atlantic from 22-27 May, and in the Mediterranean from 1-6 June), and the frequency distributions of 20 km sea surface temperature changes for the three cruise areas are plotted in Figure 9. These data show that sea surface temperature fluctuations $\pm$ 0.3 to 1.0°C with a 20 km spatial resolution occurred 68, 88, and 79% of the time, respectively, off Nova Scotia, in the mid-Atlantic, and in the Mediterranean. On the other hand, major changes in sea surface temperature (i.e., $\geq \pm$ 2°C) occurred 11% of the time off Nova Scotia, but were observed in only 2% of the observations in mid-Atlantic. None >2°C were observed in the Mediterranean.

2.2 The Microphysics of Observed Aerosols

Calspan's primary objective during NRL Cruise 77-16-04 was to acquire data with which to assess the characteristics and variability of aerosols in the lowest 20m of the marine boundary layer. Complete aerosol size spectra (0.01μm to ∿20.0μm diameter) were acquired by combining the data obtained with three different instruments: an Electrical Aerosol Analyzer (EAA) for sizes 0.01-0.75μm; a Royco Optical Particle Counter for sizes 0.3μm to >3.0μm; and a Calspan-built impactor for gelation replication of aqueous aerosols of 1.0 to >30μm diameter. In addition, total particle concentration was monitored with a Gardner Small Particle Detector, and measurements of cloud condensation nucleus (CCN) activation spectra were obtained with a Calspan-built, static thermal diffusion chamber. These data are presented and discussed within this Section, and logs of the numerical values of these data are provided in Appendices D through H.

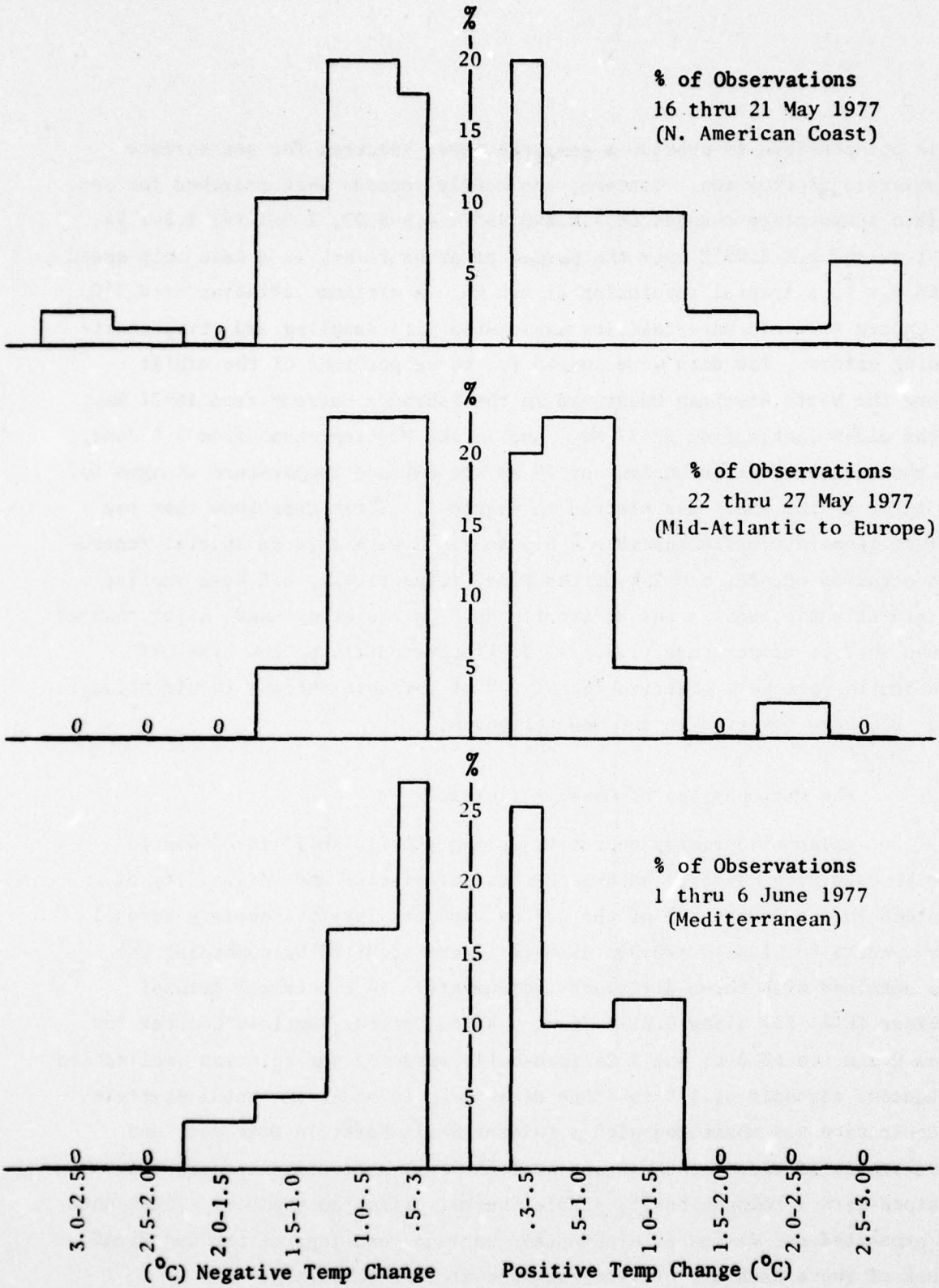

Figure 9: Frequency Distribution of 20 km (Hourly) Sea Surface Temperature Changes Observed During the Transatlantic-Mediterranean Cruise of May-June 1977

2.21 Aerosol Size Spectra, 0.01 to 3μm Diameter

Concentrations of small and large aerosols as functions of size and time for the Atlantic and Mediterranean portions of the cruise are shown in Figures 10a and b, respectively. The plotted data are the concentrations of aerosols of sizes greater than the indicated diameters: i.e., >0.01μm, >0.1μm, >0.3μm, >1.2μm, and >3.0μm. The data for size ranges >0.01 and >0.1μm were obtained with a TSI Electrical Aerosol Analyzer, and for the size ranges >0.3μm, a Royco Optical Particle Counter was utilized. The data shown are hourly values, and a log of the numerical values of these data is provided in Appendix D.

Comparison of Figures 10a and b with Figures 5a and b reveals, as expected, that the smaller particles (i.e., 0.01-0.1μm diameter) exhibited trends similar to those of total aerosol concentration. Minimum values of 30-300 cm^{-3} were observed in the mid-Atlantic from ∿0800 on 20 May to ∿0000 on 25 May, having decreased from maximum values of 5000-30000 cm^{-3} along the New England-Nova Scotia coast. Note that the decrease in concentration of aerosols >0.1μm diameter began early on 18 May--fully 24 hours prior to the observed decrease in total particle concentration--paralleling the dramatic improvement in visibility (Figure 5a) observed at that time.

On the other side of the Atlantic, concentrations of the smaller particles increased simultaneously as visibility degraded, from minimum values beginning on 25 May to ∿6000cm^{-3} early on 28 May near the Spanish coast. In the Mediterranean, the concentrations of aerosols < 0.1μm diameter were found to be 500-3500 cm^{-3}, with maximum values observed after 5 June.

Comparisons of aerosol data presented in Figures 5 and 10 suggests that, for the most part during the cruise, the observed aerosol size spectra did not extend to sizes smaller than 0.01μm. Further, the data shown in Figures 10a and b indicate that throughout most of the mid-Atlantic and to within 30 km of the Portuguese coast nearly all of the observed aerosols were larger than 0.1μm diameter.

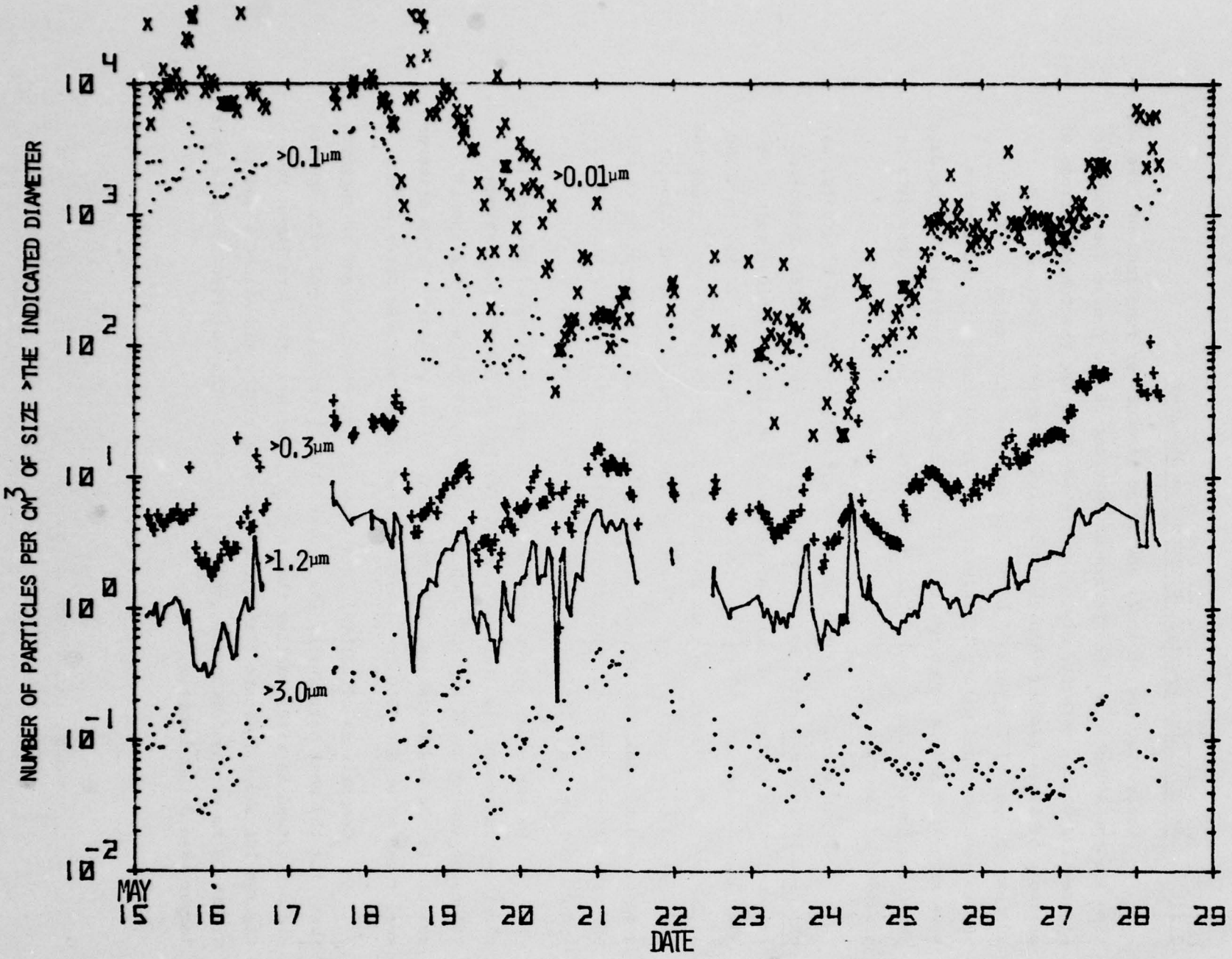

Figure 10a: Aerosol Concentrations as Functions of Size and Time for the Transatlantic Portion of NRL Cruise 77-16-04

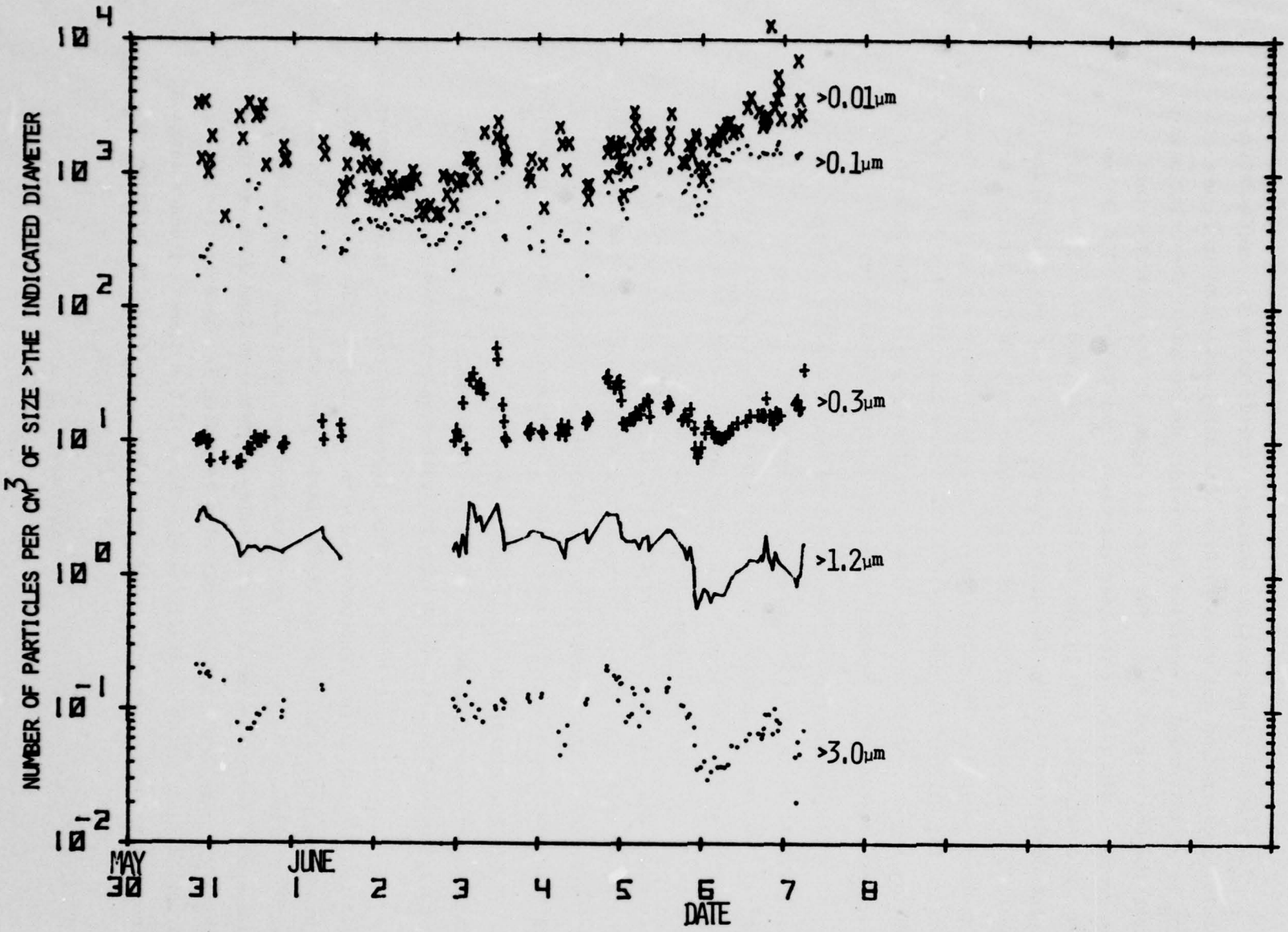

Figure 10b: Aerosol Concentrations as Functions of Size and Time for the Mediterranean Portion of NRL Cruise 77-16-04

A plot of total particle (Aitken) concentration vs. accumulative particle concentration for sizes >0.01μm (EAA data) presented in Figure 11 serves as an instrument comparison and vividly demonstrates the relationship between the two sets of data. The data in Figure 11 are separated into three groups: along the North American coast from 15 May to 1200 GMT on 20 May; mid-Atlantic, 1200 20 May to 0000 on 25 May; and from 25 May off the European coast to 7 June in the Mediterranean. The comparison in Figure 11 suggests some divergence from a 1:1 relationship only in the data for the New England coast and the mid-Atlantic. This divergence may be instrumentation-related. The Gardner may underestimate at higher concentration due to vapor depletion effects, while the EAA will underestimate at low concentration, a problem associated with "pushing" the lower limit of design feastures.

The data plotted in Figure 10 show that trends in the temporal/spatial variation in the concentrations of larger aerosols (i.e., 0.3-3.0μm diameter) were not as dramatic as, and in some instances dissimilar from, those of the smaller particles. Concentrations of larger particles increased from 2 to 40 cm^{-3} with time from 16 to 18 May along the New England-Nova Scotia coast and then decreased rapidly (as did all aerosols >0.1μm diameter) beginning at about 1200 GMT on 18 May as the ship moved away from land. Note that the trends in the concentration of aerosols >0.3μm nearly paralleled changes in measured scattering coefficient (see Figure 5a) during this period.

In the mid-Atlantic, concentrations of particles >0.3μm diameter fluctuated between ∿2 and 20 cm^{-3}, with spatial/temporal variations, again apparently correlated with variations in scattering coefficient.

Beginning about 0000 on 25 May, increasing concentrations of aerosols of 0.3 to < 3.0μm diameter were observed with proximity to the Portuguese coast. The nearly monotonic increase in these "large" particles from values of ∿3 cm^{-3} at 1200 km offshore to ∿60 cm^{-3} at 30 km from the coast was accompanied by a simultaneous, marked increase in scattering coefficient (and decrease in visibility). Smaller sized aerosols also increased in concentration during this period, but "giant"-particle (i.e., those >3.0μm diameter) concentration did not begin to increase until early on 27 May. The dramatic increase in

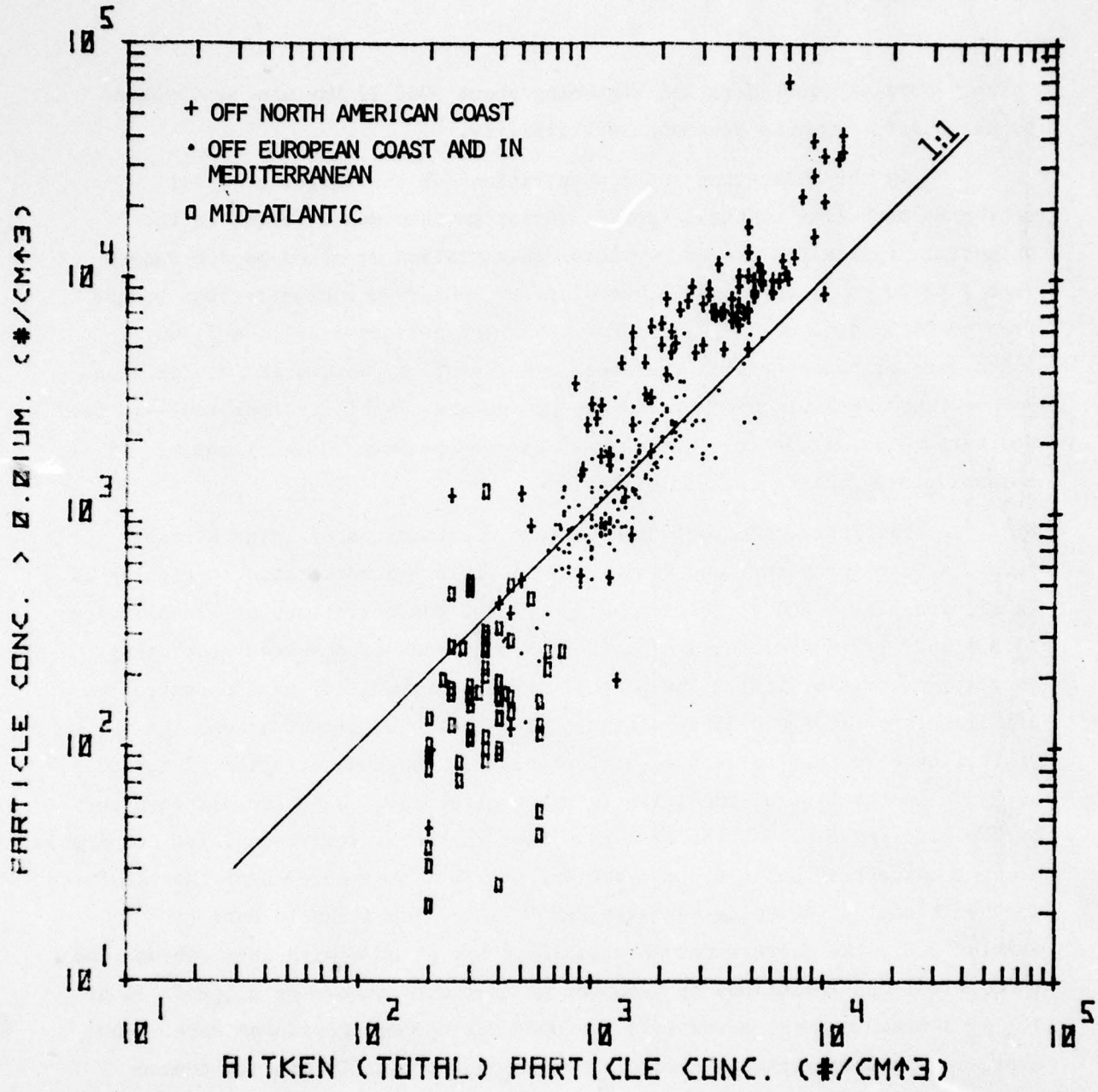

Figure 11: Total Particle Concentration vs. Concentration of Particles >0.01μm Diameter for NRL Cruise 77-16-04

"giant" particle concentration beginning about 0000 27 May was accompanied by an equally dramatic decrease in visibility.

In the Mediterranean, concentrations of the larger aerosols exhibited much less temporal/spatial variation than was observed in the Atlantic. Typical values of particle concentration at sizes >0.3μm ranged from 7 to 30 cm^{-3}; at sizes >3.0μm diameter, observed concentrations ranged from ∿0.04 to 0.15 cm^{-3}. Except for two brief periods--early on 3 June (when aerosol concentration increased and visibility decreased) and late on 5 June (when aerosol concentration decreased and visibility improved)--in the Mediterranean, little correlation was observed between fluctuations of aerosol concentration and visibility.

The apparent correlation between fluctuations of large aerosols (i.e., >0.3μm diameter) and visibility is vividly demonstrated in Figures 12. In Figures 12a, b and c, respectively, aerosol concentrations at sizes >0.1μm, >0.3μm and >1.2μm diameter are plotted as functions of observed scattering coefficient (visibility). The plot of measured visibility vs. concentration of aerosols of >0.3μm diameter (Figure 12b) shows that fluctuations in visibility were best correlated with changes in the concentration of aerosols >0.3μm. In the Figure, the Atlantic and Mediterranean data are distinguished by separate symbols, and the data show that in the Mediterranean, for comparable aerosol concentrations (>0.3μm diameter), visibilities were lower than observed in the Atlantic. Assuming sea salt aerosols for the Atlantic data (see Section 2.3), the differences in visibility are at odds with observations and theoretical considerations by a number of previous authors (e.g., Ref. 11 or 12) if a mixed natural aerosol is assumed for the Mediterranean data. However, if the Mediterranean aerosols were composed chiefly of such common salts as $CaCl_2$, $MgCl_2$ or H_2SO_4, then the observed result would be expected (Ref. 11). As will be described later in Section 2.31, a substantial fraction of the Mediterranean aerosols were composed of combinations of Cl, Ca, and S in the absence of Na.

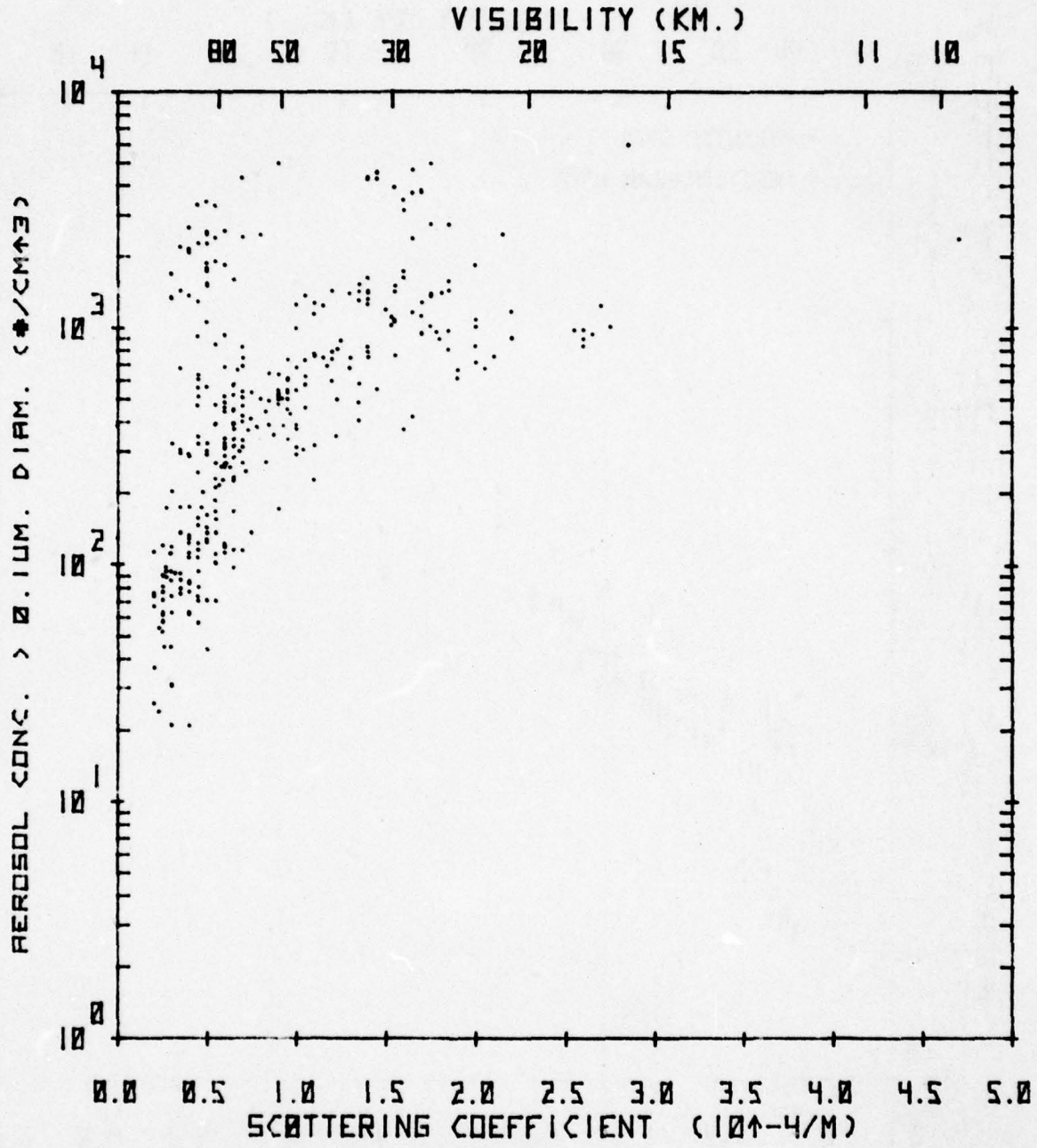

Figure 12a: Observed Scattering Coefficient (Visibility) vs. Concentration of Aerosols >0.1μm Diameter During NRL Cruise 77-16-04

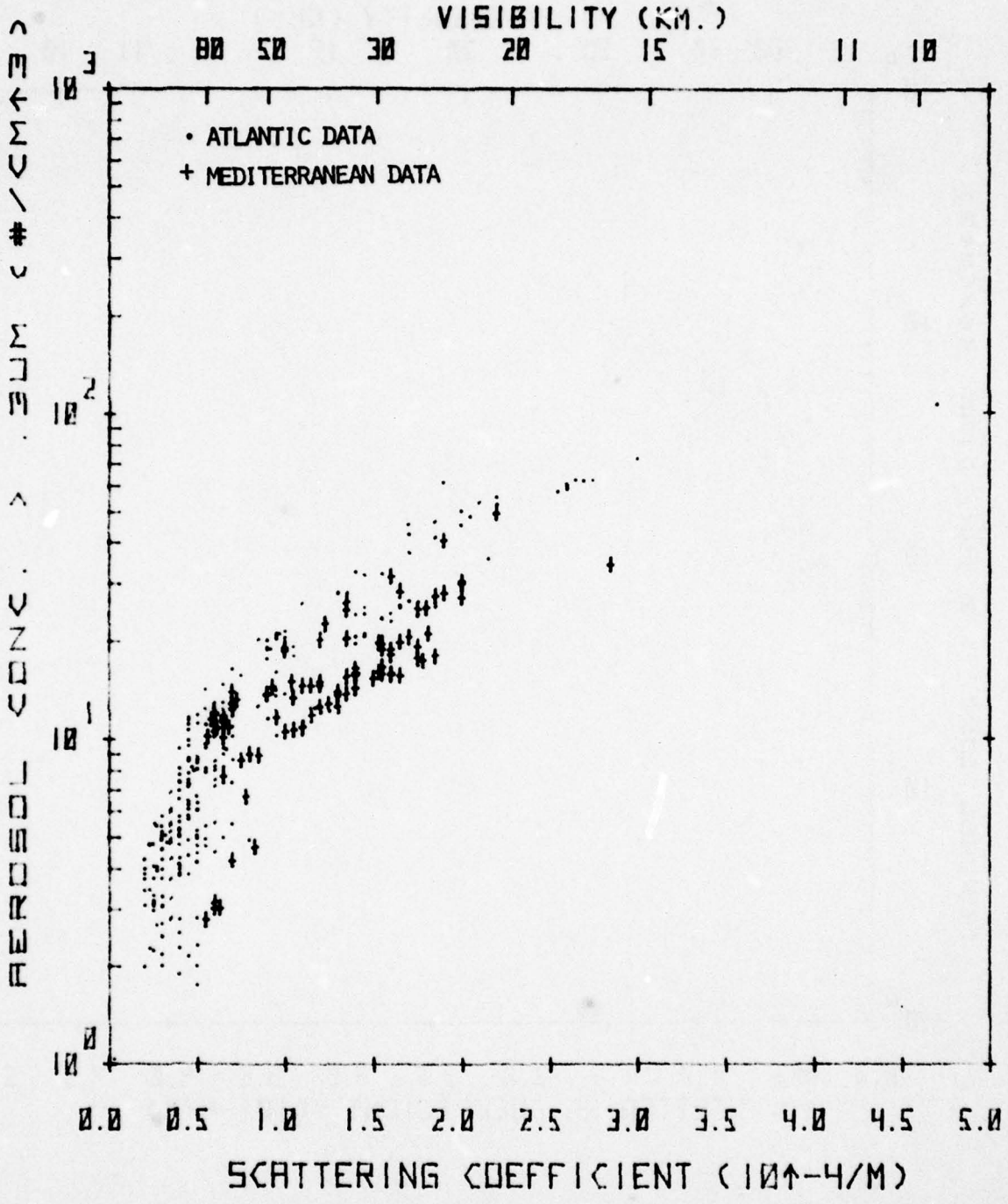

Figure 12b: Observed Scattering Coefficient (Visibility) vs. Concentration of Aerosols >0.3μm Diameter During NRL Cruise 77-16-04

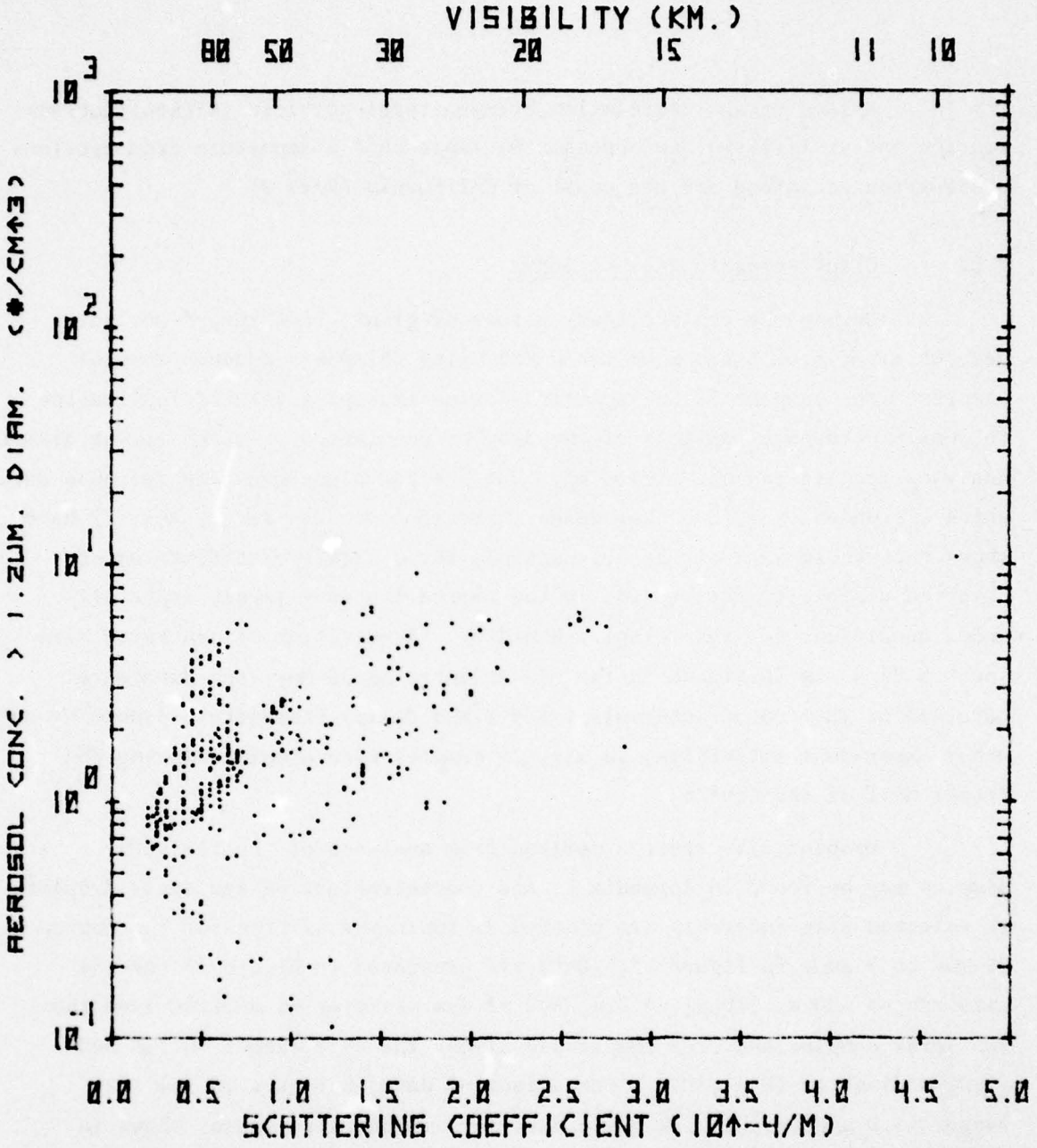

Figure 12c: Observed Scattering Coefficient (Visibility) vs. Concentration of Aerosols >1.2μm Diameter During NRL Cruise 77-16-04

A lack of any correlation between total particle (Aitken) concentration and visibility (see Appendix D) represents a departure from previous observations acquired off the coast of California (Ref. 9).

2.22 Giant Aerosols and Sea Spray

During the cruise, observations of giant, 'sea spray' aerosols were obtained from the bow of the HAYES using Calspan's aqueous-aerosol sampler. The sampler is an impaction device employing gelatin replication to obtain permanent replicas of the droplet population at sizes >1.0μm diameter. Analyses require tedious microscopy, but the technique provides reliable data which are unavailable by other means. Previous studies (e.g., Ref. 7) have shown that these aerosols are responsible for a significant fraction of observed visibility restriction in the marine boundary layer, especially under conditions of high relative humidity. Acquisition of sea spray size spectra data was initiated in the mid-Atlantic on 25 May, and data were obtained at infrequent intervals (∿1-4 times daily) thereafter, depending on other experiment activities; in all, 26 samples were acquired during the latter half of the cruise.

Droplet size spectra derived from analyses of the sea spray samples may be found in Appendix E, and concentrations of sea spray droplets at selected size intervals are plotted as functions of time for the period 25 May to 7 June in Figure 13. Data are presented in Figure 13 for the size ranges >20μm, >10μm, >4.0μm, and >1.0μm diameter as derived from the sea spray samples and, for comparable times, the size ranges >0.1μm and >0.01μm diameter (EAA data). Comparison of data in Figure 13 for size ranges >1.0 and >4.0μm with Royco data for similar size ranges shown in Figures 10a and b reveals remarkably good agreement between aerosol concentration values measured by the two different instruments.

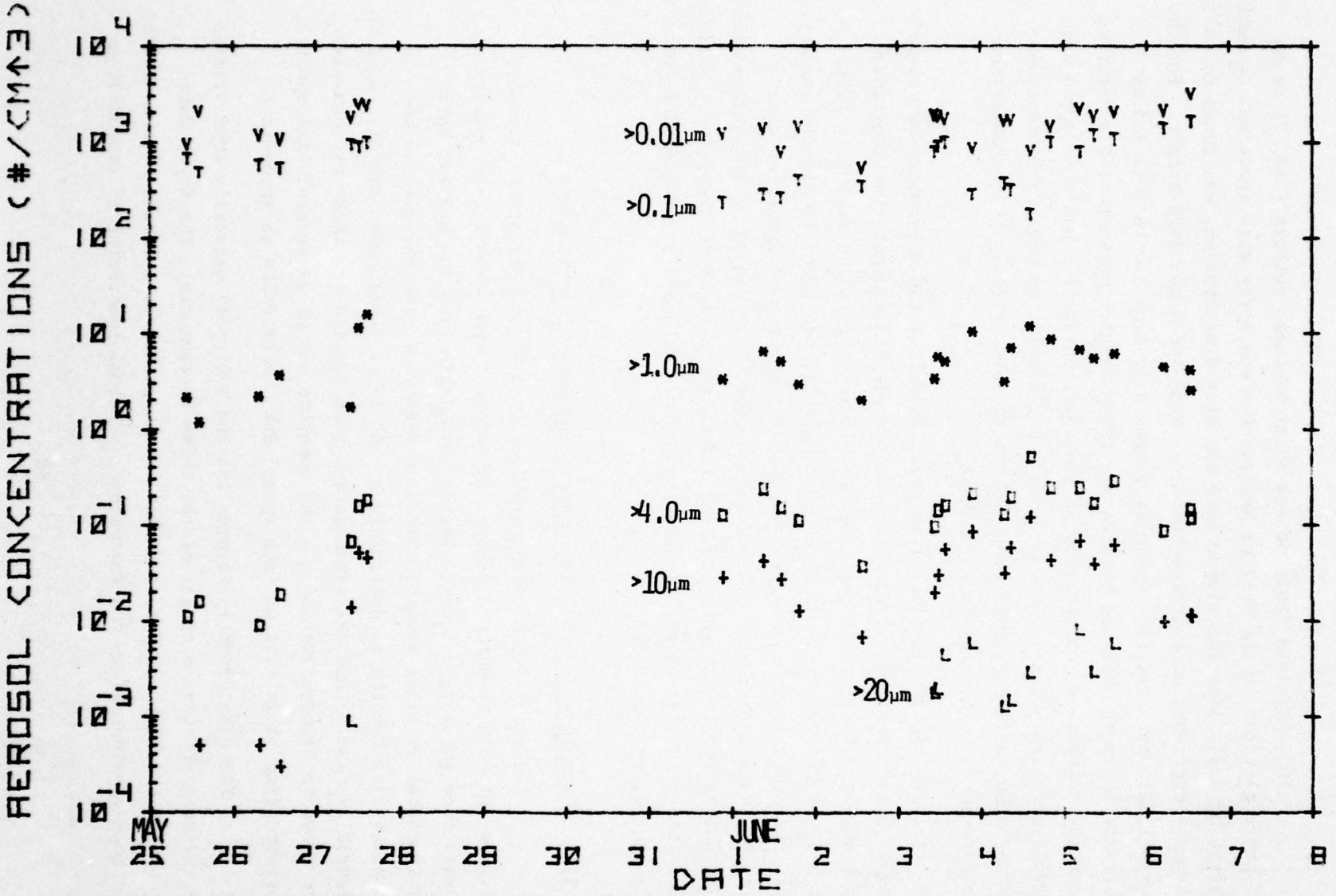

Figure 13: Concentrations of 'Sea Spray' Aerosols at Selected Size Categories as Functions of Time During NRL Cruise 77-16-04

In a previous study of sea spray by these authors (Ref. 7) on an offshore platform in the Gulf of Mexico, the sea spray size spectrum, as manifested by visibility calculated from the size distribution, was found to be strongly dependent on relative humidity, wind speed and wave height. For the current data set, relative humidity ranged only from ∿60 to 80%, and no correlations were observed between sea spray droplet parameters and relative humidity. Likewise, comparisons of sea spray parameters and wind speed were devoid of correlations. However, sea spray droplet spectra parameters were found to be correlated with crest-to-trough wave height. These comparisons are presented in Figures 14 through 18.

In Figure 14, visibility calculated from the absolute, 'sea spray' droplet size spectrum (>1.0μm diameter) is plotted against crest-to-trough wave height. While there was considerable scatter in the data (∿ a factor of 3-10 in visibility for a given wave height), the trend is clearly evident. A second order least squares fit to the data shows good agreement with previous data obtained in Gulf of Mexico (Ref. 7). Similar correlations with wave height for liquid water content and concentrations of droplets at various size intervals show comparable scatter. These data are presented in Figures 15 through 18, respectively.

2.23 Complete Aerosol Size Spectra and Junge Distributions

The acquisition of the previously discussed sea spray size data (Figure 13) permitted the extension of our measured aerosol size spectra upward from the range < 3.0μm diameter (available from the EAA and Royco instruments) to sizes greater than 20μm diameter. Two examples of the absolute size spectra as determined by the three instruments are displayed in Figures 19a and b, and the accumulative size spectra for these two examples are shown in Figures 20a and b. The complete set of 24 aerosol size spectra, corresponding to 24 sets of 'sea spray' data is provided in Appendix F.

The data shown in Figures 19a and b display extremely good overlap in the respective size ranges of the three instruments. The Royco data exhibited the most scatter, and this is thought to be a result of the optical scattering principle of the instrument. Optical scattering is dependent on

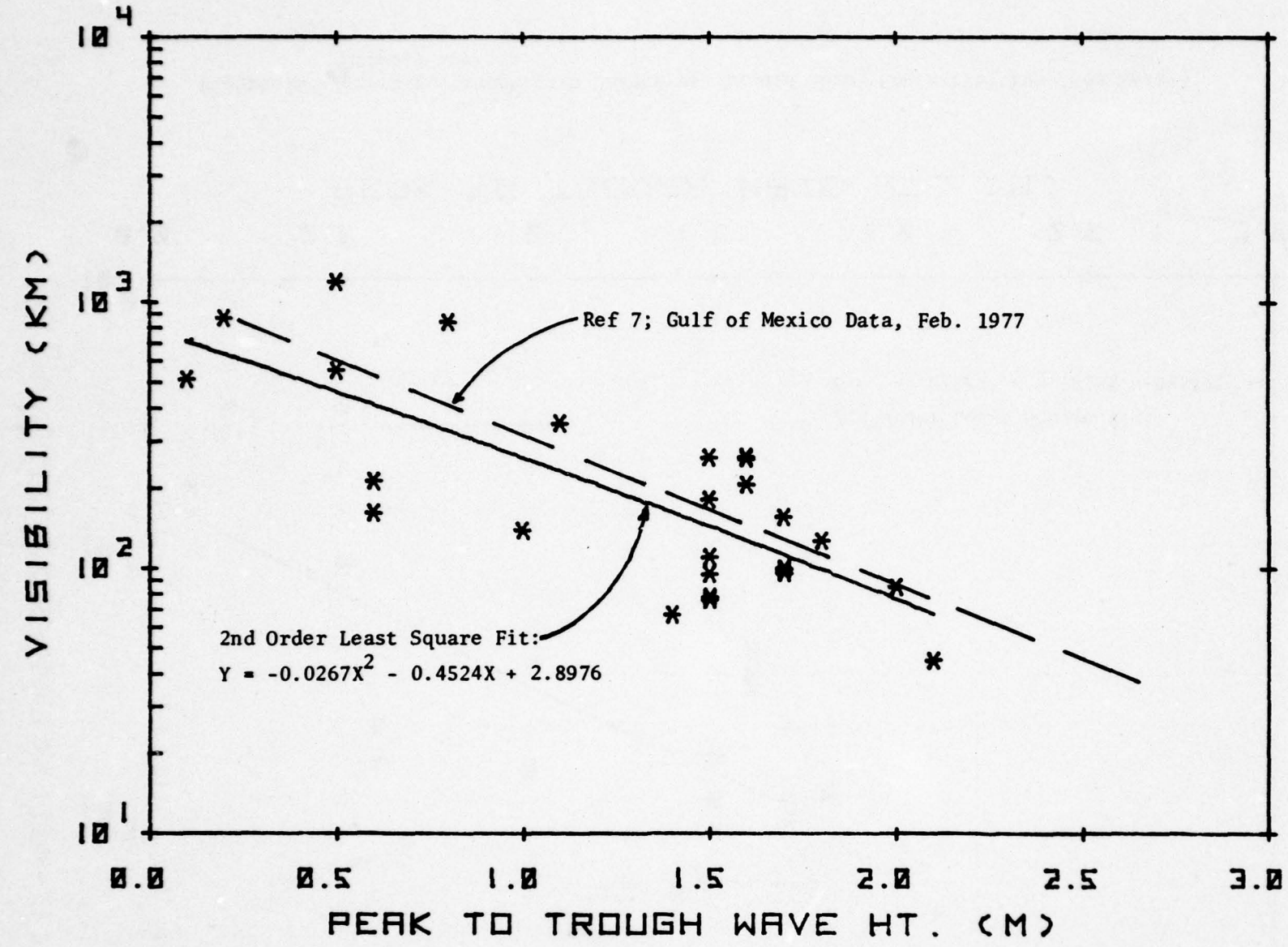

Figure 14: Crest-to-Trough Wave Height vs. Visibility Calculated from the 'Sea Spray' Drop Size Distribution

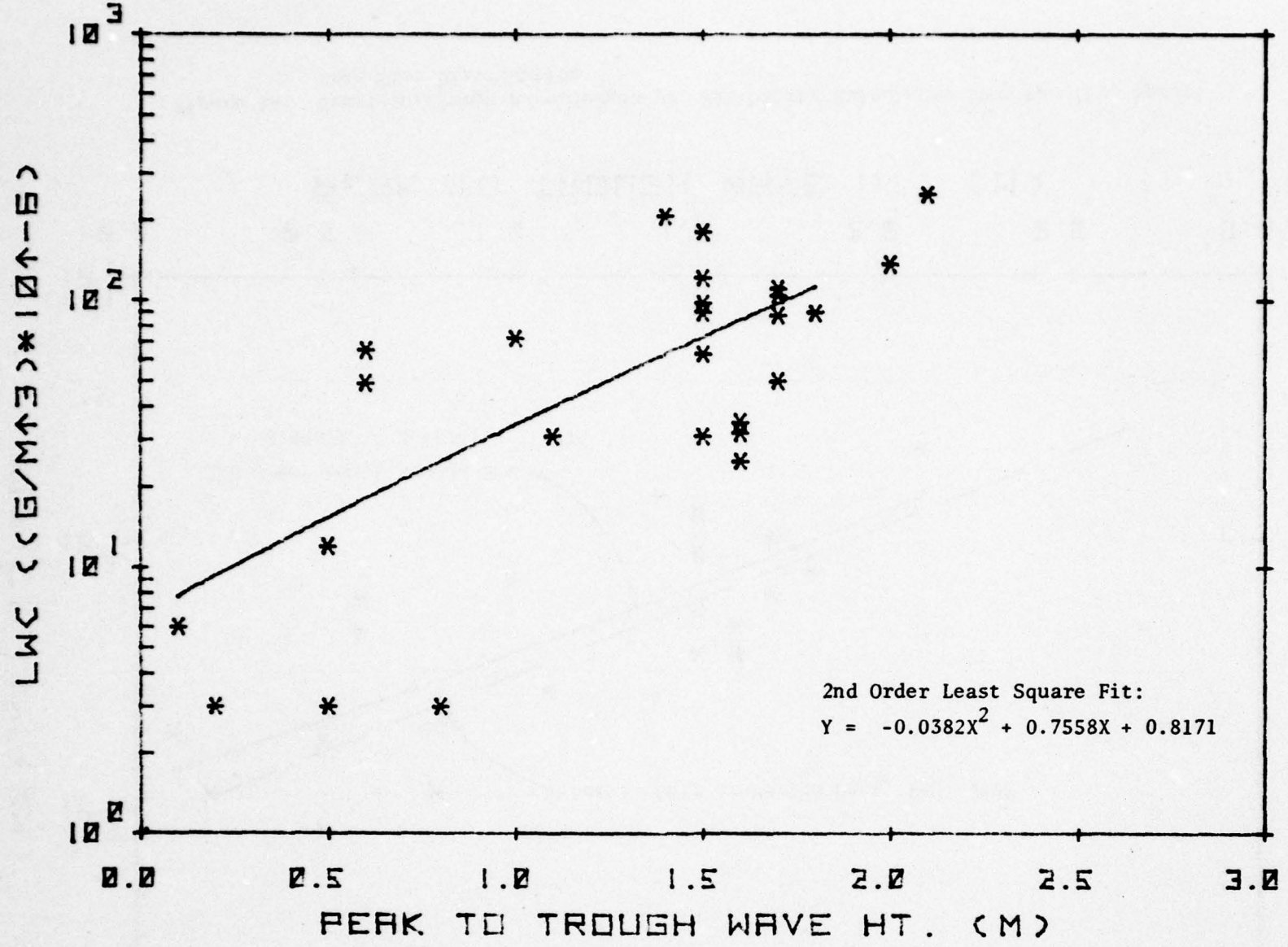

Figure 15: Crest-to-Trough Wave Height vs. Liquid Water Content of the 'Sea Spray' Droplet Spectra

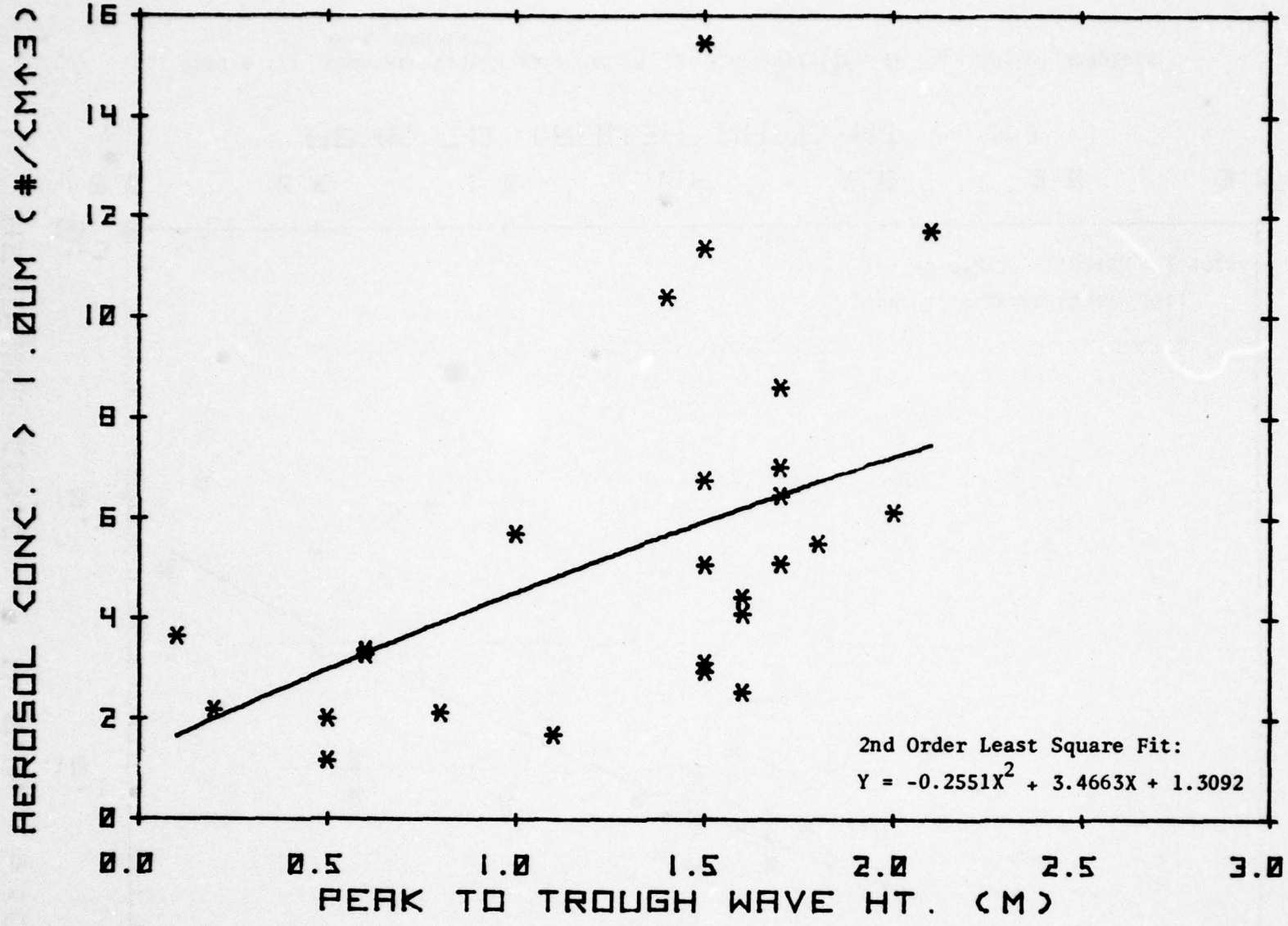

Figure 16: Crest-to-Trough Wave Height vs. Concentration of 'Sea Spray' Droplets >1μm Diameter

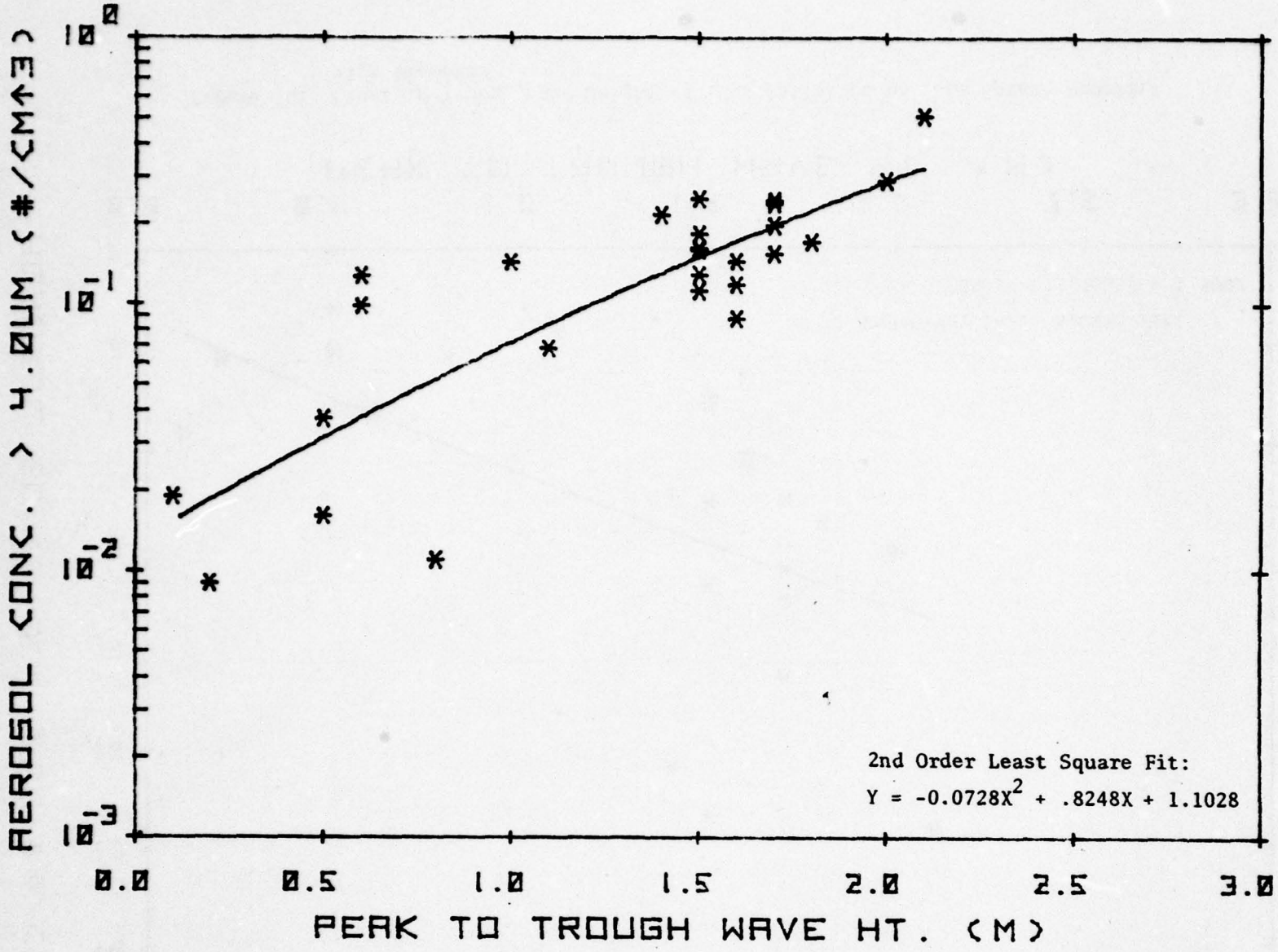

Figure 17: Crest-to-Trough Wave Height vs. Concentration of 'Sea Spray' Droplets >4μm Diameter

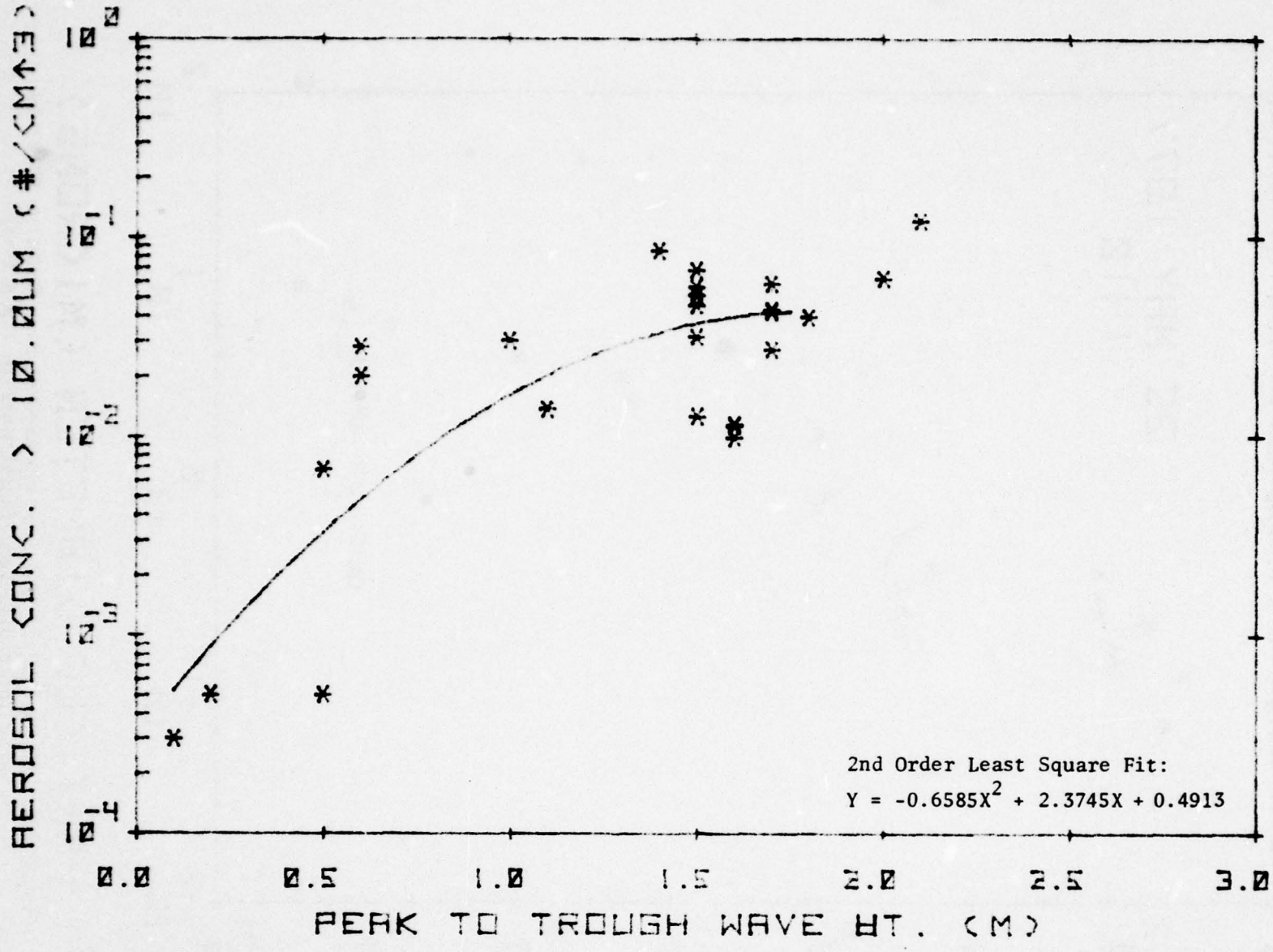

Figure 18: Crest-to-Trough Wave Height vs. Concentration of 'Sea Spray' Droplets >10μm Diameter

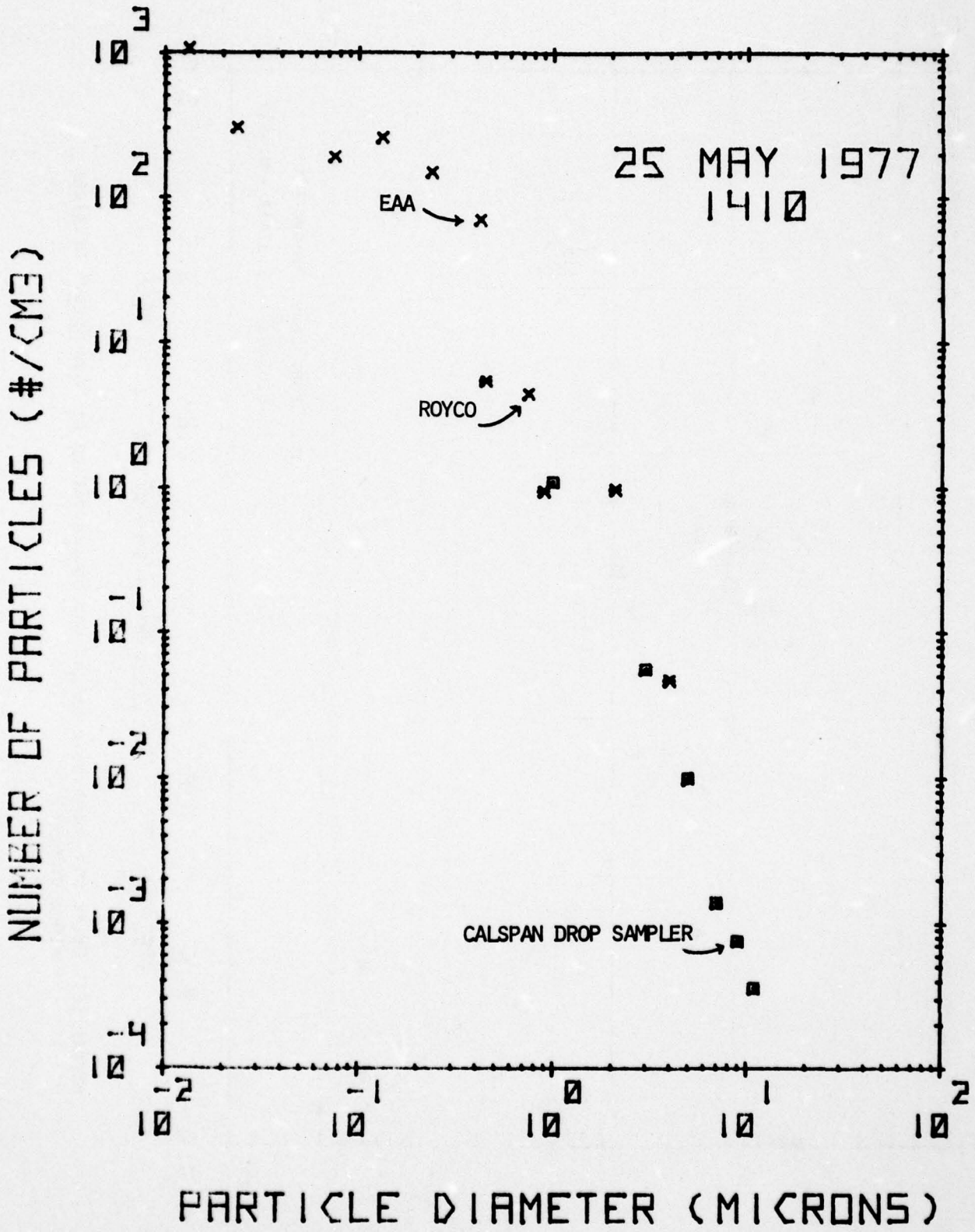

Figure 19a: An Example of the Complete Aerosol Size Spectrum Obtained with Three Different Instruments in the Atlantic

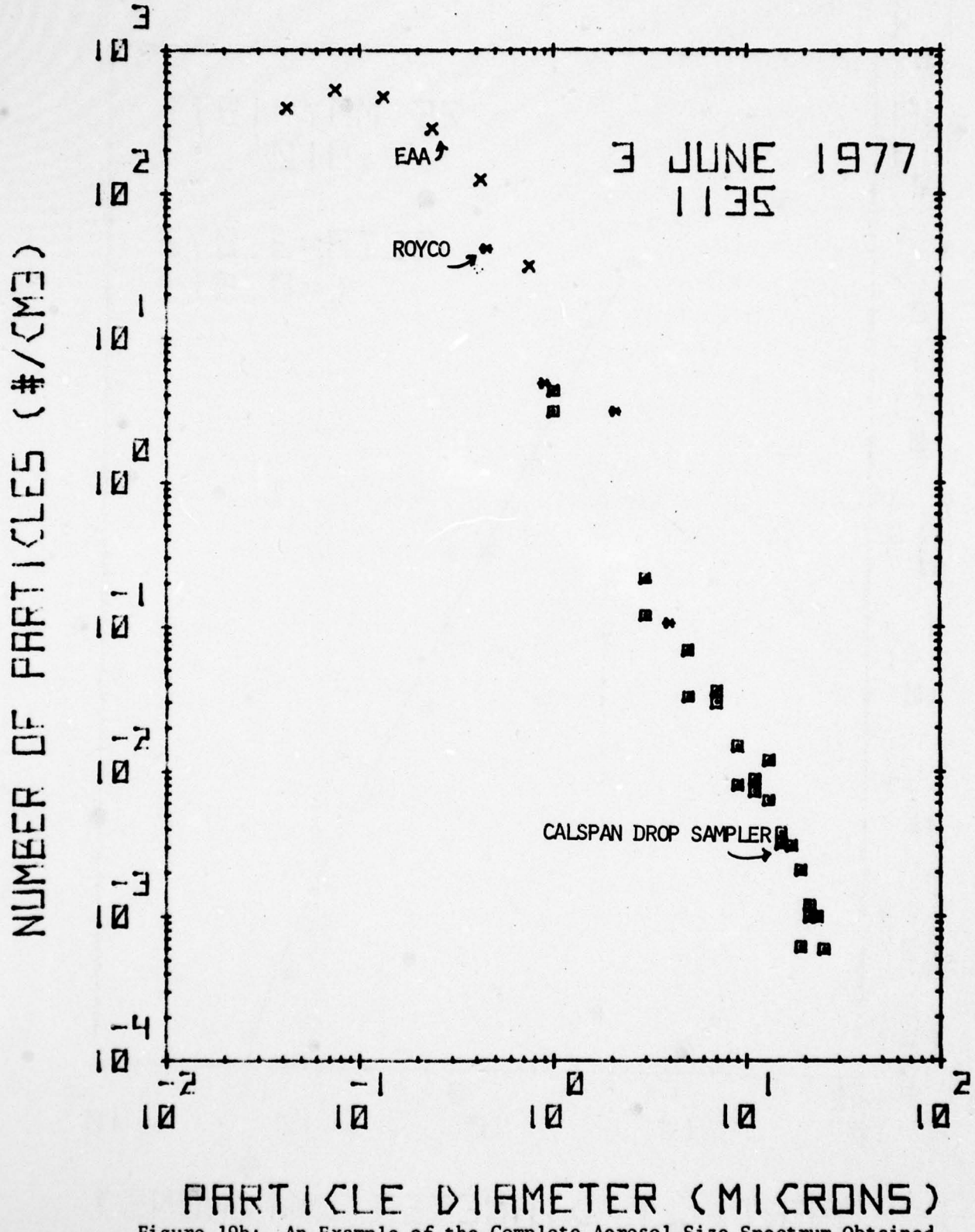

Figure 19b: An Example of the Complete Aerosol Size Spectrum Obtained with Three Different Instruments in the Mediterranean

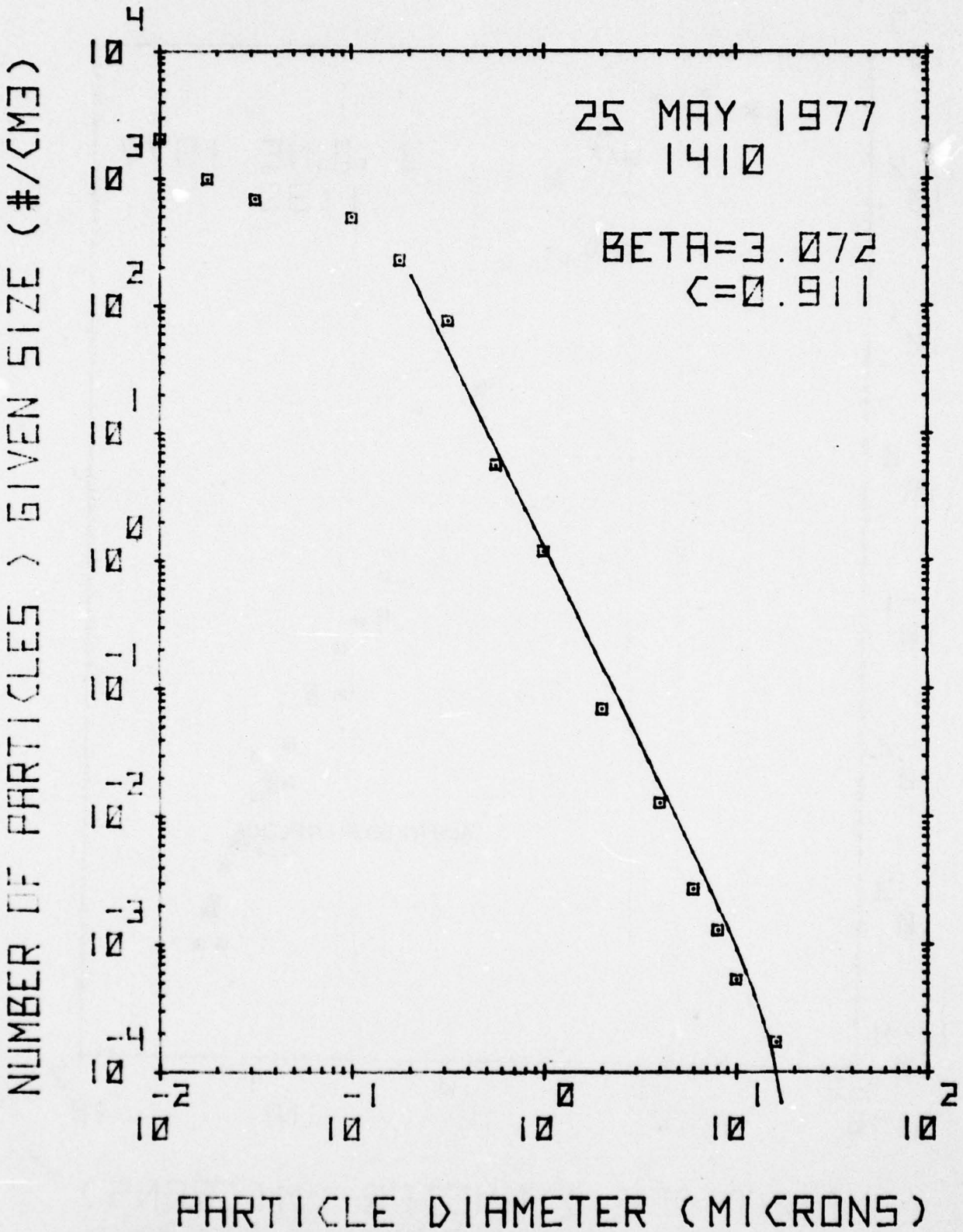

Figure 20a: Accumulative Aerosol Size Spectrum from the Atlantic Fitted with a Junge Distribution

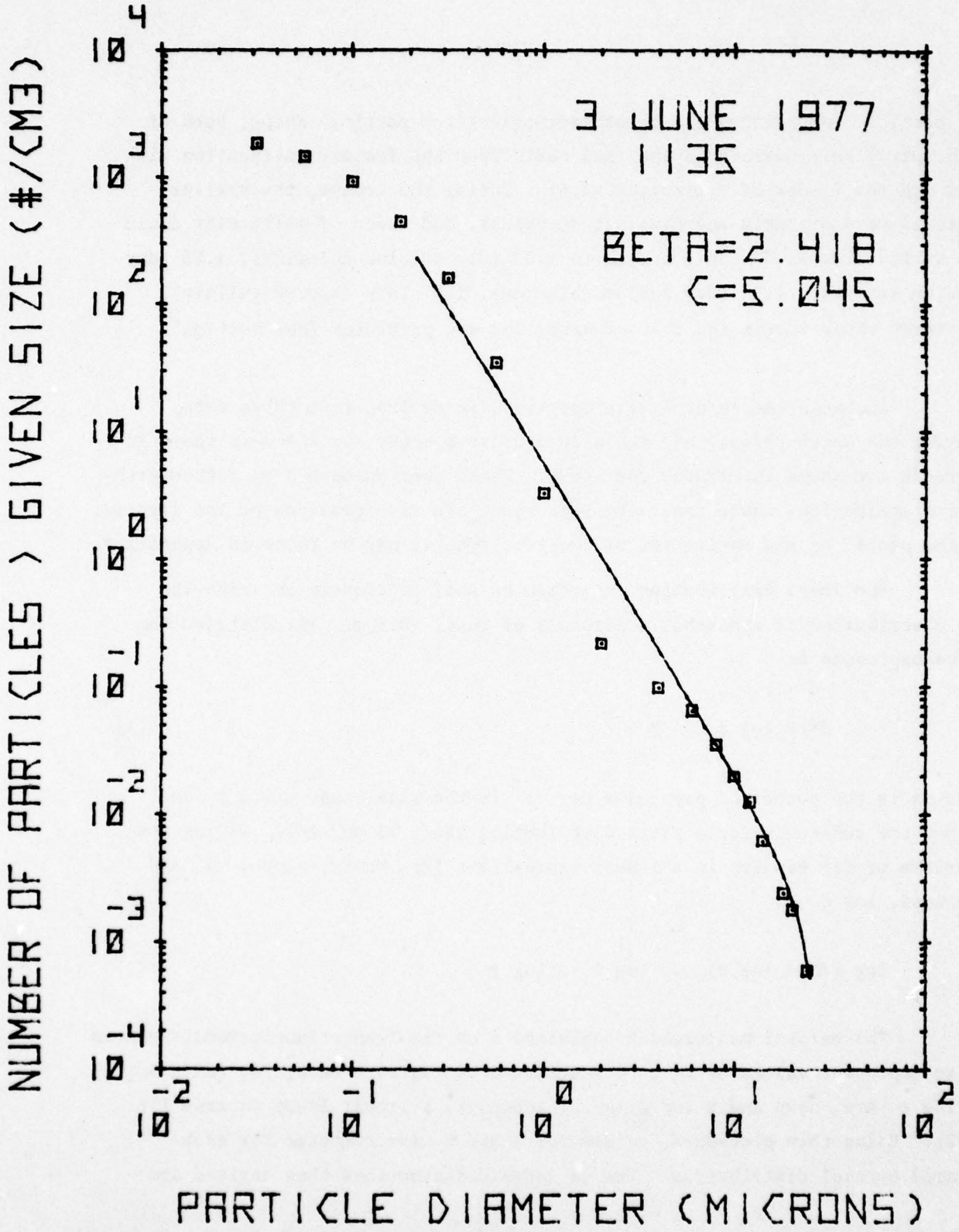

Figure 20b: Accumulative Aerosol Size Spectrum from the Mediterranean Fitted with a Junge Distribution

both particle composition (index of refraction) and particle shape, both of which very likely deviate in the real world from the factory calibration with latex spheres (index of refraction ∿1.6). During the cruise, the smaller particles were probably anything but spherical, and index of refraction could have varied from >1.33 (pure water) to 1.52 (dry calcium chloride), 1.53 (dry ammonium sulfate), 1.54 (dry sodium chloride), 1.57 (dry calcium sulfate), or between these values and that of water for wet particles (see Section 2.3).

Accumulative aerosol size spectra were derived from these data, ignoring the Royco values, and the accumulative spectra for the data shown in Figure 19 are shown in Figures 20a and b. These spectra have been fitted with Junge distributions whose constants βeta and C are also provided on the figures. Similar plots for the entire set of complete spectra may be found in Appendix F.

The Junge distribution can often be used to closely describe the size distribution of atmospheric aerosols of radii >0.1μm. The distribution may be expressed as

$$dN/d \log r = C\, r^{-\beta} \qquad (1)$$

where dN is the number of particles per cm^3 in the size range d log r, and β and C are constants for a given distribution (Ref. 13 and 14). Taking the logarithm of (1) results in a linear expression, (2), having slope, -β, and intercept, log C.

$$\log (dN/d \log r) = \log C - \beta \log r \qquad (2)$$

The aerosol measurements obtained from the Transatlantic-Mediterranean cruise represent values of dN as a function of d log r. Hence, log (dN/d log r) and log r are known and β and C may be found via a linear least squares fit of (2). Using this procedure, values for β and C were computed for each measured aerosol distribution. The 24 Junge distributions thus derived are

plotted together in Figure 21. This presentation shows that the Junge distribution changed from the Atlantic to coastal Europe to the Central Mediterranean.

The constants, β and C, and the slopes (0.5 to 5.0μm diameter) of the Junge distributions were averaged for four portions of this part of the cruise: Atlantic (25 and 26 May), Coastal Europe (27-31 May), Western Mediterranean (1-3 June), and Central Mediterranean (4-6 June). The averaged Junge distribution parameters are presented in Table 2. Given a single point measure of aerosol concentration between 0.5 and 5μm diameter,

Table 2: Junge Distribution Parameters Averaged for Four Portions of NRL Cruise 77-16-04

	β	C	Slope (0.5-5.0μm dia.)
Eastern Atlantic	3.28	1.09	-2.84
Coastal Europe	2.30	6.20	-6.21
Western Mediterranean	2.20	3.99	-3.67
Central Mediterranean	2.22	6.94	-6.31

one may be able to derive the complete aerosol spectrum for these areas under similar meteorological circumstances.

2.24 Cloud Condensation Nucleus Activation Spectra

During the Transatlantic-Mediterranean cruise of May-June 1977, approximately 90 observations of cloud condensation nucleus (CCN) activity spectra were obtained. These measurements were acquired with a Calspan-built static thermal diffusion chamber at supersaturations ranging from

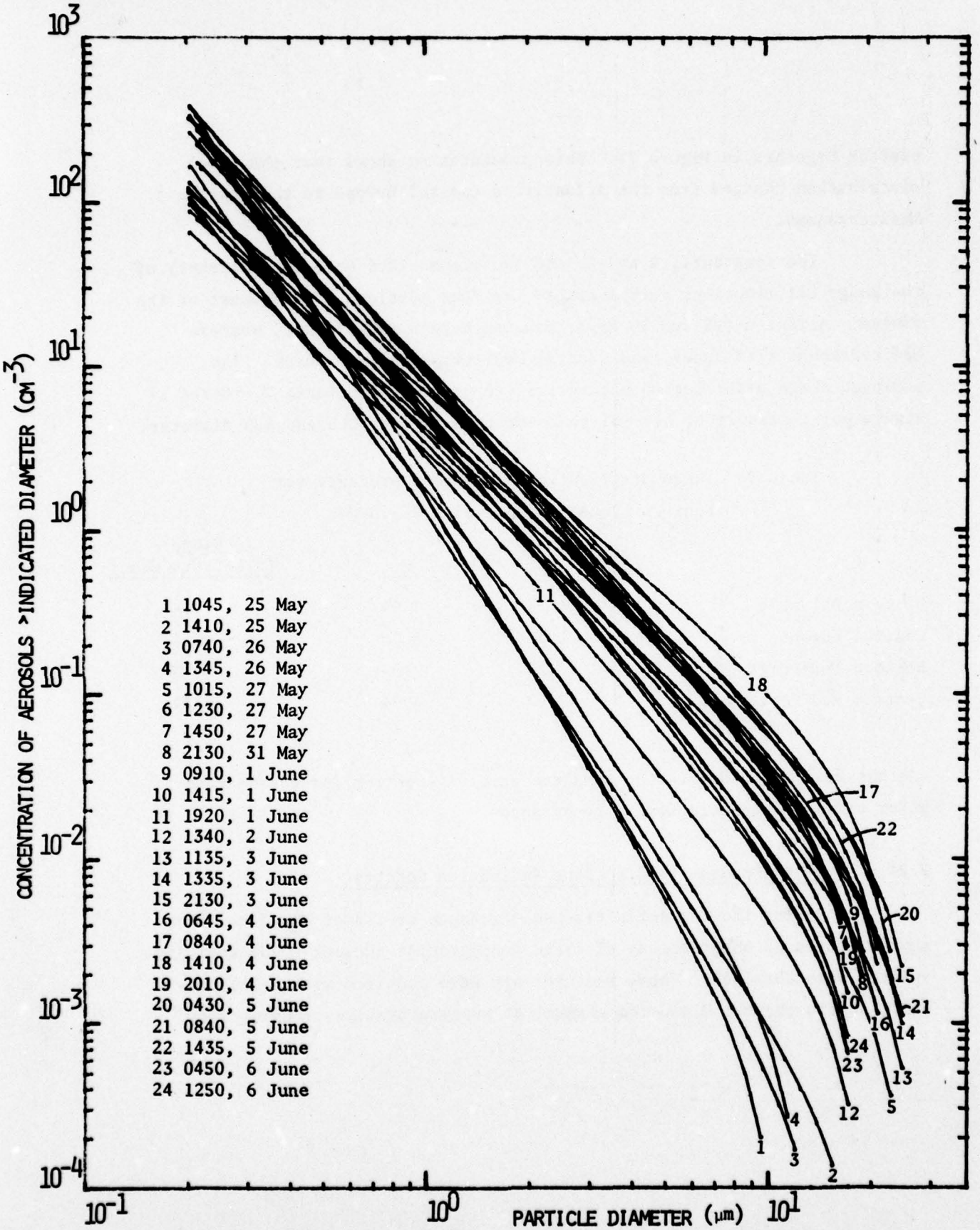

Figure 21: Junge Distributions for the 24 Complete Aerosol Spectra Measured During NRL Cruise 77-16-04

0.2% to 1.0%*. The complete set of activity spectra** are provided in Appendix G, and inferred CCN concentrations at discrete supersaturations as functions of time may be found in Appendix H. CCN concentrations at 0.2% S and Aitken nucleus concentrations at comparable times are plotted as functions of time for the Atlantic and Mediterranean portions of the cruise in Figures 22a and b, respectively.

Comparison of CCN data in Figure 22 with aerosol data presented in Figure 10 reveals that concentrations of CCN active at 0.2% S followed trends similar to those of aerosols of size >0.1μm diameter. Absolute CCN concentration at 0.2% S fell between the values observed for aerosols >0.1μm and >0.3μm, closely approximating the concentrations of aerosols >0.1μm after 19 May. The close correlation of CCN, particularly at 0.5% S, with aerosols of size >0.1 is demonstrated in Figure 23 and appears valid for the mid-Atlantic European coast and Mediterranean data.

In Figure 24, total nucleus (Aitken) concentration is plotted as a function of the simultaneous concentration of CCN active at 1.0% S. Previously reported CCN observations off the coast of California (Ref. 9) indicated that most of the aerosols observed at that location were active at 1.0% S--a result reported for marine air masses by a number of previous investigators (e.g., Ref. 17). However, the extent of departure from a 1:1 relationship, as revealed in Figure 24 suggests that a 1:1 relationship is not always the case; and, therefore, that there are, at times, differences in the production mechanisms for, or sources of, Aitken nuclei and CCN, even in the remote marine boundary layer.

---

*According to theory and experimental evidence (e.g., Ref. 15), CCN active at 0.2 and 1.0% S correspond to particles of ∿0.075 and 0.025μm diameter (dry size), respectively.

**These data have not been corrected for vapor depletion and sedimentation effects (Ref. 16).

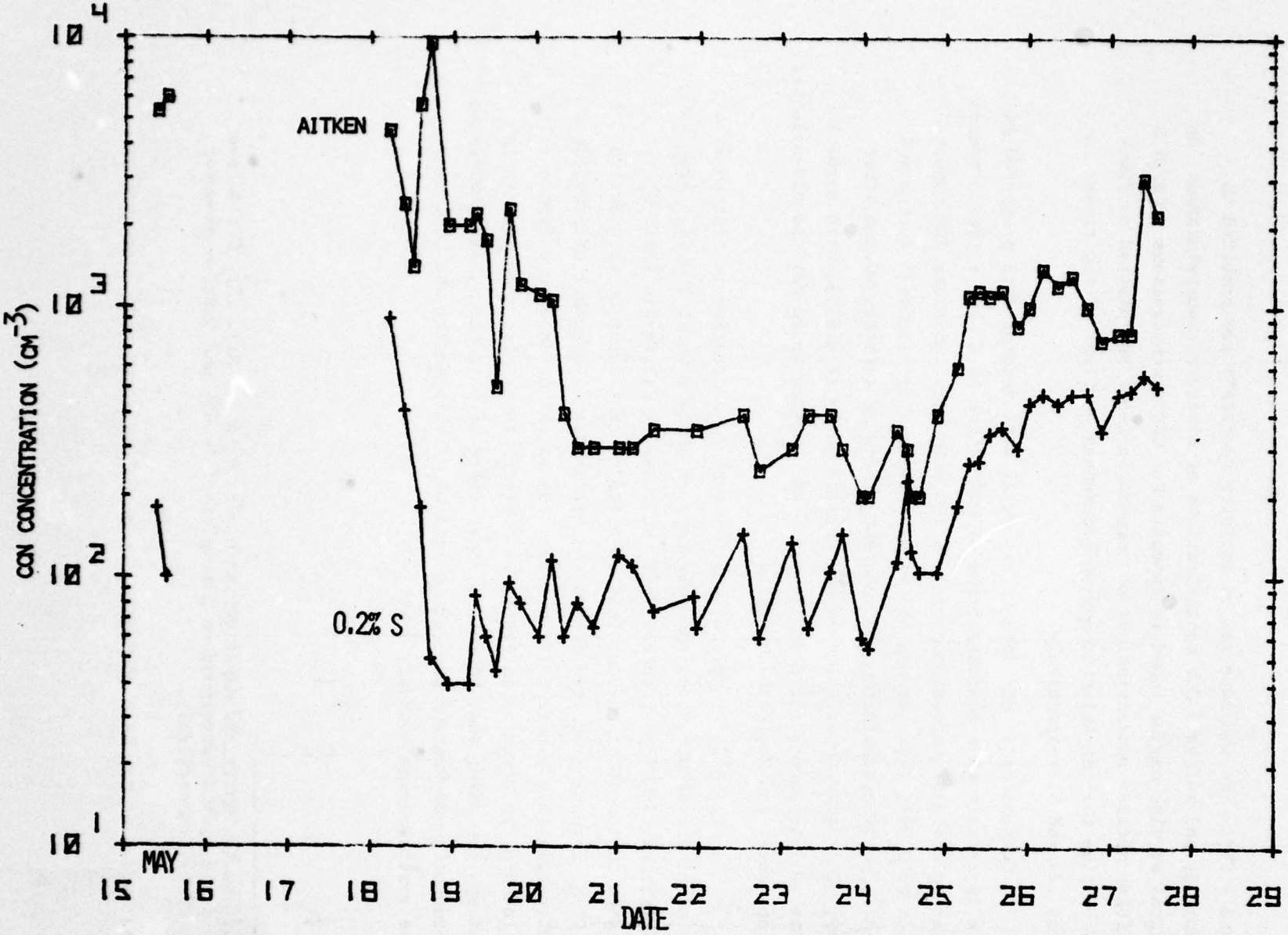

Figure 22a: Concentrations of CCN Active at 0.2% S and Aitken Nuclei as Functions of Time for the Atlantic Portion of NRL Cruise 77-16-04

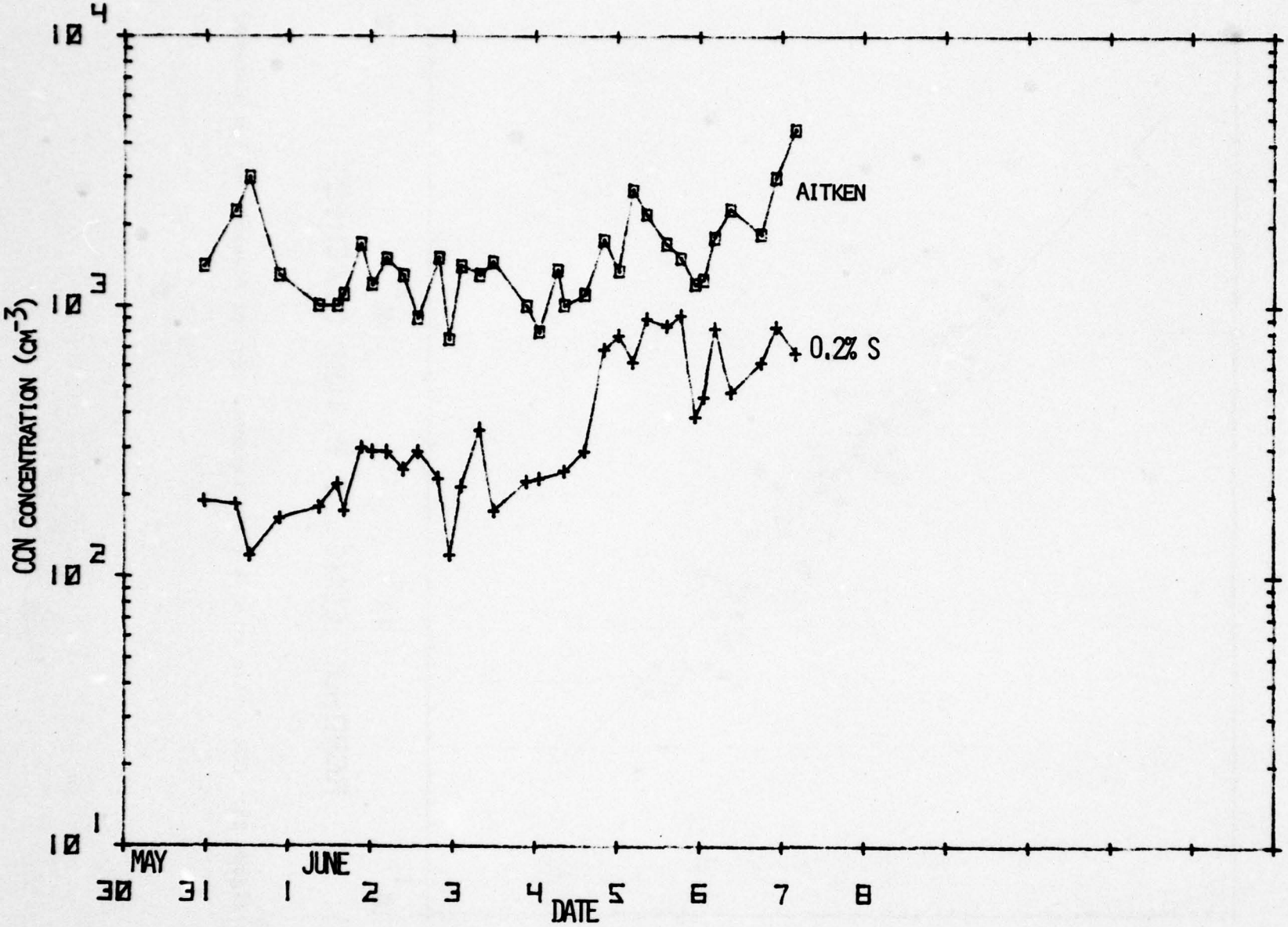

Figure 22b: Concentrations of CCN Active at 0.2% S and Aitken Nuclei as Functions of Time for the Mediterranean Portion of NRL Cruise 77-16-04

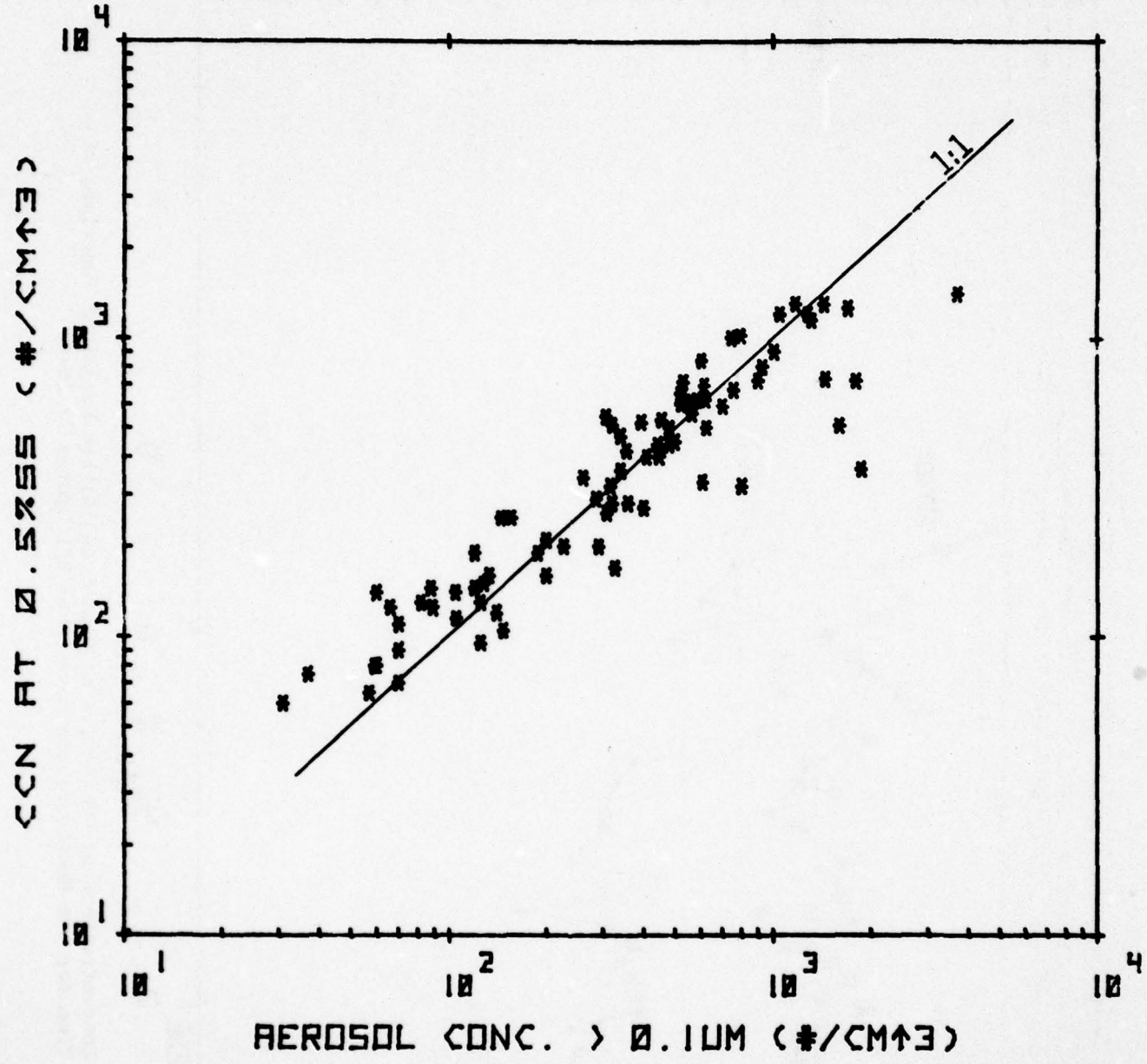

Figure 23: CCN Active at 0.5% S vs. Concentration of Aerosols >0.1μm Diameter

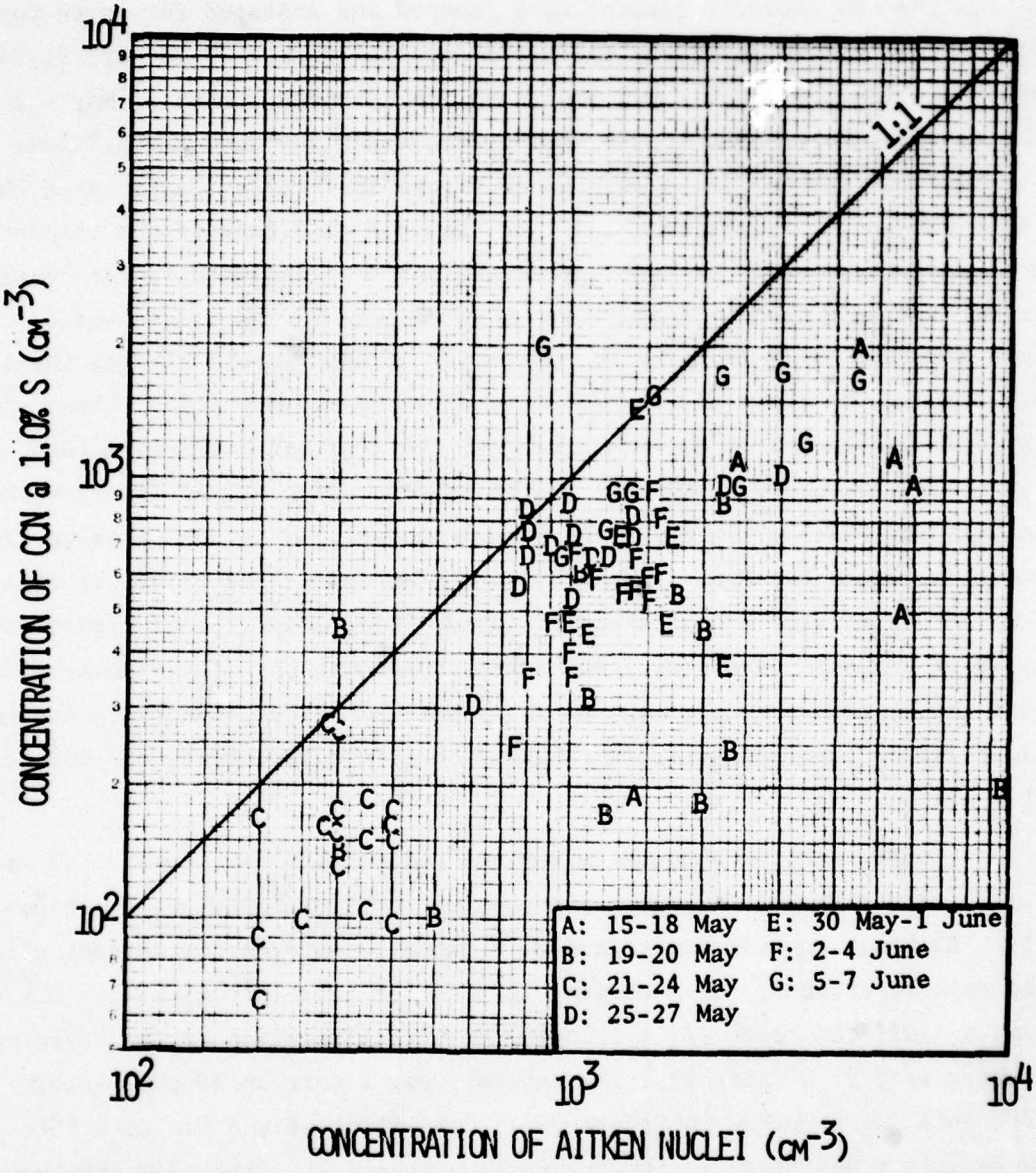

Figure 24: Concentration of CCN Active at 1.0% S vs. Concentration of Aitken Nuclei During NRL Cruise 77-16-04

The CCN activity spectra were grouped and averaged for seven portions of the cruise: 15-18 May along the North American coast; 19-20 May; 21-24 May in the mid-Atlantic; 25-27 May approaching the European coast; 30 May - 1 June in the Gibraltar area; and in the Mediterranean for 2-4 June and 5-7 June 1977. The average CCN spectra are presented in Figure 25. It is readily seen that the mean CCN spectra differed chiefly in absolute magnitude of the respective aerosol concentrations. Highest concentrations were observed in the central Mediterranean, and lowest concentrations were found in the mid-Atlantic. The spectra observed on 19-20 May were apparently 'transitional' between the aerosol observed along the coast and those observed in the mid-Atlantic. These spectra fall within the limits of data observed off the coast of California (Ref. 9) during CEWCOM-76--i.e., neither as low in concentration as was observed there in clean (natural) marine air nor as high in concentration as was observed along the coast near Los Angeles. Further, the CCN activity spectra of the Atlantic and Mediterranean were not as steeply sloped, being comprised of higher concentrations of aerosols active at lower supersaturations than those observed at sea off the West Coast. Even mid-Atlantic data exhibited higher CCN concentrations at low SS than are typically observed in clean marine air off the West Coast.

Comparisons of CCN concentrations active at 0.2% S and 0.5% S with measured scattering coefficient are presented in Figures 26a and b, respectively. Although considerable scatter (a factor of 3-4 in CCN concentrations) in the data is obvious, it is evident that better correlation is with CCN active at 0.5% S. Off the coast of California, better correlation was observed with CCN active at 0.2% S (Ref. 9). The envelope for a portion of the Eastern Pacific data is sketched in Figure 26a. Comparison of the two data sets again reveals a departure in the Atlantic/Mediterranean data from observations off the coast of California.

2.3 Chemical Composition of Boundary Layer Aerosols

During the May-June 1977 Transatlantic-Mediterranean cruise, samples of atmospheric aerosols were collected nearly continuously, weather and winds permitting, for subsequent chemical analyses. The collections consisted of

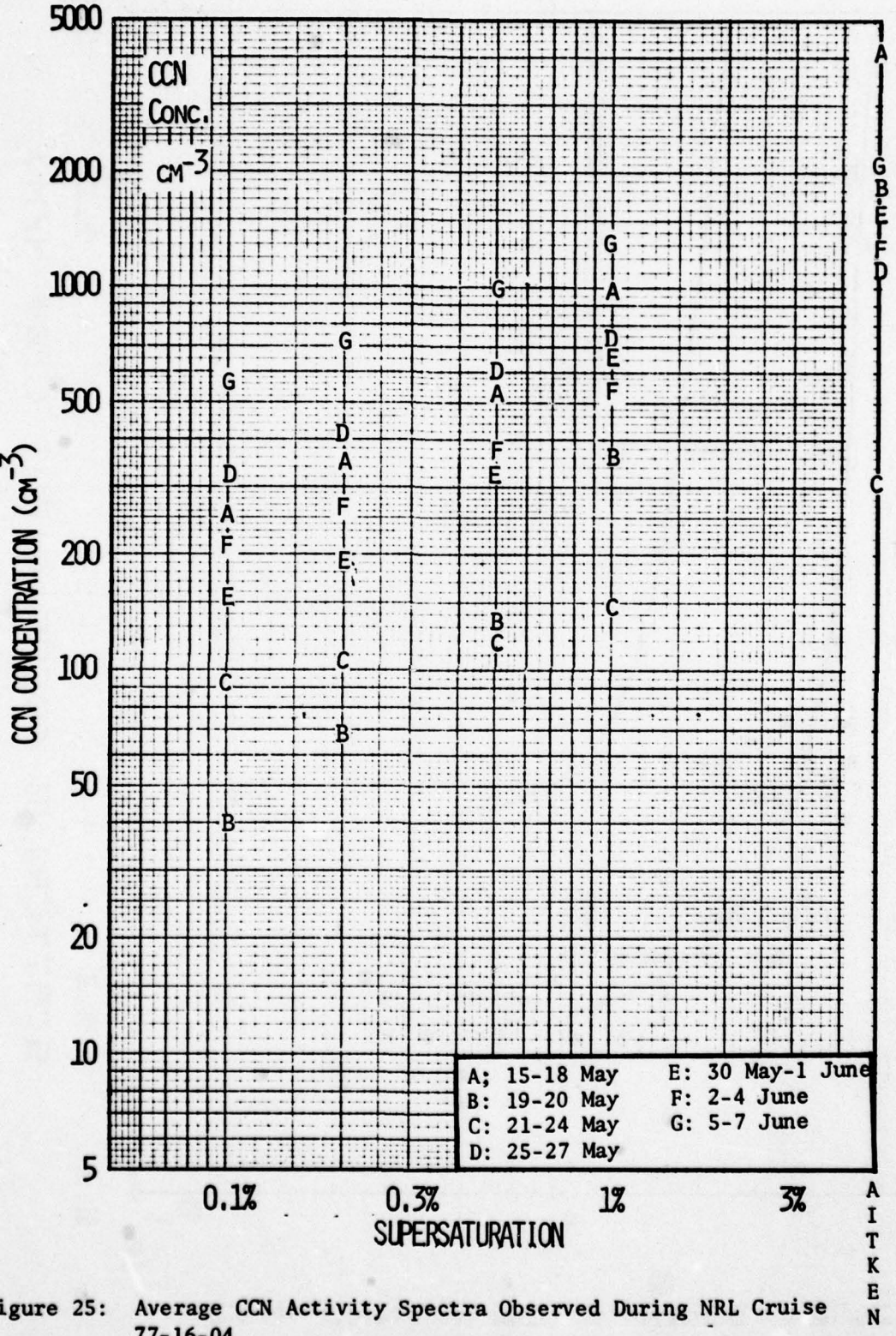

Figure 25: Average CCN Activity Spectra Observed During NRL Cruise 77-16-04

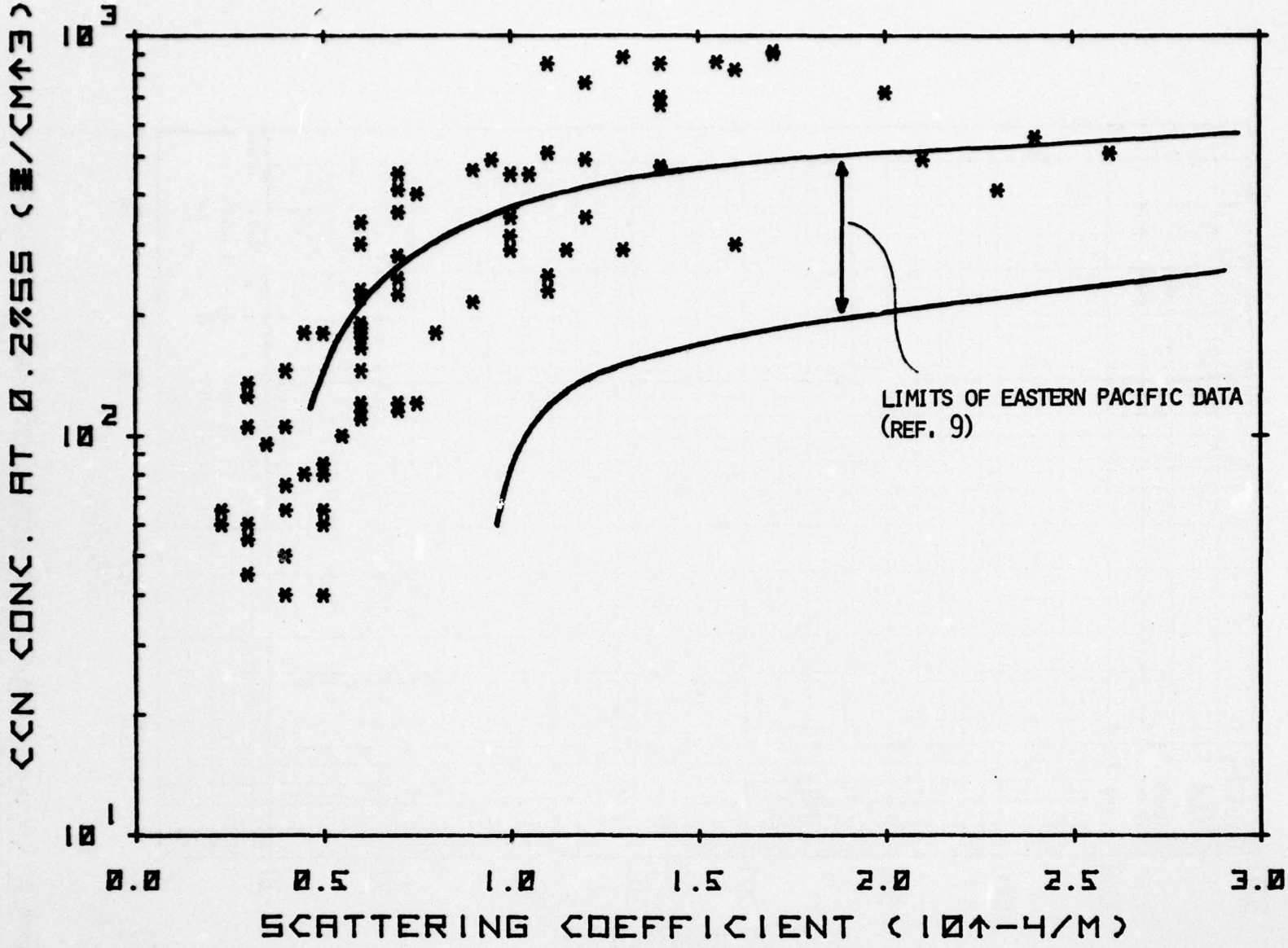

Figure 26a: CCN Active at 0.2% S vs. Measured Scattering Coefficient During the Transatlantic-Mediterranean Cruise of May-June 1977

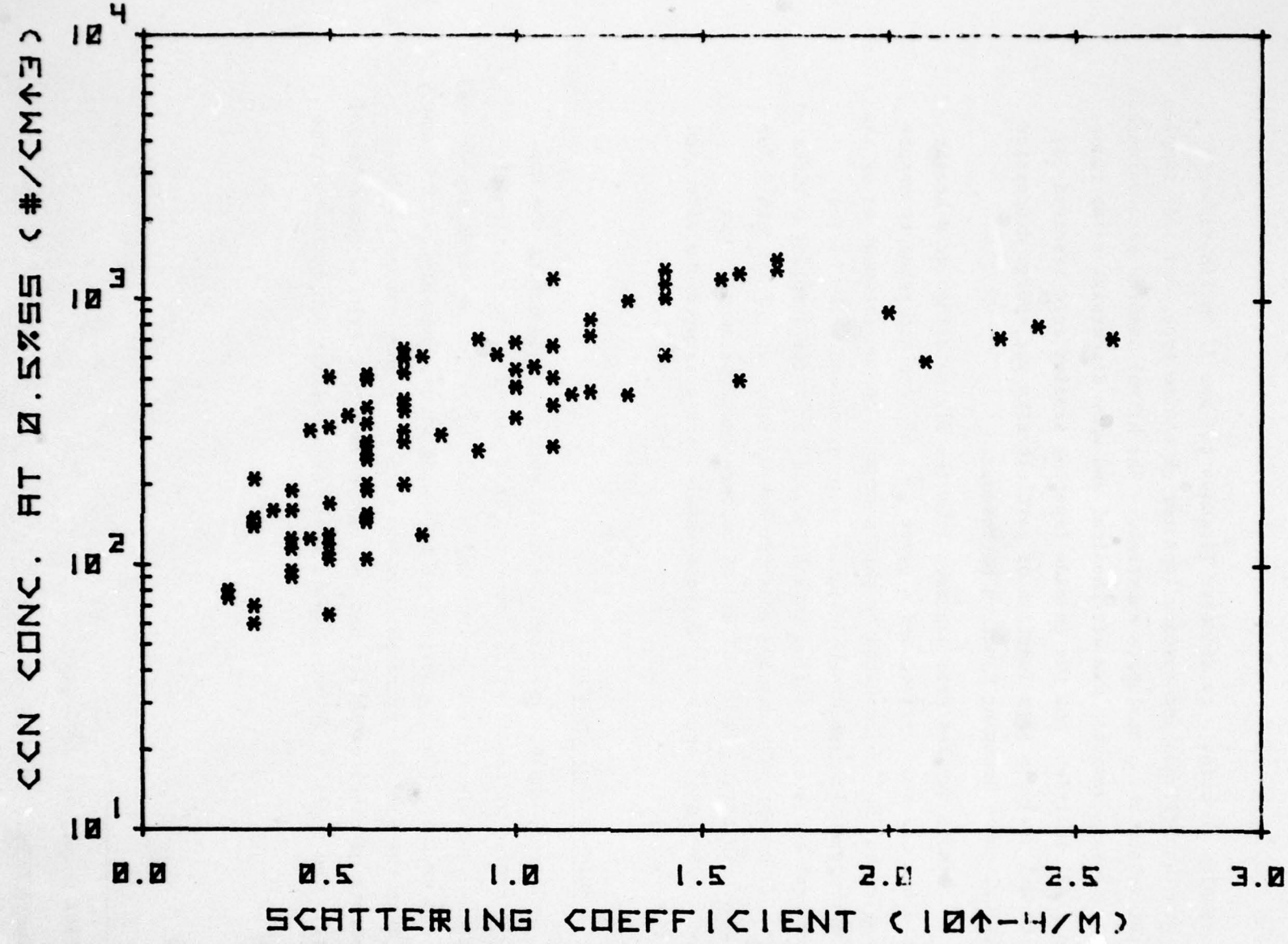

Figure 26b: CCN Active at 0.5% S vs. Measured Scattering Coefficient During the Transatlantic-Mediterranean Cruise of May-June 1977

hi-vol samples on both 10 cm diameter Tissuquartz* and 37 mm Fluoropore** teflon-membrane filters and cascade impactor (Battelle type, Ref. 18) samples on cellulose acetate proprionate substrate. The hi-vol samples were earmarked for bulk aerosol chemistry via wet-chemical and wave dispersive x-ray fluorescense (XRF) analyses, and the cascade impactor samples were reserved for compositional analysis as a function of particle size via energy dispersive x-ray in Calspan's Scanning Electron Microscope.

Aerosol samples were acquired from the Flying Bridge at a height of ∿18m above the sea surface, and a great deal of care was taken to ensure that samples not be contaminated by ship's exhaust and environment or by sea spray; any obviously contaminated samples were discarded. The hi-vol samplers were operated at a flow rate of ∿2.5 m^3 hr^{-1} for sampling periods of from 1 to 29 hours. The cascade impactor was operated at 12.5 l min^{-1} for 1 or 2 min. In total, 12 hi-vol and 35 cascade impactor samples were acquired. Results of analyses of these samples are presented and discussed within this section.

2.31 Bulk Aerosol Chemistry

Hi-vol samples of ambient aerosols were obtained during the May-June 1977 cruise at the locations depicted in Figure 27. Acquisition of samples was severely limited due to long periods of following winds experienced during the cruise. (During periods of following winds, the ship was frequently turned into the wind for brief periods--up to 1 hour--long enough to obtain measurements of other variables but not long enough to obtain adequate hi-vol samples.) Two types of filter samples were taken during each indicated time

---

*Pallflex Corp., No. 2500 QAO

**Millipore Corp., No. FHLP-037-00

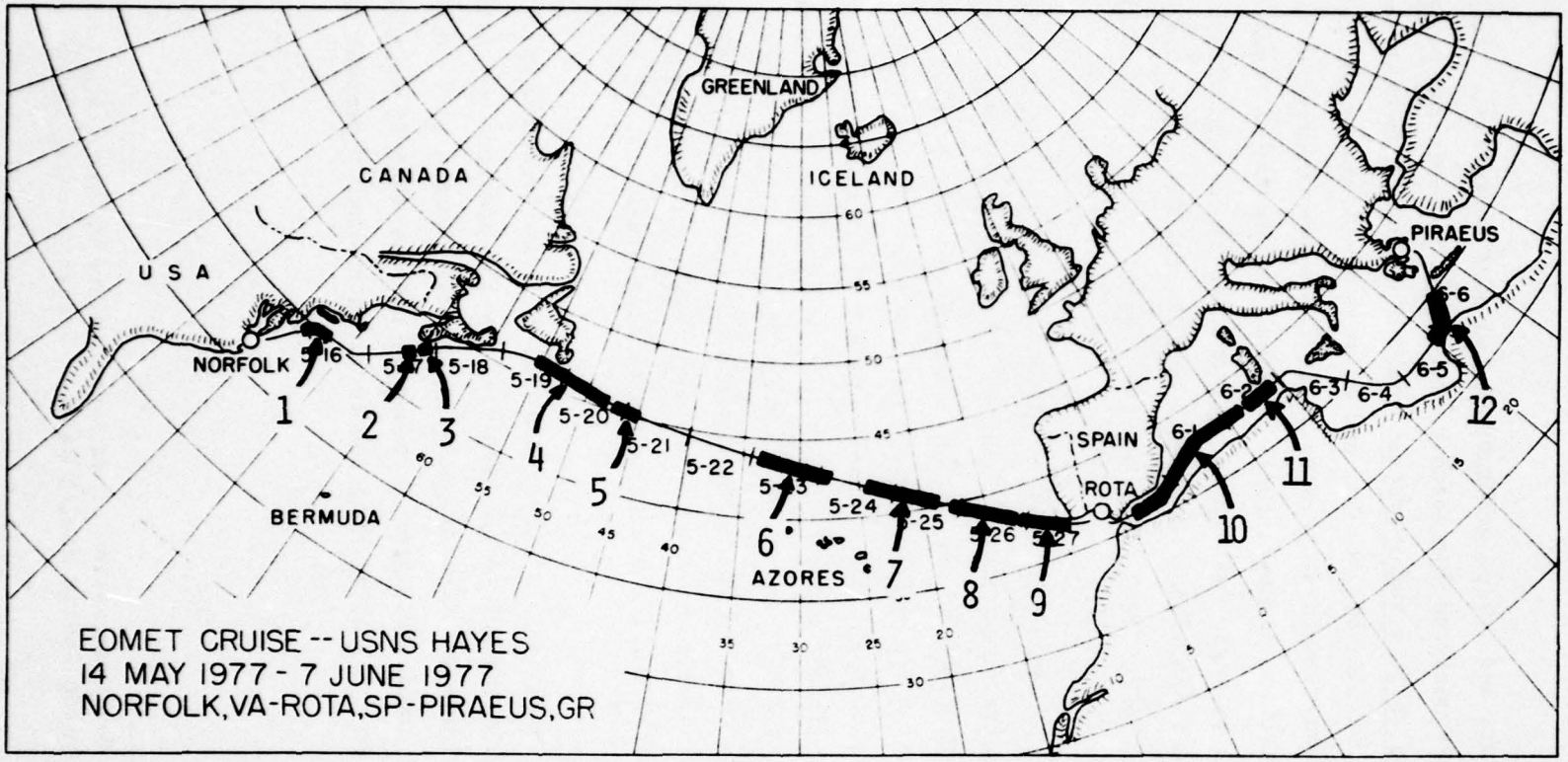

Figure 27: Sampling Locations for Hi-Vol Bulk Aerosol Sample Nos. 1-12

period: Tissuquartz and teflon membrane (0.5μm pore diameter). The Tissuquartz filters were analyzed for soluble sulfate (SO_4^{--}) via the barium chloride to barium sulfate turbidimetric* method. Total elemental analyses for Cl, S, K, Mg, Ca, Al, Si, Fe, Mn, and Na were performed on the teflon-filter samples by wavelength-dispersive X-ray fluorescence (XRF) at the Environmental Protection Agency's (EPA) National Environmental Research Center at Research Triangle Park (RTP), NC, and the assistance provided by J.L. Durham of EPA's Atmospheric Chemistry and Physics Division at RTP is gratefully acknowledged. Results of the analyses of the hi-vol filter samples are presented in Table 3.

The data presented in Table 3 in general exhibit trends consistent with previously discussed aerosol parameters. With the exceptions of Cl and Na, highest concentrations of the various chemical constituents were found off the North American coast (15-17 May), off the European coast (25-27 May) and in the Mediterranean (31 May-6 June). Lowest airborne elemental concentrations along with lowest aerosol concentrations (see Figures 5, 10 and 13) were observed in the mid-Atlantic (19-24 May). Lowest Cl and highest SO_4^{--} concentrations were observed along the coast of Europe and in the Mediterranean. Elemental S values observed in the mid-Atlantic approach background values of 0.2-0.4μg m^{-3} reported for the Northern Hemisphere by a number of authors (e.g., Ref. 19).

Gaseous sulfur dioxide (SO_2) conversion to particulate sulfate (SO_4^{--}) processes are thought to be catalyzed by the presence of certain heavy metals in aqueous solution droplets (e.g., Ref. 20 and 21). Others have postulated that SO_2 oxidation rates increase in the presence of NaCl in solution droplets (thereby releasing chlorine to the atmosphere) present in the

*"Standard Methods for Examination of Water and Waste Water", 14th Edition (1976), p.493, American Public Health Assoc., Washington, DC 20036.

Table 3: Airborne Concentrations of Selected Constituents of Hi-Vol Aerosol Samples Collected in the Atlantic and Mediterranean During May-June 1977

Absolute Concentration ($\mu g/m^3$)

Sample Number	Date (1977)	Exposure Time (GMT)	Cl	SO_4^{--}	S	K	Mg	Ca	Al	Si	Na
1	15-16 May	2300-0900	0.60	-	0.41	.06	.10	.43	.17	.31	0.11
2	17 May	1405-1500	4.03	1.36	1.86	.10	.58	.38	.22	.52	1.57
3	17 May	1935-2025	3.80	-	2.01	.08	.45	.50	.27	.50	1.41
4	19-20 May	1120-1640	0.75	0.44	0.25	.02	.06	.05	.02	.03	0.22
5	20-21 May	1705-0610	1.76	0.33	0.37	.03	.14	.08	.02	.03	0.50
6	23-24 May	0325-0450	1.62	0.19	0.30	.02	.11	.06	.02	.03	0.32
7	24-25 May	1530-1600	0.30	0.86	0.61	.01	.05	-	.04	.09	0.15
8	25-26 May	2040-1912	0.01	2.35	1.32	.03	.06	.07	.05	.13	0.15
9	26-27 May	1940-1500	0.20	3.04	2.52	.05	.14	.11	.05	.11	0.36
10	31M-2 Jun	0820-0740	0.27	2.35	1.43	.03	.11	.14	.06	.15	0.24
11	2 June	0830-2120	0.14	4.04	1.55	.03	.07	.12	.06	.13	0.12
12	5-6 June	1840-1355	0.11	5.43	2.00	.05	.09	.15	.08	.16	0.20

high humidity marine atmosphere (e.g., Ref. 9 and 22). The XRF analyses allowed the quantitative determination of the trace concentrations of the suspected heavy metal catalysts, Mn and Fe. Results of these analyses are summarized below for the four general areas of the cruise. As expected,

Average Concentrations ($\mu g/m^3$) of Heavy Metal Catalysts as Functions of Location During the Cruise

	North American Coast	Mid-Atlantic	European Coast	Mediterranean
Mn	0.01	0	0.02	0.02
Fe	0.50	0.02	0.06	0.10

the lowest concentrations were observed in the mid-Atlantic. While the data do not necessarily imply a cause and effect, inspection of Table 3 reveals that, in general, higher values of SO_4^{--} were associated with higher values of heavy metal catalysts and lower values of Cl.

Averages of the hi-vol data for the above-mentioned four general areas are compared in Table 4 with averages of data obtained by Calspan elsewhere in studies of the marine boundary layer. It is readily apparent that the mid-Atlantic values of all constituents were lower than those observed elsewhere (except for Cl off the coasts of Nova Scotia and Europe and in the Mediterranean). Coastal-area concentrations of most constituents exhibited comparable values for the different locations. It must be recognized, however, that these data were observed under specific meteorological circumstances and that they do not necessarily represent typical conditions.

The ratio of the concentration of elemental constituents to that of sodium in ambient aerosols in the marine boundary layer, when compared to that of sea water, provides a useful indicator of the continental or maritime characteristics of the aerosol. For example, the sodium ratios for Al and Si in bulk sea water are extremely small (i.e., $\sim 10^{-4}$) and any detectable airborne quantities must be attributed to continental sources. The sodium ratios for

Table 4: Average Airborne Concentrations of Selected Constituents of Hi-Vol Aerosol Samples for Portions of the 1977 Atlantic-Mediterranean Cruise Compared With 1975 Data Obtained off Nova Scotia and 1976 and 1978 Data Obtained off Southern California

Absolute Concentration ($\mu g/m^3$)

		Cl	SO_4^{--}	S	K	Mg	Ca	Al	Si	Na
Off N. American Coast	May 77	2.81	1.4	1.4	.08	.38	.44	.22	.44	1.0
Mid-Atlantic	May 77	1.38	0.3	0.3	.02	.10	.06	.02	.03	0.4
Off European Coast	May 77	0.17	2.1	1.5	.03	.08	.09	.05	.11	0.2
Mediterranean	Jun 77	0.17	3.9	1.7	.04	.09	.14	.07	.15	0.2
Off Nova Scotia	Aug 75*	< .02	4.0	-	.19	.05	.09	.22	-	0.9
Coast of S. California										
within 100 km	Oct 76**	1.2	8.4	-	.20	.31	.19	.013	-	2.1
within 100 km	May 78***	4.4	-	0.4	.36	.35	.62	.10	.54	2.1
beyond 100 km	Sept 76**	3.1	2.5	-	.14	.30	.08	.004	-	2.4

*Ref. 4

**Ref. 9

***Ref. 10

the data presented in Table 3 are tabulated in Table 5. The observed sodium ratios are compared against those of sea water to produce enrichment ratios (factors) which are tabulated in Table 6. The enrichment ratio (E) is simply the sodium ratio of an element (X) in a sample divided by the sodium

$$E(x) = \frac{(x/_{Na}) \text{ sample}}{(x/_{Na}) \text{ sea water}}$$

ratio of sea water for that species. If the sample is pure marine (sea salt) aerosol, the enrichment ratio is 1. (Due to limitations and inaccuracies imposed by sampling conditions, sample handling, trace ambient concentrations, filter background and analysis procedures, values ranging from ∿0.7 to 1.5 may be considered as pure marine.)

The analysis presented in Table 6 suggests that, averaged over the time periods for the respective hi-vol sample, pure marine aerosols (sea salt) were not observed at any time during the cruise. The closest approach to pure marine aerosol was encountered off Nova Scotia and into the mid-Atlantic 17-21 May. During that period, enrichment ratios of all elements were closest to 1 than at any other time during the cruise. However, even in the "cleanest" air observed during the cruise (i.e., in the mid-Atlantic; see Figures 5 and 10) when E values for Cl, K and Mg were in the range 1.1-2.9, large background values for SO_4^{--}, Ca, Al and Si were found. In the mid-Atlantic, enrichment factors for Al and Si were at their lowest values observed during the cruise; but, even there, Al and Si were found, respectively in relative concentrations 600-1000 and 300-600 times greater than would be expected from pure sea salt aerosols. Along the coast of Europe and in the Mediterranean, the E values were suggestive of anything but sea salt aerosol.

In contrast to these data, samples obtained beyond 100 km from shore off the coast of California have been found to be composed predominantly of sea salt aerosol mixed with some sulfate. In coastal areas off the West Coast, however, enrichment factors for all elements approach those observed off the coast of Europe and in the Mediterranean.

Table 5: Sodium Ratios for Selected Constituents of Hi-Vol Aerosol Samples Collected in the Atlantic and Mediterranean During May-June 1977

Sample Number	Date (1977)	Sodium Ratios (X/Na)						
		Cl	SO_4^{--}	K	Mg	Ca	Al	Si
1	15-16 May	5.3	3.5	.53	.83	3.80	1.40	2.70
2	17 May	2.6	1.2	.06	.33	0.24	0.14	0.33
3	17 May	2.7	1.4	.05	.32	0.35	0.19	0.35
4	19-20 May	3.3	1.2	.05	.30	0.17	0.05	0.12
5	20-21 May	3.5	0.8	.05	.28	0.14	0.03	0.06
6	23-24 May	5.2	0.9	.07	.35	0.18	0.05	0.08
7	24-25 May	2.0	4.1	.11	.40	-	0.32	0.62
8	25-26 May	0.1	8.7	.16	.36	0.48	0.39	0.85
9	26-27 May	0.5	7.0	.11	.37	0.28	0.12	0.31
10	31M-2 Jun	1.1	6.0	.15	.42	0.54	0.27	0.61
11	2 Jun	1.1	13.1	.22	.61	1.00	0.56	1.20
12	5-6 Jun	0.5	9.8	.27	.47	0.75	0.39	0.78
Sea Water		1.8	0.25	.036	.12	.038	4.7×10^{-5}	$\sim 2 \times 10^{-4}$

Table 6: Enrichment Ratios (Relative to the Sodium Ratios of Sea Water) for Selected Constituents of Hi-Vol Aerosol Samples Collected in the Atlantic and Mediterranean During May-June 1977

Enrichment Ratios $\frac{X/Na\ (Sample)}{X/Na\ (Sea\ Water)}$

Sample Number	(1977)	Cl	SO_4^{--}	K	Mg	Ca	Al ($\times 10^3$)	Si ($\times 10^3$)
1	15-16 May	2.9	13.8	14.7	6.9	98.7	30.0	13.3
2	17 May	1.4	4.7	1.7	2.8	6.3	3.0	1.7
3	17 May	1.5	5.7	1.4	2.7	9.2	4.0	1.8
4	19-20 May	1.8	4.7	1.4	2.5	4.5	1.0	0.6
5	20-21 May	2.0	3.0	1.4	2.3	3.7	0.6	0.3
6	23-24 May	2.9	3.7	1.9	2.9	4.7	1.0	0.4
7	24-25 May	1.1	16.3	3.1	3.3	-	7.0	3.1
8	25-26 May	0.04	34.7	4.4	3.0	12.6	8.0	4.3
9	26-27 May	0.3	28.0	3.1	3.1	7.4	3.0	1.6
10	31M-2 Jun	0.6	23.8	4.2	3.5	14.2	6.0	3.1
11	2 Jun	0.6	52.1	6.1	5.1	26.3	12.0	6.0
12	5-6 Jun	0.3	38.8	7.5	3.9	19.7	8.0	3.9
Coast of S. California								
within 100 km	Oct 76	0.3	16.0	2.6	1.3	2.4	0.1	-
within 100 km	May 78	1.2	-	4.7	1.4	7.9	1.0	1.3
beyond 100 km	Sept 76	0.7	4.2	1.6	1.1	0.8	0.04	-

2.32 Aerosol Chemistry as a Function of Particle Size

Previous studies of the marine atmosphere conducted by Calspan focused primarily on the microphysics of the marine boundary-layer. On the CEWCOM-76 cruise of September-October 1976 (Ref. 9), the chemistry of individual particulates was first addressed. During that cruise, aerosols were impacted on a variety of substrates (glass, aluminum foil and germanium) and the samples returned to Calspan for analysis via scanning electron microscopy (SEM) and elemental energy dispersive x-ray analysis (EDXA). The combination of these two techniques allowed (1) visualization of the impacted particle where size measurements could be obtained and (2) elemental composition of particles with specific identification of elements from sodium (atomic number 11) and greater in atomic number.

During the Transatlantic-Mediterranean cruise, samples were acquired at 35 locations (numbered consecutively as shown in Figure 28) using a six-stage Battelle cascade impactor. Air was drawn through the impactor at 12.5 l min^{-1} (limiting-orifice regulated), and the sample impacted on cellulose acetate proprionate substrate. The substrate is a smooth, carbonaeous material devoid of interfering elemental composition. (A phosphorus peak from a plasticizer in the material is occasionally seen in the x-ray energy spectrum when count times are long.)

Calspan's scanning electron microscope is an ETEC AUTO SCAN with a working distance of 17 mm and a 20 KV electron beam. The energy dispersive x-ray analysis was obtained on a KEVEX unit with a counting time of 100 seconds. Particle length and width dimensions were measured from the SEM viewing CRT screen at 6000 magnification. The SEM internal micron marker with an error of less than 2% was used as a standard length.

Because of the tedious (and expensive) nature of the operation, SEM and EDXA analyses were performed on only 21 of the 35 available samples. Guided by the previously discussed aerosol and visibility data (Sections 2.1 and 2.2), analyses were performed on the 21 selected samples in the following grouping:

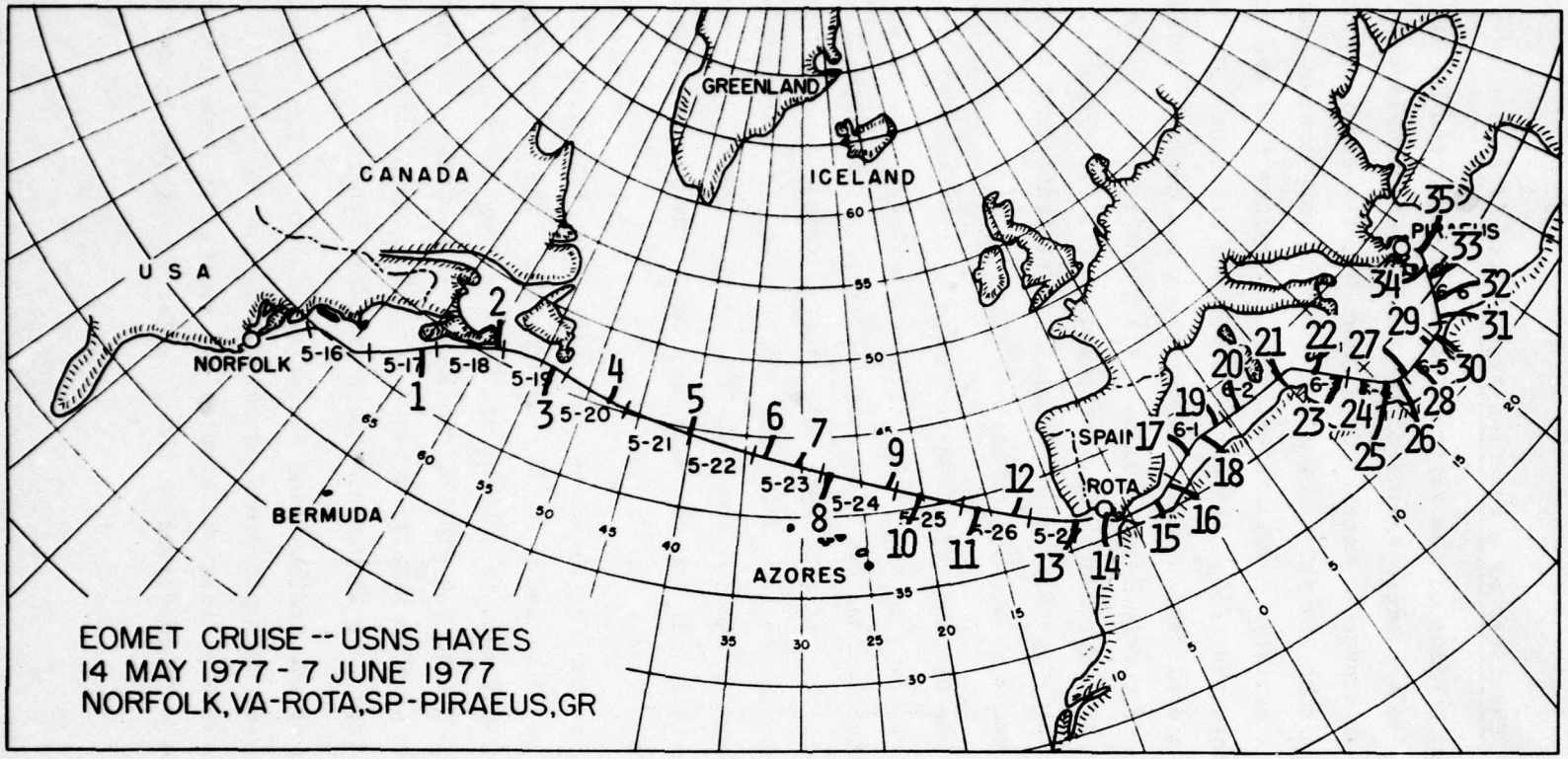

Figure 28: Sampling Locations for Cascade Impactor Sample Nos. 1-35

Cascade Impactor Data Grouping

Group Area	Sample Numbers
North American Coast	1, 2, 3
Mid-Atlantic	4, 5, 6, 7, 8, 9
European Coast	10, 11, 12, 13
Western Mediterranean	16, 20, 23, 26
Central Mediterranean	28, 30, 32, 34

Only slides from stages 4 and 5 of the impactor were examined by SEM and EDXA. The selection of these two stages allowed for analysis of individual particles primarily in the size range 0.5-5μm diameter. As an example, SEM photographs for stages 4 and 5 from the mid-Atlantic sample #6 (see above) are shown in Figure 29. For each sampling site, 25 particles on each substrate from both stages 4 and 5 were examined. The particles were selected objectively from randomly chosen 50μm wide swaths until a total of 50 particles had been examined for each sampling location. Of the particles counted, only a few readily identifiable cubic NaCl crystals were seen. The particles, as shown in Figure 29, were either rectangular, globular, or irregular in shape. In most cases, the particles were not perfect crystals. The examined particles were divided into two size groups, based on area calculated from the length and width dimensions: $< 1.0\mu m^2$ ($< \sim 1.0\mu m$ diameter) and $\geq 1.0\mu m^2$ ($\geq 1.0\mu m$ diameter). The smallest particles examined were $\sim 0.2\mu m$ diameter and the largest, 10.0μm diameter.

The percentage of particles examined in each size grouping for each of the 5 composite sampling groups is shown below. The largest fraction of the examined particles was in the $\geq 1\mu m$ size range. Compared to the Atlantic samples, a slightly higher proportion of the particles examined for the Mediterranean were in the size range $< 1.0\mu m$ diameter.

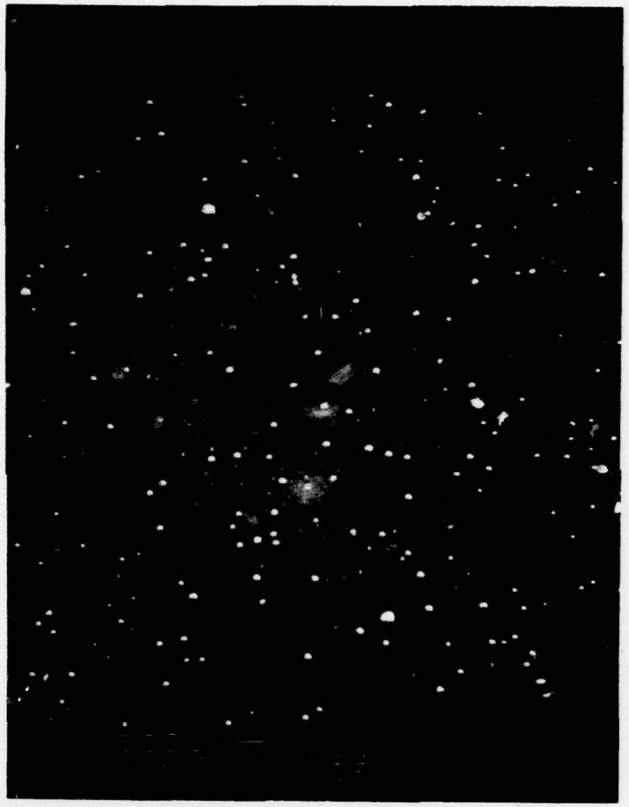

CASCADE IMPACTOR STAGE 6

CASCADE IMPACTOR STAGE 5

Figure 29: Examples of Scanning Electron Microscope Microphotographs of the Cascade Impactor Sample #6 Obtained in the Mid-Atlantic on 23 May 1977

Number of Particles Examined and Percent in Each Size Group at Each Sampling Location

Location	Number of Particles Examined	Size Groups <1.0μm	Size Groups ≥1.0μm
North American Coast	150	22%	78%
Mid-Atlantic	300	37%	62%
European Coast	200	34%	66%
Western Mediterranean	200	42%	58%
Central Mediterranean	200	40%	60%

After length and width dimensions were measured, the elemental composition of each individual particle (a total of 1050 particles) was determined using energy-dispersive x-ray analysis. Examples of the x-ray energy spectrum for an individual particle at each of the indicated sampling sites are presented in Figure 30. In Figure 30, 'A' shows the x-ray energy spectrum for a particle at Site 1 (See Figure 28); 'B' from Site 6; 'C' from Site 5; and 'D' from Site 23. 'A' shows the spectrum for a frequently observed group of particles which contained no elements of atomic number equal to or >Na. (The phosphorus peak, P, came from a placticizer in the cellulose acetate substrate when long count-times were required.) 'B' shows an example of a 'pure' NaCl particle, thought to be sea salt. 'C' shows the spectrum of an aerosol particle of mixed inorganic salts, heavy metals and silicate composition. 'D' shows the spectrum of a particle of mixed composition containing only inorganic salts. From this kind of analysis, it was found that individual particles could be grouped into five categories according to total elemental composition:

(1) those with atomic numbers lower than Na;
(2) NaCl only--sea salt;
(3) NaCl with minor amounts of other inorganic salts;
(4) inorganic salts without NaCl;
(5) and Si containing compounds.

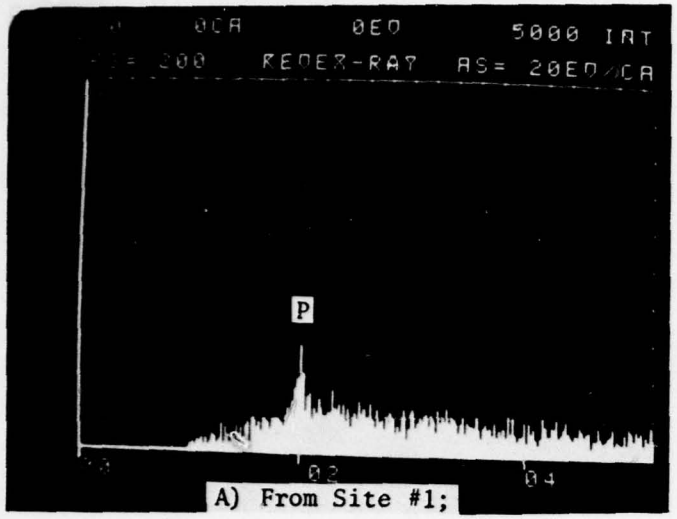

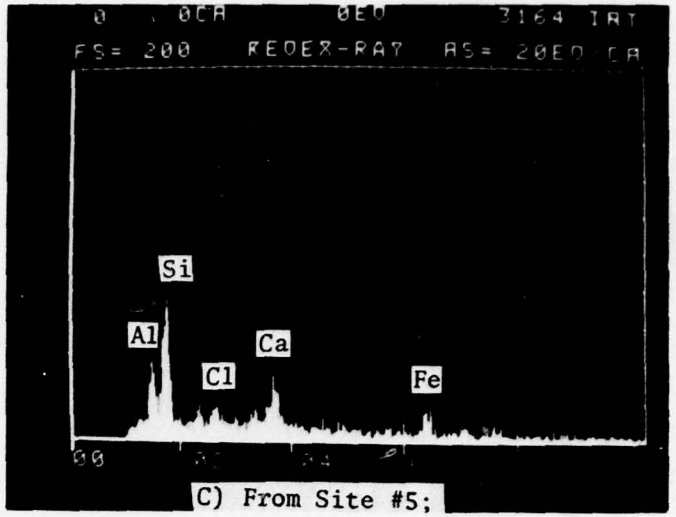

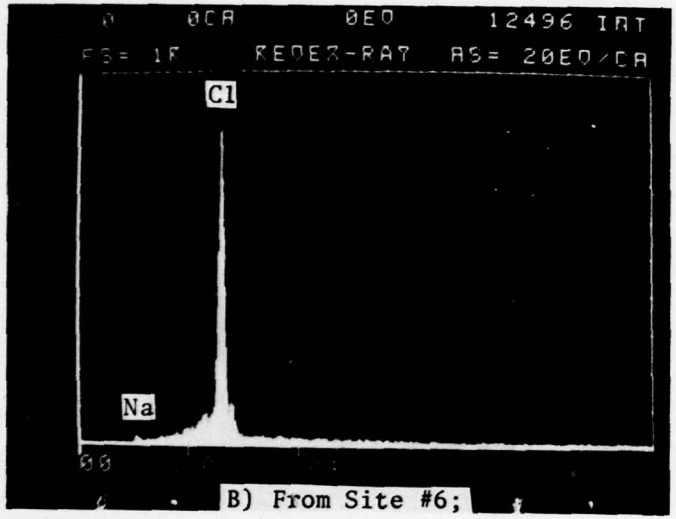

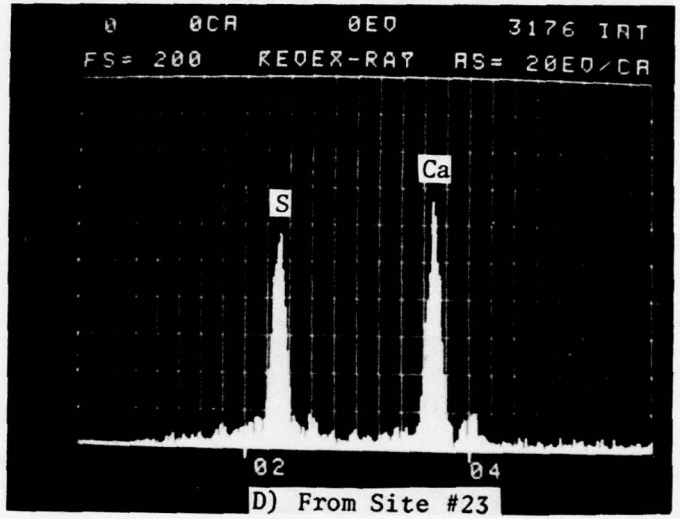

Figure 30: Examples of Elemental X-Ray Energy Spectra of an Individual Particle Sampled at Each of the Four Indicated Locations During the Transatlantic-Mediterranean Cruise of May-June 1977

The percentages of particles found in each of these five composition groups for each of the individual sampling sites are plotted in Figure 31, schematically as a function of location during the cruise. The average percentage values for each of the five composite sample groups are plotted to the right of the figure. Inspection of the data reveals a dramatic shift in particle composition from the Atlantic to the Mediterranean. Off the coast of North America and in the mid-Atlantic, the percentage of particles which were comprised solely of sea salt (NaCl) averaged 80% and 65%, respectively. Note that these data correspond well with hi-vol data in Tables 3-6 which show that aerosols sampled off North America and in the mid-Atlantic more closely resembled sea salt than those sampled elsewhere.

In contrast, along the European coast and in the Mediterranean, the percent of NaCl particles dropped to ~25%, while the percentage of inorganic, non-NaCl salts increased ultimately to an average 40-50%. Particles composed of Si and those of elemental composition <Na in atomic number both peaked along the European coast at values of 14 and 33%, respectively. These data are, qualitatively, also in good agreement with analytical analyses of hi-vol data presented in Section 2.31.

A summary of the distribution of chemical composition as a function of particle size is presented in Table 7 and illustrated graphically in Figure 32. In both Table 7 and Figure 32, the percentages of particles of a given size group (i.e. $< 1\mu m$ or $\geq 1\mu m$) are presented as functions of composition for each sample group of the cruise. From these data, it is obvious that the Si and mixed NaCl and non-NaCl salts were aerosols of $>1.0\mu m$ in both the Atlantic and the Mediterranean. The proportions of the aerosol population, for the two size ranges, comprised of 'pure' sea salt aerosols and non-NaCl salts were similar, respectively, and the dramatic shift in particle composition from the Atlantic to the Mediterranean was observed in both size

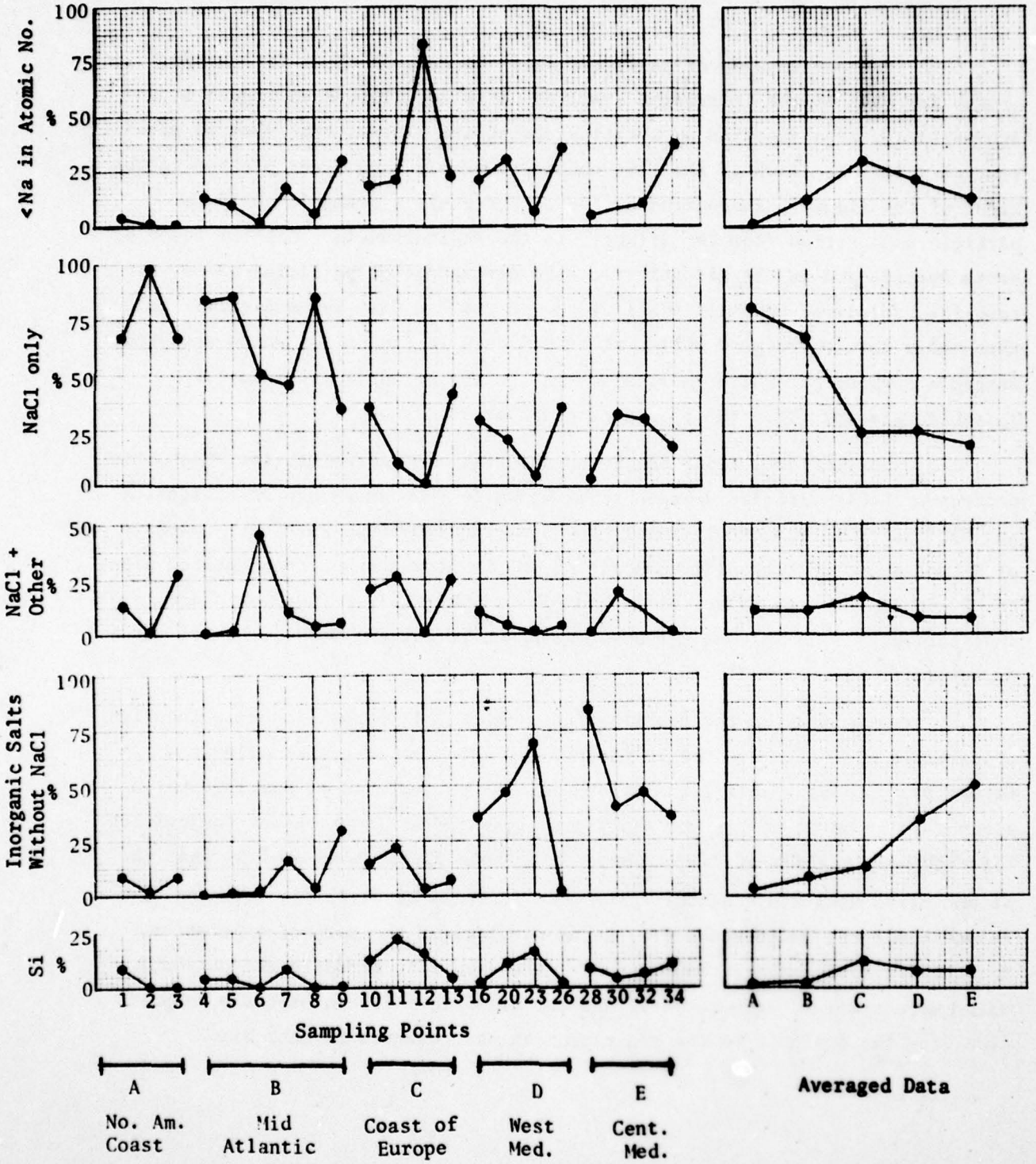

Figure 31: The Percentage of Particles in Each Composition Group as Functions of Sampling Location During the Transatlantic-Mediterranean Cruise of May-June 1977

Table 7: Percent of Particles In Each Size Category as Functions of Composition and Sample Location

	North American Coast		Mid-Atlantic		Europe. Coast		West Mediterr.		Central Mediterr.	
	$<1.0\mu$	$\geq 1.0\mu$	$<1.0\mu$	$\geq 1.0\mu$	$<1.0\mu$	$\geq 1.0\mu$	$<1.0\mu$	$\geq 1.0\mu$	$<1.0\mu$	$\geq 1.0\mu$
<Na	0%	1%	19%	10%	71%	14%	30%	17%	23%	7%
NaCl	91%	79%	65%	66%	18%	24%	23%	31%	23%	20%
NaCl & other	5%	12%	3%	16%	0%	27%	0%	9%	5%	10%
Other salts	5%	5%	14%	5%	9%	15%	42%	33%	43%	55%
Si	0%	3%	0%	3%	3%	20%	5%	10%	7%	8%

categories. Aerosols comprised solely of elements of <Na in atomic number were primarily in the size range < 1μm. These aerosols of elemental composition <Na were found in their highest relative proportions along the European coast and in the Western Mediterranean, accounting for >70% of the particles in the size range < 1μm observed along the European coast.

2.33 Discussion

The differences in the chemical species comprising the aerosol populations, respectively, of the Atlantic, Coastal Europe and the Mediterranean suggest significant implications in terms of response to changes in relative humidity and to effects on electro-optical propagation, depending on the compositional combination of the observed elements. The individual particles of the aerosol population sampled during the cruise were grouped into five broad compositional categories and these are discussed in this Section.

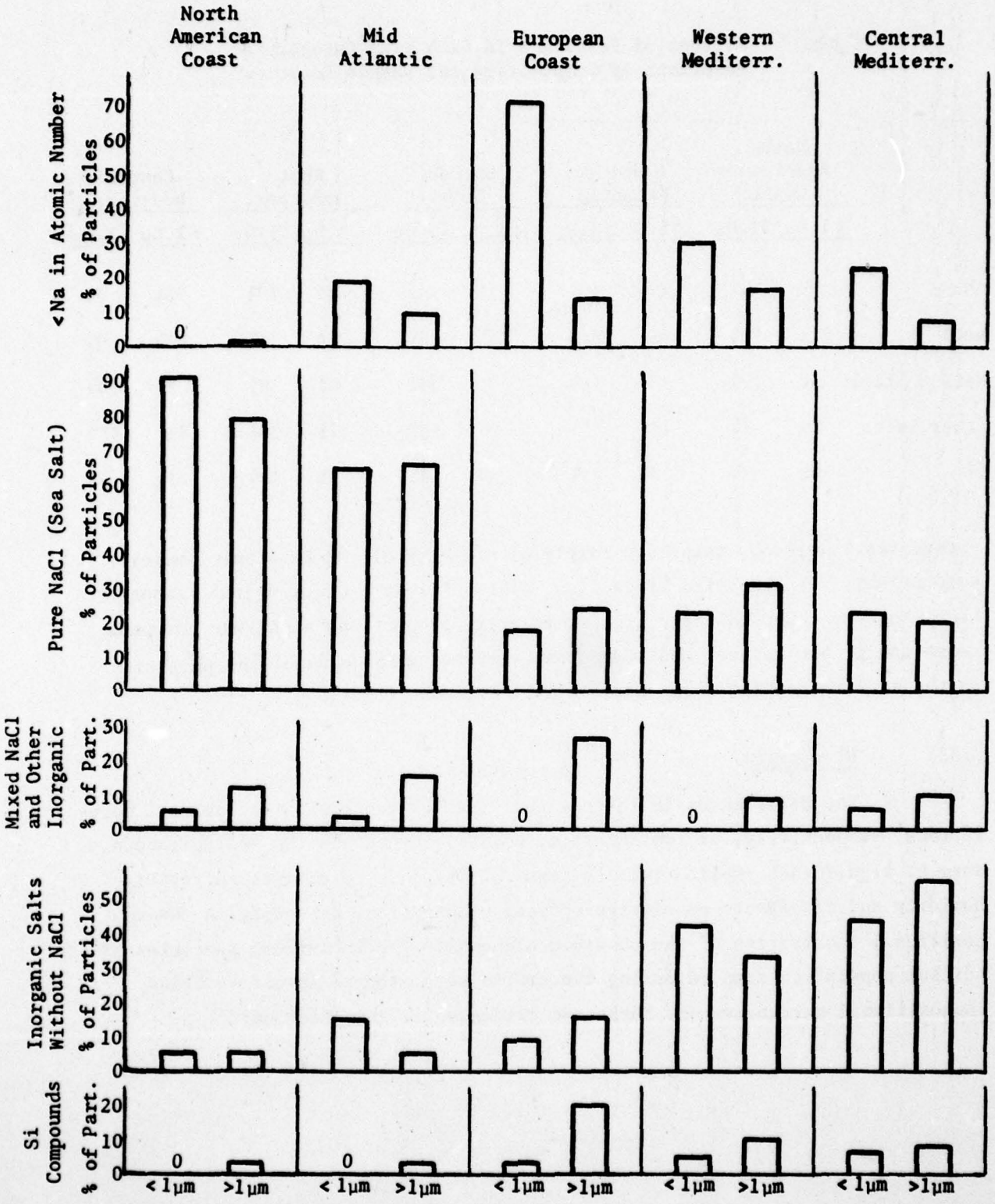

Figure 32: Percentage of Particles in Each of Two Size Ranges as Functions of Composition and Sampling Location During the Transatlantic-Mediterranean Cruise of May-June 1977

Chemical Species Composed of Elements of Atomic Number Less Than Na

There are ten elements of atomic number less than sodium which could make-up the particulates containing only those elements. However, only four of those have a high probability of being found in the atmosphere: H, N, C, O. There is a good probability that these particles were organic in nature, their sources being either combustion products, photochemical processes, or natural continental material (i.e., humic acid).

If the particles are inorganic, then a cation and an anion combination must be formed from those four elements. The only logical cation formed from H, N, C and O in the atmosphere as a particulate is the ammonium ion (NH_4^+). It is unlikely that the hydrogen ion would combine to form a solid inorganic particulate. There are several combinations of C, N, O and H which may form inorganic anions, the most likely of which are NO_3^- and CO_3^{--}. It is unlikely, however, that ammonium nitrate was the primary aerosol, since it sublimes under the evacuated conditions of the SEM and wouldn't have been detected as a particle. The possible cation and anion combinations for this group of aerosols are as follows:

Potential Cation and Anion Possibilities for Particulates With Elemental Composition Less Than Na in Atomic Number

Cation	Anion
Organic	Organic
NH_4^+	NO_2^-
	NO_3^-
	HCO_3^-
	CO_3^{--}

These particles comprised up to 33% of the ambient aerosol burden (and >70% of those 0.2-1.0 μm diameter) in the region along the European Coast. Elsewhere, except along North America, these particles accounted for ∿20% of the total (in the measurable size range >0.2μm diameter). The lack of available inorganic ions, leaves the strong possibility that these aerosols were organic material.

Particles Composed Solely of NaCl

A second categorization of the aerosols observed during the cruise were those composed solely of NaCl. In general, these particles were cubic in shape, but a few round, globular particles were also found. These particles are thought to be sea salt aerosols whose other major constituents are at least an order of magnitude lower in concentration and hence did not show up in the x-ray analyses (e.g., Fig. 30b).

Mixed Aerosols Composed of NaCl and other Inorganic Salts

The third chemical classification contained particles that were primarily NaCl with a small amount of co-precipitated inorganic salt. The relative amount of inorganic salt that was observed co-precipitated with NaCl was always less than 10 percent of the amount of NaCl present, based on the Cl x-ray peak.

Table 8 illustrates the elemental composition for each of the particles examined which were found to have co-precipitate inorganic salt with sodium chloride. In the table, the number of particles observed of specific elemental composition (in addition to NaCl) at each sampling location is shown. For these elemental combinations, there are four probable ionic species: SO_4^{--}, Ca^{++}, K^{+} and Mg^{++}. As shown by the data, S was the most common co-precipitate, and a combination of S and Ca was the most common mixture associated with NaCl. The data show that the elemental admixtures to NaCl were uniformly distributed over the Atlantic and Mediterranean.

Aerosols Comprised on Non-NaCl Inorganic Salts

The fourth chemical classification of aerosols observed during the cruise was that of inorganic salts which did not contain NaCl. These particles were found to comprise ∿10% of the aerosol population in the Atlantic but 40-50% of those sampled in the Mediterranean (See Figures 31 and 32). Table 9

Table 8: Number of Particles of Mixed Composition Containing NaCl Plus Other Inorganic Salts as Functions of Elemental Composition and Sampling Location

Element Combinations In Addition to NaCl	Sampling Sites																		
	North American Coast			Mid-Atlantic						European Coast				Western Mediterr.				Central Mediterr.			
	1	2	3	4	5	6	7	8	9	10	11	12	13	16	20	23	26	28	30	32	34
S	1		1			8	1	1			1	2	1						5	1	1
S, Ca, K	1					2	1	1					1		1				2		
Ca	2					1															
Si, S	1																				
Si	1						1														
S, Ca			4		1	8			1		10		6		1		1		4	4	1
S, Fe			1																		
S, Ca, K, Mg						2															
Ca, K						1															
S, Fe, Ca															1						

illustrates the number of particles of each elemental composition found at each specific sampling site. These data exhibit two major groupings of salts. The first group was found in the mid-Atlantic, along the European coast, and through most of the Mediterranean. This group consisted primarily of particles which contained only Ca and/or S (e.g., Figure 30d). The candidate chemical species containing only Ca and elements of $<$Na in atomic number is probably limited to CaO, $CaCO_3$ (calcite) or $Ca(NO_3)_2$. Particles which contained only elemental S were very likely ammonium sulfate $(NH_4)_2SO_4$ aerosols since the NH_4^+ ion is the only available cation from the group of elements of $<$Na in atomic number.

Table 9: Number of Particles of Non-NaCl Inorganic Salts of Indicated Mixed Elemental Composition as Function of Sampling Location

Element Combinations	Sampling Sites																			
	North American Coast			Mid-Atlantic						European Coast				Western Mediterr.				Central Mediterr.			
	1	2	3	4	5	6	7	8	9	10	11	12	13	16	20	23	26	28	30	32	34
S,Ca,Na	1																				
S,Ca,K,Cl	1																				
Ca,Cl			1													1				2	1
Al			1							1											
Ca						1	1	1		4	1		4	1	1	8	1				
S							3	3	2	1	7	1	11		9	10	1	4	1		
S,Na							1		1						7						
S,Al,K,Cl							1														
Fe,Cl							2							1						1	
Al,Cl							1									1					
S,K									1		1		1					1		1	
S,Fe,K										1											
S,Cl,K										1											
K,Cl										1											
S,Ca,Cl											1							1	4		
S,Ca													1		1	5		1		1	3
S,Cl														3		4		1		1	2
S,Fe,Cl														1							
Cl														4		7	1	27	8	16	12
S,Fe															3						
S,Fe,Ca,Na															1						
S,Ca,K																		1			
S,Fe,Cl,Cr																			1		

The second group of particles, found primarily in the Mediterranean samples were inorganic salts containing combinations of S and Ca, S and Cl, and Cl alone. Possible species for these groups of elements include mixed aerosols of $(NH_4)_2SO_4$, $Ca(NO_3)_2$, $CaCO_3$ and NH_4Cl. Of course, a strong possibility also exists for a combination of Ca and S (observed primarily off the North American coast and in the Mediterranean) in the form of $CaSO_4$, the common sedimentary mineral, gypsum.

A major fraction of the particulate population found only in the Central Mediterranean was comprised only of Cl (and elements < Na in atomic number). These particles were probably NH_4Cl. The proportion of this type of particle increased from the Western Mediterranean into the Central Mediterranean. In the Western Mediterranean, there were 12 particles seen and in Eastern Mediterranean, 63 particles were observed.

Silicate-Containing Aerosols

The final chemical composition group consisted of particles which contained the element Si. In all, 40 different elemental combinations were observed containing the Si element, and these are listed according to location of observation in Table 10. Of these 40 different elemental combinations, 31 were seen only at one site each, 6 recurred at two sites, 2 were sampled at three sites, and one combination was seen at 8 sites. The most frequently observed Si containing compound (seen at 8 sites from the mid-Atlantic to the Mediterranean) was pure Si and is presumed to have been SiO_2. However, as shown by the presentation in Figure 10, the remainder of the Si-containing compounds generally were different in chemical composition at different sampling sites. The most complex of these apparently mixed aerosols were observed in the Central Mediterranean.

2.4 Discussion and Summary

In summary, analyses of aerosol parameters (i.e., visibility, size spectra, supersaturation activity, and chemical composition), qualified by wind and humidity circumstances, suggest that at least four distinct airmass conditions (in terms of aerosols) were encountered during the Transatlantic-Mediterranean cruise of May-June 1977. The data from which these conclusions were drawn are summarized in Table 11. Briefly recapping,

1. Clean marine air, with background levels of continental-originated material, was observed in the mid-Atlantic (51°W-22°W longitude) from ∿0800 GMT on 20 May until ∿0100 on 25 May. The

Table 10: Number of Particles Containing Si as Functions of Additional Elemental Composition and Sampling Location

Element Combination In Addition to Si	Sampling Sites																			
	North American Coast			Mid-Atlantic						European Coast				Western Mediterr.				Central Mediterr.			
	1	2	3	4	5	6	7	8	9	10	11	12	13	16	20	23	26	28	30	32	34
Ca,Fe,Al																					1
Na,Cl,S	1	-	-																		
Al,K	1	-	-													1					
S,K				1																	
Si				1	1		1				2	1			2	4		2			
Ca,Cl,S					1																
Ca,Al					1																
Ca,S,Cl,Fe						1	1														
Ca,S,Cl,Na,K							1														
Ca,S,K,Cl							1														
S,Cl,Fe							2														
S,K,Al							1						1			1					
S,K,Al,Fe										3											
S,Cl,K,Fe										2											
S,Ca,K,Al										1											
S,Cl,Fe,Mn											1										
S,Ca,Al,Mg											1										
S,Ca,Na,Cl											1										
S,K,Fe											2										
S											1										
S,Ca,Fe,Al											1								1	1	1
S,Ca,K,Fe,Al											2										
S,Ca,Cl,Ni												1									
S,Al												1							1		
Al												1						1			
Na,Ca,K,Al													1								
K,Cl,Fe														1							
S,Ca,Fe															1			1			
S,Ca,Na															1						
S,Ca															1						
S,Cl																2					
Fe,Cl																1					
Fe,Al																	1				1
K,Cl																		3			
S,Ca,K,Fe,Cl,Al																			1		
Cl,Ca,Fe																				1	1
Ca,K,Fe,Cl,Al																				1	1
Mn																					1
Ca,S,Cl,Fe,Al																					1
Ca,K,Al																					1

Table 11. Summary of Aerosol-Related Characteristics of the Marine Boundary Layer Observed During the Transatlantic/Mediterranean Cruise of May-June 1977

		50-200 km Off New England/ Nova Scotia	Mid-Atlantic 50°W-22°W	1200-200 km Off Coast of Portugal	200-30 km Off Coast of Portugal	Western Mediterranean ~150 km Offshore	Central Mediterranean 150-250 km Offshore
Visibility (km)		20-80	>80	80	15-50	40-80	30-80
b_{scat} ($x10^{-4}m^{-1}$)		0.4-2.0	0.2-0.8	0.5-1.0	1.0-4.0	0.5-2.0	0.5-2.0
Aerosol Concentration ($\#/cm^3$)	Total	4000-15000	200-500	900-1500	1000-5000	800-2000	1000-3500
	$>.01\mu$	5000-30000	30-500	700-1200	900-3000	500-2000	800-3500
	$>.1\mu$	1000-5000	30-150	400-800	700-2000	250-800	250-1500
	$>.3\mu$	2-30	3-15	7.0-20	30-60	7.0-30.	9.0-30.
	>1.2	0.3-6.0	0.8-4.0	0.9-3.0	3.0-6.0	1.5-3.0	0.7-3.0
	>3.0	0.03-0.2	0.04-0.3	0.03-0.1	0.03-0.2	.08-0.2	.04-0.2
	>10.0	-	-	.0003-.0006	0.02-0.05	.007-.05	.01-0.1
	>20.	-	-	<.0005	.001	<.0005-.003	.001-.008
CCN ($\#/cm^3$)	0.2%S	-	60-100	300-500	-	150-300	400-900
	1.0%S	-	90-200	600-1000	-	400-900	600-2000
Aerosol Composition (% of Part. >0.2μm dia. of indicated composition)	<Na	2	12	33	-	21	13
	NaCl	81%	68%	25	-	25	19
	NaCl & Other	11	10	17		8	7
	Other Salts	3	8	13	-	36	51
	Si & Other	2	2	12	-	8	9

airmass(es), under northwesterly wind conditions, were characterized by visibilities >80 km and total particle concentrations of 200-500 cm^{-3}; concentrations of particles >0.1μm were 30-150 cm^{-3} and CCN active at 0.2%S were found in concentrations of 60-100 cm^{-3}. Of the particles >0.2μm diameter, ∿70% were pure NaCl, 10% were NaCl plus other inorganic salts, 8% were other inorganic salts without NaCl and 12% were, perhaps, organics.

2. Prior to that period, the ship encountered modified-marine air, with much higher levels of continental material, along the North American coast. During the period along the coast from Cape Cod to Nova Scotia, winds were west-southwesterly, relative humidities ranged from 75-98%, and visibilities ranged from 20-80 km. Total aerosol concentration was 5000-20000 cm^{-3}, while concentrations of aerosols >0.1μm diameter fell between 1000 and 5000 cm^{-3}. Of the particles >0.2μm diameter, ∿80% were pure NaCl, 11% were mixed composition of NaCl and other inorganic salts. Evidently, a significant fraction of the particles < 0.2μm diameter were sulfates and silicates (i.e., material of continental origin). From ∿1100, 18 May to 0800, 20 May, with increasing distance out into the Atlantic and a shift in wind trajectories to southeasterly (away from continental sources), aerosol concentrations and composition gradually evolved to those of clean marine conditions.

3. Beginning early on 25 May at a distance of ∿1200 km off the Iberian Peninsula, with southerly winds, aerosol concentration began to increase and visibility began to degrade, in the face of decreasing average relative humidity. Total aerosol concentration peaked at ∿5000 cm^{-3}, and the concentration of aerosols >0.1μm diameter increased to ∿1000 cm^{-3}, after a frontal passage which brought northwesterly winds late on 26 May. Composition of the aerosol population (particles >0.2μm)

AD-A062 888 CALSPAN ADVANCED TECHNOLOGY CENTER BUFFALO NY F/G 4/2
AEROSOL CHARACTERISTICS OF THE MARINE BOUNDARY LAYER OF THE NOR--ETC(U)
OCT 78 E J MACK, R J ANDERSON, C K AKERS N00019-78-C-0179
UNCLASSIFIED CALSPAN-6232-M-1 NL

2 OF 3
ADA
062888

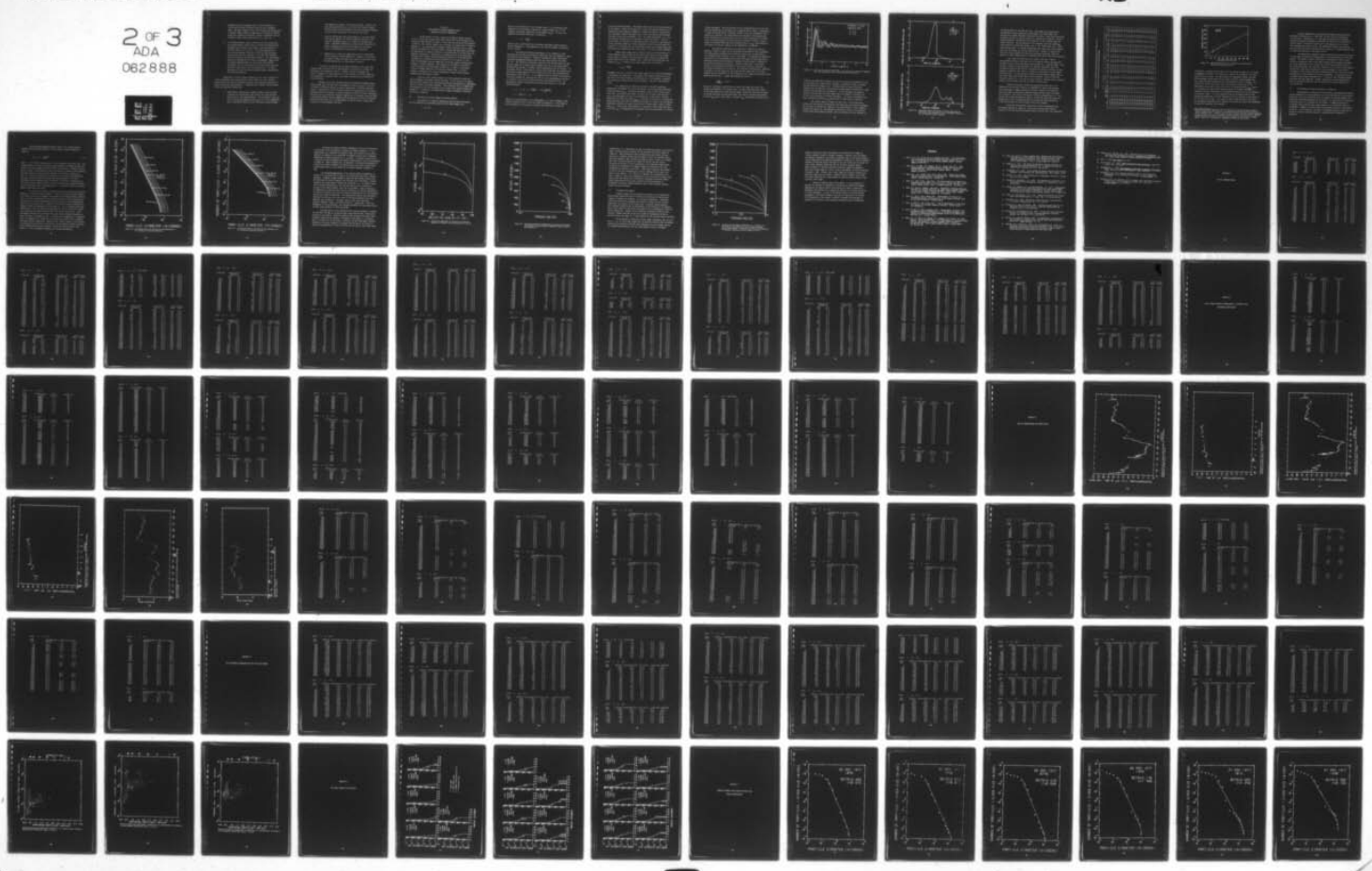

changed from one of primarily NaCl in the mid-Atlantic to that of only 25% NaCl, 17% NaCl mixed with other inorganic salts, 13% other inorganic salts, 12% silicates and 33% particles of perhaps organic material--suggesting an influence of Coastal Europe and a modified-continental airmass in agreement with conclusions of other cruise participants (e.g., Ref. 12).

4. In the Mediterranean, aerosol concentrations and visibilities were midway between values observed off the North American and European coasts, however, the aerosol consisted primarily of the heavy metals, Ca, S and Cl. The aerosol population at sizes >0.2μm diameter consisted of ∿22% pure NaCl particles, 8% mixed NaCl and other inorganic salts, 44% other inorganic salts, 9% silicates and 17% perhaps organics. The observations, along with consideration for winds and geography, suggest that the observed Mediterranean air masses were also modified-continental, but of a substantially different nature than that observed in the Atlantic off the European Coast. The data definitely show that the observed Mediterranean airmasses were not of marine character.

Comparison of various aerosol parameters of the clean 'natural' air of the mid-Atlantic with data obtained by these authors in clean 'natural' marine air off the coast of California disclosed some important differences in airmass and aerosol characteristics. Comparing clean 'natural' marine aerosol in the two locations revealed that:

1. Total aerosol concentration exhibited similar values in both locations, but off the West Coast, nearly all those aerosols were active at 1.0% supersaturation. In the Atlantic, only one-half of the aerosol population was active at 1.0% S, suggesting that a significant portion of the mid-Atlantic aerosol burden

was comprised of smaller, less active particles. However, the most active particles (i.e., at 0.2% S) were found in higher concentrations in the mid-Atlantic than were previously observed in clean marine situations at sea off the West Coast.

2. Aerosols off the West Coast were primarily of sea salt origin with varying amounts of a sulfate component; whereas in the Atlantic, background levels of a variety of materials were found. Apparently differences in origin of the respective air masses and downwind distances from respective land masses account for differences in total aerosol composition.

3. Apparently as a result of compositional and size differences in the respective aerosol populations, response of the aerosol to humidity changes and hence their impact on visibility, also differed between the two clean marine situations.

It must be recognized that the data discussed in this report were acquired under a specific set of meteorological circumstances, and what was observed is not necessarily typical. However, the data do suggest that what is thought to be clean marine air in one location at one time should not be extrapolated to describe other clean marine situations nor necessarily be termed 'natural'.

Analyses of the data acquired during the Transatlantic-Mediterranean cruise of May-June 1977 show that considerable variation can occur in the concentration and chemical make-up of aerosol populations in different maritime locales. Consideration of the refractive indices and hygroscopicity of various observed aerosols and changes in relative humidity (caused by diurnal influences, advection over sea surface of different temperature, or adiabatic expansion aloft in well-mixed boundary layers) suggests that considerable variation in resultant visibility restriction or in the performance of electro-optical systems (particularly at IR wavelengths) can occur.

Section 3
THE INFLUENCE OF MARINE BOUNDARY LAYER AEROSOLS ON OPTICAL PROPAGATION

On NRL Cruise 77-16-04, a total of 24 complete aerosol spectra ($0.01 < d < 30\mu m$) were obtained from about 1100 km west of the European coast through the Mediterranean to Greece. These data were presented and discussed in Section 2.23, and the complete set of aerosol size spectra may be found in Appendix F. The availability of complete aerosol spectra as well as simultaneous measurements of visibility from an integrating nephelometer presented the opportunity to compare visibilities calculated from the aerosol data with measured visibilities. Additionally, the demonstration of the representativeness of the aerosol spectra through calculations of visibility allows extrapolation to probable extinction properties of the aerosol as functions of wavelength, aerosol composition and aerosol growth resulting from changes in relative humidity. Such comparisons can offer an indication of the accuracy of the measurement systems and, in light of the present interest in EOMET properties of the marine boundary layer, can prove valuable as measures of the likely performance of modern electro-optical communications and weapons systems.

The aim of the current program is directed primarily toward the basic microphysics of marine aerosols and fogs. In this section, we expound upon the marine aerosol data, calculating extinction as functions of wavelength, refractive index and relative humidity. These exercises serve to demonstrate the relevance as well as the quality of the aerosol data acquired during the expedition. In addition, the significance of aerosol parameters affecting extinction is explored.

3.1 Calculation of Visual Range from Aerosol Spectra

Calculations of visibility degradation from the measured aerosol size distributions were performed using the well-known Bouguer law:

$$I = I_o e^{-\beta x} \qquad (1)$$

where I_o is the intensity of the incident light, I is the observed light intensity at some distance x through the aerosol medium, and β is the composite scattering coefficient of the aerosol (b_{scat}). In turn, the composite scattering coefficient is defined as

$$\beta = \pi \sum_i k_i r_i \qquad (\ )$$

where k_i and r_i are the particle scattering coefficient and the particle radius, respectively. The summation is over the total number of particles per unit volume.

The particle scattering coefficient, k, is a function of the wavelength of the light and refractive index (both real and imaginary), shape, and structure of the particle. Rigorous solutions for light scattered by individual homogeneous spherical particles have been found by Mie (1908; Ref. 23). The laborious calculations required to use the Mie theory to determine the effect of an aerosol upon incident light are not necessary unless extremely high accuracy or angular scattering properties are of interest. For the present effort, calculations of the particle scattering cross-section were made using an approximation of Van De Hulst (1957; Ref. 24) and modified by Deirmendjian (1969; Ref. 25). It is suggested that the values of the particle scattering coefficient resulting from the use of the approximation are within 2 percent of the values obtained from the cumbersome Mie series. The approximation defines the particle scattering cross-section, k, for non-absorbing spheres

$$k = (1 + D) \left[2 - \frac{4 \sin Z}{Z} + 4\frac{(1 - \cos Z)}{Z^2}\right] \qquad (3)$$

$$Z = \frac{4 \pi r}{\lambda} (n - 1), \qquad (4)$$

where D is the modification due to Deirmendjian, λ is the wavelength of the incident radiation, and n is the real index of refraction. A more complex form of Equation 3 can be used to calculate the extinction of light by

partially absorbing spheres. The present effort does not consider absorption by the aerosol. Since the aerosols will contain considerable quantities of liquid water whose imaginary component of refractive index is insignificant for wavelengths smaller than about 2.5μm, these calculations should produce excellent results for wavelengths < 2.5μm. At longer wavelengths, i.e., the far-infrared, extinction due to absorption can be significant. Later in this Section, we calculate the expected extinction due only to scattering of 10.6μm wavelength radiation. Since absorption at the 10.6μm wavelength was neglected, it is likely that our calculation significantly underestimates the extinction and overestimates the visual range at the far-infrared wavelength.

Rather than present data in terms of optical visibility which is a rather ambiguous term, results are presented with respect to visual range. Visual range is defined as the optical path length required to produce 98 percent extinction of the incident light. Based upon this definition, the composite b_{scat} is related to the visual range (V) by the relation

$$b_{scat} = \frac{3.912}{V}. \tag{5}$$

Throughout this text, visibility and visual range will be used interchangeably in accordance with Equation 5. According to this general definition, we can now discuss the visual range at all wavelengths of electromagnetic radiation not necessarily confined to the visible spectrum. Such data are presented below.

The information on visibility provided by the MRI Integrating Nephelometer is probably not as good as desired. The integrating nephelometer actually measures b_{scat}. The basic measurement itself is not without controversy (Ref. 26), but in this effort, we prefer not to begin correcting basic data; such adjustments are left to the discretion of the reader. However, manipulations of the basic data (b_{scat}) to present visibility will be addressed. Using broad band light with an effective wavelength of 0.474μm, the integrating nephelometer measures the light scattered over a broad angular range to determine b_{scat}. Rather than using Equation 5 to determine visual range from these values of b_{scat}, the nephelometer extrapolates from the measurement at 0.474μm to

0.55μm wavelengths. The justification for the extrapolation lies in the fact that the sensitivity of the human eye is peaked at about 0.55μm. Consequently, in order to provide better correlation between visual and instrumental determination of visibility, the extrapolation was employed by the manufacturer. Since calculations of visibility can be just as easily performed for 0.474μm as for 0.55μm wavelength, our quoted values of measured visibility (visual range) are actually determined from measured values of b_{scat} using Equation 5. The values of visibility offered by the nephelometer are ignored.

The particle scattering cross-section as a function of particle diameter is shown in Figure 33 as calculated from Equation 4 for a wavelength of 0.474μm and the indicated real refractive indices of 1.33 (pure water), 1.37 (saturated NaCl solution), and 1.5 (dry NaCl). To eliminate the possibility that the use of discrete groups of particles (from particle measuring instrumentation) would have mean diameters centered at either peaks or valleys of the particle scattering coefficient (shown in Figure 33), a continuous aerosol size distribution was used for each of the 24 aerosol data sets in the actual calculations of visibility. The continuous distributions, discussed in Section 2.23 (see Figure 21), are valid over the range from 0.2 to 20μm diameter and were obtained by a least squares fit of a Junge distribution to the measured aerosol data. A Junge distribution has the form

$$\frac{dN}{d \log r} = Cr^{-\beta} \qquad (6)$$

where N is the number of particles in a given size range and C and β are constants determined by the aerosol data. To assure that particles outside of the valid range do not significantly affect visibility, the discrete groups of aerosol particles and their mean radii were used to calculate the percent of total b_{scat} due to each family. Percent b_{scat} as functions of aerosol size

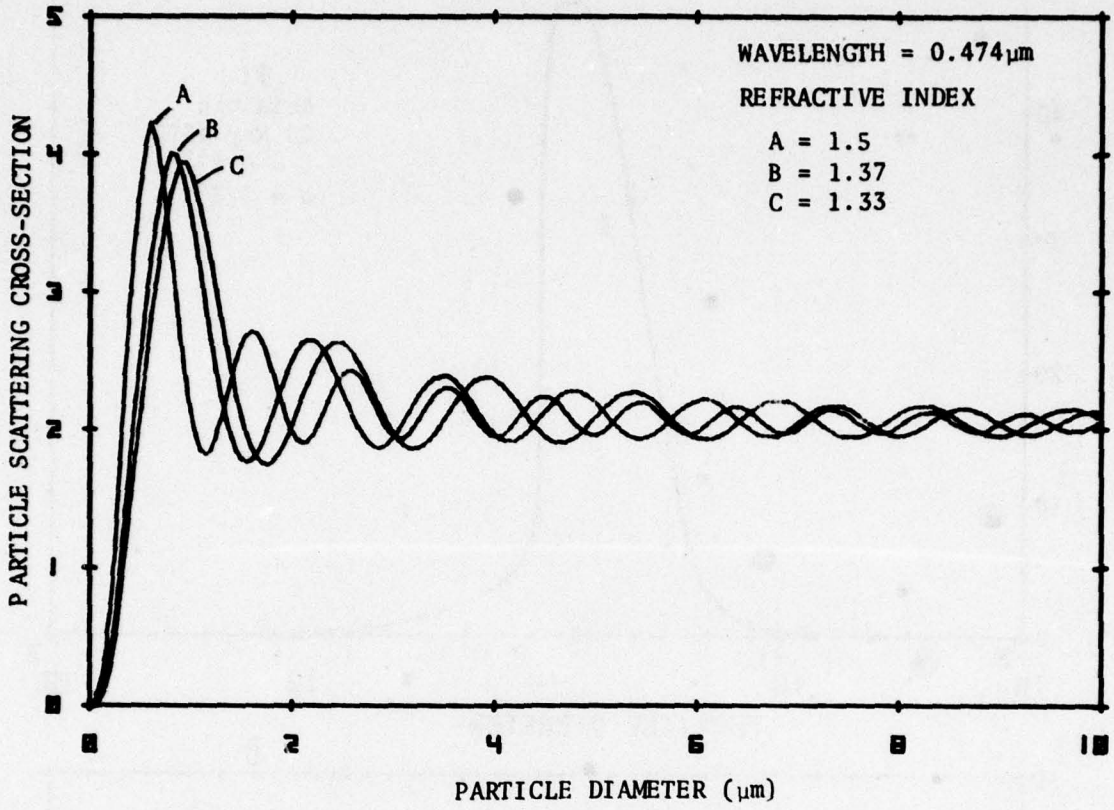

Figure 33: Particle Scattering Coefficient as a Function of Particle Diameter for 0.474μm Radiation and Indicated Refractive Indices

intervals are presented in Figures 34a and b for aerosol distributions #1 and 18 (see Figure 21), respectively, assuming a wavelength of light of 0.474μm and real refractive index of 1.37. The data shown in Figures 34a and b indicate that the families of particles providing maximum contribution to light extinction are located near 1μm diameter. For the measured size spectra, particles smaller than 0.2μm and larger than 20μm diameter contributed < 5% to the total extinction at visible wavelengths. For longer wavelengths, however, the peak in percent b_{scat} would shift to larger particle diameters.

The results shown in Figures 34a and b are, in the broad sense, similar for both aerosol distributions even though the distributions represent the extremes of the data set (Figure 21) and are different in other respects. Aerosol distribution #1, was acquired at 1045 GMT on 25 May in the Atlantic, ∿1100 km from the European continent, while distribution #18 was obtained in

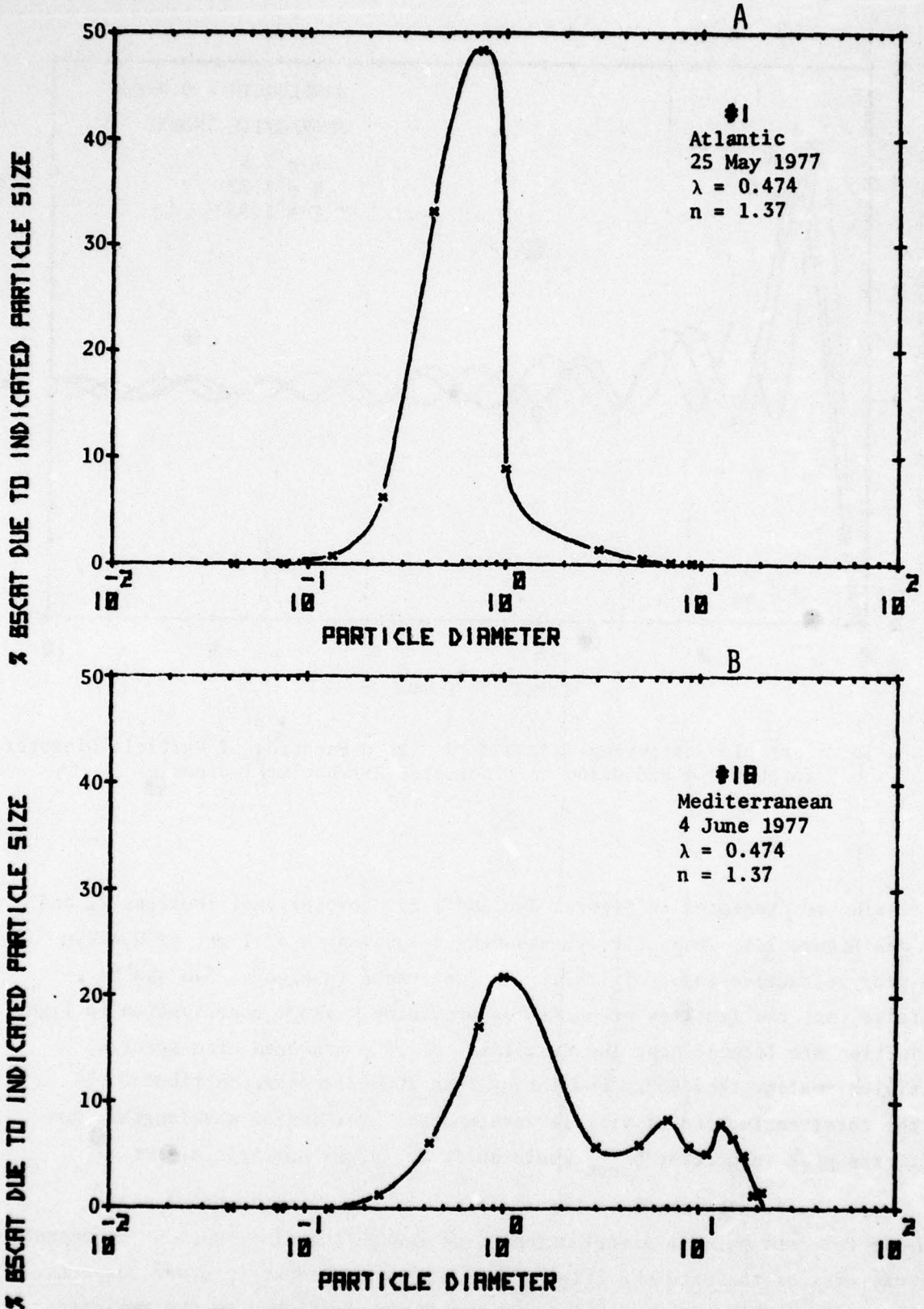

Figure 34: Calculated Values of Percent of Total B_{scat} Due to Individual Size Categories at the Indicated Diameters For Two Measured Aerosol Spectra

the Mediterranean at 1410 GMT on 4 June. The former may be more nearly representative of the clean marine environment, the latter might more accurately be termed continental influenced by marine. While total extinction resulting from the two aerosol spectra was substantially different, the percentage extinction contributed by the particles in the 0.2-20μm range was nearly identical. For the particles < 0.2μm diameter, particle scattering cross-section was relatively minimal, and, in the larger sizes (i.e., >20μm) concentrations were ∿3 orders of magnitude lower than those of 1μm diameter particles (see Figure 13) in both distributions. However, in spectra #18 particles ≥1.0μm accounted for 50% of the observed extinction, while for spectra #1, these larger aerosols contributed only ∿15% of the total extinction.

The values of calculated visual range, using Eqs. 4 and 6, are presented in Table 12 for each of the 24 complete aerosol distributions. Included in Table 12 for each aerosol distribution are: spectrum number, date, and time; observed relative humidity (%); measured visibility (km); and, calculated visibility (km) for the indicated real refractive indices and wavelengths of radiation (μm). Again, it should be noted that the visual ranges calculated for λ = 10.6μm are gross estimates and represent an upper limit to the visual range since absorption has been neglected. Values of the real refractive index (1.33, 1.37, and 1.5) were chosen to simulate water, saturated aqueous saline solution, and dry salt (NaCl), respectively.

From the calculated visibilities presented in Table 12, it is immediately obvious that visibility is dependent not only on the absolute size distribution (compare spectra #1 and #18 in Figure 21 and Table 12) but on the index of refraction (chemical composition and state of wetness) of the aerosol. Note that if the aerosol had been saturated NaCl (n = 1.37) and for the visible wavelength (0.474μm), visibilities would have been overestimated by ∿5-15% if pure water had been assumed and underestimated by 10-25% had dry NaCl (or other inorganic salt) been assumed.

Calculated and observed visibilities (visible wavelengths only) are further compared in Figure 35. Since much of the soluble material expected in the true marine environment should be wetted salt, the calculated

Table 12 Visibility Calculated From Measured Aerosol Size Spectra as a Function of Index of Refraction and Wavelength

#	Date	RH (%)	Vsby (km)	n=1.33 λ 0.474	n=1.33 λ 1.0	n=1.33 λ 2.5	n=1.33 λ 10.6	n=1.37 λ 0.474	n=1.37 λ 1.0	n=1.37 λ 2.5	n=1.37 λ 10.6	n=1.5 λ 0.474	n=1.5 λ 1.0	n=1.5 λ 2.5	n=1.5 λ 10.6
1	25 May 1045	81	56	112.1	304.9	1163.4	19598.1	98.5	263.8	993.7	15260.5	71.5	180.4	650.1	7821.5
2	25 May 1410	76	64	184.8	394.4	1077.5	7726.2	116.9	352.3	954.6	6323.6	129.7	262.7	693.2	3901.8
3	26 May 0740	81	37	115.1	303.7	1097.6	12792.2	101.5	263.8	943.2	10197.2	74.2	182.5	629.8	5676.3
4	26 May 1345	76	40	102.0	233.3	708.4	7930.6	91.4	206.5	618.4	6294.1	69.6	150.1	434.9	3455.2
5	27 May 1015	78	15	58.6	92.2	170.5	597.7	54.9	85.8	157.6	517.2	46.9	71.4	128.3	383.2
6	27 May 1230	78	15	33.8	47.6	77.0	239.1	32.2	44.9	72.0	204.9	28.5	38.9	61.0	150.5
7	27 May 1450	83	16	31.5	43.0	67.6	241.0	30.0	40.8	63.5	201.1	26.9	35.7	54.1	135.2
8	31 May 2130	65	69	88.9	101.6	126.8	268.1	86.9	98.9	121.9	232.8	82.8	92.6	111.5	181.5
9	1 June 0910	69	49	64.4	73.3	91.0	190.7	63.0	71.4	87.5	165.7	60.1	67.0	80.2	129.3
10	1 June 1415	63	56	87.5	111.0	159.2	502.0	84.4	106.3	151.0	420.2	77.6	95.6	132.1	286.2
11	1 June 1920	72	51	106.5	153.9	259.4	1010.6	101.0	144.8	241.8	841.5	88.8	124.1	201.8	559.9
12	2 June 1340	76	39	166.7	255.6	463.0	1978.6	156.8	238.5	428.2	1643.7	135.2	200.1	350.1	1082.0
13	3 June 1135	81	17	53.2	76.0	124.3	346.8	50.5	71.6	116.3	307.5	44.6	61.7	98.1	242.2
14	3 June 1335	77	39	47.4	60.1	85.0	190.8	45.7	57.6	80.7	171.0	42.0	51.8	71.1	140.3
15	3 June 2130	78	56	53.1	58.7	69.4	116.1	52.2	57.4	67.2	105.7	50.4	54.5	62.5	91.9
16	4 June 0645	74	53	73.7	92.1	128.1	298.7	71.1	88.5	122.2	263.0	65.7	80.0	108.0	208.9
17	4 June 0840	76	54	54.2	63.0	79.9	161.2	52.9	61.2	77.0	142.8	50.1	56.9	70.0	116.4
18	4 June 1410	80	41	33.6	36.2	41.3	69.6	33.1	35.6	40.3	62.2	32.2	34.1	37.9	52.4
19	4 June 2010	72	20	32.9	45.6	73.0	266.0	31.4	43.2	68.4	221.8	28.0	37.6	57.9	148.7
20	5 June 0430	74	29	35.7	42.0	54.0	111.7	34.8	40.7	52.0	98.9	32.8	37.7	47.1	80.2
21	5 June 0840	67	23	37.5	50.8	78.1	198.8	35.8	48.3	73.6	177.1	32.2	42.4	63.2	141.9
22	5 June 1435	70	24	28.4	35.8	50.4	119.6	27.4	34.4	48.0	105.2	25.2	31.0	42.3	83.4
23	6 June 0450	55	36	57.1	94.3	186.8	894.1	53.2	87.1	171.1	740.6	44.8	71.2	136.4	481.1
24	6 June 1250	66	28	62.0	95.9	175.6	760.7	58.2	89.4	162.2	631.7	50.1	74.7	132.2	415.2

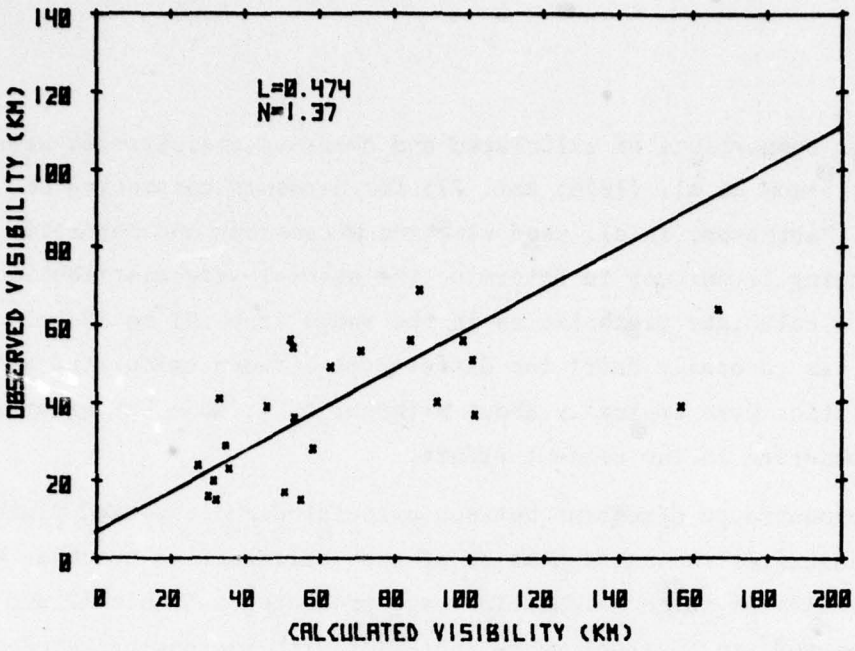

Figure 35: Measured Visibility vs. Visibility Calculated From 26 Discrete Aerosol Spectra

visibilities in Figure 35 were based on a real refractive index of 1.37* using a wavelength of 0.474μm. The solid line in Figure 35 corresponds to a least squares fit to the data. The data display fair agreement overall, but much better agreement particularly for the lower visibility, Mediterranean data. The reasons for better agreement in the Mediterranean data are unknown. For visibilities greater than about 50 km, the measured visibilities of the nephelometer are suspect because of the error in measuring small b_{scat} values. It is possible that much of the observed scatter in the data presented in Figure 35 is due to uncertainty in the measured visibility and in the assumption of refractive index. It is also possible that the systematic error in the integrating nephelometer could be responsible for the variation of the slope of the fit from a unit slope. The scatter of data further justifies the use of the Deirmendjian approximation as opposed to the exact Mie series for determining the particle scattering cross-section.

*The observed aerosol population for this portion of the cruise was of mixed chemical composition (see Section 2.3) containing ∿25% NaCl particles and ∿50% other inorganic salts. However, the refractive indices of most of those materials in the dry state are ∿1.5, but wetted, as the aerosols must have been at 80% RH, ambient refractive indices would have been between that value and 1.33 (pure water)--hence 1.37 is probably a reasonable estimate of the actual.

Similar comparisons of calculated and observed visibilities were performed by Patterson et al. (1976; Ref. 27) for aerosols consisting of soil particles. Patterson, et al. used electron microscopy and automatic imaging and scanning techniques to determine the aerosol size distributions, and Mie theory to calculate visibilities in the range from .01 to 10 km. While agreement was generally fair, the differences between calculated and observed visibilities were typically about a factor of 4, somewhat greater than the variations observed in the present effort.

The demonstrated agreement between calculated and observed visibility to some extent justifies the extrapolation of such calculations to other wavelengths. The results of these calculations are presented in Table 12 and indicate, as expected, that visual range increases with increasing wavelength. The values presented in Table 12 show that visual range estimates at 2.5μm and 10.6μm wavelengths were, typically, factors of 1.5-5 and 3-15 times greater respectively, than those estimated for visual wavelengths. These factors correspond to total extinction values (scattering only) only 20-60% and 10-30%, respectively, of that expected for visual wavelengths. As indicated earlier, the large visual ranges calculated for λ = 10.6μm are over estimated because absorption has been neglected. However, absorption for wavelengths shorter than $\sim$2.5μm should be minimal, and the results more accurate estimates of total extinction.

3.2 The Influence of Relative Humidity on Visibility

Calculations of visibility can be carried a step further by considering the influence of relative humidity on the size distribution of the aerosol. Variations in the size distribution due to changes in relative humidity will modify the scattering properties of the aerosol. To facilitate the calculation of particle size, it is assumed that the aerosol is composed entirely of an aqueous saline solution whose vapor pressure is at equilibrium with the environment. Examples of these results are presented for aerosol distributions #1 and 18. In this exercise, the effect of changing refractive index due to dilution of aerosol solution droplets by changing relative humidity is neglected.

The relationship between particle radius r at a given relative humidity and the particle radius r_o at zero percent relative humidity is given by

$$\frac{r}{r_o} = \left[1 + \frac{\sigma}{1-S}\right]^{1/3} \tag{7}$$

where $\sigma = 1.22$ for NaCl droplets and S is the saturation ratio (Ref. 12). This relationship has been used to produce relative humidity dependent aerosol size spectra for aerosol samples #1 and 18 shown, respectively, in Figures 36 and 37. We have chosen to allow particle sizes to increase continuously with increasing relative humidity as natural marine aerosols are observed to behave (e.g., Ref. 12). This size variation is in contrast to the theoretical behavior of pure NaCl particles in which the particles remain dormant in size with increasing relative humidity until a value near 75 percent is attained; near 75 percent relative humidity the size of the salt particles abruptly increases due to deliquesence and the ensuing growth is a continuous function of relative humidity described by Equation 7.

The expected variations of observed aerosol size spectra with relative humidity are shown in Figures 36 and 37. These two particular aerosol spectra were chosen because they represent the extremes of our observed aerosol spectra. That is, aerosol distribution #1 was obtained farthest from the European coast ($\sim$1100 km) while aerosol distribution #18 was obtained in the central Mediterranean near the African coast. Further, the two aerosol spectra exhibited the largest variation in parameters for the Junge fit. It is recognized that some differences in the two aerosol distributions are likely to be due to significant continental influence, particularly on the latter distribution. Since continental aerosols will not exhibit the same relative humidity dependence as marine aerosols, the common use of $\sigma = 1.22$ may not be appropriate. Fitzgerald (Ref. 12) suggests that σ values of $\sim$0.2 may be more realistic for a modified continental aerosol population. However, since a major fraction of our aerosol scattering cross-section was due directly to liquid droplets (direct sea spray), we are dealing with sea water aerosols. Within the limited scope of this effort, $\sigma = 1.22$ is probably acceptable for illustrative purposes.

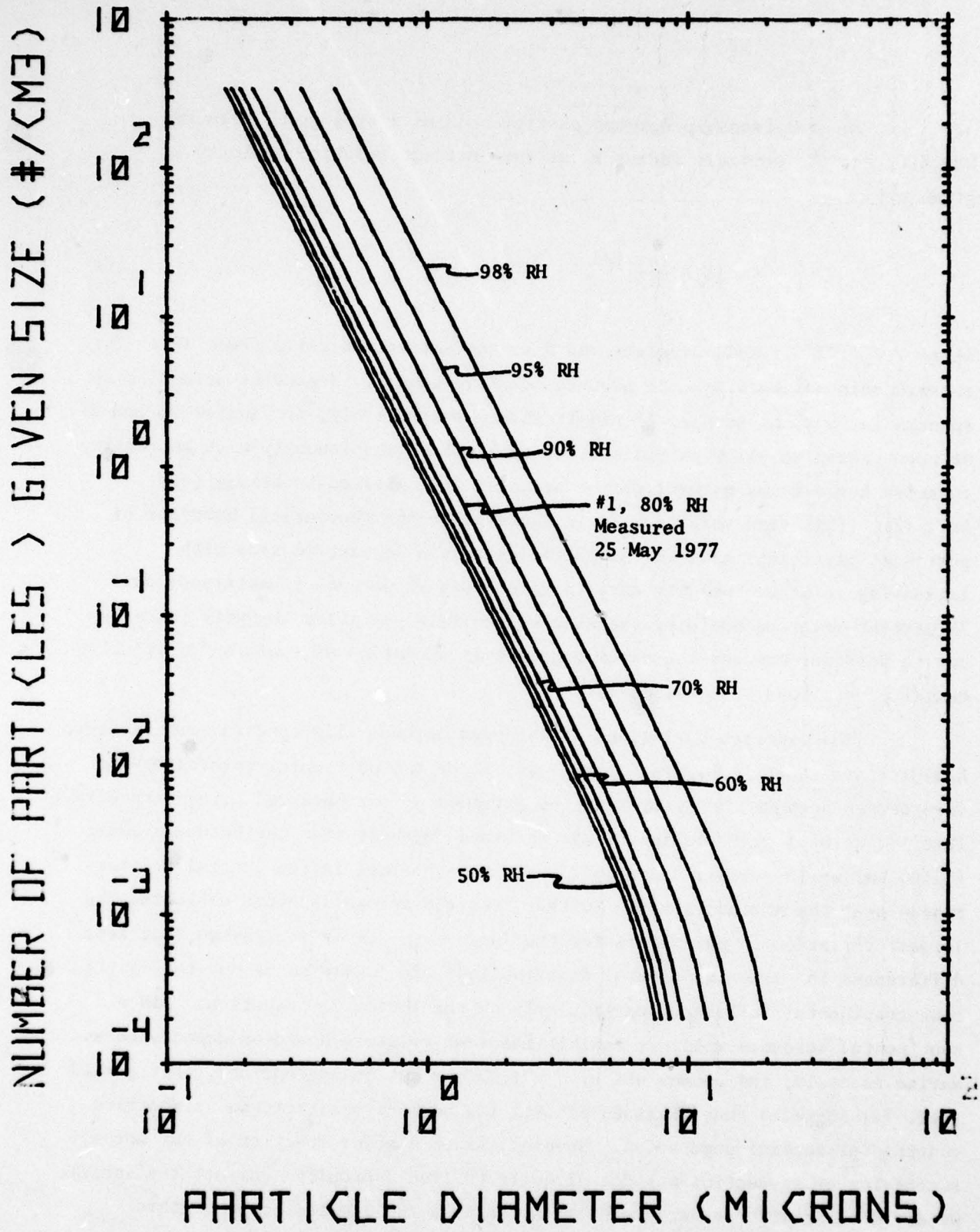

Figure 36: Calculated Growth of Aerosol Size Distribution #1 As a Function of Relative Humidity

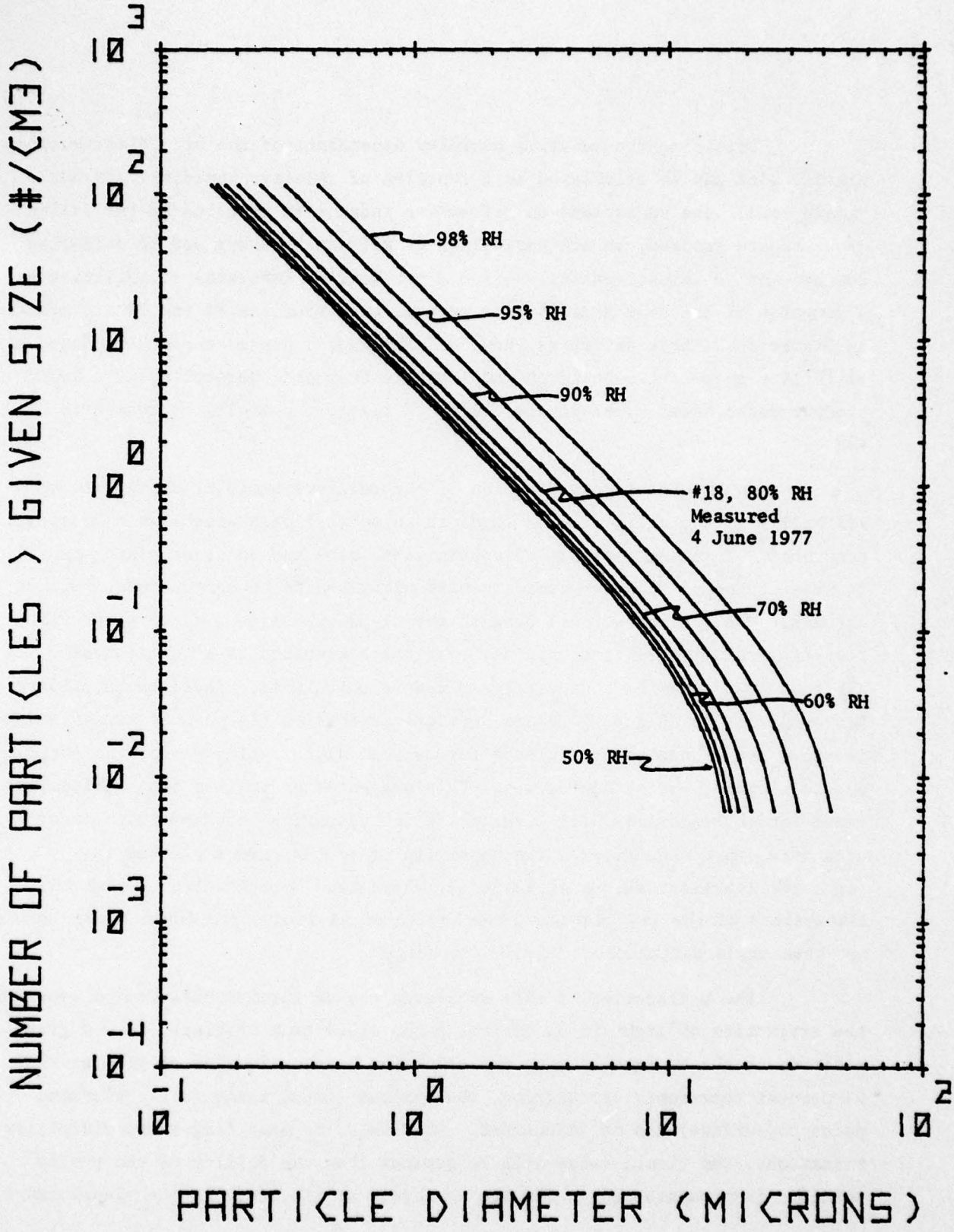

Figure 37: Calculated Growth of Aerosol Size Distribution #18 As a Function of Relative Humidity

Utilizing the relative humidity dependence of the size distribution, visibilities can be calculated as a function of relative humidity. In our simple model, the variations of refractive index with dilution of the saline droplets are ignored, as are variations of refractive index due to differing composition of aerosol particles (i.e., not NaCl). Estimated visibilities as a function of relative humidity for aerosol distributions #1 and 18 are presented in Figure 38. These estimates show, as expected, a considerable dependence of visibility on relative humidity and indicate that both aerosol spectra would produce dense hazes of ∿1 km visibility if relative humidity increased to ∿98%.

An interesting application of the relative humidity dependence of visibility is the extinction of light in an optical path which has a vertical component. Assuming a simple adiabatic lapse rate and constant mixing ratio, the variations of relative humidity with altitude can be calculated. Further, assuming a well mixed aerosol beneath the cloud base (i.e., no vertical variation in aerosol concentration), the vertical extinction as a function of altitude in the marine boundary layer can be calculated. These calculations are summarized in Figure 39 where vertical extinction (in percent transmission) is shown as a function of altitude for aerosol distribution #1 for the indicated surface-level relative humidities. This presentation implies that substantial reduction in visibility will occur aloft in the marine boundary layer under adiabatic lapse conditions. The upper limits of the curves plotted in Figure 39 represent values at 98.5% RH, where Eq. 7 breaks-down. Under the assumptions of the calculations, the indicated altitudes for these upper limits are then crude estimates of cloud base height.

The application of this reasoning can be further extended to consider the extinction of light in an optical path, other than vertical, from a given altitude to the surface. Using the criterion that extinction of greater than 98 percent represents obscuration, the maximum visual range (i.e., elevated point to surface) can be calculated. Obviously, in many long-range visibility situations, the visual range will be greater than the ability of the eye or specific instrumentation to resolve an object at the limit of the visual range.

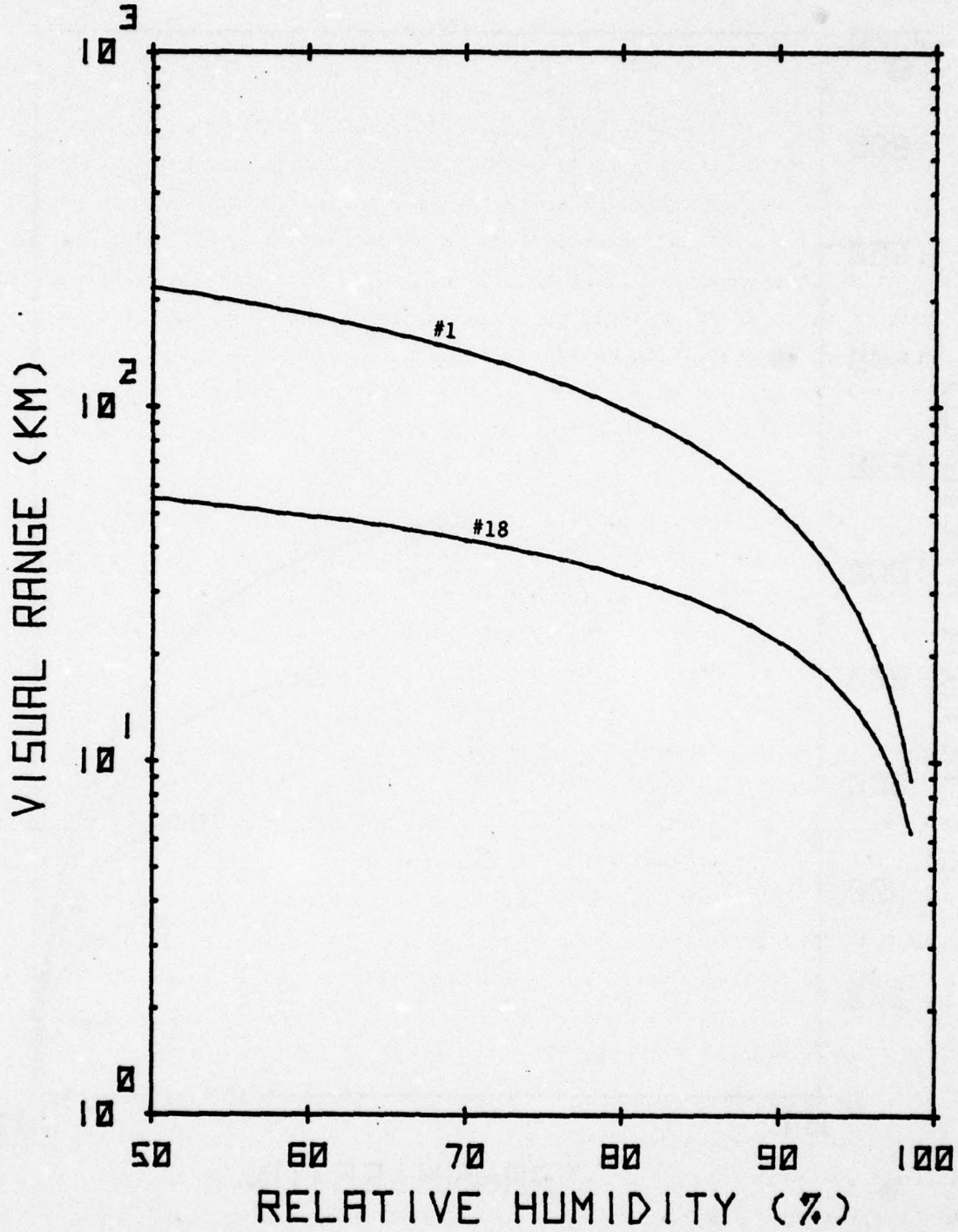

Figure 38: Calculated Dependence of Visibility on Relative Humidity for Aerosol Size Distributions #1 and 18

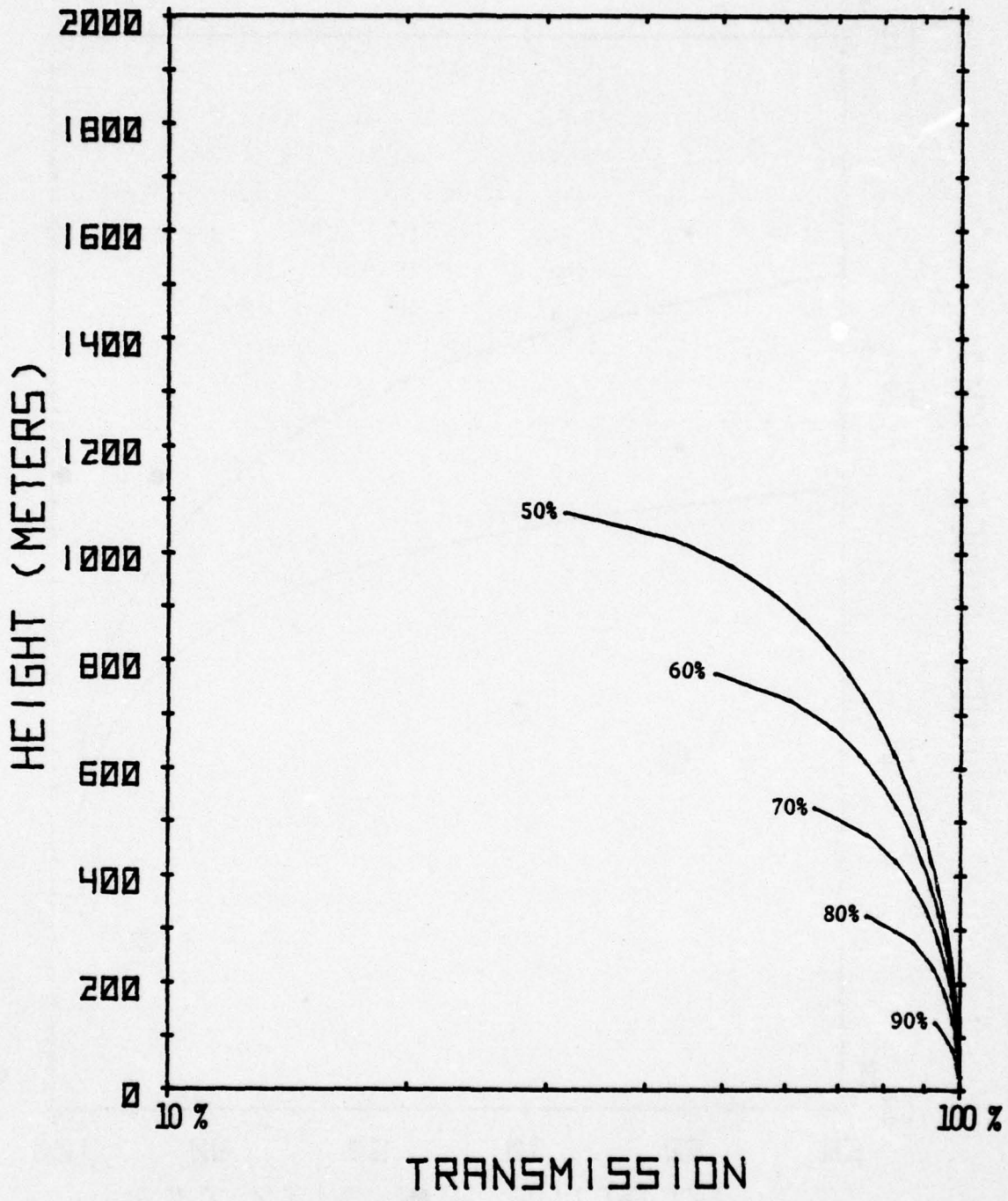

Figure 39: Calculated Vertical Transmission as Function of Altitude and Indicated Surface Relative Humidities Using Aerosol Distribution #1

Transmission (i.e., the percent of light not extincted through a given optical path) is plotted against altitude for the indicated observation angles in Figure 40. These calculations were performed using the Atlantic aerosol spectrum #1, assuming surface relative humidity of 50% and constant mixing ratio and adiabatic lapse conditions through the layer. (Since, at a surface RH of 80%, cloud base would be at ∿400m, the 50% RH value was used to illustrate the utility of such calculations.) The observation angles shown in Figure 40 are defined as the angles between the surface and the line connecting the observer to the object. These angles necessary fall between 0° and 90°, with 90° representing the observer looking directly down at an object on the surface. It is obvious in comparing this presentation with that in Figure 40, that while transmission in the vertical may be good, slant range values drop rapidly with altitude for decreasing observation angles. Obvious applications of this type calculation include evaluation of performance of tactical weapons systems as well as less military-oriented search and rescue missions.

3.3 Discussion and Summary

Complete aerosol size distributions obtained on the Transatlantic-Mediterranean cruise were used to calculate the extinction of various wavelengths of radiation as functions of a variety of parameters. Calculated visibilities showed fair agreement with observed visibilities and served to demonstrate the validity of the aerosol data. Deviation between observed and calculated visibility may be attributable to uncertainties in the measurement of both visibility and aerosol size spectra and the assumption of NaCl for aerosol composition. Results of the visibility calculations indicated that, typically, greater than 90% of the total visibility degradation was due to particles within the range 0.2 to 20μm diameter for the observed aerosol spectrum.

The calculation of visibility at much longer wavelengths than the visible (i.e., at 2.5 and 10.6μm) showed that the observed aerosols under the ambient surface-level conditions of 80% RH, were responsible for only minimal obscuration (neglecting absorption) near the ocean surface at those wavelengths.

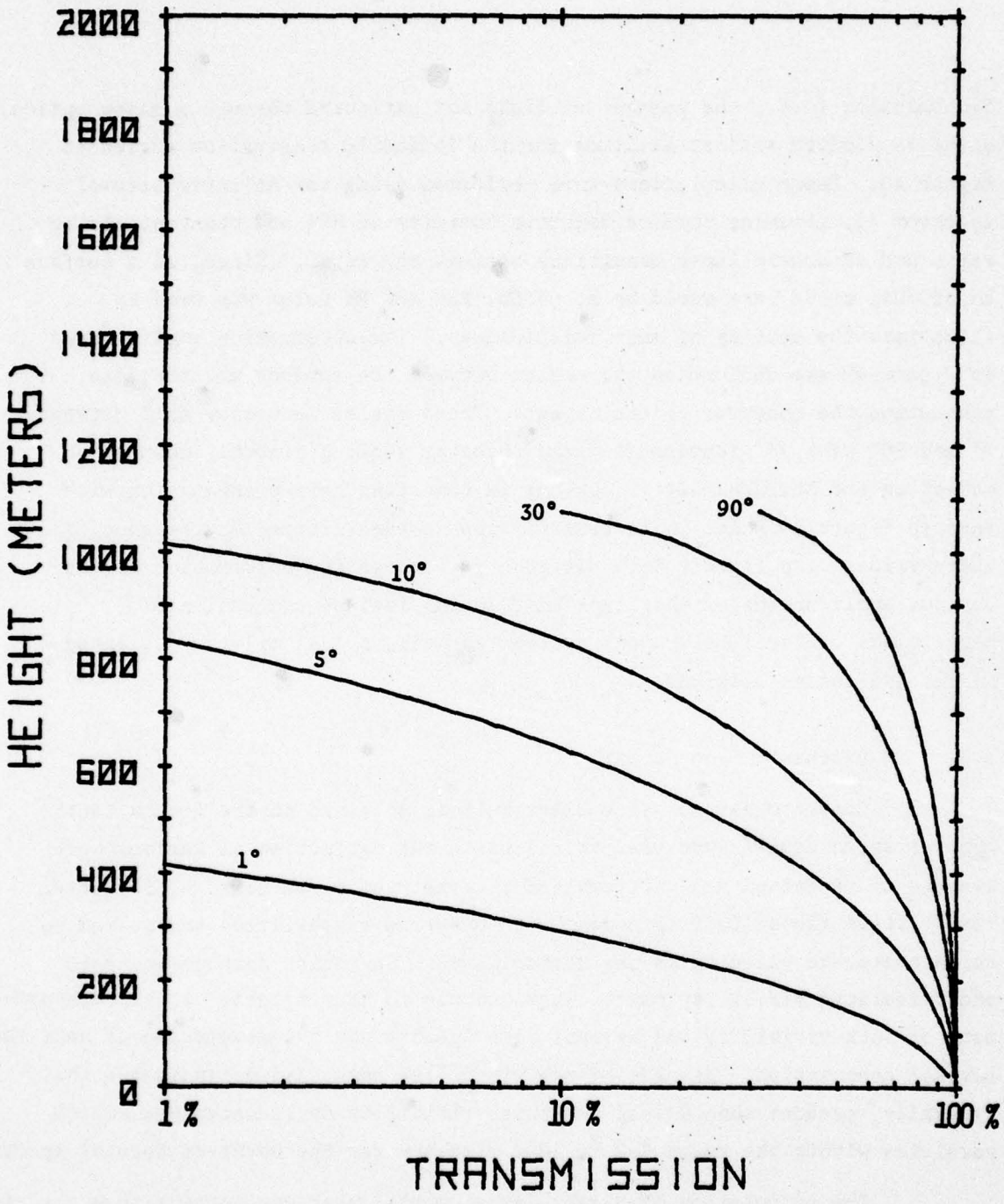

Figure 40: Calculated Slant Range Transmission as a Function of Altitude for Observations at the Indicated Viewing Angles (With Respect to Surface) for Aerosol Distribution #1 Assuming a Surface Relative Humidity of 50%

However, extension of these calculations to consideration of changes in relative humidity (caused by diurnal influences, advection over sea surface of different temperature, or adiabatic expansion aloft in well-mixed boundary layers) demonstrated an important dependence of visibility on relative humidity. Assuming the observed aerosol consisted of sea salt (which was not always the case), these exercises showed that any one of the 24 complete aerosol spectra (Figure 21) obtained during the cruise was capable of producing dense haze (visual range of < 1 km at visible wavelengths) if relative humidity increased to ∿98%. Further, while visual range may be nearly unlimited over horizontal paths near the surface, increased relative humidity aloft under well-mixed conditions will produce growth of aerosols, thereby severely limiting slant visual range.

Within the limited scope of this effort, it was not possible to consider the influence of absorption on extinction at infrared wavelengths. Depending on the specific aerosol size spectra and chemical composition, absorption could account for a substantial fraction of the total extinction at 10.6μm wavelength. In view of the current interest in electro-optical propagation in the marine boundary layer and the availability of the data set incorporated in this report, an effort to consider the influence of absorption on extinction at far-infrared wavelengths should be undertaken.

References

1. Mack, E.J., R.J. Pilié, and W.C. Kocmond, May 1973: "An Investigation of the Microphysical and Micrometeorological Properties of Sea Fog," Project SEA FOG, First Annual Summary Report, Calspan Report CJ-5237-M-1.

2. Mack, E.J., U. Katz, C.W. Rogers, and R.J. Pilié, July 1974: "The Microstructure of California Coastal Stratus and Fog at Sea," Project SEA FOG: Second Annual Summary Report, Calspan Report CJ-5404-M-1.

3. Mack, E.J., R.J. Pilié, and U. Katz, March 1975: "Marine Fog Studies Off the California Coast," Project SEA FOG: Third Annual Summary Report, Calspan Report No. CJ-5606-M-1.

4. Mack, E.J. and U. Katz, June 1976: "The Characteristics of Marine Fog Occurring Off the Coast of Nova Scotia," Project SEA FOG: Fourth Annual Summary Report, Part 1, Calspan Report No. CJ-5756-M-1.

5. Mack, E.J. and C.W. Rogers, June 1976: "Simulation of Marine Advection Fog With the Calspan Advection Fog Model Using Prognostic Equations for Turbulent Energy," Project SEA FOG: Fourth Annual Summary Report, Part 2, Calspan Report No. CJ-5756-M-2.

6. Mack, E.J. and U. Katz, March 1977: "Measurements of Aerosol and Micrometeorological Characteristics of the Marine Boundary Layer in the Gulf of Mexico," Calspan Report.

7. Katz, U. and E.J. Mack, April 1977: "Direct Measurements of Sea Spray Size Spectra at the NCSL Offshore Platform," Calspan Report No. CH-6067-M-1.

8. Katz, U. and E.J. Mack, September 1977: "Measurements of Aerosol and Micrometeorological Characteristics of the Marine Boundary Layer During the Transatlantic/Mediterranean Cruise of the USNS Hayes, May-June 1977," Calspan Report.

9. Mack, E.J., U. Katz, C.W. Rogers, D.W. Gaucher, K.R. Piech, C.K. Akers, and R.J. Pilié, October 1977: "An Investigation of the Meteorology, Physics, and Chemistry of Marine Boundary Layer Processes," Project SEA FOG: Fifth Annual Summary Report, Calspan Report No. CJ-6017-M-1.

10. Mack, E.J. and T.A. Niziol, October 1978: "Reduced Data from Calspan's Participation in the CEWCOM-78 Field Experiment off the Coast of Southern California During May 1978", Project SEA FOG, Sixth Annual Summary Report: Part 2, Calspan Report No. 6232-M-2.

11. Winkler, P., 1973: "The Growth of Atmospheric Aerosol Particles as a Function of the Relative Humidity -II. An Improved Concept of Mixed Nuclei", Aerosol Sci, Vol 4, pp 373-387.

12. Fitzgerald, J.W., 1978: "On the Growth of Aerosol Particles with Relative Humidity", Naval Research Lab. Memorandum Rept. 3847, August, 11 pp.

13. Davies, C.N., 1974: "Size Distribution of Atmospheric Particles", Aerosol Sci, Vol 5, pp 293-300.

14. Jaenicke, R. and Davies, C.N., 1976: "The Mathematical Expression of the Size Distribution of Atmospheric Aerosols", J. Aerosol Sci, Vol 7, pp 255-259.

15. Gerber, H.E., Hoppel, W.A., and Wojciechowski, T.A., 1977: "Experimental Verification of the Relationship Between Size and Critical Supersaturation of Salt Nuclei", Presented at the Fifth Annual Marine Fog Investigation Program Review Meeting, Buffalo, NY, 5-6 April 1977.

16. Alofs, D.J. and Carstens, D.J., 1976: "Numerical Simulation of a Widely Used Cloud Nucleus Counter," J. Appl. Met., Vol 15, pp 350-354.

17. Blanchard, D.C., 1969: "The Oceanic Production Rate of Cloud Nuclei", J. de Rech. Atmospheriques, Vol. IV, 1, pp 1-6.

18. Mitchell, R.I. and J.M. Pilcher, 1959: "Improved Cascade Impactor for Measuring Aerosol Particle Sizes", Industrial Engineering and Chemistry, Vol 51, 9, pp 1039-1042.

19. Lawson, D.R. and Winchester, J.W., 1978: "Sulfur and Crustal Reference Elements in Nonurban Aerosols from Squaw Mountain, Colorado", Environ. Sci. and Tech., Vol 12, pp 716-721.

20. Barrie, L.A., and H.W. Georgii, 1976: "An Experimental Investigation of the Absorption of Sulfur Dioxide by Water Drops Containing Heavy Metal Ions", Atmos. Environ., 10, 743.

21. Anderson, R.J., Pilié, R.J., Mack, E.J., and Kocmond, W.C., 1978: "A Laboratory Investigation of the Photooxidation of SO_2 in Irradiated $HC+NO_x+SO_2$ Systems and the Catalytic Oxidation of SO_2 in Hazes, Clouds and Fogs", Calspan Report for EPA, March 1978.

22. Mohnen. V.A., and Yue, G.K., 1974: "Free HCl Acid in the Atmosphere Resulting from Scavenging Processes", Precipitation Scavenging 1974, U.S. Atomic Energy Commission Symposium Series (in press).

23. Mie, G., 1908, Ann. Physik 25, p 377.

24. Van de Hulst, H.C., 1957, Light Scattering by Small Particles, John Wiley & Sons, Inc., New York.

25. Deirmendjian, D., 1969, Electromagnetic Scattering on Spherical Polydispersions, American Elsevier Publishing Co., Inc., New York.

26. Fitzgerald, J.W., 1977, "Angular Truncation Error of the Integrating Nephelometer in the Fog Droplet Size Range", J. Appl. Meteor. 16, p. 198-204.

27. Patterson, E.M., D.A. Gillette, and G.W. Grams, 1976, "The Relation Between Visibility and the Size-Number of Airborne Soil Particles," J. Appl. Meteor. 15, p. 470-478.

Appendix A

LOG OF COMPUTED WINDS

DATE 5 15 1977

TIME(GMT)	WINDS(M/SEC) MAGNETIC		WINDS(MI/HR) RELATIVE		SHIP(MI/HR)	
	DIR.	SP.	DIR.	SP.	HEAD.	SPEED
1700	355	5.8	340	23.8	35	13.0
1800	16	2.4	355	17.3	33	13.0
1900	352	0.8	355	13.2	34	13.0
2000	35	0.2	360	12.2	35	13.0
2100	35	0.6	360	13.2	35	13.0
2200	254	5.1	300	7.1	33	13.0
2300	239	4.3	315	4.6	31	13.0

DATE 5 16 1977

TIME(GMT)	WINDS(M/SEC) MAGNETIC		WINDS(MI/HR) RELATIVE		SHIP(MI/HR)	
	DIR.	SP.	DIR.	SP.	HEAD.	SPEED
0	222	6.6	75	9.6	89	13.0
100	242	7.3	265	7.1	30	13.0
200	242	9.1	105	11.2	99	13.0
300	249	8.5	110	8.6	99	13.0
400	252	8.1	115	6.6	97	13.0
500	240	7.3	90	8.1	97	13.0
600	229	6.3	70	10.1	99	13.0
700	233	5.6	65	8.1	98	13.0
800	248	7.4	100	6.6	98	13.0
900	263	9.3	145	7.1	97	13.0
1000	275	8.4	170	4.1	98	13.0
1100	277	8.0	170	3.0	100	13.0
1200	280	4.8	0	0.0	100	13.0
1300	284	4.8	0	0.0	104	13.0
1500	280	8.7	170	4.6	103	13.0
1600	273	8.9	275	15.2	38	13.0
1700	327	7.2	340	27.4	3	13.0
1815	265	10.4	180	8.6	85	13.0
1900	265	9.5	180	6.6	85	13.0
2000	265	9.1	180	5.6	85	13.0
2200	256	11.6	180	11.7	76	13.0
2300	256	11.0	180	10.1	76	13.0

DATE 5 17 1977

TIME(GMT)	WINDS(M/SEC) MAGNETIC		WINDS(MI/HR) RELATIVE		SHIP(MI/HR)	
	DIR.	SP.	DIR.	SP.	HEAD.	SPEED
0	273	10.7	220	11.2	73	13.0
100	281	9.4	235	9.1	76	13.0
200	252	10.6	180	9.1	72	13.0
300	249	10.8	180	9.6	69	13.0
400	245	11.7	200	12.2	55	13.0
500	253	11.7	215	13.2	55	13.0
600	259	11.9	230	15.2	51	13.0
700	263	11.4	240	15.2	49	13.0
800	261	11.4	240	15.2	47	13.0
900	3	11.3	215	12.2	165	13.0
1000	264	10.9	215	11.2	67	13.0
1100	266	11.7	225	14.2	62	13.0
1200	264	11.7	225	14.2	60	13.0
1300	253	11.3	215	12.2	55	13.0
1355	264	11.9	210	13.2	68	13.0
1402	266	9.8	360	23.5	266	2.0
1415	266	9.1	360	21.7	266	2.0
1430	270	4.9	360	23.3	270	13.0
1455	259	8.8	350	20.9	270	2.0
1610	268	11.9	230	15.2	60	13.0
1700	268	12.9	225	17.3	62	13.0
1800	271	12.3	240	17.8	55	13.0
1900	303	8.2	50	23.3	220	13.0
1945	278	6.2	5	26.4	268	13.0
2000	279	6.2	5	26.4	269	13.0
2015	281	7.0	5	28.4	272	13.0
2030	258	7.4	355	29.4	267	13.0
2200	135	3.2	25	15.2	60	13.0
2300	260	11.4	210	12.2	65	13.0

DATE 5 18 1977

TIME(GMT)	WINDS(M/SEC) MAGNETIC		WINDS(MI/HR) RELATIVE		SHIP(MI/HR)	
	DIR.	SP.	DIR.	SP.	HEAD.	SPEED
0	264	12.7	210	15.2	67	13.0
100	275	10.9	235	13.2	66	13.0
145	311	9.5	280	18.3	68	13.0
210	5	3.3	340	17.3	62	13.0
230	305	2.9	330	10.1	62	13.0
300	258	8.3	180	3.5	78	13.0
540	289	8.4	260	10.1	72	13.0
700	309	7.5	280	11.7	79	13.0
800	308	8.0	275	12.2	79	13.0

DATE: 5 18 1977 CONTINUED

900	326	12.1	275	24.4	80	13.0
1000	50	9.4	340	33.0	82	13.0
1100	25	10.8	260	17.3	157	13.0
1200	14	9.6	315	28.4	84	13.0
1300	45	5.2	340	22.3	88	13.0
1400	9	8.1	315	24.4	84	13.0
1500	46	3.7	345	19.3	85	13.0
1610	112	3.0	10	18.3	82	13.0
1700	156	2.4	20	14.2	82	13.0
1800	161	5.9	40	19.3	82	13.0
1900	54	3.4	350	19.3	81	13.0
2000	44	4.1	345	20.3	81	13.0
2200	27	11.1	325	34.5	80	13.0
2300	359	9.4	295	22.3	98	13.0

DATE 5 19 1977

TIME(GMT)	WINDS(M/SEC) MAGNETIC		WINDS(MI/HR) RELATIVE		SHIP(MI/HR)	
	DIR.	SP.	DIR.	SP.	HEAD.	SPEED
0	353	6.7	300	15.2	102	13.0
100	0	6.8	300	15.7	108	13.0
300	333	7.3	280	11.2	104	13.0
420	344	7.9	280	13.2	110	13.0
500	338	8.0	275	12.2	109	13.0
600	351	7.3	285	12.7	116	13.0
700	357	6.9	295	14.2	112	13.0
800	11	6.8	305	17.3	111	13.0
900	35	5.7	325	20.3	106	13.0
1000	54	5.6	335	22.3	105	13.0
1100	72	5.3	345	23.3	104	13.0
1200	100	5.3	360	24.4	100	13.0
1300	99	4.0	360	21.3	99	13.0
1400	130	3.0	10	18.3	100	13.0
1500	115	2.8	5	18.3	100	13.0
1600	153	2.6	15	16.2	103	13.0
1700	172	4.6	30	18.3	103	13.0
1800	178	5.1	35	18.3	102	13.0
1830	197	6.3	50	17.3	102	13.0
1900	184	5.6	40	18.3	102	13.0
2000	187	3.0	20	16.2	126	13.0
2100	199	2.6	20	14.7	128	13.0
2200	126	1.9	360	16.2	126	13.0
2250	163	2.2	10	16.2	126	13.0

DATE 5 20 1977

TIME(GMT)	WINDS(M/SEC) MAGNETIC		WINDS(MI/HR) RELATIVE		SHIP(MI/HR)	
	DIR.	SP.	DIR.	SP.	HEAD.	SPEED
0	157	2.8	10	17.8	126	13.0
100	141	2.4	5	17.3	124	13.0
200	125	2.8	360	18.3	125	13.0
300	129	2.5	360	17.8	129	13.0
400	160	3.0	10	18.3	130	13.0
500	163	0.8	355	13.2	205	13.0
600	162	3.0	10	18.3	132	13.0
700	168	4.1	15	20.3	131	13.0
800	139	3.7	5	20.3	126	13.0
900	115	4.5	355	22.3	126	13.0
1000	125	4.4	360	22.3	125	13.0
1100	148	5.1	10	23.3	126	13.0
1200	133	4.9	5	23.3	122	13.0
1300	107	4.9	355	23.3	118	13.0
1400	99	4.6	350	22.3	122	13.0
1500	136	4.5	5	22.3	125	13.0
1600	102	4.2	350	21.3	126	13.0
1700	103	4.6	350	22.3	126	13.0
1800	104	5.1	350	23.3	126	13.0
2100	88	6.9	345	27.4	116	13.0
2300	85	6.8	340	26.4	122	13.0

DATE 5 21 1977

TIME(GMT)	WINDS(M/SEC) MAGNETIC		WINDS(MI/HR) RELATIVE		SHIP(MI/HR)	
	DIR.	SP.	DIR.	SP.	HEAD.	SPEED
0	92	6.9	345	27.4	120	13.0
100	84	6.8	340	26.4	121	13.0
200	88	6.0	340	24.4	127	13.0
300	76	7.1	335	26.4	121	13.0
400	73	6.7	335	25.4	119	13.0
500	61	7.9	325	26.4	121	13.0
600	44	7.7	315	23.3	121	13.0
700	30	9.5	305	25.4	115	13.0
800	25	10.5	295	25.4	120	13.0
900	8	12.4	275	25.4	121	13.0
1000	6	13.6	275	28.4	116	13.0
1100	9	16.0	270	33.5	120	13.0
1230	352	14.2	260	26.4	116	13.0
1400	348	14.1	245	23.3	125	13.0
1500	343	13.3	240	20.3	125	13.0
2000	324	10.4	245	13.2	110	13.0
2305	320	8.4	360	20.0	320	2.0
2355	330	8.4	360	20.0	330	2.0

DATE 5 22 1977

TIME(GMT)	WINDS(M/SEC) MAGNETIC		WINDS(MI/HR) RELATIVE		SHIP(MI/HR)	
	DIR.	SP.	DIR.	SP.	HEAD.	SPEED
100	308	11.0	190	10.1	123	13.0
200	303	11.0	180	10.1	123	13.0
300	303	11.0	180	10.1	123	13.0
400	296	13.1	180	15.2	116	13.0
600	297	13.1	180	15.2	117	13.0
700	323	12.9	225	17.3	117	13.0
800	335	13.6	235	20.3	120	13.0
1200	327	9.5	20	22.6	305	2.0
1230	310	9.5	360	22.6	310	2.0
1250	316	9.9	15	23.5	300	2.0
1500	318	8.4	220	5.1	124	13.0
1710	329	8.0	5	19.1	323	2.0
1730	313	8.8	5	20.9	307	2.0
1750	321	8.8	7	20.9	313	2.0
2030	333	3.4	230	4.3	115	2.0
2300	328	6.4	280	7.1	111	13.0

DATE 5 23 1977

TIME(GMT)	WINDS(M/SEC) MAGNETIC		WINDS(MI/HR) RELATIVE		SHIP(MI/HR)	
	DIR.	SP.	DIR.	SP.	HEAD.	SPEED
0	321	6.6	260	3.0	121	13.0
200	334	4.5	310	5.1	122	13.0
300	337	2.8	335	7.1	121	13.0
400	341	3.1	330	7.1	122	13.0
500	348	3.0	330	8.1	121	13.0
600	342	2.3	340	8.1	121	13.0
700	357	2.9	330	9.1	122	13.0
800	13	3.4	325	11.2	124	13.0
900	45	3.2	335	15.2	120	13.0
1000	61	3.0	340	16.2	122	13.0
1100	44	4.7	325	17.3	124	13.0
1200	37	4.2	325	15.2	125	13.0
1330	38	4.2	325	15.2	126	13.0
1500	40	5.3	320	17.3	125	13.0
1600	30	5.2	315	15.2	127	13.0
1700	24	6.8	305	17.3	124	13.0
1915	22	7.6	300	18.3	124	13.0
2200	350	5.2	300	8.1	124	13.0
2240	334	6.1	280	5.1	124	13.0
2300	322	6.9	250	3.0	124	13.0
2330	312	7.3	270	8.1	95	13.0

DATE 5 24 1977

TIME(GMT)	WINDS(M/SEC) MAGNETIC		WINDS(MI/HR) RELATIVE		SHIP(MI/HR)	
	DIR.	SP.	DIR.	SP.	HEAD.	SPEED
0	307	7.6	180	2.0	127	13.0
115	253	4.2	85	7.8	156	2.0
145	246	3.7	75	7.0	158	2.0
300	129	2.3	360	5.2	129	2.0
400	341	2.9	335	6.6	128	13.0
600	180	1.4	35	2.6	124	2.0
600	286	4.2	35	3.0	124	13.0
700	195	9.7	50	27.4	118	13.0
800	196	7.9	45	23.8	120	13.0
900	193	7.7	45	23.3	116	13.0
1000	190	8.1	45	24.4	115	13.0
1100	191	9.2	45	27.4	120	13.0
1200	180	8.7	40	27.4	115	13.0
1255	233	9.0	75	18.3	120	13.0
1330	195	9.2	45	27.4	124	13.0
1400	191	8.7	40	27.4	126	13.0
1500	193	8.4	40	26.4	126	13.0
1600	195	8.0	40	25.4	127	13.0
1800	187	7.5	35	25.4	126	13.0
1900	187	5.6	30	21.3	126	13.0
2000	191	4.9	30	19.3	125	13.0
2100	192	4.9	30	19.3	126	13.0
2200	192	5.1	30	19.8	127	13.0
2300	206	6.7	45	20.3	123	13.0

DATE 5 25 1977

TIME(GMT)	WINDS(M/SEC) MAGNETIC		WINDS(MI/HR) RELATIVE		SHIP(MI/HR)	
	DIR.	SP.	DIR.	SP.	HEAD.	SPEED
0	204	7.0	45	21.3	123	13.0
100	202	7.7	45	23.3	125	13.0
300	202	7.4	45	22.3	123	13.0
400	216	7.7	55	20.3	123	13.0
500	196	6.6	40	21.5	122	13.0
600	193	7.6	40	24.4	124	13.0
700	217	8.2	50	23.3	134	13.0
800	193	8.8	45	26.4	120	13.0
900	198	8.8	45	26.4	125	13.0
1000	195	8.7	40	27.4	130	13.0
1100	199	8.8	45	26.4	126	13.0
1200	197	8.4	40	26.4	130	13.0
1300	199	8.0	40	25.4	131	13.0
1400	200	8.4	40	26.4	133	13.0
1500	200	8.0	40	25.4	132	13.0
1600	200	7.7	45	23.3	123	13.0
1800	207	7.0	45	21.3	126	13.0
2015	210	5.6	40	18.3	128	13.0
2100	210	5.6	40	18.3	128	13.0
2200	213	5.6	40	18.3	131	13.0
2230	238	5.4	240	10.4	360	0.5

DATE 5 26 1977

TIME(GMT)	WINDS(M/SEC) MAGNETIC		WINDS(MI/HR) RELATIVE		SHIP(MI/HR)	
	DIR.	SP.	DIR.	SP.	HEAD.	SPEED
0	207	5.1	35	18.3	131	13.0
200	215	5.1	40	16.7	128	13.0
300	222	5.5	45	16.2	128	13.0
400	220	4.2	35	15.2	132	13.0
500	228	4.1	35	14.7	138	13.0
600	226	3.7	35	13.2	128	13.0
700	216	3.9	35	14.2	123	13.0
800	217	3.3	30	13.7	126	13.0
850	206	2.3	20	13.7	127	13.0
1000	229	3.7	355	20.3	242	13.0
1110	235	2.1	340	9.1	4	13.0
1200	229	3.0	330	8.1	2	13.0
1300	199	4.3	30	17.3	126	13.0
1400	206	3.8	30	15.7	126	13.0
1500	202	1.7	15	13.2	126	13.0
1540	188	1.2	10	13.2	124	13.0
1700	278	1.7	10	8.1	124	13.0
1900	320	1.5	355	8.1	126	13.0
2200	1	3.7	320	9.1	126	13.0
2300	6	4.2	315	10.1	126	13.0

DATE 5 27 1977

TIME(GMT)	WINDS(M/SEC) MAGNETIC		WINDS(MI/HR) RELATIVE		SHIP(MI/HR)	
	DIR.	SP.	DIR.	SP.	HEAD.	SPEED
0	6	5.3	305	11.2	125	13.0
100	2	6.8	290	12.2	125	13.0
200	18	5.6	310	14.7	121	13.0
300	22	6.3	305	15.7	126	13.0
400	12	8.2	290	17.3	124	13.0
500	17	8.5	290	18.3	127	13.0
600	11	10.0	285	21.3	120	13.0
700	5	9.8	280	19.3	121	13.0
800	359	9.9	275	18.3	120	13.0
905	348	10.3	330	33.5	34	13.0
1000	338	10.7	325	33.5	31	13.0
1100	338	10.7	325	33.5	31	13.0
1200	339	7.4	355	29.4	348	13.0
1300	332	7.5	350	29.4	350	13.0
1430	317	8.8	340	31.5	350	13.0
1500	0	11.7	200	12.2	170	13.0
1700	352	9.9	185	7.6	170	13.0
1900	347	16.1	255	30.4	112	13.0
2000	331	9.4	255	12.2	113	13.0
2200	305	6.8	260	4.1	102	13.0
2300	306	7.8	245	5.6	103	13.0

DATE 5 28 1977

TIME(GMT)	WINDS(M/SEC) MAGNETIC		WINDS(MI/HR) RELATIVE		SHIP(MI/HR)	
	DIR.	SP.	DIR.	SP.	HEAD.	SPEED
0	309	6.2	270	3.0	108	13.0
100	317	4.8	305	4.6	108	13.0
300	10	6.8	305	17.3	110	13.0
400	21	2.7	335	13.2	110	13.0
500	207	2.5	25	11.2	100	13.0
600	161	3.0	20	16.2	100	13.0
700	118	7.4	360	29.4	118	13.0

DATE 5 30 1977

TIME(GMT)	WINDS(M/SEC) MAGNETIC		WINDS(MI/HR) RELATIVE		SHIP(MI/HR)	
	DIR.	SP.	DIR.	SP.	HEAD.	SPEED
2000	235	7.0	360	28.4	235	13.0
2100	279	10.0	75	21.3	170	13.0
2200	270	10.2	80	20.3	156	13.0
2300	273	9.9	85	18.3	152	13.0

DATE 5 31 1977

TIME(GMT)	WINDS(M/SEC) MAGNETIC		WINDS(MI/HR) RELATIVE		SHIP(MI/HR)	
	DIR.	SP.	DIR.	SP.	HEAD.	SPEED
0	273	9.9	85	18.3	152	13.0
100	234	9.8	125	10.1	80	13.0
200	256	9.7	170	7.1	80	13.0
300	244	10.3	120	12.2	95	13.0
400	243	8.9	130	7.1	83	13.0
500	272	11.4	180	11.2	92	13.0
600	273	11.0	180	10.1	93	13.0
800	298	10.4	75	22.3	190	13.0
900	312	13.0	95	24.4	190	13.0
1000	301	9.1	260	12.2	80	13.0
1100	57	8.5	280	15.2	179	13.0
1200	317	8.2	290	17.3	69	13.0
1300	306	9.3	275	16.2	70	13.0
1400	295	8.4	260	10.1	78	13.0
1445	298	7.0	270	7.1	84	13.0
1700	267	8.3	245	7.1	62	13.0
1900	242	9.7	180	7.1	62	13.0
2000	208	11.8	120	16.2	63	13.0
2100	221	9.6	130	9.1	63	13.0
2105	202	7.5	90	15.6	105	2.0
2130	228	11.1	35	26.1	190	2.0
2155	222	11.8	30	27.8	190	2.0
2230	233	10.5	170	9.1	58	13.0

DATE 6 1 1977

TIME(GMT)	WINDS(M/SEC) MAGNETIC		WINDS(MI/HR) RELATIVE		SHIP(MI/HR)	
	DIR.	SP.	DIR.	SP.	HEAD.	SPEED
0	208	11.3	125	14.2	58	13.0
100	213	12.1	135	15.2	58	13.0
300	215	13.1	140	17.3	58	13.0
400	219	11.5	140	13.2	60	13.0
500	213	10.7	130	12.2	59	13.0
600	219	11.5	140	13.2	60	13.0
800	233	10.1	170	8.1	57	13.0
845	238	4.9	360	23.3	238	13.0
845	238	8.4	360	20.0	238	2.0
915	226	8.4	350	20.0	237	2.0
1100	241	11.0	180	10.1	61	13.0
1200	241	9.9	180	7.6	61	13.0
1300	265	9.8	235	10.1	59	13.0
1410	244	5.1	5	12.2	238	2.0
1430	246	4.8	5	11.3	240	2.0
1445	124	0.5	355	11.2	238	13.0
1545	177	2.8	25	13.7	92	13.0
1630	168	1.7	15	13.2	92	13.0
1800	153	2.0	15	14.2	88	13.0
1900	181	1.0	10	11.7	87	13.0
2000	176	1.6	15	12.2	87	13.0
2100	179	3.3	30	13.7	88	13.0
2130	188	3.1	30	12.2	87	13.0
2200	245	8.8	115	8.6	93	13.0
2300	192	4.3	40	13.7	93	13.0

DATE 6 2 1977

TIME(GMT)	WINDS(M/SEC) MAGNETIC		WINDS(MI/HR) RELATIVE		SHIP(MI/HR)	
	DIR.	SP.	DIR.	SP.	HEAD.	SPEED
0	186	3.7	34	13.7	92	13.0
30	201	3.0	30	11.2	92	13.0
100	204	2.0	20	10.7	92	13.0
200	205	1.5	15	10.7	92	13.0
300	338	0.5	355	11.2	92	13.0
400	62	1.2	355	14.2	92	13.0
500	49	0.8	355	13.2	91	13.0
600	275	0.2	360	11.2	95	13.0
700	164	0.6	5	12.2	95	13.0
800	168	1.1	10	12.7	95	13.0
900	163	1.1	10	12.7	90	13.0
1000	322	1.1	350	10.1	90	13.0

DATE: 6 2 1977 CONTINUED

1100	310	1.8	345	8.6	90	13.0
1200	306	3.9	320	6.1	90	13.0
1300	320	5.4	300	9.1	90	13.0
1400	336	6.2	300	13.2	91	13.0
1445	329	7.1	290	13.2	90	13.0
1600	335	7.8	290	15.7	90	13.0
1800	329	7.8	285	14.2	90	13.0
1900	335	8.7	285	17.3	90	13.0
2000	317	6.6	290	11.2	83	13.0
2100	297	7.0	270	7.1	83	13.0
2215	307	5.2	300	7.6	83	13.0
2300	23	7.9	325	26.4	83	13.0

DATE 6 3 1977

TIME(GMT)	WINDS(M/SEC) MAGNETIC		WINDS(MI/HR) RELATIVE		SHIP(MI/HR)	
	DIR.	SP.	DIR.	SP.	HEAD.	SPEED
0	359	10.2	305	27.4	82	13.0
100	4	7.6	315	22.8	82	13.0
200	11	7.3	320	23.3	82	13.0
300	9	6.9	320	22.3	82	13.0
400	0	2.4	340	7.6	144	13.0
500	348	3.3	335	5.1	145	13.0
600	5	3.1	330	7.1	146	13.0
700	347	5.1	300	3.0	145	13.0
800	351	5.5	290	3.5	146	13.0
900	350	8.5	240	7.1	146	13.0
1000	8	8.1	265	10.1	148	13.0
1100	5	7.3	270	8.1	148	13.0
1140	326	6.6	355	15.6	332	2.0
1210	320	6.8	350	16.1	331	2.0
1340	327	9.8	355	23.5	332	2.0
1400	328	10.9	355	26.1	333	2.0
1420	321	10.9	350	26.1	332	2.0
1440	306	7.3	345	28.4	333	13.0
1600	334	13.1	190	15.2	148	13.0
1700	344	12.3	210	14.2	148	13.0
1800	343	11.0	210	11.2	148	13.0
1900	341	9.3	215	7.1	147	13.0
2000	336	9.6	200	7.1	148	13.0
2100	336	9.6	200	7.1	148	13.0
2110	325	8.8	350	20.9	336	2.0
2130	325	8.0	350	19.1	336	2.0
2150	314	9.2	340	21.7	336	2.0
2205	327	11.0	180	10.1	147	13.0
2300	334	10.8	200	10.1	145	13.0

DATE 6 4 1977

TIME(GMT)	WINDS(M/SEC) MAGNETIC		WINDS(MI/HR) RELATIVE		SHIP(MI/HR)	
	DIR.	SP.	DIR.	SP.	HEAD.	SPEED
0	331	11.0	190	10.1	146	13.0
55	337	15.4	200	21.3	144	13.0
110	320	8.8	350	20.9	331	2.0
130	323	9.5	355	22.6	328	2.0
200	335	10.1	205	8.6	144	13.0
300	334	11.7	200	12.2	144	13.0
400	327	9.3	190	6.1	143	13.0
500	326	8.4	190	4.1	143	13.0
610	346	7.5	295	16.5	57	2.0
650	336	8.7	285	19.1	57	2.0
810	304	8.0	360	19.1	304	2.0
850	292	8.0	350	19.1	303	2.0
1000	311	9.3	145	7.1	145	13.0
1100	323	9.7	170	7.1	147	13.0
1200	322	9.7	170	7.1	146	13.0
1300	327	9.3	180	6.1	147	13.0
1355	327	9.3	180	6.1	147	13.0
1410	305	9.9	345	23.5	321	2.0
1430	301	9.2	340	21.7	323	2.0
1450	294	8.5	335	20.0	322	2.0
1505	312	9.7	145	8.1	147	13.0
1545	312	9.7	145	8.1	147	13.0
1700	331	9.7	190	7.1	147	13.0
1800	330	9.7	190	7.1	146	13.0
1900	334	9.2	200	6.1	146	13.0
1955	321	10.3	270	18.3	85	13.0
2010	312	8.0	350	19.1	323	2.0
2030	317	7.7	355	18.2	323	2.0
2030	317	7.7	355	18.2	323	2.0
2050	317	7.3	355	17.4	323	2.0
2105	319	9.7	270	16.2	86	13.0
2230	317	10.1	265	16.2	87	13.0
2315	309	9.1	260	12.2	88	13.0
2355	315	9.7	265	15.2	87	13.0

DATE 6 5 1977

TIME(GMT)	WINDS(M/SEC) MAGNETIC		WINDS(MI/HR) RELATIVE		SHIP(MI/HR)	
	DIR.	SP.	DIR.	SP.	HEAD.	SPEED
10	305	10.2	350	24.3	316	2.0
30	312	10.9	355	26.1	317	2.0
50	307	9.8	350	23.5	318	2.0
200	326	11.1	270	20.3	88	13.0
300	350	7.5	270	15.6	87	2.0
415	309	6.3	335	14.8	337	2.0
450	299	6.2	350	14.8	310	2.0
600	318	9.0	270	14.2	88	13.0
700	313	9.1	265	13.2	88	13.0
830	312	6.6	360	15.6	312	2.0
850	294	7.0	350	16.5	305	2.0
1100	302	9.4	250	11.2	88	13.0
1200	308	9.6	255	12.7	89	13.0
1200	308	9.6	255	12.7	89	13.0
1300	345	6.2	265	12.2	88	2.0
1355	349	5.9	270	11.7	88	2.0
1410	243	7.6	300	18.3	345	13.0
1430	277	3.9	345	19.8	315	13.0
1450	279	8.1	300	19.8	18	13.0
1545	311	8.7	250	9.1	100	13.0
1815	312	6.1	315	18.3	40	13.0
1900	303	6.3	310	17.3	38	13.0
2000	320	3.7	330	15.2	42	13.0
2055	302	7.3	70	14.2	184	13.0
2200	322	4.7	325	17.3	42	13.0
2215	317	4.3	325	15.7	42	13.0
2300	317	5.6	320	18.3	39	13.0

DATE 6 6 1977

TIME(GMT)	WINDS(M/SEC) MAGNETIC		WINDS(MI/HR) RELATIVE		SHIP(MI/HR)	
	DIR.	SP.	DIR.	SP.	HEAD.	SPEED
0	302	6.0	310	16.2	40	13.0
100	306	6.6	310	18.3	39	13.0
200	310	6.9	310	19.3	40	13.0
300	319	6.7	315	20.3	42	13.0
400	334	6.8	325	23.3	38	13.0
500	318	7.9	310	22.3	42	13.0
600	338	6.8	325	23.3	42	13.0
700	321	7.4	315	22.3	40	13.0
800	314	8.2	310	23.3	37	13.0
900	313	9.0	310	25.4	33	13.0
1030	313	8.6	310	24.4	34	13.0
1300	303	9.8	295	23.3	41	13.0
1410	298	10.1	290	22.8	41	13.0
1630	271	9.4	295	22.3	10	13.0
1740	267	11.0	290	25.4	7	13.0
1800	266	9.1	295	21.3	7	13.0
1820	255	8.5	290	18.3	5	13.0
1900	258	8.9	290	19.3	6	13.0
2000	293	3.2	335	15.2	8	13.0
2100	244	3.3	325	9.1	9	13.0
2150	153	1.3	10	9.6	17	13.0
2210	147	1.0	5	9.6	354	13.0
2230	153	1.1	5	9.1	354	13.0
2300	174	0.6	360	10.1	354	13.0

DATE 6 7 1977

TIME(GMT)	WINDS(M/SEC) MAGNETIC		WINDS(MI/HR) RELATIVE		SHIP(MI/HR)	
	DIR.	SP.	DIR.	SP.	HEAD.	SPEED
330	271	2.0	345	14.2	336	13.0
400	279	3.3	340	17.3	336	13.0
430	297	6.0	340	24.4	336	13.0
500	294	4.1	345	20.3	331	13.0
600	183	0.6	355	10.7	315	13.0
700	313	9.1	265	13.2	88	13.0

Appendix B

LOG OF TOTAL PARTICLE CONCENTRATION, VISIBILITY AND SCATTERING COEFFICIENT

DATE: 5 15 1977

TIME (GMT)	AITKEN COUNT (/CM↑3)	BSCAT (10↑-4/M)	VISIBILITY (KM)
400		0.8	64
500	4700	0.5	80
600	2700	0.5	80
700	3400	0.5	80
800	4000	0.6	77
900	4700	0.5	80
1000	6000	0.5	80
1100	6400	0.7	72
1200	5400	0.5	80
1300	6600	0.6	72
1400	10000	0.6	80
1500	5400	0.5	80
1600	8000	0.6	80
1700	10000	0.9	48
1800	11500	0.7	63
1900	9000	0.5	80
2000	7000	0.4	80
2100	7400	0.5	80
2200	6000	0.5	80
2300	5400	0.5	80

DATE: 5 16 1977

TIME (GMT)	AITKEN COUNT (/CM↑3)	BSCAT (10↑-4/M)	VISIBILITY (KM)
0	5300	0.5	80
100	7000	0.4	80
200		0.3	80
300	3700	0.3	80
400	3300	0.3	80
500	3400	0.4	80
600	3600	0.3	80
700	4700	0.4	80
800	4300	0.4	80
900	12000	0.5	80
1000	20000	0.5	80
1100	5000	0.5	80
1200	6000	0.4	80
1300	4300	0.4	80
1400		0.7	64
1500	11000	0.7	72
1600	4000	0.6	80
1700	4000	0.5	80

DATE: 5 17 1977

TIME (GMT)	AITKEN COUNT (/CM↑3)	BSCAT (10↑-4/M)	VISIBILITY (KM)
1355	60000	1.7	26
1405	4500	1.3	37
1415	5000	1.4	32
1430	5000	1.5	32
1455	4500	1.5	32
1900	4300	1.4	34
1945	5000	1.4	32
2000	5000	1.4	32
2015	5000	1.5	31
2030	6800	1.5	31

DATE: 5 18 1977

TIME (GMT)	AITKEN COUNT (/CM↑3)	BSCAT (10↑-4/M)	VISIBILITY (KM)
145	5200	1.8	27
210	4300	1.6	29
230	4700	1.7	27
500	4700	1.7	27
520		1.7	27
540	4300	1.7	27
600	4300	1.6	29
700	4200	1.6	28
800	3000	1.8	26
830	2800	1.9	25
900	3700	2.2	22
909			
930	2700	2.4	19
1000	2000	2.2	21
1100	1800	1.4	31
1200	1400	0.6	72
1300	3000	0.6	72
1400	9000	0.5	72
1500	2100	0.4	80
1610	12000	0.3	80
1700	10000	0.4	80
1800	9000	0.4	80
1900	4700	0.4	80
2000	2200	0.4	80
2200	1500	0.3	80
2300	2400	0.4	80

DATE: 5 19 1977

TIME (GMT)	AITKEN COUNT (/CM↑3)	BSCAT (10↑-4/M)	VISIBILITY (KM)
0	2600	0.4	80
100	3200	0.5	80
300	3200	0.5	80
420	2000	0.5	80
440	2000	0.5	80
500	2300	0.5	80
600	2100	0.5	80
640	2200	0.5	80
700	1700	0.5	80
800	1800	0.5	80
900	1800	0.4	80
1000	1700	0.3	80
1100	1200	0.3	80
1200	500	0.3	80
1300	500	0.3	80
1400	450	0.3	80
1500	1300	0.3	80
1600	1200	0.4	80
1700	3500	0.3	80
1800	1350	0.4	80
1830	1200	0.4	80
1900	1500	0.5	80
1930	1500	0.5	80
2000	960	0.4	80
2100	900	0.4	80
2200	900	0.4	80
2250	1500	0.4	80

DATE: 5 20 1977

TIME (GMT)	AITKEN COUNT (/CM↑3)	BSCAT (10↑-4/M)	VISIBILITY (KM)
0	850	0.4	80
100	1000	0.5	80
130	1200	0.4	80
200	0	0.5	80
300	1100	0.5	80
400	1100	0.6	80
500	1050	0.7	80
600	920	0.5	80
700	550	0.5	80
800	450	0.5	80
900	400	0.5	80
1000	250	0.5	80
1100	200	0.3	80
1200	200	0.5	80
1300	400	0.5	80
1400	300	0.5	80
1500	600	0.4	80
1600	200	0.4	80
1700	300	0.4	80
1800	750	0.5	80
1930	300	0.5	80
2100	300	0.6	72
2300	450	0.7	64

DATE: 5 21 1977

TIME (GMT)	AITKEN COUNT (/CM↑3)	BSCAT (10↑-4/M)	VISIBILITY (KM)
0	350	0.7	64
100	300	0.8	60
200	330	0.6	72
300	300	0.6	64
400	350	0.7	72
430	300	0.6	72
500	250	0.6	77
600	300	0.6	77
700	350	0.6	77
800	350	0.6	80
900	650	0.5	80
1000	300	0.4	80
1100	400	0.4	80
1230		0.4	80
2010			
2300	400	0.5	
2315	350	0.5	80
2335	350	0.5	80
2355	280	0.5	80

DATE: 5 22 1977

TIME (GMT)	AITKEN COUNT (/CM↑3)	BSCAT (10↑-4/M)	VISIBILITY (KM)
1200	350	0.4	
1230	450	0.4	
1250	400	0.4	80
1710	200	0.2	80
1730	250	0.2	80
1750	300	0.3	80
2300	250	0.3	80

DATE: 5 23 1977

TIME (GMT)	AITKEN COUNT (/CM↑3)	BSCAT (10↑-4/M)	VISIBILITY (KM)
200	270	0.3	80
300	350	0.3	80
400	300	0.3	80
500	250	0.3	80
600	250	0.2	80
700	400	0.2	80
800	400	0.2	80
900	600	0.2	80
1000	550	0.2	80
1100	400	0.3	80

DATE: 5 23 1977 CONTINUED

1200	400	0.3	80
1330	450	0.4	80
1500	400	0.4	80
1600	650	0.5	80
1700	350	0.6	80
1745	305	0.6	72
1915	200	0.3	80
2200	200	0.2	80
2240	-	0.2	80
2330	200	0.2	80

DATE: 5 24 1977

TIME (GMT)	AITKEN COUNT (/CM↑3)	BSCAT (10↑-4/M)	VISIBILITY (KM)
115	200	0.3	80
145	200	0.3	80
300	270	0.2	80
400	200	0.3	80
430	0	0.3	80
500	200	0.4	80
600	200	0.3	80
700	600	3.0	16
800	600	1.9	26
900	400	1.1	43
1000	300	0.4	80
1100	350	0.3	80
1200	250	0.3	80
1255	300	0.6	80
1330		0.3	80
1400	230	0.3	80
1500		0.3	80
1600		0.3	80
1800	350	0.3	80
1900		0.3	80
2000	600	0.3	
2100	430	0.3	80
2200	400	0.3	80
2300	450	0.4	80

DATE: 5 25 1977

TIME (GMT)	AITKEN COUNT (/CM↑3)	BSCAT (10↑-4/M)	VISIBILITY (KM)
0	420	0.3	80
100	500	0.5	80
200	520	0.5	
300	600	0.6	80
400	580	0.5	80

DATE: 5 25 1978 CONTINUED

500	650	0.5	80
600	1000	0.7	72
700	1200	0.7	64
800	950	0.7	64
900	1100	0.7	72
1000	1200	0.7	64
1100	1200	0.7	64
1200	1000	0.6	72
1300	1200	0.6	
1400	100	0.6	72
1500	970	0.6	72
1600	900	0.7	64
1630	1150	0.7	69
1800	740	0.5	80
2015	800	0.6	72
2100	860	0.6	
2200	900	0.7	69
2230		0.7	64

DATE: 5 26 1977

TIME (GMT)	AITKEN COUNT (/CM↑3)	BSCAT (10↑-4/M)	VISIBILITY (KM)
0	1000	0.7	69
200	1000	0.8	60
300	1300	1.0	48
400	1380	1.1	42
500	1250	1.2	39
600	1300	1.1	39
700	1200	1.1	45
800	1250	1.1	45
850	1100	1.0	45
1000	1200	1.0	48
1030	1350	1.0	45
1110	1200	0.9	51
1200	1250	0.9	48
1300	1350	1.0	45
1400	880	1.0	47
1500	760	0.9	48
1540	700	0.9	47
1700	1001	0.9	48
1900	1000	0.9	48
2000	830	0.9	48
2030	1100	1.0	45
2045	800		
2100	760	1.0	45
2130	720	1.0	45
2200	700	1.0	43
2300	680	1.0	44

DATE: 5 27 1977

TIME (GMT)	AITKEN COUNT (/CM↑3)	BSCAT (10↑-4/M)	VISIBILITY (KM)
0	730	1.0	45
100	650	0.9	55
200	800	1.4	54
300	760	1.6	29
400	800	1.5	32
500	760	2.1	23
600	800	2.1	23
700	760	2.0	23
800	1100	1.9	27
905	3000	2.2	21
1000	3000	2.7	19
1100	2300	2.8	17
1200	4500	2.6	19
1300	2500	2.6	18
1330	2200	2.6	18
1430	2700	2.6	18

DATE: 5 28 1977

TIME (GMT)	AITKEN COUNT (/CM↑3)	BSCAT (10↑-4/M)	VISIBILITY (KM)
0	4700	2.2	22
100	4800	1.7	27
300	2300	1.7	27
400	5400	4.7	10
500	3500	2.7	16
600	2500	2.0	23
700	2800	1.9	'25

DATE: 5 30 1977

TIME (GMT)	AITKEN COUNT (/CM↑3)	BSCAT (10↑-4/M)	VISIBILITY (KM)
2000	2900	0.7	64
2100	2300	0.7	64
2200	1500	0.6	80
2300	1700	0.6	76
2330	1400	0.6	80

DATE: 5 31 1977

TIME (GMT)	AITKEN COUNT (/CM↑3)	BSCAT (10↑-4/M)	VISIBILITY (KM)
0	1900	0.6	76
400			
800	2400	0.6	80
900	2100	0.6	80
1100	2100	0.6	80
1200	2700	0.6	77
1300	3300	0.7	64
1400	2700	0.7	64
1445	2400	0.7	61
1600		0.7	61
2110	1300	0.6	77
2130	1300	0.6	76
2155	1550	0.6	71

DATE: 6 1 1977

TIME (GMT)	AITKEN COUNT (/CM↑3)	BSCAT (10↑-4/M)	VISIBILITY (KM)
845	1800	0.9	48
915	1500	0.8	56
1410	1000	0.7	61
1430	900	0.6	74
1445	1100	0.6	69
1545	1100	0.6	77
1630	1150	0.6	77
1800	1600	0.7	61
1900	1350	0.8	53
2000	1350	0.8	56
2100	1900	1.2	37
2130	1600	1.6	29
2230	900	1.4	32
2300	900	1.3	34
			32

DATE: 6 2 1977

TIME (GMT)	AITKEN COUNT (/CM↑3)	BSCAT (10↑-4/M)	VISIBILITY (KM)
0	1700	1.4	32
30	1150	1.2	39
100	1100	1.1	43
200	900	1.3	37
300	920	1.3	35
400	1400	1.2	40
500	1600	1.1	43
600	1900	1.2	42

DATE: 6 2 1977 CONTINUED

700	1200	1.2	40
800	1400	1.2	40
900	1300	1.1	40
1000	1300	1.1	45
1100	1300	1.1	40
1200	1050	1.1	40
1300	900	1.1	42
1400	900	1.0	47
1445	870	1.1	43
1600	1400	1.0	47
1800	900	1.0	45
1900	1200	1.0	45
2000	1500	1.1	40
2100	1000	1.2	37
2215	1150	1.4	51
2300	750	0.6	48
2330		0.6	

DATE: 6 3 1977

TIME (GMT)	AITKEN COUNT (/CM↑3)	BSCAT (10↑-4/M)	VISIBILITY (KM)
0	1150	0.6	72
100	1050	0.7	64
200	1400	1.0	45
300	1350	0.8	56
400	1500	1.7	27
500	1600	1.6	29
600	1300	1.4	34
700	1400	1.4	34
800	1300	1.2	37
1140	1600	2.2	21
1200	1600	1.9	23
1340	3400	1.0	45
1400	1800	0.7	61
1420	1100	0.6	68
1440	1300	0.7	64
2110	1150	0.7	64
2130	1000	0.7	64
2150	1000	0.7	61

DATE: 6 4 1977

TIME (GMT)	AITKEN COUNT (/CM↑3)	BSCAT (10↑-4/M)	VISIBILITY (KM)
110	750	0.6	64
130	800	0.6	69
610	1100	0.7	64
650	1600	0.7	61
810	1050	0.7	64
850	1000	0.7	61
1410	1100	0.9	48
1430	1000	1.0	43
1450	1100	0.9	47
1700			
2010	1700	2.0	23
2030	1800	2.0	23
2050	2000	1.9	24
2230	1850	1.8	27
2315	1500	2.0	23
2355	1550	1.9	23

DATE: 6 5 1977

TIME (GMT)	AITKEN COUNT (/CM↑3)	BSCAT (10↑-4/M)	VISIBILITY (KM)
10	1550	1.8	25
30	1350	1.2	37
50	1250	0.9	66
200	1400	1.1	45
300	1500	1.2	37
400	2000	1.1	37
415	2200	1.2	37
450	3200	1.4	32
600	3000	1.5	31
700	3500	1.6	29
810	2700	1.7	27
830	2200	1.7	27
850	2000	1.5	31
1355	1700	1.6	29
1410	1900	1.5	30
1430	1550	1.6	29
1450	1500	1.6	29
1815	1500	1.2	37
1900	1550	1.4	32
2000	1500	1.4	32
2055	1700	1.8	26
2200	1600	1.3	34
2215	1150	0.9	51
2300	1250	0.7	69

DATE: 6 6 1977

TIME (GMT)	AITKEN COUNT (/CM↑3)	BSCAT (10↑-4/M)	VISIBILITY (KM)
0	1150	0.8	55
100	1250	1.0	48
200	1350	1.3	35
300	1800	1.3	35
400	1600	1.1	42
500	2000	1.1	43
600	2200	1.0	45
700	2200	1.1	42
800	2300	1.2	40
900	2300	1.2	39
1030	2400	1.4	32
1300	2500	1.4	52
1410	2200	1.4	32
1630	1750	1.4	32
1740	1800	1.4	32
1800	1850	1.4	33
1820	1900	1.4	32
1900	2100	1.8	25
2000	3800	1.7	27
2100	2300	1.3	33
2150	2400	1.6	31
2210	3000	1.6	29
2230	4500	1.6	29
2300	2000	1.6	30

DATE: 6 7 1977

TIME (GMT)	AITKEN COUNT (/CM↑3)	BSCAT (10↑-4/M)	VISIBILITY (KM)
330	5000	1.8	27
400	4500	1.4	32
430	2500	1.8	27
500	2100	1.9	24
600	12000	2.9	15

Appendix C

LOGS OF TEMPERATURES AND MIXING RATIO

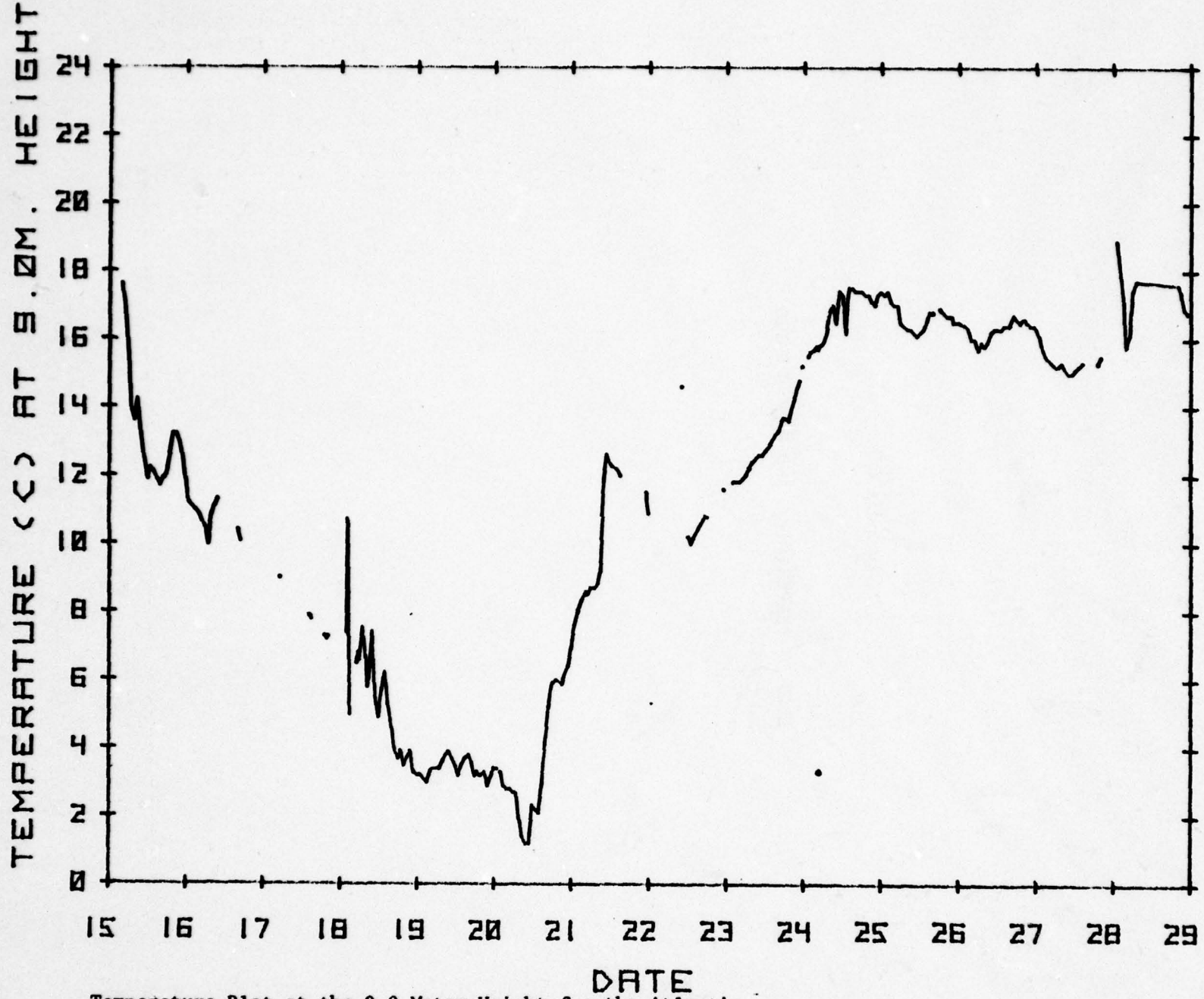

Temperature Plot at the 9.0 Meter Height for the Atlantic Portion of the NRL Cruise, 77-16-04

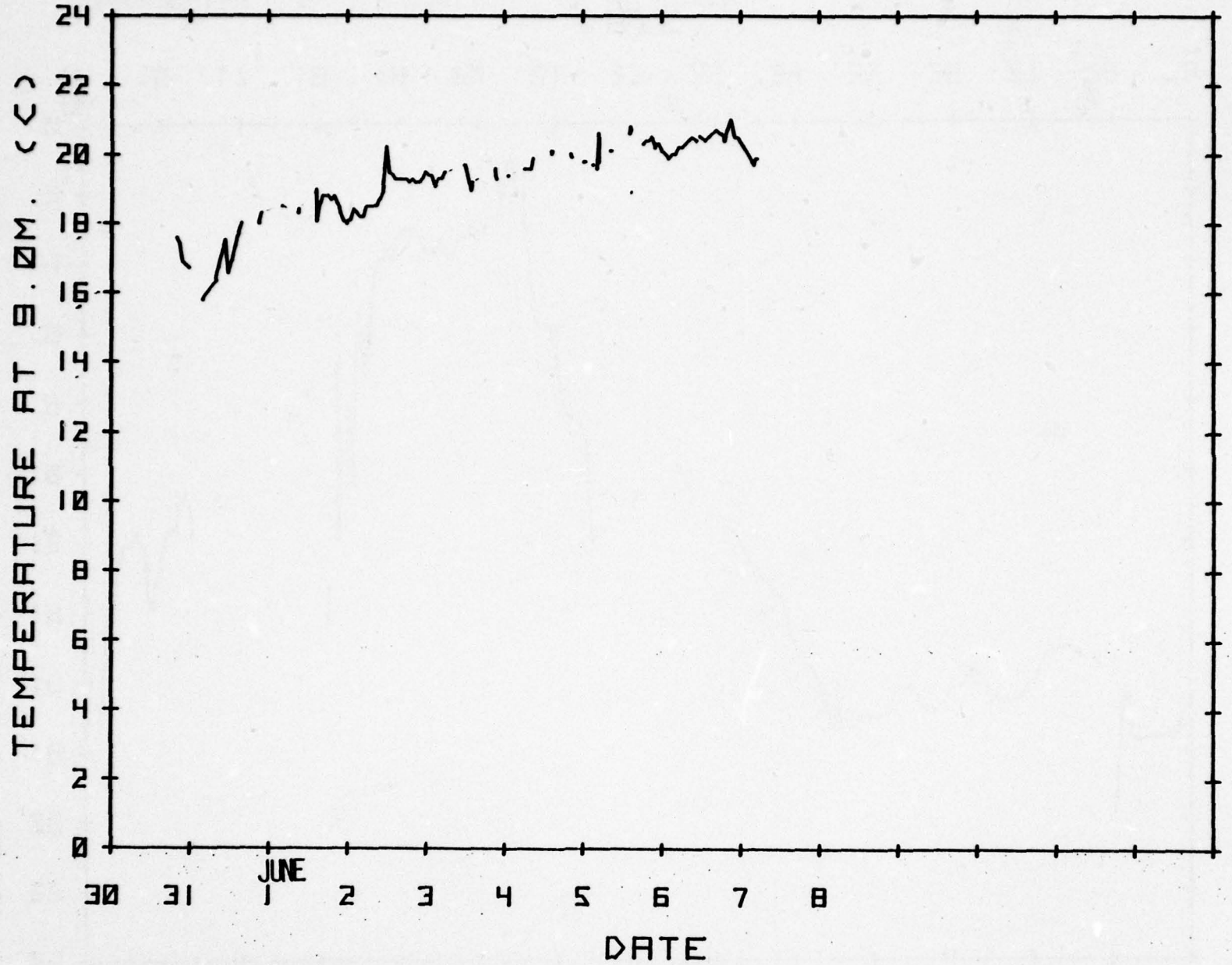

Temperature Plot at the 9.0 Meter Height for the Mediterranean Portion of the NRL Cruise, 77-16-04

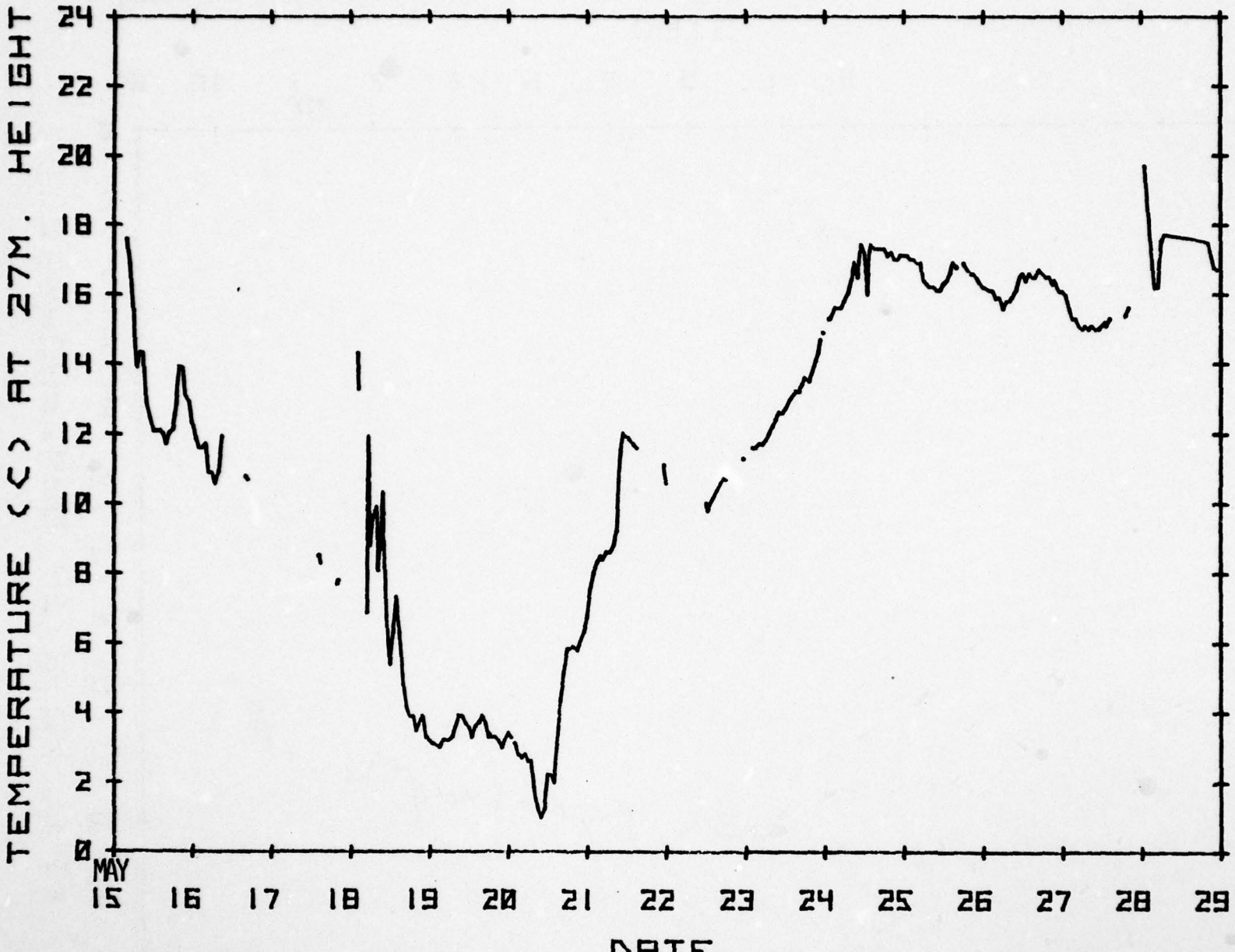

Temperature Plot at the 27.0 Meter Height for the Atlantic Portion of the NRL Cruise, 77-16-04

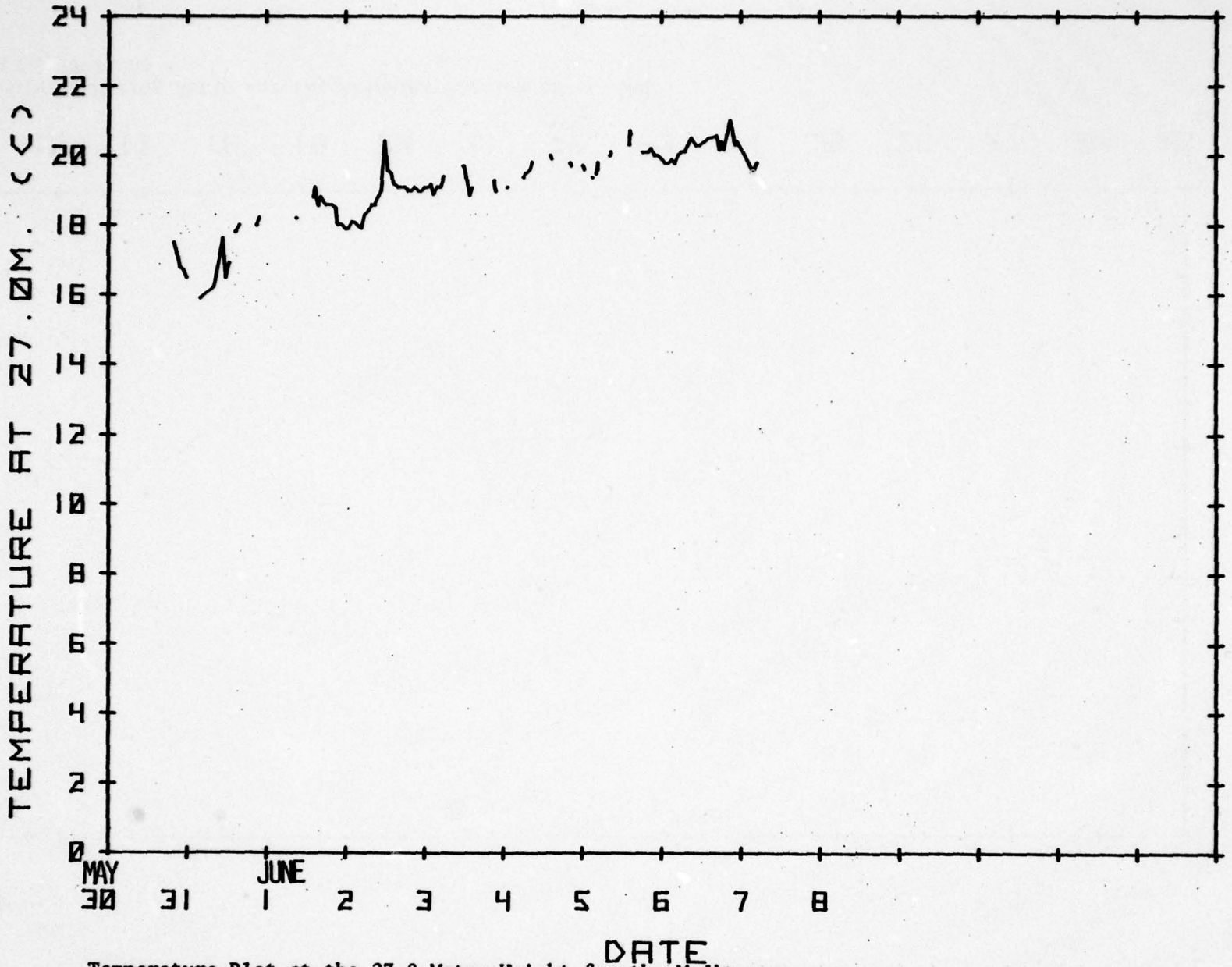

Temperature Plot at the 27.0 Meter Height for the Mediterranean Portion of the NRL Cruise, 77-16-04

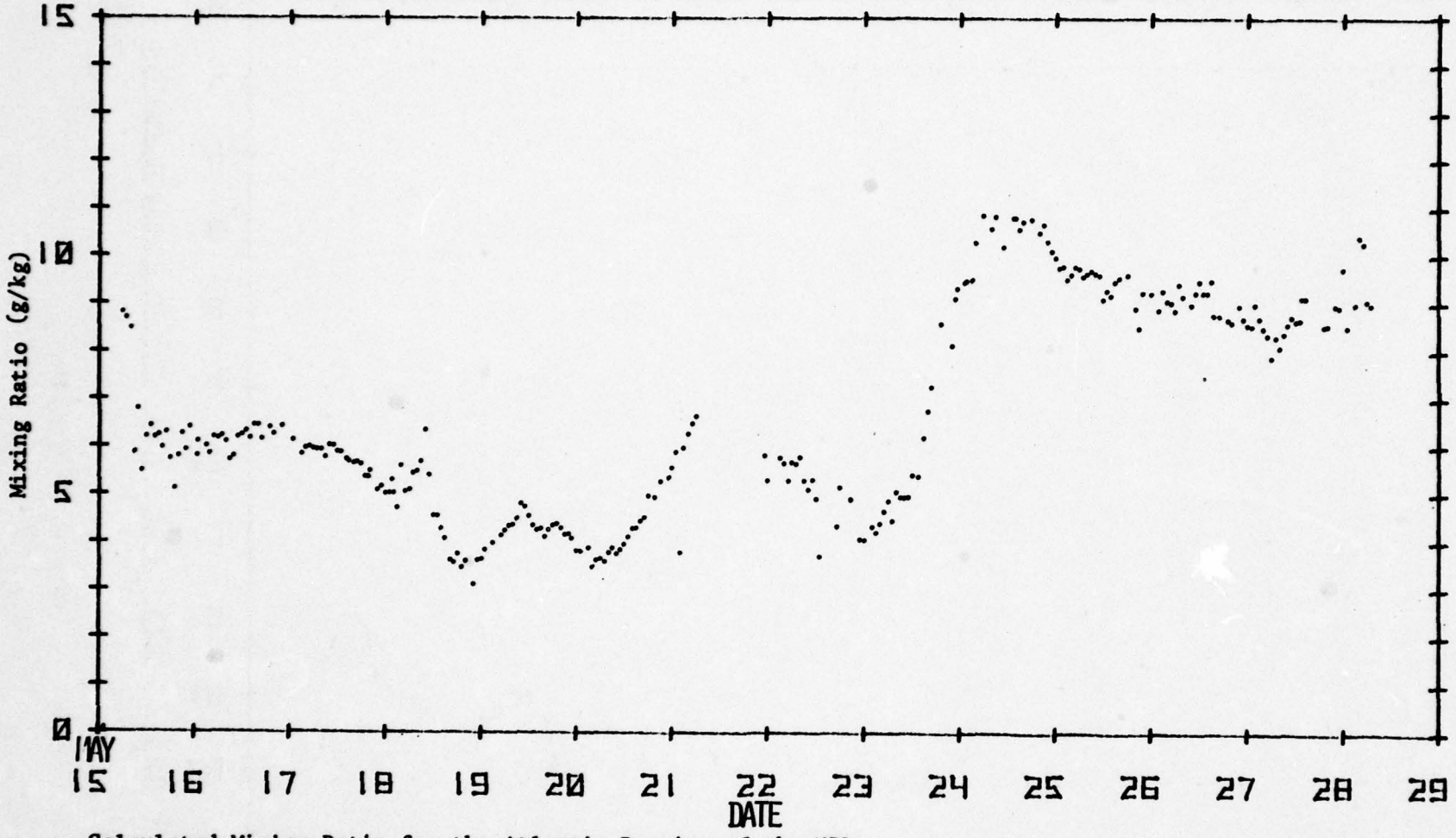

Calculated Mixing Ratio for the Atlantic Portion of the NRL Cruise, 77-16-04

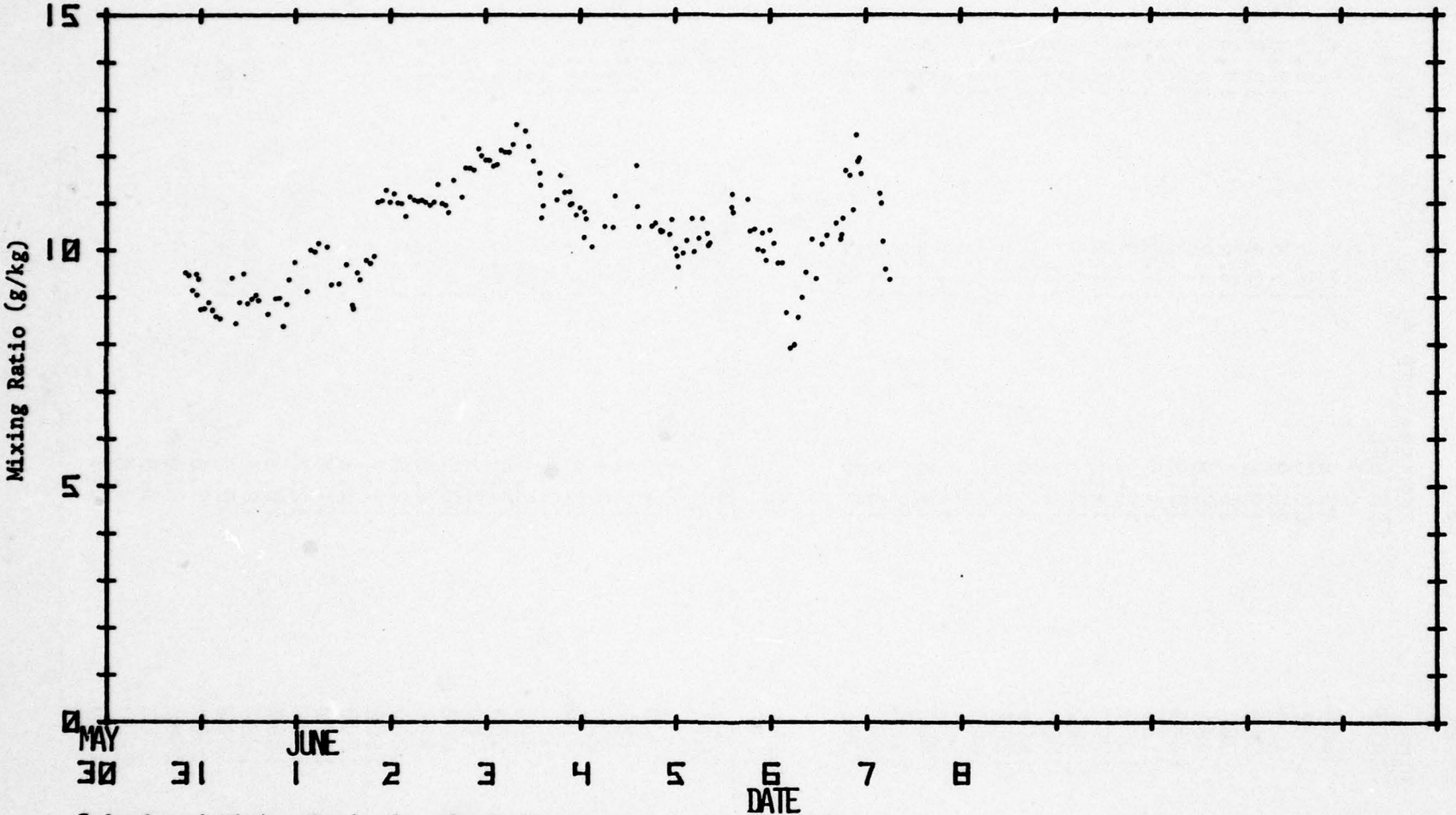

Calculated Mixing Ratio for the Mediterranean Portion of the NRL Cruise, 77-16-04

DATE: 5 15 1977

TIME (GMT)	TEMPERATURE AT SELECTED LEVELS SEA SFC. (C)	9M. (C)	27M. (C)
400	23.8	17.6	17.6
500	20.5	16.9	16.9
600	20.0	15.6	15.6
700	19.3	13.9	13.9
800	18.1	13.6	14.3
900	16.8	14.2	14.3
1000	15.3	13.2	12.9
1100	14.3	12.5	12.5
1200	13.3	11.9	12.1
1300	14.3	12.2	12.1
1400	13.6	12.1	12.1
1500	14.1	11.9	12.0
1600	13.6	11.7	11.7
1700	13.6	11.9	12.0
1800	13.6	12.0	12.1
1900	13.9	12.6	12.8
2000	14.8	13.2	13.9
2100	14.3	13.2	13.9
2200	13.5	13.0	13.1
2300	13.3	12.6	12.9

DATE: 5 16 1977

TIME (GMT)	TEMPERATURE AT SELECTED LEVELS SEA SFC. (C)	9M. (C)	27M. (C)
0	14.5	11.9	12.3
100	13.8	11.2	11.9
200	14.1	11.1	11.6
300	13.8	11.0	11.6
400	13.7	10.9	11.7
500	13.9	10.7	10.9
600	12.8	10.5	10.9
700	12.9	10.0	10.6
800	13.1	10.8	10.9
900	12.8	11.1	11.9
1000	12.8	11.3	
1100	11.7		
1200	12.2		
1300	11.5		
1400	12.7		
1500	10.3		
1600	10.7	10.4	10.8
1700	9.5	10.1	10.7
1900	9.0		
2000	8.0		
2100	9.9		
2200	10.0		
2300	10.1		

DATE: 5 17 1977

TIME (GMT)	TEMPERATURE AT SELECTED LEVELS SEA SFC. (C)	9M. (C)	27M. (C)
0	10.1		
100	9.9		
200	9.6		
300	9.5		
400	9.0		
500	9.0	9	
600	9.0		
700	8.3		
800	8.2		
900	8.0		
1000	9.0		
1100	7.7		
1200	7.4		
1300	6.4		
1355	0.0		
1405	6.0	7.9	8.5
1415			0.0
1430		7.9	8.5
1455		7.8	8.3
1610	6.3		
1700	6.3		
1800	6.3		
1900	5.8	7.3	
1945	5.8	7.2	7.7
2000	5.5	7.3	7.8
2030	5.3	7.3	7.8
2200	4.9		
2300	5.0		

DATE: 5 18 1977

TIME (GMT)	TEMPERATURE AT SELECTED LEVELS SEA SFC. (C)	9M. (C)	27M. (C)
0	5.0		
100	5.7		
145	5.4	7.4	
210	4.7	10.7	14.3
230	4.5	7.7	13.3
300	4.2	5.0	
400	4.0		
500	5.5	6.5	6.9
540	5.9	6.8	11.9
600	5.1	6.6	8.8

DATE: 5 18 1977 CONTINUED

700	4.1	7.5	9.6
800	4.4	6.7	9.9
830	4.1	5.8	8.1
900	4.1	6.0	8.7
1000	4.3	7.4	10.3
1100	4.3	5.5	6.8
1200	3.9	4.9	5.4
1300	3.9	5.7	6.3
1400	3.9	6.2	7.3
1500	4.3	5.3	6.3
1610	5.4	4.6	4.8
1700	5.9	4.0	4.2
1800	5.9	3.7	3.9
1900	9.0	3.9	3.9
2000	6.3	3.5	3.5
2200	3.2	3.9	3.9
2300	3.2	3.3	3.3

DATE: 5 19 1977

TIME (GMT)	TEMPERATURE AT SELECTED LEVELS SEA SFC. (C)	9M. (C)	27M. (C)
0	3.0	3.2	3.2
100	3.3	3.2	3.1
300	3.6	3.0	3.0
420	3.9	3.3	3.2
440	4.0	3.4	3.2
500	3.4	3.4	3.2
600	3.6	3.4	3.2
700	3.3	3.4	3.3
800	3.6	3.6	3.6
900	3.8	3.8	3.9
1000	4.0	3.9	3.9
1100	4.5	3.7	3.7
1200	4.4	3.5	3.6
1300	4.6	3.2	3.3
1400	4.0	3.5	3.6
1500	4.3	3.7	3.7
1600	4.9	3.8	3.9
1700	4.3	3.6	3.7
1800	4.1	3.2	3.3
1830	3.8	3.3	3.4
1900	3.3	3.3	3.3
1930		3.2	3.3
2000	3.8	3.2	3.3
2100	4.5	3.3	3.2
2200	4.2	2.9	3.0

DATE: 5 20 1977

TIME (GMT)	TEMPERATURE AT SELECTED LEVELS SEA SFC. (C)	9M. (C)	27M. (C)
0	4.6	3.4	3.4
100	4.9	3.4	3.3
130			
200	5.0	3.3	3.1
300	4.8	2.9	2.8
400	4.8	2.8	2.7
500	4.7	2.8	2.8
600	4.4	2.7	2.6
700	4.7	2.7	2.6
800	5.0	2.0	1.9
900	4.9	1.4	1.3
1000	5.0	1.2	1.0
1100	4.1	1.2	1.2
1200	4.0	2.3	2.2
1300	3.9	2.2	2.2
1400	2.9	2.1	2.0
1500	2.6	2.9	3.1
1600	4.0	4.1	4.3
1700	6.3	5.2	5.1
1800	7.3	5.9	5.8
1930	7.3	6.0	5.9
2100	7.7	5.9	5.8
2300	7.9	6.4	6.3

DATE: 5 21 1977

TIME (GMT)	TEMPERATURE AT SELECTED LEVELS SEA SFC. (C)	9M. (C)	27M. (C)
0	7.4	6.9	6.7
100	8.2	7.6	7.5
200	8.9	8.0	8.0
300	9.0	8.3	8.3
400	9.3	8.5	8.5
430	10.6	8.6	8.4
500	9.8	8.5	8.4
600	9.5	8.7	8.6
700	8.7	8.7	8.6
800	9.0	8.8	8.8
900	9.2	9.2	9.2
1000	14.0	11.8	11.4
1100	17.0	12.6	12.0
1230	16.4	12.3	11.9
1400	17.4	12.2	11.7
1500	17.4	12.0	11.6
1600			
1800	14.3		
2000	14.4		
2200	14.5		
2305	13.5	11.5	11.1
2355	13.5	10.9	10.6

DATE: 5 22 1977

TIME (GMT)	TEMPERATURE AT SELECTED LEVELS SEA SFC. (C)	9M. (C)	27M. (C)
100	13.5		
200	13.6		
500	13.1		
600	13.6		
700	13.5		
800	14.4		
900	15.4		
1000	14.6	14.6	
1100	15.0	0.0	
1200		10.2	10.0
1230		10.1	9.8
1250		10.0	9.9
1710		10.8	10.7
1750	15.0	10.8	10.7
2030	15.5		
2300	15.9	11.6	11.3

DATE: 5 23 1977

TIME (GMT)	TEMPERATURE AT SELECTED LEVELS SEA SFC. (C)	9M. (C)	27M. (C)
0	15.7		
200	15.0	11.8	11.6
300		11.8	11.6
400		11.8	11.7
500		11.9	11.7
600		12.0	11.8
700		12.2	12.0
800		12.4	12.2
900		12.5	12.4
1000		12.6	12.6
1100		12.6	12.6
1200		12.7	12.7
1330		12.9	13.0
1500		13.2	13.2
1600		13.3	13.2
1700		13.6	13.4
1745		13.7	13.6
1915		13.6	13.5
2200	16.8	14.6	14.3
2240	16.9	14.8	14.7
2300	17.1		
2330	17.1	15.2	14.9

DATE: 5 24 1977

TIME (GMT)	TEMPERATURE AT SELECTED LEVELS SEA SFC. (C)	9M. (C)	27M. (C)
0	17.1		
50	17.3		
115	17.0	15.5	15.3
145	17.1	15.6	15.3
300	17.2	15.7	15.6
400	17.5	15.8	15.6
430	17.0	15.7	15.6
500	17.4	15.8	15.6
600	16.6	15.9	15.8
700	16.8	16.2	16.0
800	16.7	16.9	16.4
900	16.9	17.0	16.9
1000	17.5	16.5	16.5
1100	17.4	17.4	17.4
1200	18.0	17.3	17.2
1255	18.0	16.2	16.0
1330	17.5	17.2	17.2
1400	17.7	17.5	17.4
1500	17.8	17.5	17.3
1600	17.9	17.4	17.3
1800	17.5	17.4	17.3
1900	17.3	17.3	17.1
2000	17.3	17.3	17.2
2100	17.3	17.1	17.0
2200	16.7	17.0	17.0
2300	17.7	17.3	17.1

DATE: 5 25 1977

TIME (GMT)	TEMPERATURE AT SELECTED LEVELS SEA SFC. (C)	9M. (C)	27M. (C)
0	17.5	17.4	17.1
100	17.5	17.3	17.1
200	17.6	17.4	17.0
300	17.6	17.1	17.0
400	17.5	17.0	16.9
500	17.7	17.0	16.9
600	17.1	16.5	16.4
700	16.7	16.4	16.3
800	16.7	16.3	16.2
900	16.6	16.3	16.2
1000	16.2	16.2	16.1
1100	16.2	16.1	16.1
1200	16.2	16.2	16.3
1300	16.4	16.3	16.4
1400	16.6	16.5	16.6
1500	17.1	16.8	16.9
1600	17.4	16.8	16.8
1630			
1800	17.7	16.9	16.9
2015	17.5	16.7	16.6
2100	17.1	16.7	16.6
2200	17.0	16.7	16.5
2230	16.9	16.5	16.4

DATE: 5 26 1977

TIME (GMT)	TEMPERATURE AT SELECTED LEVELS SEA SFC. (C)	9M. (C)	27M. (C)
0	16.9	16.5	16.2
200	16.6	16.4	16.1
300	16.6	16.3	16.1
400	16.5	16.0	15.9
500	16.1	16.0	15.9
600	16.1	15.7	15.6
700	15.9	15.9	15.8
800	15.9	15.8	15.8
850	16.1	15.9	15.9
1000	16.9	16.2	16.1
1110	16.7	16.3	16.5
1200	16.7	16.3	16.6
1300	16.7	16.3	16.4
1400	16.9	16.4	16.6
1500	17.1	16.4	16.5
1540	17.2	16.4	16.5
1700	17.4	16.7	16.7
1900	17.7	16.5	16.5
2000	17.7	16.6	16.5
2030	17.5	16.6	16.4
2100	17.3	16.5	16.3
2130	17.6	16.5	16.4
2200	16.6	16.4	16.3
2300	17.3	16.4	16.1

DATE: 5 27 1977

TIME (GMT)	TEMPERATURE AT SELECTED LEVELS SEA SFC. (C)	9M. (C)	27M. (C)
0	16.9	16.3	16.1
100	16.8	16.1	16.0
200	16.6	15.7	15.6
300	16.1	15.5	15.3
400	16.5	15.4	15.3
500	16.5	15.3	15.1
600	16.4	15.2	15.0
700	16.2	15.2	15.1
800	16.2	15.3	15.0
905	15.9	15.1	15.1
1000	15.9	15.0	15.0
1000	15.9	15.0	15.0
1100	15.9	15.0	15.0
1200	15.8	15.1	15.1
1300	15.9	15.2	15.2
1330	15.7	15.2	15.1
1430	15.7	15.3	15.3
1700	15.7		
1900	14.7	15.3	15.4
2000	14.7	15.5	15.6
2200	15.5		
2300	15.4		

DATE: 5 28 1977

TIME (GMT)	TEMPERATURE AT SELECTED LEVELS SEA SFC. (C)	9M. (C)	27M. (C)
0	17.7	-	
100	17.8	18.9	19.7
300	17.1	17.3	17.2
400	15.8	15.8	16.2
500	15.9	16.1	16.2
600	16.5	17.4	17.5
700	17.8	17.7	17.7

DATE: 5 30 1977

TIME (GMT)	TEMPERATURE AT SELECTED LEVELS SEA SFC. (C)	9M. (C)	27M. (C)
2000	18.7	17.6	17.5
2100	17.6	17.4	17.2
2200	17.0	16.9	16.8
2300	17.0	16.8	16.7

DATE: 5 31 1977

TIME (GMT)	TEMPERATURE AT SELECTED LEVELS SEA SFC. (C)	9M. (C)	27M. (C)
0	16.8	16.7	16.5
100	-		
300	16.7		
400	15.6	15.8	15.9
800	17.5	16.3	16.2
900	17.5	16.7	16.5
1100	17.1	17.5	17.6
1200	16.3	16.6	16.5
1300	16.6	16.9	16.9
1400	17.3	17.3	0.0
1445	17.9	17.6	17.8
1600	18.0	18.0	18.0
1700	19.6		
1900	18.2		
2000	17.9		
2100	18.4		
2105	18.0	18.0	18.0
2155	18.3	18.3	18.2
2230	18.6		

DATE: 6 1 1977

TIME (GMT)	TEMPERATURE AT SELECTED LEVELS SEA SFC. (C)	9M. (C)	27M. (C)
0	18.1		
100	18.4		
200	18.6		
400	18.5	18.5	
500	18.8		
600	18.6		
800	18.7		
845	18.7	18.3	18.2
915	18.7	18.4	18.2
1100	18.6		
1200	18.6		
1300	19.0		
1410	19.1	18.9	18.8
1430		19.0	19.0
1445	19.1	18.1	19.1
1545	19.1	18.6	18.6
1630	19.4	18.8	18.8
1800	19.5	18.8	18.6
1900	19.5	18.7	18.6
2000	19.5	18.8	18.6
2100	19.3	18.6	18.5
2130	19.1	18.5	18.1
2200	19.2	18.3	18.0
2300	19.2	18.1	18.0

DATE: 6 2 1977

TIME (GMT)	TEMPERATURE AT SELECTED LEVELS SEA SFC. (C)	9M. (C)	27M. (C)
0	19.1	18.0	17.9
30	19.4	18.1	17.9
100	19.5	18.1	17.9
200	19.5	18.4	18.1
300	19.2	18.3	18.1
400	19.1	18.2	18.0
500	18.1	18.2	17.9
600	19.1	18.5	18.3
700	19.3	18.5	18.4
800	19.7	18.5	18.6
900	19.8	18.5	18.6
1000	20.3	18.7	18.8
1100	20.3	18.9	19.0

DATE: 6 2 1977 CONTINUED

1200	20.4	20.2	20.4
1300	20.4	19.5	19.6
1400	20.0	19.4	19.5
1445	20.0	19.3	19.2
1600	20.2	19.3	19.1
1800	19.9	19.3	19.1
1900	19.6	19.2	19.0
2000	19.6	19.3	19.0
2100	19.7	19.2	19.1
2215	19.6	19.2	19.0
2300	19.9	19.3	19.0

DATE: 6 3 1977

TIME (GMT)	TEMPERATURE AT SELECTED LEVELS SEA SFC. (C)	9M. (C)	27M. (C)
0	19.7	19.5	19.1
100	19.7	19.4	19.1
200	19.7	19.4	19.2
300	20.1	19.1	18.9
400	20.0	19.3	19.1
500	20.1	19.3	19.1
600	19.9	19.5	19.4
700	19.9		
900	20.1		
1000	19.2		
1140	19.8	19.7	19.7
1210	19.8	19.7	19.7
1400	19.9	19.0	18.9
1420	20.0	19.2	19.0
1440	19.8	19.2	19.1
1600	19.5		
1700	19.6		
1800	19.7		
1900	19.7		
2000	20.3		
2100			
2110	20.0	19.6	19.3
2130	20.0	19.4	19.1
2150	19.9	19.3	19.0
2205	19.8		
2300	20.5		

DATE: 6 4 1977

TIME (GMT)	TEMPERATURE AT SELECTED LEVELS SEA SFC. (C)	9M. (C)	27M. (C)
0	20.6		
55	20.3		
110	20.1	19.4	19.1
130	20.1	19.4	19.1
200	20.1		
300	20.3		
400	20.4		
500	20.3		
610	20.3	19.6	19.4
650	20.2	19.6	19.5
810	20.4	19.6	19.6
850	20.5	19.9	19.8
1000	20.2		
1100	20.3		
1200	20.6		
1300	20.6		
1355	20.2		
1410	20.2	20.1	20.0
1430	20.1	20.0	20.0
1450	20.2	20.1	19.9
1505			
1545	20.7		
1700	20.7		
1800	20.4		
1900	20.9		
1955	20.6		
2010	20.6	20.0	19.8
2030	20.6	19.9	19.8
2050	20.6	19.9	19.7
2105	20.6		
2230	20.6		
2315	20.8		
2355	20.6		

DATE: 6 5 1977

TIME (GMT)	TEMPERATURE AT SELECTED LEVELS SEA SFC. (C)	9M. (C)	27M. (C)
10	20.5	19.8	19.7
30	20.5	19.8	19.7
50	20.6	19.8	19.6
200	20.5	0.0	0.0
300	20.7	19.7	19.4
400			
415	20.6	19.6	19.5
420	19.6	20.6	19.8
450	20.6	19.8	19.6
600	20.6		
700	20.8		
810	20.9	20.1	20.0
830	20.8	20.1	20.0
850	20.9	20.1	20.1
1100	21.0		
1200	21.0		
1300	21.4		
1355	21.4		
1410	21.1	20.6	20.3
1430	21.1	20.8	20.7
1450	21.1	20.7	20.6
1545	21.0		
1700	21.2		
1815	21.3	20.3	20.1
1900	21.4	20.4	20.1
2000	21.4	20.4	20.1
2055	21.5	20.5	20.2
2200	21.3	20.2	20.0
2215	21.2	20.3	20.0
2300	21.4	20.3	20.0

DATE: 6 6 1977

TIME (GMT)	TEMPERATURE AT SELECTED LEVELS SEA SFC. (C)	9M. (C)	27M. (C)
0	21.4	20.1	19.9
100	21.2	20.0	19.8
200	21.0	19.9	19.8
300	21.1	20.0	19.9
400	21.4	20.0	19.8
500	21.6	20.2	20.0
600	20.3	20.2	20.1
700	21.5	20.3	20.1
800	20.8	20.4	20.3
900	21.0	20.5	20.5
1030	21.0	20.4	20.3
1130	21.0	20.5	20.3
1300	20.2	20.4	20.4
1410	20.5	20.5	20.5
1630	21.3	20.7	20.6
1740	21.0	20.6	20.2
1800	20.9	20.6	20.4
1820	21.0	20.6	20.4
1900	21.1	20.4	20.2
2000	21.1	20.7	20.6
2100	21.0	21.0	21.0
2150	21.0	20.7	20.6
2210	21.0	20.5	20.4
2230	21.0	20.5	20.3
2300	21.0	20.5	20.4

DATE: 6 7 1977

TIME (GMT)	TEMPERATURE AT SELECTED LEVELS SEA SFC. (C)	9M. (C)	27M. (C)
330	19.7	19.8	19.6
400	20.1	19.7	19.6
430	19.9	19.9	19.7
500	20.7	19.9	19.8

Appendix D

LOG OF AEROSOL CONCENTRATIONS FOR FIVE SIZE RANGES

DATE: 5 15 1977

TIME (GMT)	AEROSOL CONCENTRATIONS FOR SIZES > INDICATED DIAMETER				
	>0.01 /CM↑3	>0.1 /CM↑3	>0.3 /CM↑3	>1.2 /CM↑3	>3.0 /CM↑3
400	28150	2474	4.9	0.9	0.09
500	4950	1055	4.2	0.9	0.13
600	9207	1301	3.8	0.9	0.11
700	7230	1754	5.0	1.1	0.17
800	8118	2563	4.5	0.8	0.09
900	12870	1809	4.2	0.8	0.09
1000	9844	1553	4.5	1.0	0.13
1100	9795	1616	5.0	1.1	0.14
1200	10630	1872	5.1	1.1	0.16
1300	11950	1861	5.5	1.2	0.18
1400	8552	1914	4.7	1.1	0.14
1500	9443	2263	4.7	1.0	0.12
1600	22190	3288	4.9	0.8	0.08
1700	21130	4953	11.5	1.0	0.06
1800	32110	4328	5.5	0.6	0.05
1900	38500	3413	2.8	0.4	0.03
2000	68880	2157	2.3	0.3	0.03
2100	12320	3309	2.2	0.3	0.03
2200	8789	2541	2.3	0.4	0.03
2300	9673	1740	2.0	0.3	0.03

DATE: 5 16 1977

TIME (GMT)	AEROSOL CONCENTRATIONS FOR SIZES > INDICATED DIAMETER				
	>0.01 /CM↑3	>0.1 /CM↑3	>0.3 /CM↑3	>1.2 /CM↑3	>3.0 /CM↑3
0	10750	1518	1.8	0.3	0.03
100	10000	1383	1.9	0.4	0.04
200	N/A	N/A	2.2	0.5	0.06
300	7203	1353	2.5	0.6	0.07
400	7157	1344	3.1	0.8	0.09
500	6931	1438	2.8	0.6	0.07
600	6994	1698	2.5	0.5	0.06
700	7364	2655	2.8	0.4	0.05
800	6245	2183	2.8	0.4	0.05
900	34430	2268	4.4	0.8	0.08
1000	47990	1935	5.2	1.1	0.13
1100	N/A	N/A	5.2	1.2	0.13
1200	8662	2139	4.0	1.0	0.10
1300	9265	2092	4.1	1.0	0.10
1400	8338	2411	14.4	3.5	0.45
1500	N/A	N/A	11.7	2.2	0.17
1600	6987	2412	5.4	1.4	0.11
1700	6530	2473	6.0	1.7	0.14

DATE: 5 17 1977

TIME (GMT)	AEROSOL CONCENTRATIONS FOR SIZES > INDICATED DIAMETER				
	>0.01 /CM↑3	>0.1 /CM↑3	>0.3 /CM↑3	>1.2 /CM↑3	>3.0 /CM↑3
1355	N/A	N/A	37.0	9.2	0.50
1405	N/A	N/A	28.2	7.0	0.34
1415	8593	4308	24.0	6.1	0.32
1430	8325	4298	24.2	6.3	0.35
1455	7029	4268	25.2	6.6	0.36
1900	7567	4273	N/A	N/A	0.00
1945	8721	4300	19.6	4.4	0.28
2000	8776	4369	20.6	4.8	0.33
2015	9787	4538	20.7	4.9	0.32
2030	10460	4603	20.9	4.9	0.32

DATE: 5 18 1977

TIME (GMT)	AEROSOL CONCENTRATIONS FOR SIZES > INDICATED DIAMETER				
	>0.01 /CM↑3	>0.1 /CM↑3	>0.3 /CM↑3	>1.2 /CM↑3	>3.0 /CM↑3
145	11500	4991	26.5	5.6	0.33
210	10230	3934	23.4	4.1	0.25
230	10220	4657	25.2	5.0	0.31
500	7164	3834	26.4	4.6	0.29
520	7856	3748	26.6	4.7	0.30
540	7608	3694	25.7	4.5	0.28
600	7573	3510	24.4	4.4	0.23
700	6686	3150	22.9	3.7	0.17
800	5151	2753	24.1	3.1	0.15
830	4786	2739	25.6	2.9	0.15
900	4963	2497	35.6	3.6	0.17
909	N/A	N/A	40.5	5.2	0.63
930	5084	2044	N/A	N/A	0.00
1000	2481	1603	59.0	11.4	0.00
1100	1814	1283	32.4	4.2	0.10
1200	1169	685	10.1	1.9	0.10
1300	7729	934	8.0	1.1	0.05
1400	15020	909	4.9	0.6	0.03
1500	8088	679	3.7	0.3	0.01
1610	40760	204	3.7	0.9	0.05
1700	33100	129	5.0	1.3	0.09
1800	27250	79	5.2	1.4	0.09
1900	16420	294	5.5	1.4	0.10
2000	5858	79	6.1	1.7	0.12
2200	5806	74	5.2	1.5	0.09
2300	7270	174	6.9	2.2	0.17

DATE: 5 19 1977

TIME (GMT)	AEROSOL CONCENTRATIONS FOR SIZES > INDICATED DIAMETER				
	>0.01 /CM↑3	>0.1 /CM↑3	>0.3 /CM↑3	>1.2 /CM↑3	>3.0 /CM↑3
0	7932	292	7.8	2.6	0.22
100	9051	471	8.6	2.8	0.22
300	8456	556	8.7	2.8	0.26
420	6341	347	9.9	3.3	0.25
440	5149	326	10.7	3.6	0.30
500	5247	326	11.2	3.8	0.33
600	3846	513	11.4	3.8	0.34
640	4801	607	11.6	3.9	0.34
700	4356	292	11.9	4.1	0.41
800	6188	245	9.6	3.3	0.28
900	3090	305	4.8	1.6	0.12
1000	3187	174	2.7	0.8	0.06
1100	1758	90	2.2	0.7	0.06
1200	511	58	3.1	0.9	0.07
1300	1193	76	3.2	0.9	0.07
1400	119	71	3.2	0.8	0.03
1500	193	94	2.7	0.6	0.03
1600	528	75	3.2	0.6	0.03
1700	11480	324	2.0	0.4	0.02
1800	4319	289	2.5	0.6	0.03
1830	1728	176	4.1	1.0	0.05
1900	2354	74	6.1	1.6	0.09
1930	4993	71	5.8	1.4	0.09
2000	2346	62	4.8	1.1	0.08
2100	1438	77	4.1	0.9	0.05
2200	537	84	3.9	0.8	0.05
2250	806	108	5.6	1.5	0.11

DATE: 5 20 1977

TIME (GMT)	AEROSOL CONCENTRATIONS FOR SIZES > INDICATED DIAMETER				
	>0.01 /CM↑3	>0.1 /CM↑3	>0.3 /CM↑3	>1.2 /CM↑3	>3.0 /CM↑3
0	3532	84	5.3	1.5	0.09
100	2875	81	5.7	1.7	0.10
130	1581	63	5.8	1.7	0.09
200	N/A	N/A	6.1	1.8	0.10
300	2843	124	8.9	3.0	0.18
400	1722	168	9.7	3.2	0.18
500	2493	226	10.8	3.0	0.15
600	1509	162	6.0	1.6	0.06
700	871	123	6.3	1.8	0.08
800	370	630	6.3	1.8	0.09
900	411	57	8.6	2.9	0.15
1000	1174	57	7.3	2.4	0.15
1100	45	45	4.0	1.2	0.06

DATE: 5 20 1977 CONTINUED

1200	92	44	0.7	0.2	0.12
1300	94	94	7.3	2.4	0.12
1400	119	71	8.1	2.9	0.20
1500	156	108	4.3	1.0	0.04
1600	132	84	3.8	0.9	0.05
1700	161	113	5.2	1.4	0.08
1800	256	157	6.5	1.8	0.11
1930	491	137	6.4	1.7	0.09
2100	467	113	11.3	3.7	0.26
2300	163	116	14.7	5.2	0.41

DATE: 5 21 1977

TIME (GMT)	AEROSOL CONCENTRATIONS FOR SIZES > INDICATED DIAMETER				
	>0.01 /CM↑3	>0.1 /CM↑3	>0.3 /CM↑3	>1.2 /CM↑3	>3.0 /CM↑3
0	1232	115	16.3	5.6	0.47
100	181	137	15.7	5.5	0.49
200	171	123	12.2	4.3	0.31
300	169	121	10.9	3.9	0.27
400	98	98	12.9	4.5	0.36
430	168	120	12.9	4.6	0.37
500	168	120	12.3	4.4	0.40
600	150	102	11.1	4.0	0.38
700	217	71	11.1	4.1	0.38
800	259	112	12.4	4.8	0.47
900	254	108	11.1	4.4	0.32
1000	162	63	7.4	3.2	0.14
1100	N/A	N/A	7.0	2.5	0.06
1230	N/A	N/A	4.3	1.6	0.08
2010	286	93	0.0	0.0	0.00
2300	191	143	8.8	2.9	0.24
2315	293	147	8.7	2.8	0.24
2335	310	116	7.5	2.4	0.20
2355	262	116	7.1	2.2	0.17

DATE: 5 22 1977

TIME (GMT)	AEROSOL CONCENTRATIONS FOR SIZES > INDICATED DIAMETER				
	>0.01 /CM↑3	>0.1 /CM↑3	>0.3 /CM↑3	>1.2 /CM↑3	>3.0 /CM↑3
1200	269	123	7.4	1.3	0.09
1230	490	85	9.3	2.1	0.15
1250	133	133	8.1	1.6	0.11
1710	102	54	4.8	0.9	0.05
1730	N/A	N/A	4.7	0.9	0.06
1750	111	63	5.1	1.0	0.09
2300	450	45	5.5	1.1	0.09

DATE: 5 23 1977

TIME (GMT)	AEROSOL CONCENTRATIONS FOR SIZES > INDICATED DIAMETER				
	>0.01 /CM↑3	>0.1 /CM↑3	>0.3 /CM↑3	>1.2 /CM↑3	>3.0 /CM↑3
200	86	86	5.8	1.2	0.11
300	88	88	5.4	1.1	0.08
400	108	61	4.8	0.9	0.05
500	177	81	4.8	1.0	0.08
600	124	76	4.0	0.9	0.07
700	26	26	3.4	0.7	0.04
800	166	67	3.9	0.9	0.07
900	114	114	3.7	0.8	0.06
1000	428	74	4.3	0.9	0.06
1100	99	52	4.1	0.7	0.03
1200	160	112	4.9	0.9	0.06
1330	140	92	4.9	0.9	0.04
1500	134	86	5.5	1.4	0.12
1600	214	116	7.8	2.1	0.19
1700	201	102	10.2	3.0	0.30
1745	N/A	N/A	10.4	3.1	0.32
1915	21	21	3.3	1.0	0.05
2200	N/A	N/A	2.0	0.5	0.04
2240	N/A	N/A	2.3	0.6	0.06
2330	37	37	3.1	0.8	0.07

DATE: 5 24 1977

TIME (GMT)	AEROSOL CONCENTRATIONS FOR SIZES > INDICATED DIAMETER				
	>0.01 /CM↑3	>0.1 /CM↑3	>0.3 /CM↑3	>1.2 /CM↑3	>3.0 /CM↑3
115	N/A	N/A	3.1	0.7	0.06
145	80	31	3.3	0.7	0.07
300	72	24	3.4	0.7	0.06
400	21	21	4.6	0.9	0.08
430	N/A	N/A	4.8	0.8	0.05
500	21	21	5.1	0.9	0.09
600	31	31	5.4	0.8	0.06
700	42	37	72.0	7.4	0.35
800	53	39	61.0	5.6	0.16
900	322	227	26.2	2.7	0.15
1000	N/A	N/A	6.6	1.7	0.19
1100	259	112	5.0	1.3	0.10
1200	267	120	4.7	1.2	0.13
1255	510	156	14.2	1.8	0.12
1330	N/A	N/A	4.3	1.2	0.10
1400	193	98	4.1	1.1	0.08
1500	94	94	4.0	1.1	0.09
1600	204	57	3.7	1.0	0.09
1800	111	63	3.3	0.8	0.07
1900	N/A	N/A	3.1	0.8	0.07
2000	124	76	3.1	0.7	0.07
2100	169	121	3.1	0.7	0.07
2200	189	90	3.0	0.7	0.06
2300	283	137	6.0	0.8	0.06

DATE: 5 25 1977

TIME (GMT)	AEROSOL CONCENTRATIONS FOR SIZES > INDICATED DIAMETER				
	>0.01 /CM↑3	>0.1 /CM↑3	>0.3 /CM↑3	>1.2 /CM↑3	>3.0 /CM↑3
0	286	92	5.1	0.8	0.06
100	250	202	8.0	0.9	0.07
200	128	128	8.4	0.9	0.06
300	232	137	9.4	1.0	0.05
400	317	174	8.2	0.9	0.06
500	370	562	8.6	1.1	0.07
600	520	374	10.9	1.6	0.11
700	897	448	10.5	1.5	0.08
800	799	509	10.9	1.6	0.08
900	863	574	10.4	1.6	0.09
1000	930	688	10.1	1.6	0.09
1100	952	663	9.3	1.4	0.07
1200	1208	517	8.5	1.2	0.06
1300	813	476	8.1	1.2	0.05
1400	2049	483	7.5	1.0	0.05
1500	751	462	8.3	1.2	0.06
1600	964	467	8.6	1.2	0.07
1630	1212	454	8.3	1.2	0.07
1800	850	302	6.7	0.9	0.04
2015	586	443	7.2	1.0	0.04
2100	781	393	7.9	1.1	0.05
2200	632	393	9.4	1.3	0.06
2230	849	509	7.3	1.3	0.07

DATE: 5 26 1977

TIME (GMT)	AEROSOL CONCENTRATIONS FOR SIZES > INDICATED DIAMETER				
	>0.01 /CM↑3	>0.1 /CM↑3	>0.3 /CM↑3	>1.2 /CM↑3	>3.0 /CM↑3
0	713	522	9.0	1.2	0.06
200	630	535	8.7	1.2	0.05
300	1020	734	10.2	1.3	0.06
400	1143	759	11.3	1.4	0.07
500	3070	693	12.4	1.5	0.06
600	922	731	14.0	1.7	0.06
700	2195	629	18.0	3.0	0.06
800	1174	579	19.3	2.5	0.05
850	885	547	20.4	2.4	0.03
1000	840	550	16.0	1.9	0.04
1030	868	677	13.7	1.6	0.04
1110	735	640	12.6	1.4	0.05
1200	872	634	13.6	1.6	0.04
1300	1513	608	13.5	1.6	0.06
1400	1068	533	14.1	1.7	0.04
1500	976	478	17.6	2.2	0.04

DATE: 5 26 1977 CONTINUED

1540	893	504	18.9	2.4	0.04
1700	967	530	18.8	2.4	0.04
1900	934	498	19.0	2.5	0.04
2000	855	518	20.1	2.5	0.04
2030	941	505	20.2	2.5	0.04
2045	729	386	19.9	2.5	0.04
2100	681	340	20.8	2.7	0.05
2130	697	455	20.3	2.7	0.04
2200	565	374	21.4	2.7	0.04
2300	777	436	21.0	2.7	0.03

DATE: 5 27 1977

TIME (GMT)	AEROSOL CONCENTRATIONS FOR SIZES > INDICATED DIAMETER				
	>0.01 /CM↑3	>0.1 /CM↑3	>0.3 /CM↑3	>1.2 /CM↑3	>3.0 /CM↑3
0	884	502	20.9	2.6	0.04
100	685	392	20.2	2.5	0.04
200	680	584	28.0	3.2	0.05
300	1001	763	32.0	3.6	0.06
400	842	556	31.7	3.8	0.06
500	1280	681	47.9	5.2	0.07
600	1050	760	53.1	5.8	0.07
700	1237	836	50.2	5.1	0.07
800	903	807	46.3	4.5	0.06
905	2460	907	52.2	4.6	0.12
1000	1785	947	62.1	5.3	0.16
1100	2204	1009	62.5	5.5	0.15
1200	2417	977	57.3	5.6	0.19
1300	2460	840	58.5	5.8	0.19
1330	2179	900	60.9	5.9	0.20
1430	2351	986	59.8	6.2	0.22

DATE: 5 28 1977

TIME (GMT)	AEROSOL CONCENTRATIONS FOR SIZES > INDICATED DIAMETER				
	>0.01 /CM↑3	>0.1 /CM↑3	>0.3 /CM↑3	>1.2 /CM↑3	>3.0 /CM↑3
0	6415	1180	54.8	4.7	0.16
100	5761	1122	45.4	3.1	0.08
300	2339	956	42.5	3.0	0.08
400	5528	2391	106.5	10.9	0.24
500	3319	1252	61.9	5.7	0.12
600	5738	1849	45.3	3.5	0.07
700	2464	1598	41.5	3.1	0.05
2000	3307	169	10.0	2.5	0.22
2100	1282	234	10.3	3.0	0.19
2200	3418	231	10.7	3.2	0.21
2300	1012	266	9.7	2.7	0.18
2330	1247	212	10.0	2.8	0.19

DATE: 5 30 1977

TIME (GMT)	AEROSOL CONCENTRATIONS FOR SIZES > INDICATED DIAMETER				
	>0.01 /CM↑3	>0.1 /CM↑3	>0.3 /CM↑3	>1.2 /CM↑3	>3.0 /CM↑3
0	1875	289	7.1	2.6	0.17
400	472	131	7.3	2.3	0.16
800	2608	394	6.7	1.7	0.08
900	1777	271	6.9	1.4	0.06
1100	3311	852	8.6	1.6	0.07
1200	N/A	N/A	8.5	1.6	0.07
1300	2653	746	10.5	1.6	0.08
1400	2772	826	10.0	1.5	0.09
1445	3225	539	9.9	1.5	0.09
1600	1130	401	10.6	1.6	0.10
2110	1575	217	8.8	1.5	0.09
2130	1214	227	9.4	1.5	0.10
2155	1265	326	9.4	1.5	0.11

DATE: 5 31 1977

TIME (GMT)	AEROSOL CONCENTRATIONS FOR SIZES > INDICATED DIAMETER				
	>0.01 /CM↑3	>0.1 /CM↑3	>0.3 /CM↑3	>1.2 /CM↑3	>3.0 /CM↑3
845	1686	358	13.9	2.2	0.15
915	1356	273	10.2	1.9	0.14
1410	633	248	13.0	1.3	0.08
1430	804	270	10.8	1.2	0.06
1445	791	260	3.0	0.2	0.01
1545	1151	262	3.0	0.2	0.01
1630	850	315	3.2	0.2	0.01
1800	1798	426	4.2	0.3	0.01

DATE: 6 1 1977

TIME (GMT)	AEROSOL CONCENTRATIONS FOR SIZES > INDICATED DIAMETER				
	>0.01 /CM↑3	>0.1 /CM↑3	>0.3 /CM↑3	>1.2 /CM↑3	>3.0 /CM↑3
1445	791	260	3.0	0.2	0.01
1545	1151	262	3.0	0.2	0.01
1630	850	315	3.2	0.2	0.01
1800	1798	426	4.2	0.3	0.01
1900	1736	446	4.7	0.2	0.01
2000	1112	383	6.7	0.2	0.02
2100	1632	811	6.4	0.1	0.01
2130	1204	624	8.1	0.1	0.01
2230	793	456	6.1	0.1	0.00
2300	674	432	6.3	0.1	0.00

DATE: 6 2 1977

TIME (GMT)	AEROSOL CONCENTRATIONS FOR SIZES > INDICATED DIAMETER				
	>0.01 /CM↑3	>0.1 /CM↑3	>0.3 /CM↑3	>1.2 /CM↑3	>3.0 /CM↑3
0	1127	596	6.4	0.1	0.00
30	1071	443	5.2	0.0	0.00
100	685	396	4.9	0.1	0.00
200	629	386	5.8	0.1	0.00
300	701	411	5.7	0.1	0.00
400	829	380	5.1	0.1	0.00
500	924	488	4.9	0.1	0.00
600	730	440	4.6	0.1	0.00
700	714	425	4.8	0.1	0.00
800	809	472	4.3	0.0	0.00
900	837	448	4.2	0.0	0.00
1000	837	448	4.0	0.0	0.00
1100	1032	436	4.1	0.1	0.00
1200	899	463	4.4	0.1	0.00
1300	572	381	4.8	0.1	0.00
1400	527	336	4.5	0.1	0.00
1445	485	342	4.9	0.1	0.00
1600	578	289	4.3	0.1	0.00
1800	484	293	4.9	0.1	0.00
1900	504	313	5.2	0.1	0.00
2000	954	320	5.7	0.2	0.01
2100	692	352	5.5	0.2	0.01
2215	909	409	5.8	0.3	0.03
2300	576	188	2.8	0.2	0.01
2330	N/A	N/A	10.2	1.6	0.12

DATE: 6 3 1977

TIME (GMT)	AEROSOL CONCENTRATIONS FOR SIZES > INDICATED DIAMETER				
	>0.01 /CM↑3	>0.1 /CM↑3	>0.3 /CM↑3	>1.2 /CM↑3	>3.0 /CM↑3
0	804	270	12.0	1.7	0.11
100	883	301	10.8	1.4	0.10
200	870	390	19.0	2.0	0.08
300	1279	414	8.6	1.5	0.13
400	1263	426	28.3	3.4	0.16
500	1163	373	31.5	3.3	0.11
600	919	483	24.8	2.5	0.09
700	N/A	N/A	26.2	2.7	0.10
800	2002	500	22.5	2.1	0.08
1140	1832	912	49.2	3.2	0.11
1200	2405	614	40.5	3.4	0.10
1340	1720	997	18.6	2.2	0.12
1400	1380	335	14.0	1.9	0.12
1420	1281	342	10.6	1.6	0.10
1440	1256	317	10.1	1.7	0.11
2110	983	397	11.7	2.0	0.12
2130	868	285	11.4	2.0	0.13
2150	1273	272	12.3	2.1	0.11

DATE: 6 4 1977

TIME (GMT)	AEROSOL CONCENTRATIONS FOR SIZES > INDICATED DIAMETER				
	>0.01 /CM↑3	>0.1 /CM↑3	>0.3 /CM↑3	>1.2 /CM↑3	>3.0 /CM↑3
110	1165	308	11.9	2.0	0.12
130	554	262	11.5	1.9	0.13
610	2200	341	11.5	1.8	0.07
650	1645	368	13.1	1.6	0.05
810	1060	318	11.2	1.4	0.05
850	1672	313	12.8	1.8	0.08
1410	806	173	13.7	2.2	0.11
1430	650	306	15.0	1.9	0.11
1450	824	388	14.4	1.8	0.12
1700	N/A	N/A	N/A	N/A	N/A
2010	1443	1007	30.0	2.9	0.20
2030	955	717	30.5	2.9	0.21
2050	1718	976	27.4	2.8	0.20
2230	1615	1020	25.0	2.8	0.18
2315	1432	1095	27.2	2.8	0.17
2355	1245	662	28.0	2.5	0.12

DATE: 6 5 1977

TIME (GMT)	AEROSOL CONCENTRATIONS FOR SIZES > INDICATED DIAMETER				
	>0.01 /CM↑3	>0.1 /CM↑3	>0.3 /CM↑3	>1.2 /CM↑3	>3.0 /CM↑3
10	1726	896	25.3	2.5	0.18
30	1102	602	20.2	2.1	0.16
50	691	548	13.6	1.9	0.16
200	1043	464	13.4	1.8	0.08
300	1532	745	14.5	1.8	0.09
400	2879	775	14.6	1.8	0.09
415	2442	794	15.0	1.9	0.15
450	1937	795	16.4	1.8	0.13
600	1690	1108	16.0	1.6	0.08
700	N/A	N/A	18.8	1.9	0.11
810	1918	1290	20.4	2.0	0.14
830	1702	1173	19.8	1.9	0.14
850	1998	1205	15.3	1.6	0.10
1355	N/A	N/A	18.1	2.2	0.15
1410	1560	1029	19.8	2.1	0.14
1430	2034	1084	19.6	2.1	0.15
1450	2818	1058	18.9	2.2	0.17
1815	1228	741	14.6	1.7	0.11
1900	1188	752	15.8	1.6	0.11
2000	1626	836	14.3	1.3	0.09
2055	1396	964	17.4	1.6	0.09
2200	1922	680	12.5	1.2	0.08
2215	1802	495	8.9	0.7	0.05
2300	1120	582	7.7	0.6	0.04

DATE: 6 6 1977

TIME (GMT)	AEROSOL CONCENTRATIONS FOR SIZES > INDICATED DIAMETER				
	>0.01 /CM↑3	>0.1 /CM↑3	>0.3 /CM↑3	>1.2 /CM↑3	>3.0 /CM↑3
0	886	504	8.9	0.7	0.04
100	1102	615	11.6	0.8	0.04
200	1697	747	13.9	0.8	0.03
300	1518	885	12.7	0.6	0.03
400	1778	1154	10.8	0.7	0.04
500	2106	1387	10.7	0.7	0.04
600	1890	1269	10.5	0.7	0.04
700	2357	1284	10.9	0.7	0.04
800	2417	1245	11.8	0.8	0.04
900	2027	1448	12.5	1.0	0.05
1030	2115	1539	13.7	1.1	0.05
1300	3146	1637	14.3	1.2	0.06
1410	3714	1428	15.6	1.3	0.07
1630	2917	1346	15.8	1.3	0.07
1740	2253	1453	15.7	1.4	0.06
1800	2395	1433	15.5	1.3	0.07
1820	2478	1415	15.8	1.4	0.07
1900	2687	1419	21.1	2.0	0.09
2000	12720	2398	15.6	1.4	0.09
2100	3114	1408	13.6	1.1	0.07
2150	3609	1513	16.6	1.5	0.10
2210	5344	1643	15.9	1.4	0.09
2230	4315	1743	15.7	1.3	0.07
2300	2585	1429	15.8	1.3	0.08

DATE: 6 7 1977

TIME (GMT)	AEROSOL CONCENTRATIONS FOR SIZES > INDICATED DIAMETER				
	>0.01 /CM↑3	>0.1 /CM↑3	>0.3 /CM↑3	>1.2 /CM↑3	>3.0 /CM↑3
330	2536	1374	19.2	0.9	0.04
400	6993	1313	20.3	0.8	0.02
430	3595	1409	17.6	1.0	0.06
500	2764	1455	18.0	1.0	0.05
600	34600	5977	34.3	1.7	0.07

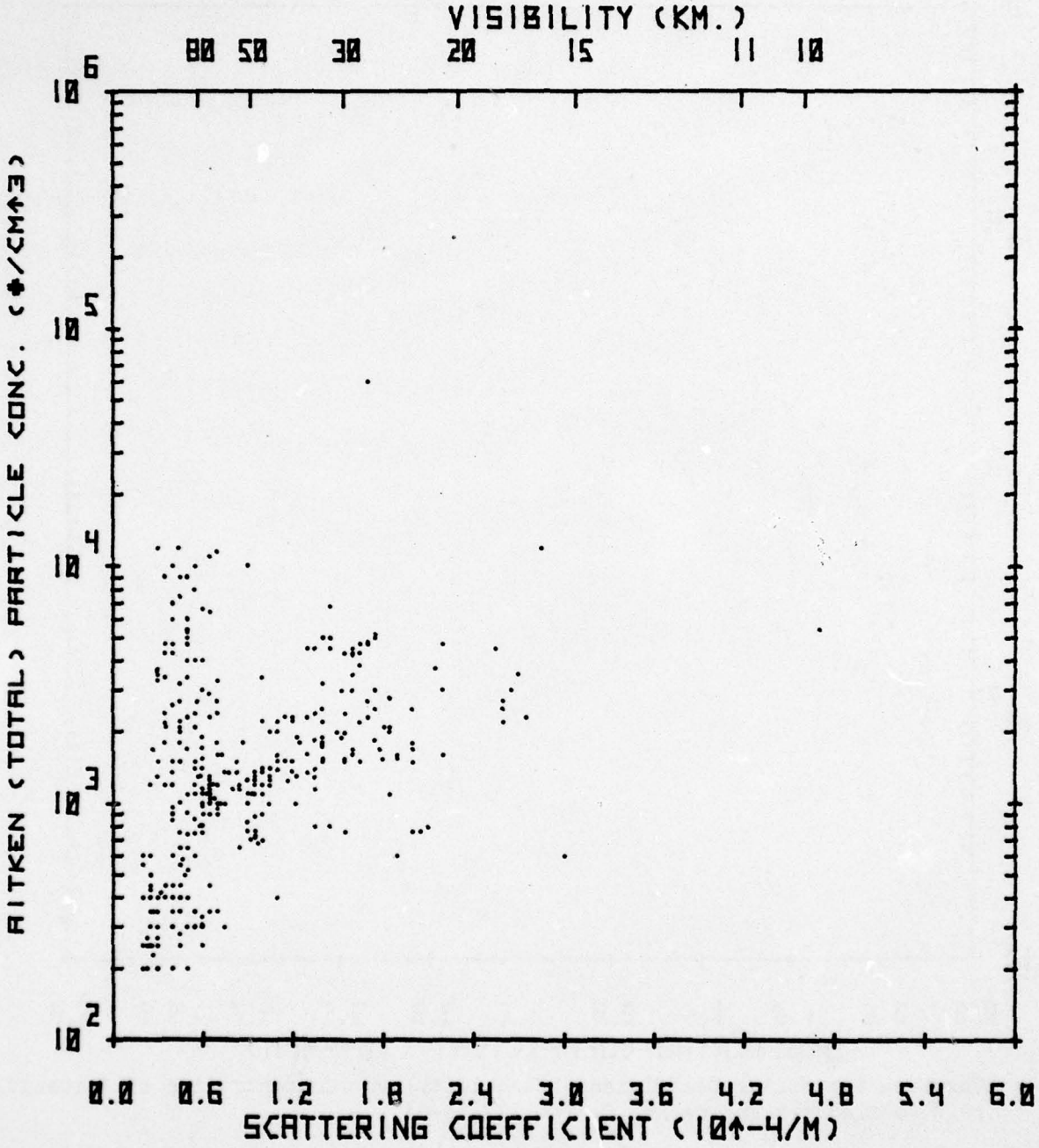

Observed Scattering Coefficient (Visibility) vs. Aitken (Total) Particle Concentration During NRL Cruise, 77-16-04

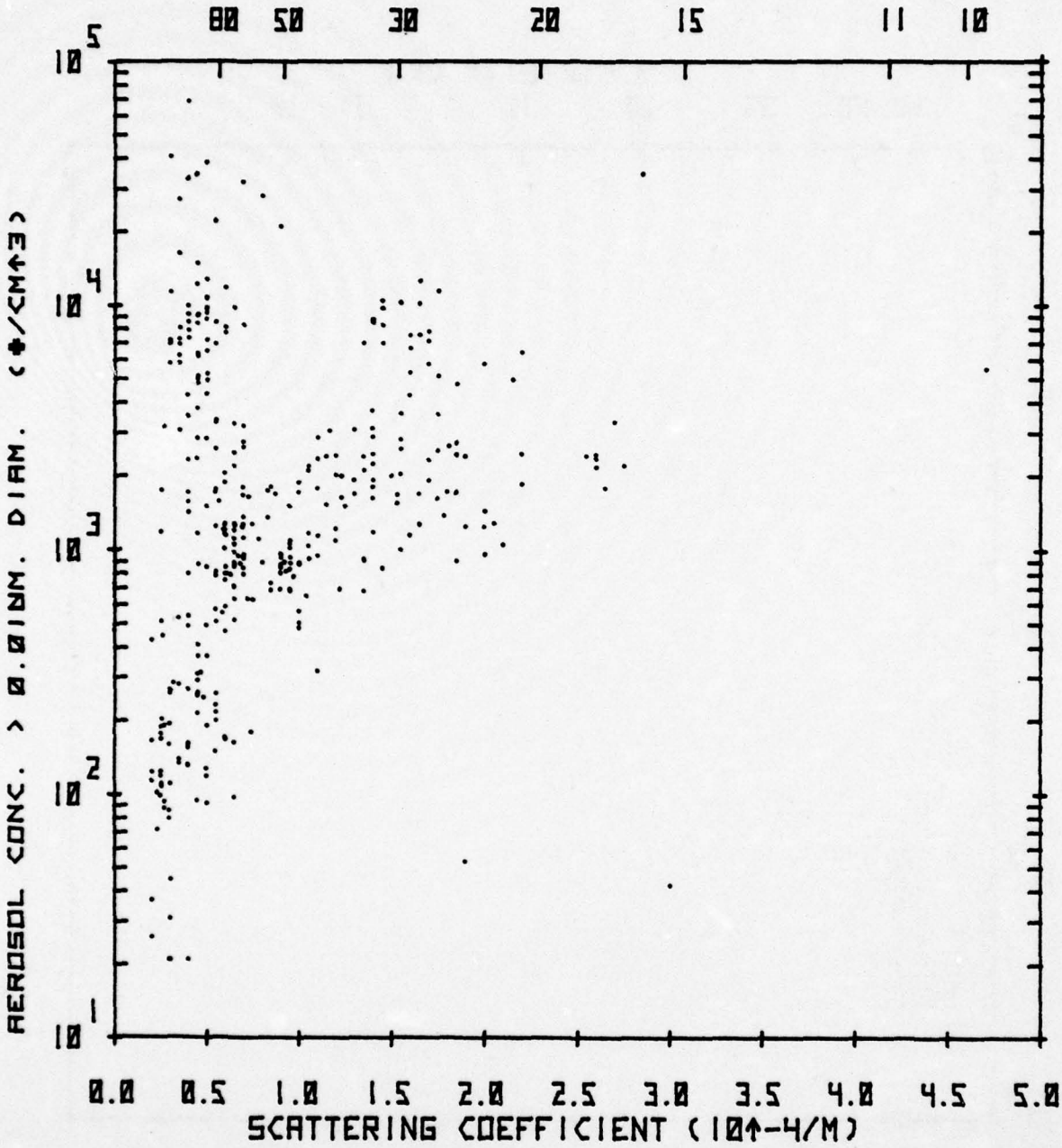

Observed Scattering Coefficient (Visibility) vs. Concentration of Aerosols >0.01μm Diameter During NRL Cruise, 77-16-04

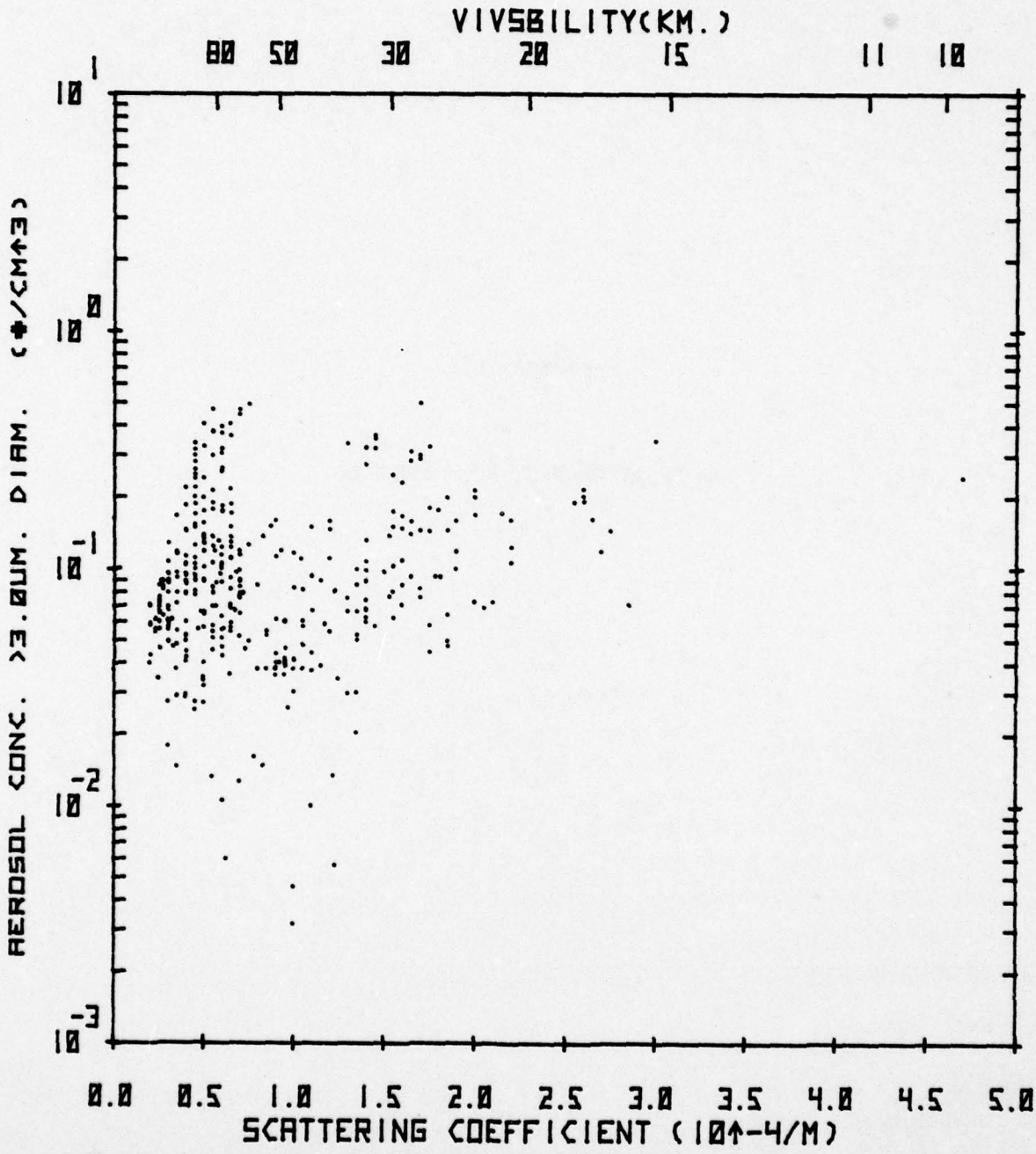

Observed Scattering Coefficient (Visibility) vs. Concentration of Aerosols >3.0μm Diameter During NRL Cruise, 77-16-04

Appendix E

SEA SPRAY DROPLET SIZE SPECTRA

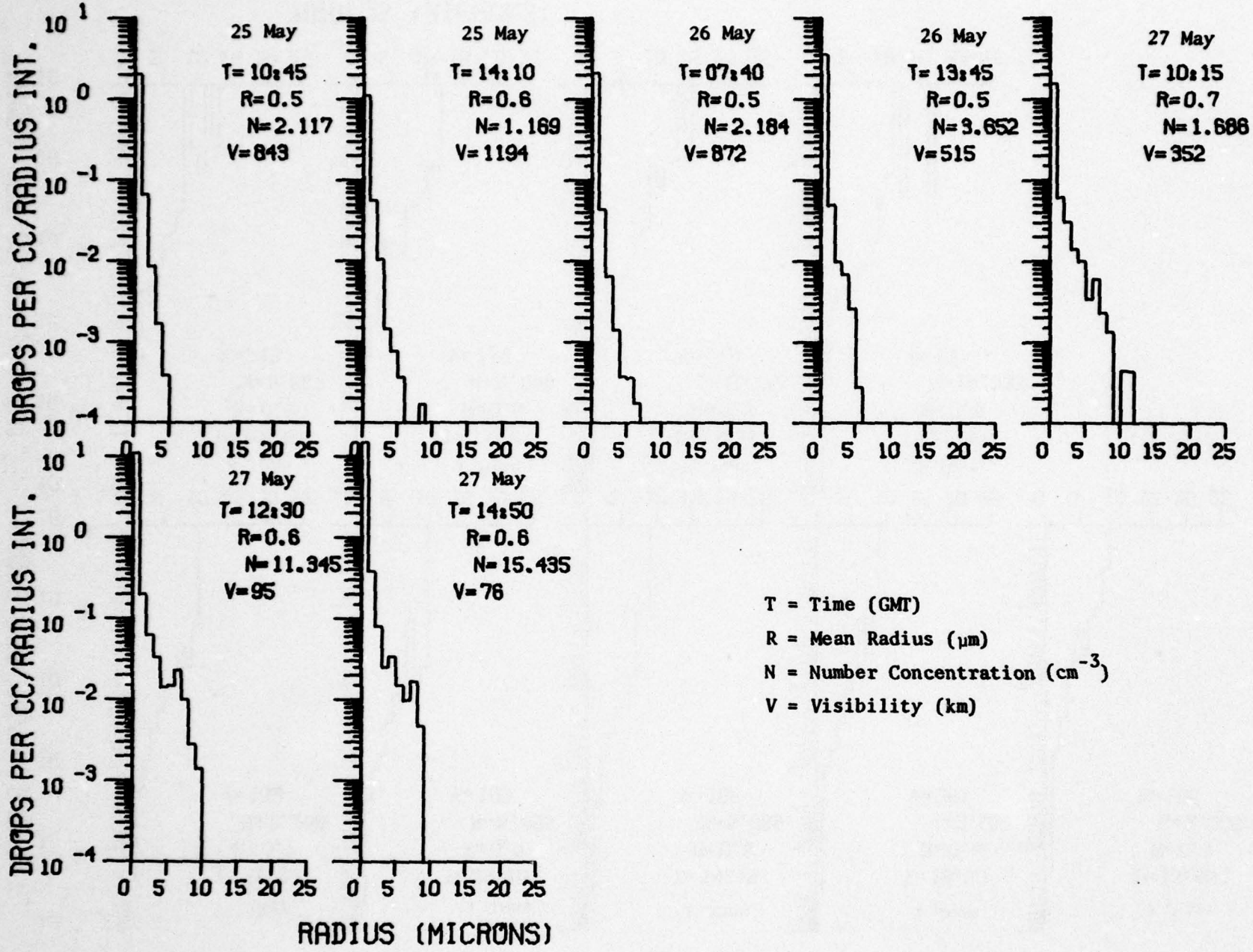
25 May
T= 10:45
R=0.5
N=2.117
V=843
25 May
T= 14:10
R=0.6
N=1.169
V=1194
26 May
T= 07:40
R=0.5
N=2.184
V=872
26 May
T= 13:45
R=0.5
N=3.652
V=515
27 May
T= 10:15
R=0.7
N=1.686
V=352
27 May
T= 12:30
R=0.6
N=11.345
V=95
27 May
T= 14:50
R=0.6
N=15.435
V=76
T = Time (GMT)
R = Mean Radius (μm)
N = Number Concentration (cm^{-3})
V = Visibility (km)
DROPS PER CC/RADIUS INT.
DROPS PER CC/RADIUS INT.
RADIUS (MICRONS)

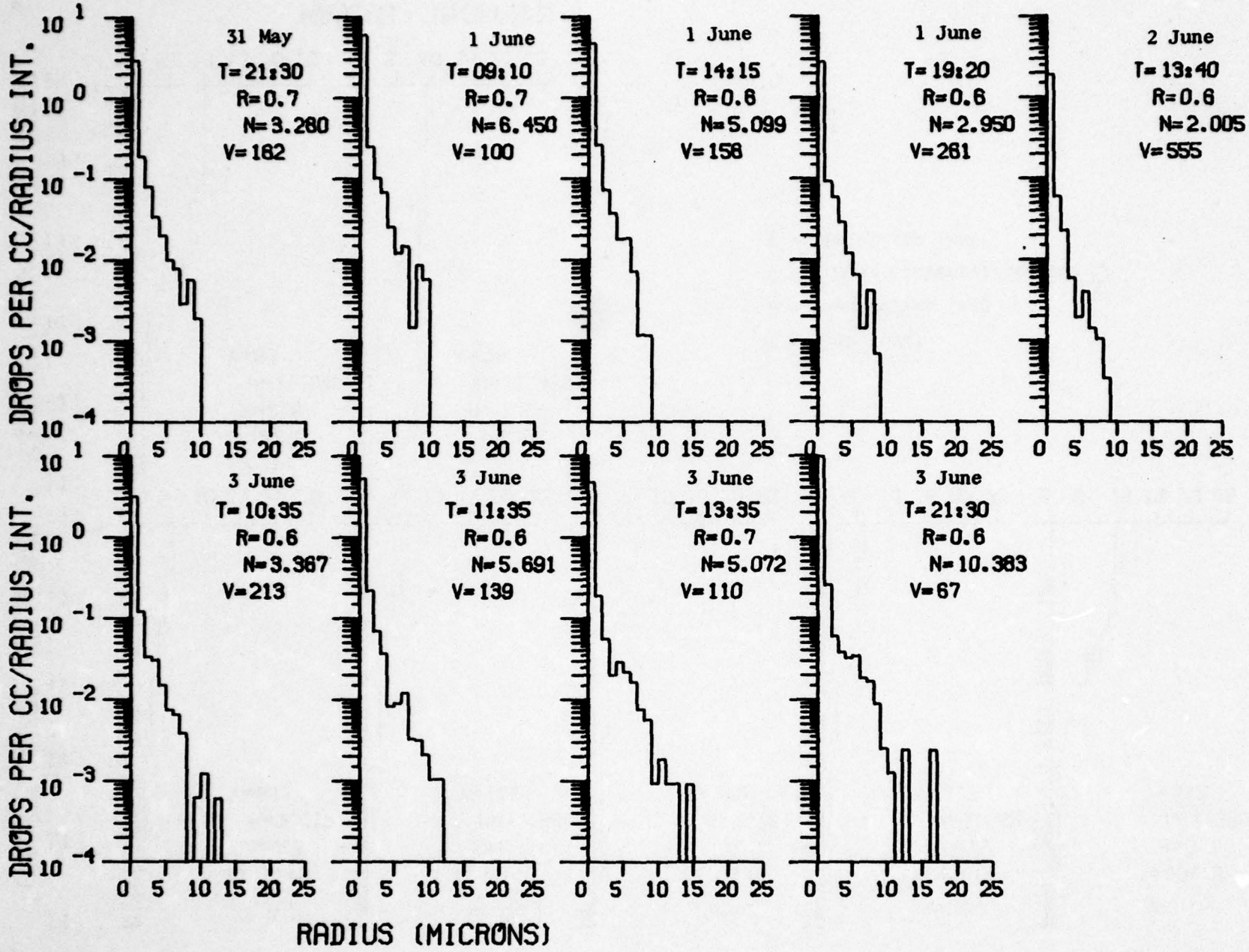
31 May
T=21:30
R=0.7
N=3.280
V=162
1 June
T=09:10
R=0.7
N=6.450
V=100
1 June
T=14:15
R=0.6
N=5.099
V=158
1 June
T=19:20
R=0.6
N=2.950
V=261
2 June
T=13:40
R=0.6
N=2.005
V=555
3 June
T=10:35
R=0.6
N=3.367
V=213
3 June
T=11:35
R=0.6
N=5.691
V=139
3 June
T=13:35
R=0.7
N=5.072
V=110
3 June
T=21:30
R=0.6
N=10.383
V=67
DROPS PER CC/RADIUS INT.
DROPS PER CC/RADIUS INT.
RADIUS (MICRONS)

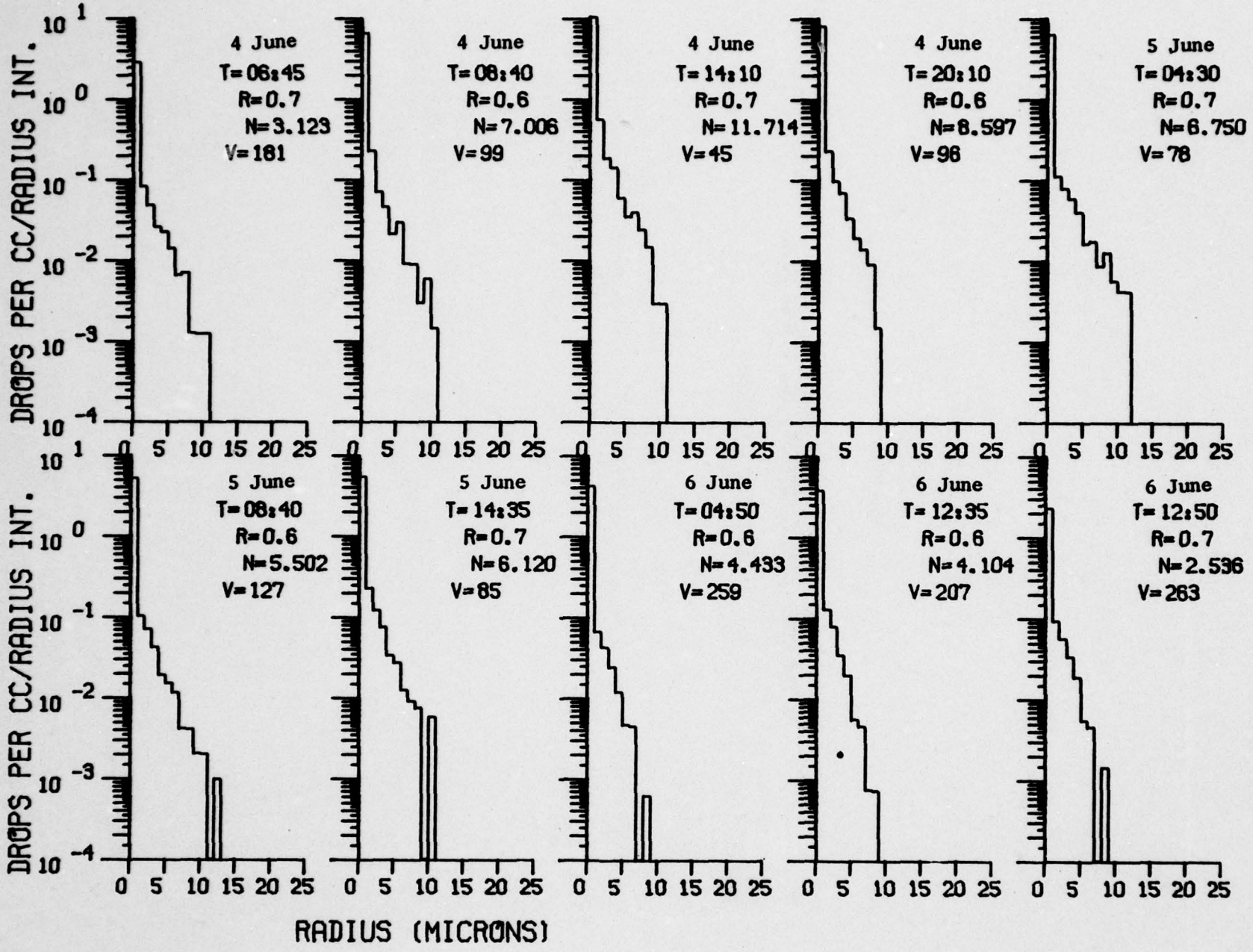
4 June
T=06:45
R=0.7
N=3.123
V=181
4 June
T=08:40
R=0.6
N=7.006
V=99
4 June
T=14:10
R=0.7
N=11.714
V=45
4 June
T=20:10
R=0.6
N=8.597
V=98
5 June
T=04:30
R=0.7
N=6.750
V=78
5 June
T=08:40
R=0.6
N=5.502
V=127
5 June
T=14:35
R=0.7
N=6.120
V=85
6 June
T=04:50
R=0.6
N=4.433
V=259
6 June
T=12:35
R=0.6
N=4.104
V=207
6 June
T=12:50
R=0.7
N=2.536
V=263
DROPS PER CC/RADIUS INT.
RADIUS (MICRONS)

Appendix F

COMPLETE AEROSOL SIZE SPECTRA FITTED WITH JUNGE DISTRIBUTIONS

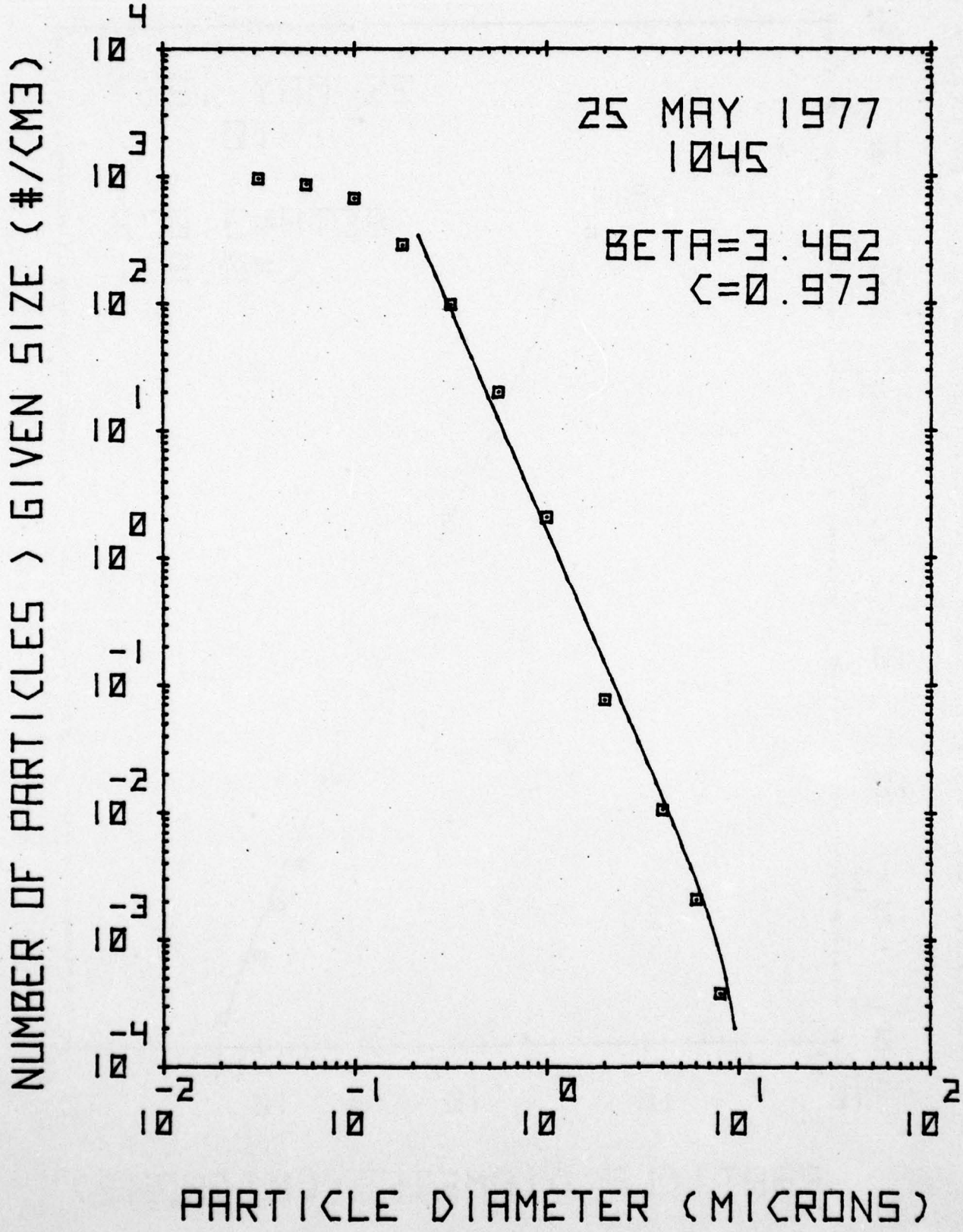
25 MAY 1977
1045
BETA=3.462
C=0.973
NUMBER OF PARTICLES > GIVEN SIZE (#/CM3)
PARTICLE DIAMETER (MICRONS)
10^4
10^3
10^2
10^1
10^0
10^-1
10^-2
10^-3
10^-4
10^-2
10^-1
10^0
10^1
10^2

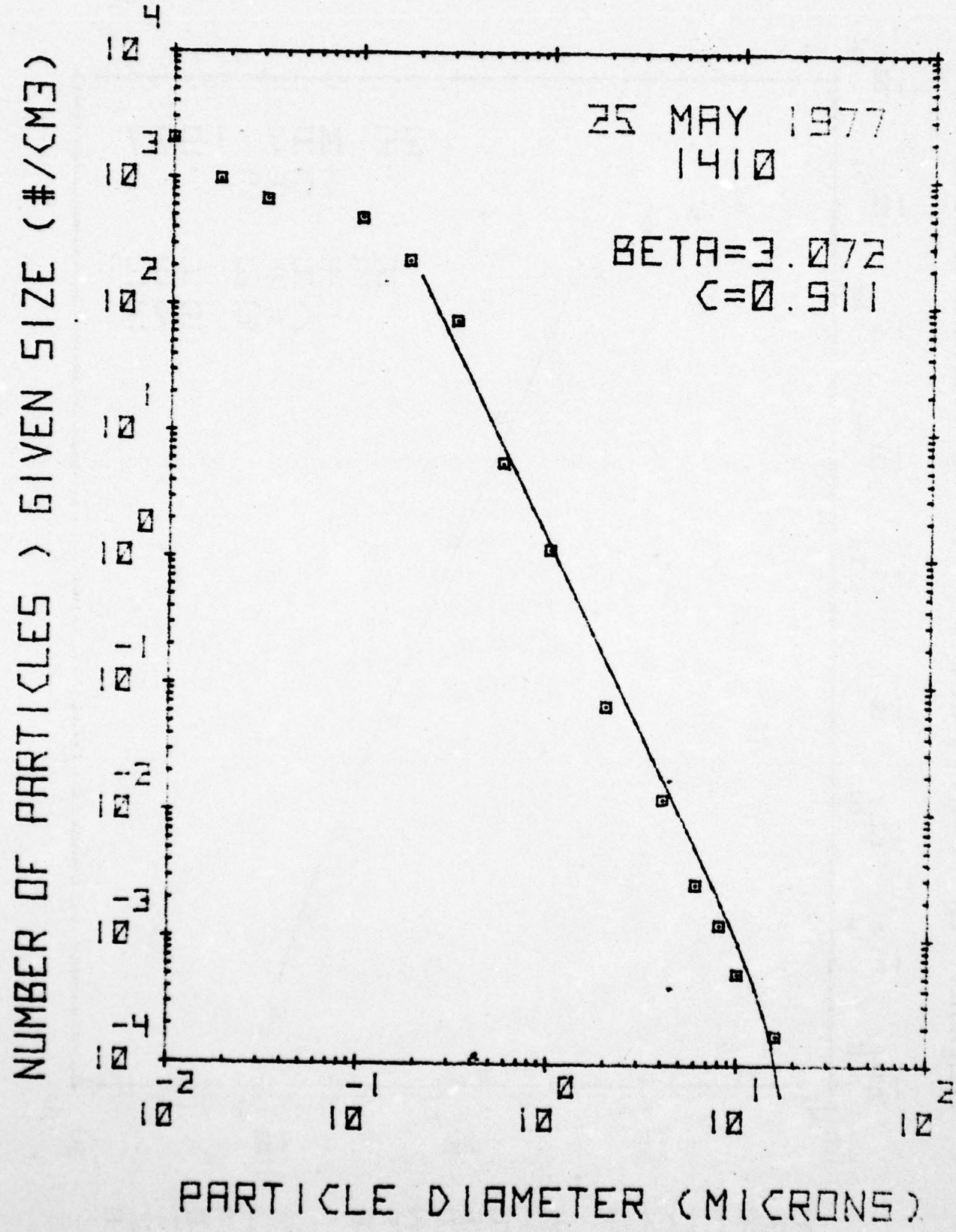
25 MAY 1977
1410
BETA=3.072
C=0.911
NUMBER OF PARTICLES > GIVEN SIZE (#/CM3)
PARTICLE DIAMETER (MICRONS)

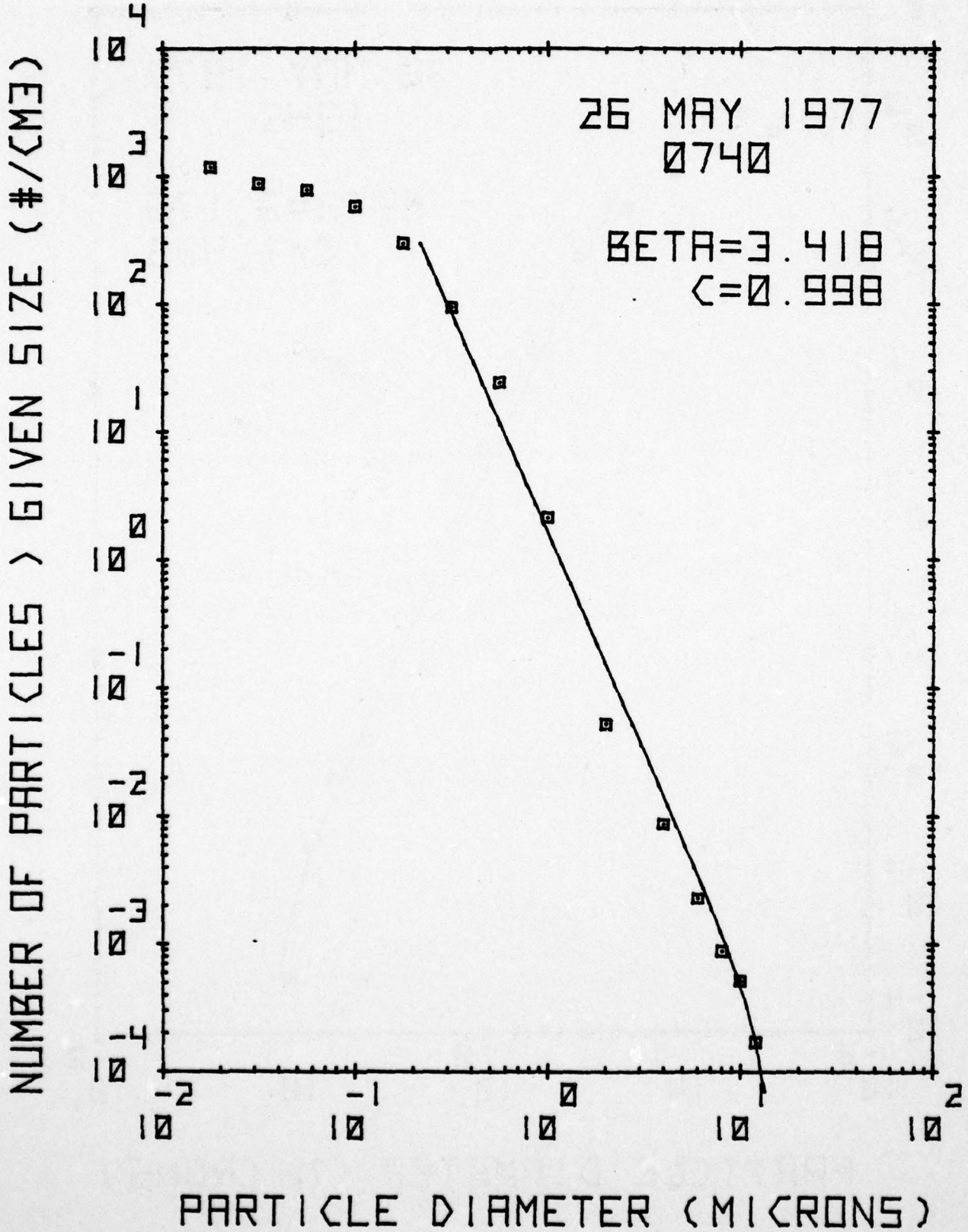
26 MAY 1977
0740
BETA=3.418
C=0.998
NUMBER OF PARTICLES > GIVEN SIZE (#/CM3)
PARTICLE DIAMETER (MICRONS)
10^4
10^3
10^2
10^1
10^0
10^-1
10^-2
10^-3
10^-4
10^-2
10^-1
10^0
10^1
10^2

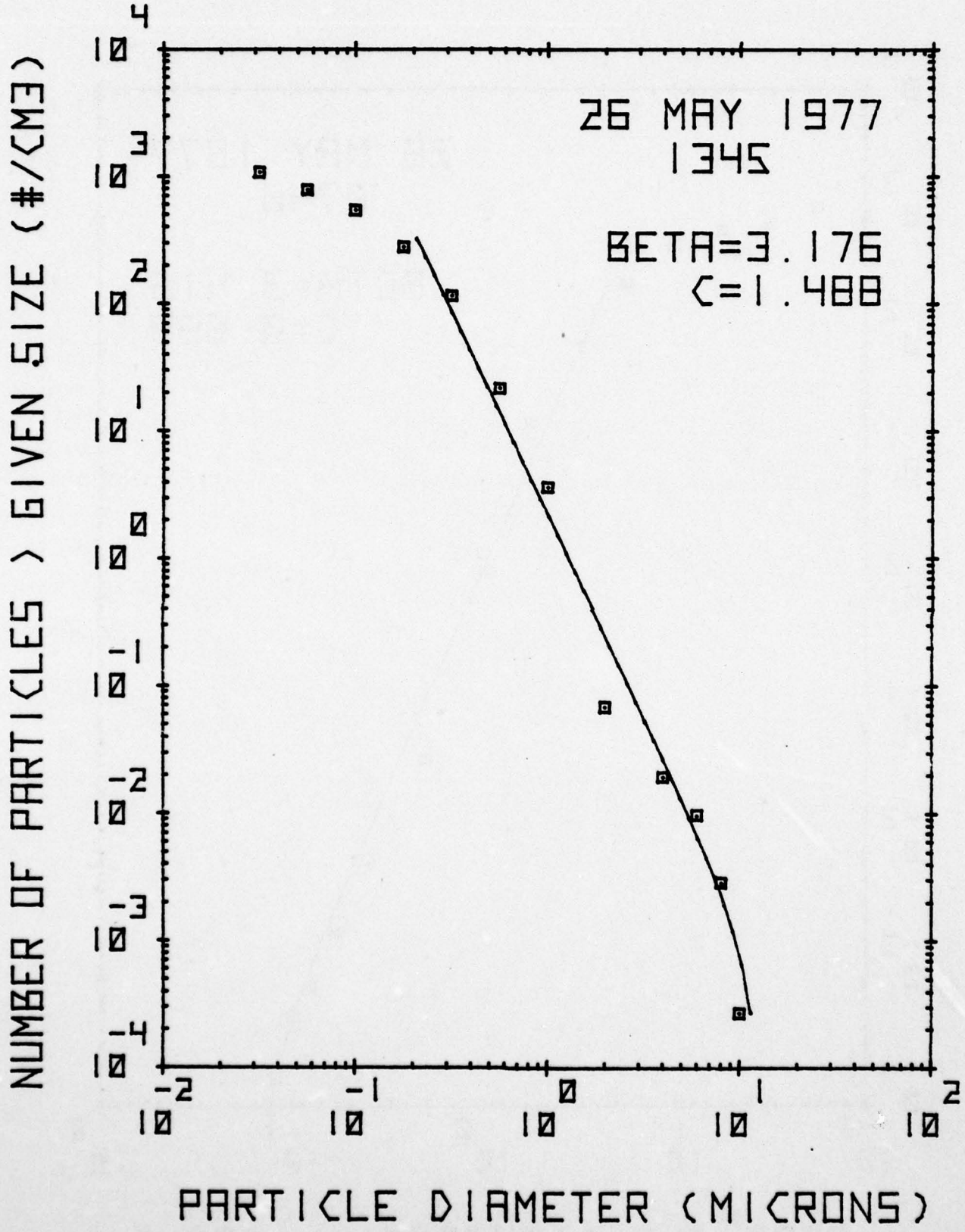
26 MAY 1977
1345
BETA=3.176
C=1.488
NUMBER OF PARTICLES > GIVEN SIZE (#/CM3)
PARTICLE DIAMETER (MICRONS)
10^4
10^3
10^2
10^1
10^0
10^-1
10^-2
10^-3
10^-4
10^-2
10^-1
10^0
10^1
10^2

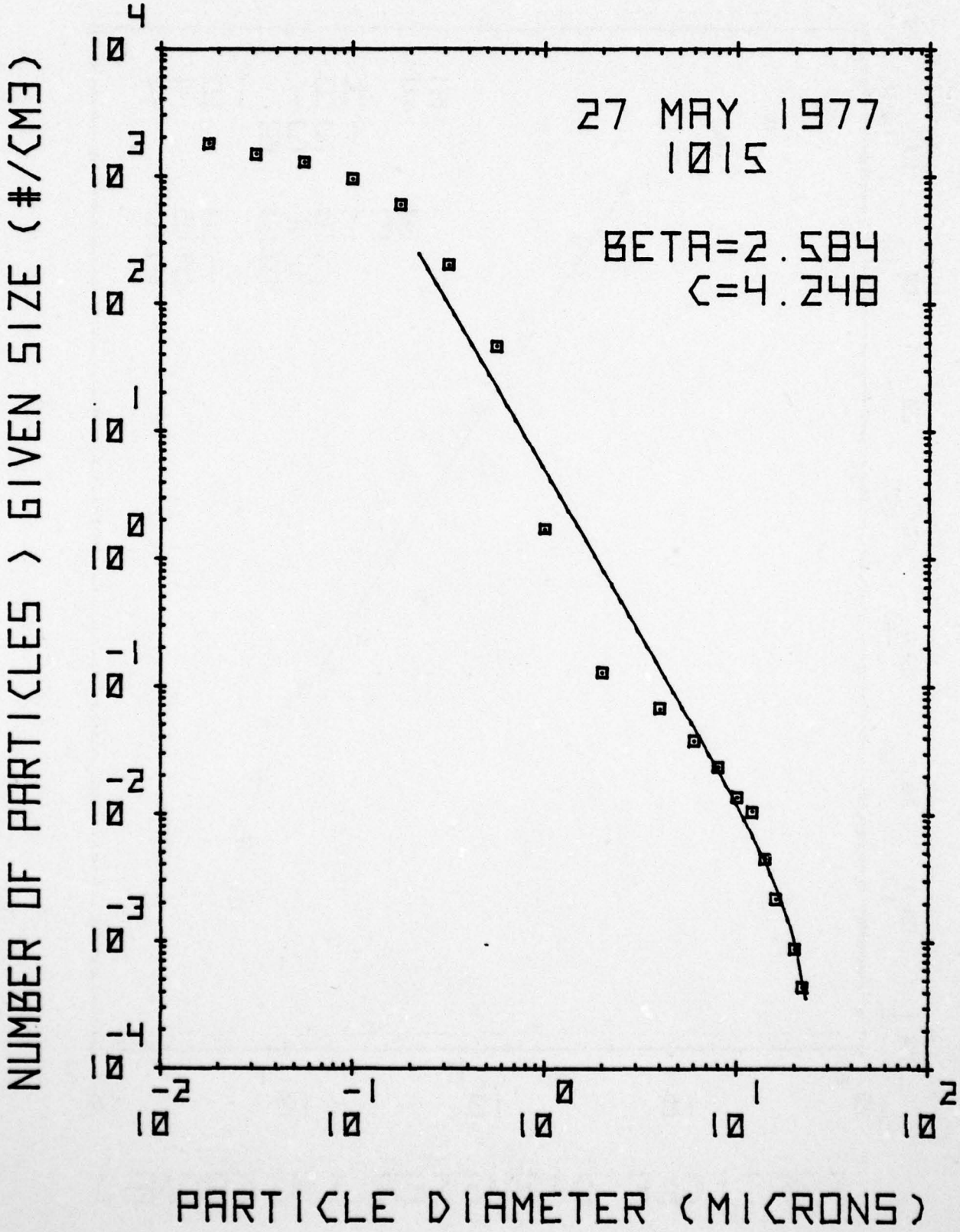
27 MAY 1977
1015
BETA=2.584
C=4.248
NUMBER OF PARTICLES > GIVEN SIZE (#/CM3)
PARTICLE DIAMETER (MICRONS)
10^4
10^3
10^2
10^1
10^0
10^-1
10^-2
10^-3
10^-4
10^-2
10^-1
10^0
10^1
10^2

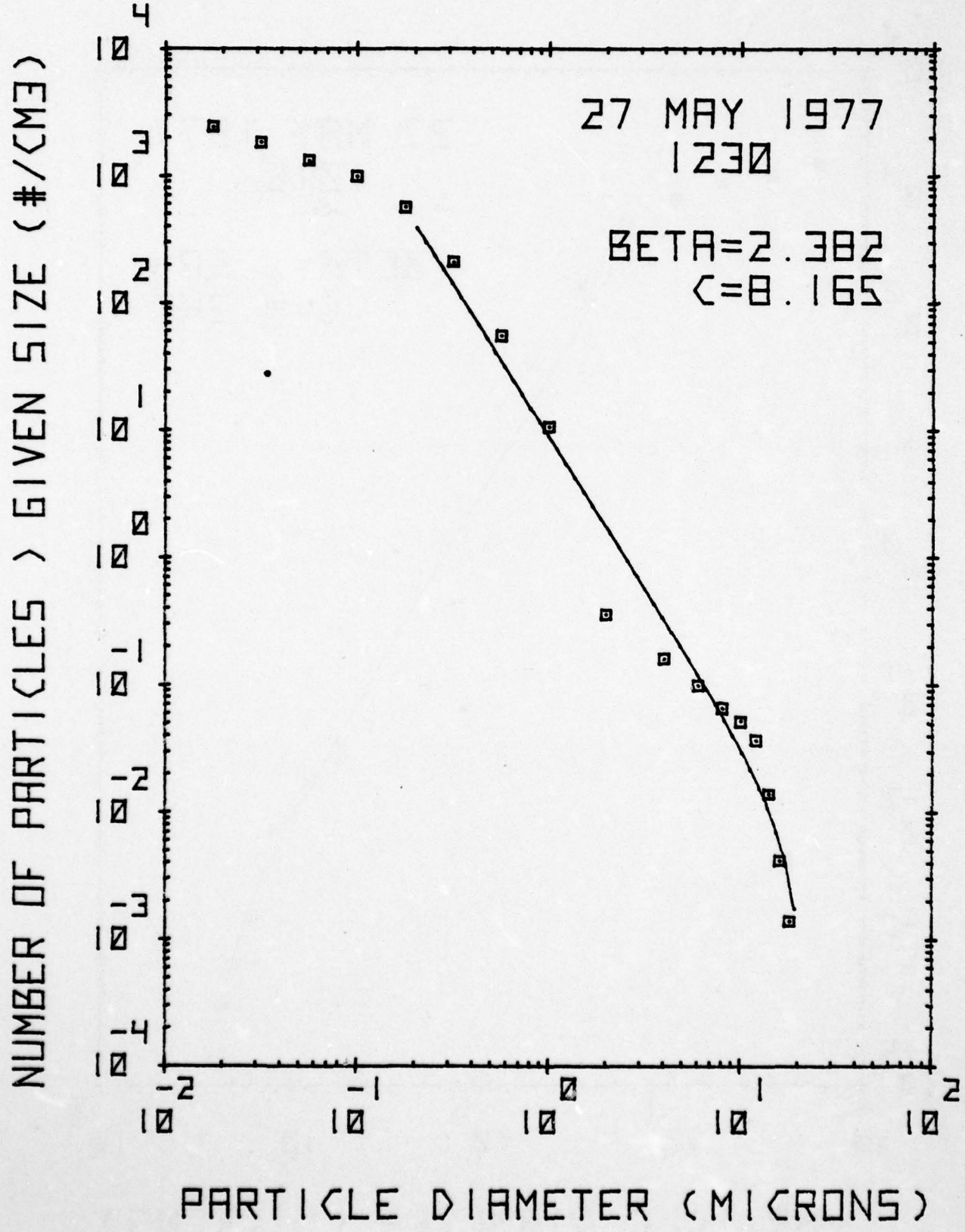
27 MAY 1977
1230
BETA=2.382
C=8.165
NUMBER OF PARTICLES > GIVEN SIZE (#/CM3)
PARTICLE DIAMETER (MICRONS)

AD-A062 888 CALSPAN ADVANCED TECHNOLOGY CENTER BUFFALO NY F/G 4/2
AEROSOL CHARACTERISTICS OF THE MARINE BOUNDARY LAYER OF THE NOR--ETC(U)
OCT 78 E J MACK, R J ANDERSON, C K AKERS N00019-78-C-0179
UNCLASSIFIED CALSPAN-6232-M-1 NL

3 OF 3
ADA
062888

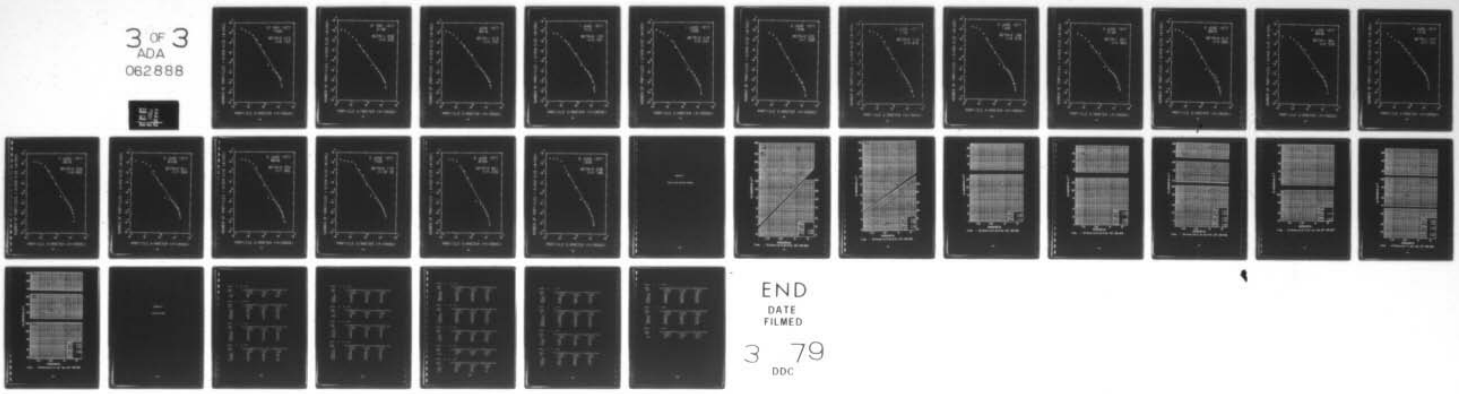

END
DATE FILMED
3 79
DDC

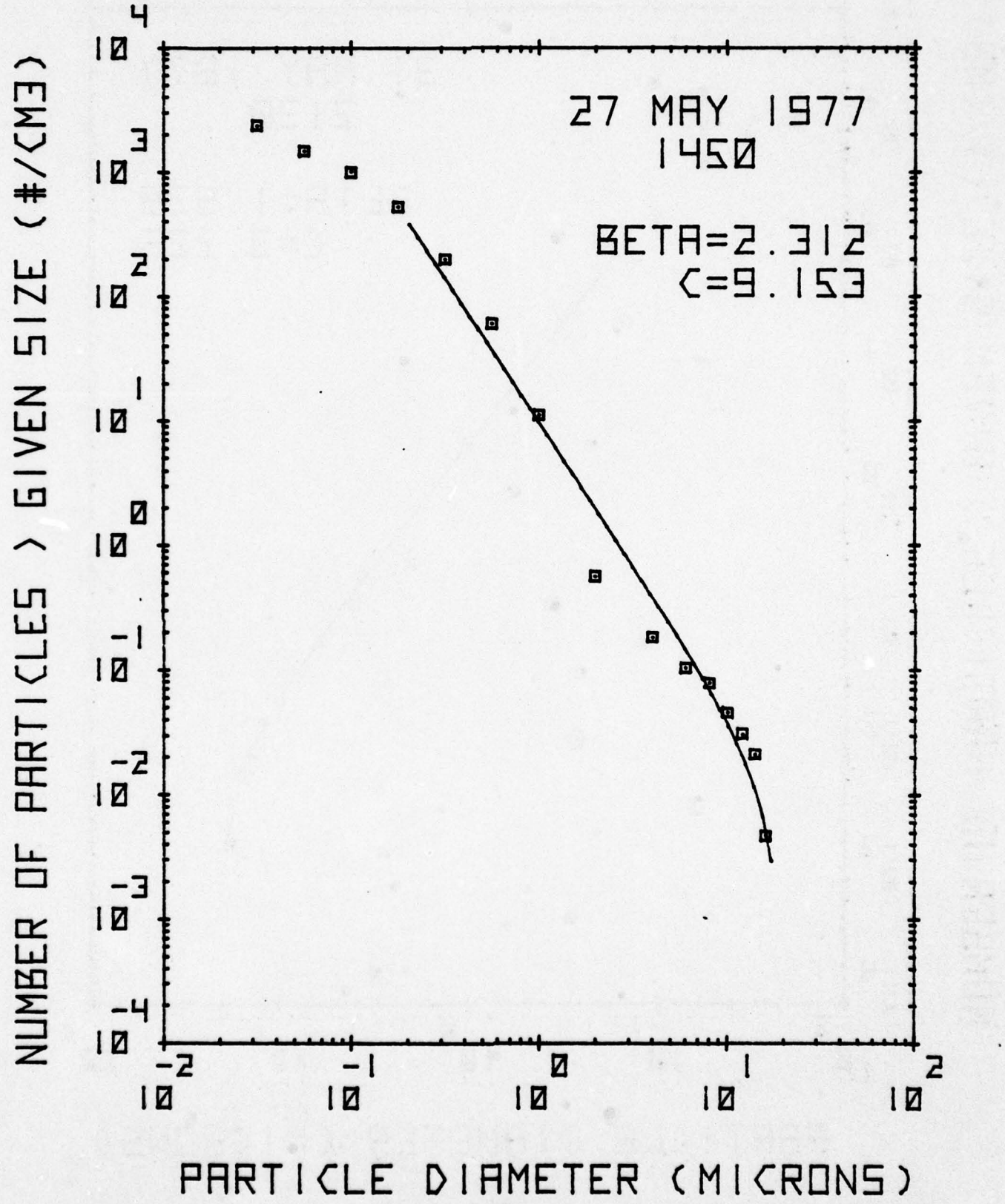
27 MAY 1977
1450
BETA=2.312
C=9.153
NUMBER OF PARTICLES > GIVEN SIZE (#/CM3)
PARTICLE DIAMETER (MICRONS)
10^4
10^3
10^2
10^1
10^0
10^-1
10^-2
10^-3
10^-4
10^-2
10^-1
10^0
10^1
10^2

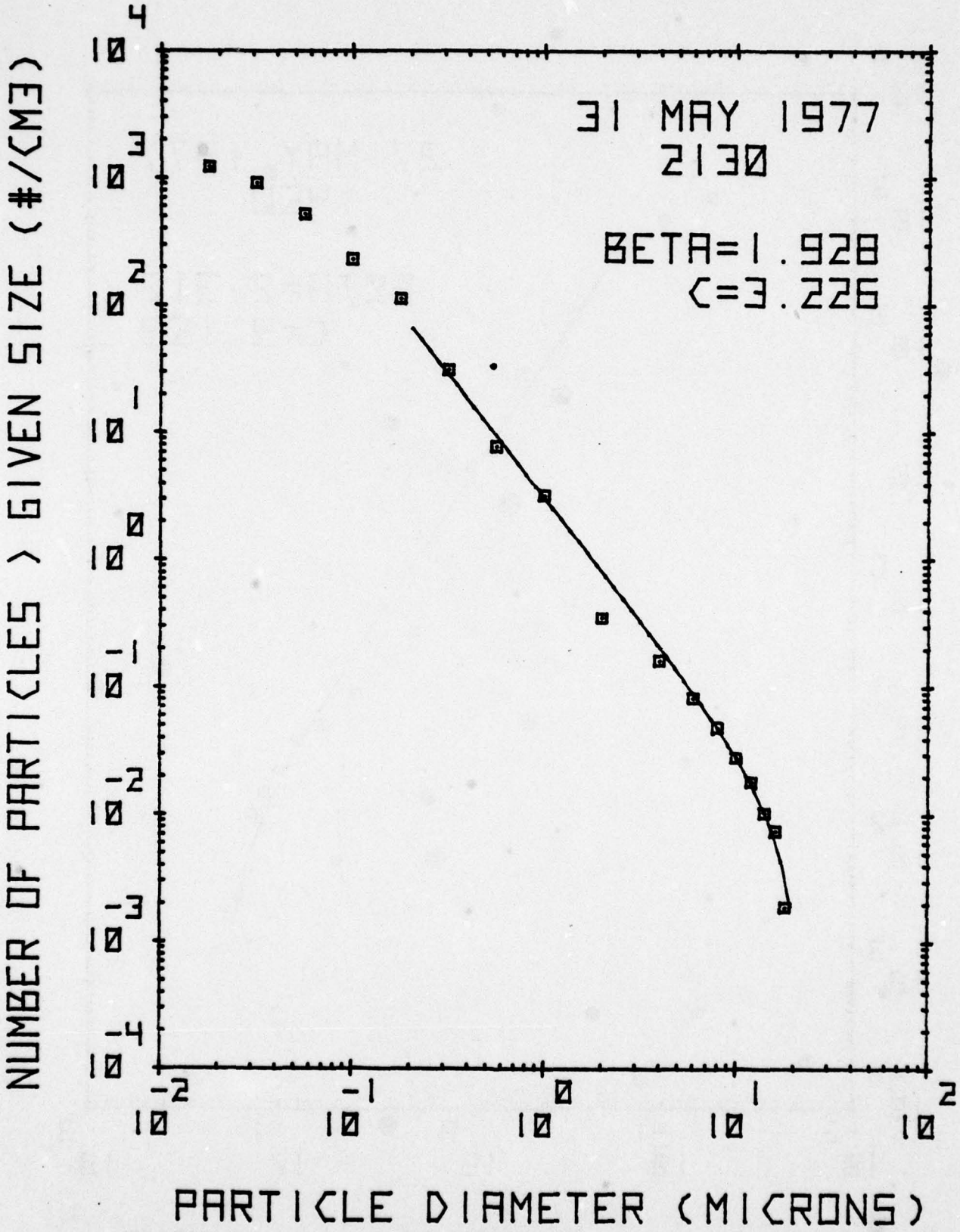
NUMBER OF PARTICLES > GIVEN SIZE (#/CM3)
10^4
10^3
10^2
10^1
10^0
10^-1
10^-2
10^-3
10^-4
31 MAY 1977
2130
BETA=1.928
C=3.226
10^-2
10^-1
10^0
10^1
10^2
PARTICLE DIAMETER (MICRONS)

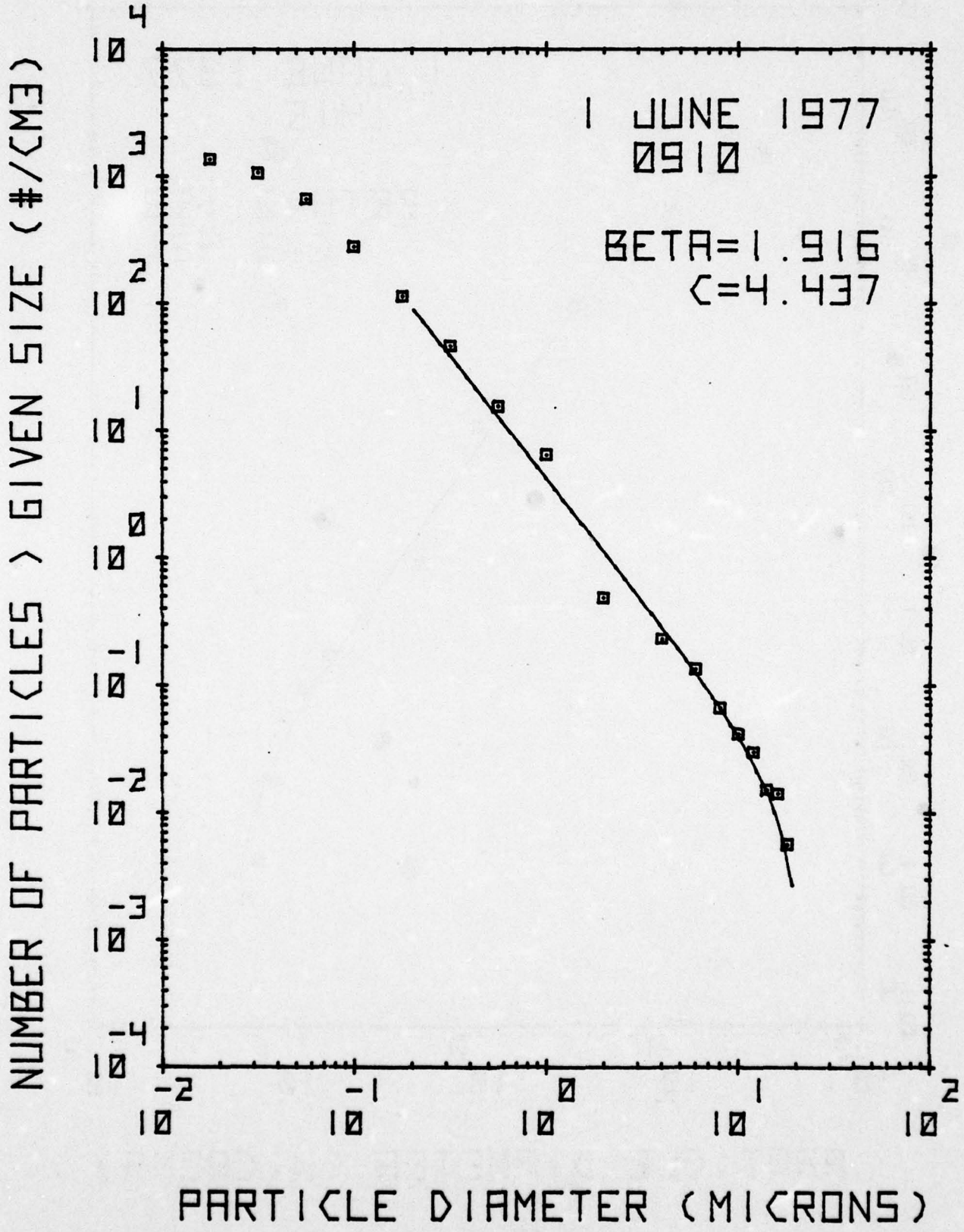
1 JUNE 1977
0910
BETA=1.916
C=4.437
NUMBER OF PARTICLES > GIVEN SIZE (#/CM3)
PARTICLE DIAMETER (MICRONS)

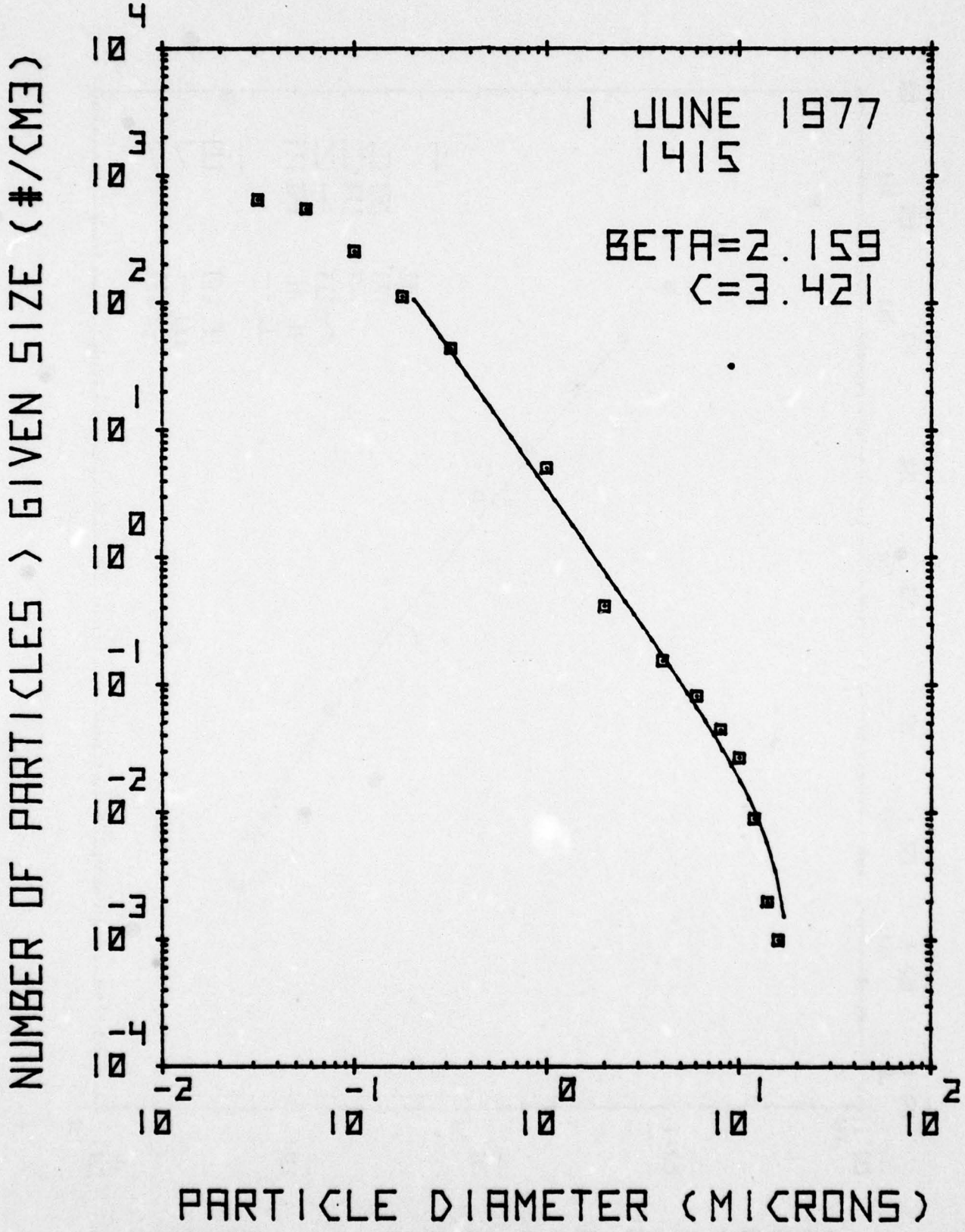
1 JUNE 1977
1415
BETA=2.159
C=3.421
NUMBER OF PARTICLES > GIVEN SIZE (#/CM3)
PARTICLE DIAMETER (MICRONS)

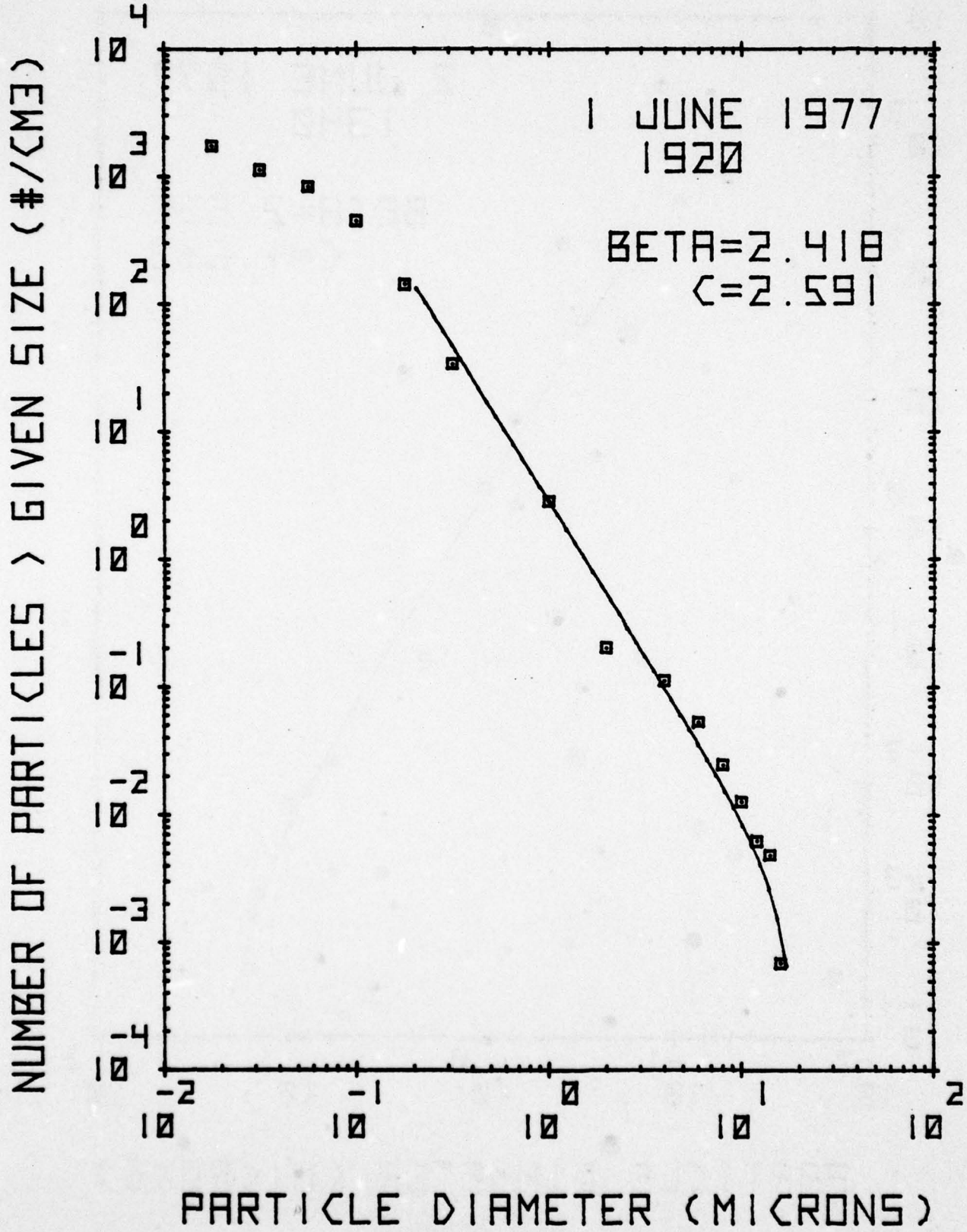
1 JUNE 1977
1920
BETA=2.418
C=2.591
NUMBER OF PARTICLES > GIVEN SIZE (#/CM3)
PARTICLE DIAMETER (MICRONS)

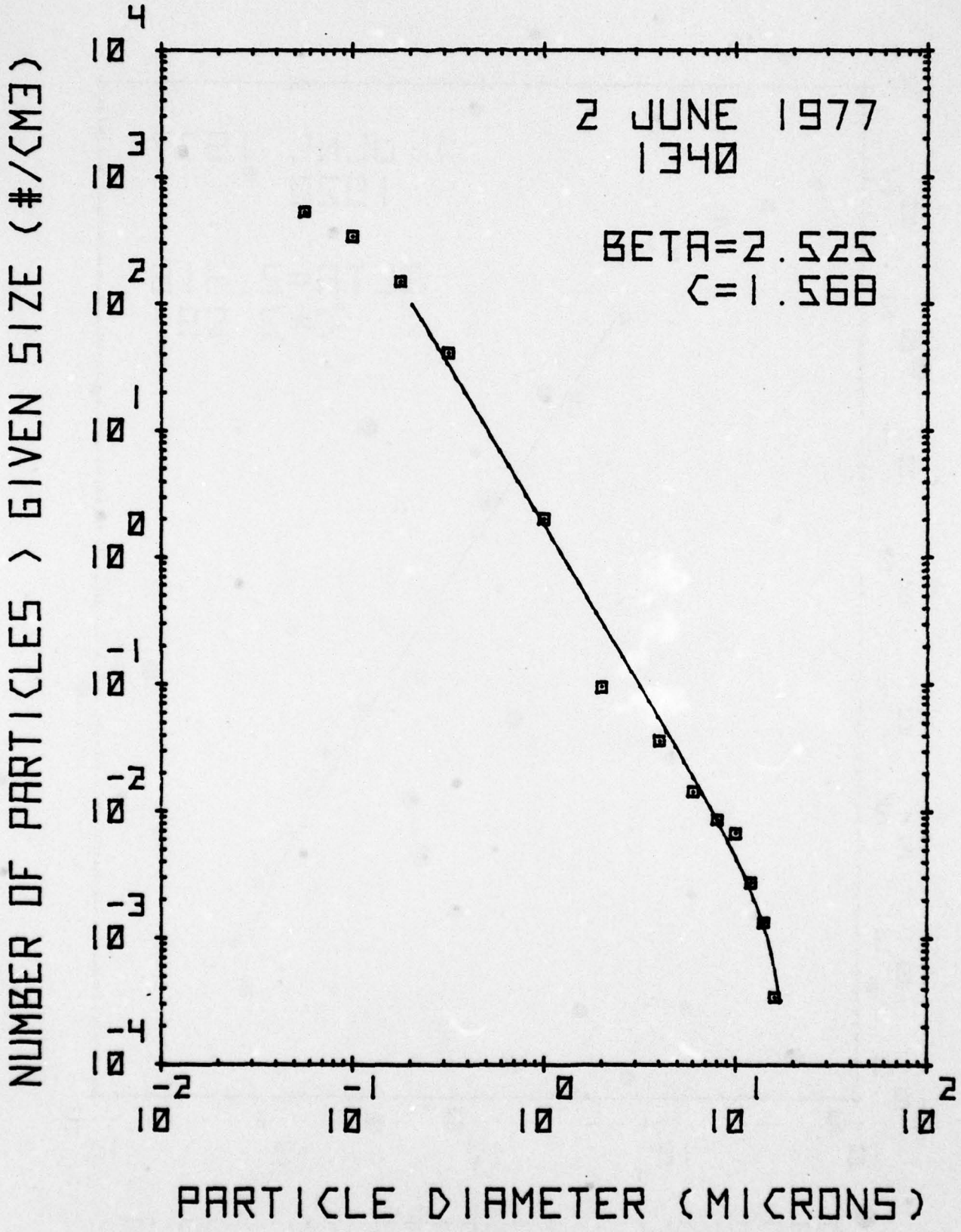
2 JUNE 1977
1340
BETA=2.525
C=1.568
NUMBER OF PARTICLES > GIVEN SIZE (#/CM3)
PARTICLE DIAMETER (MICRONS)

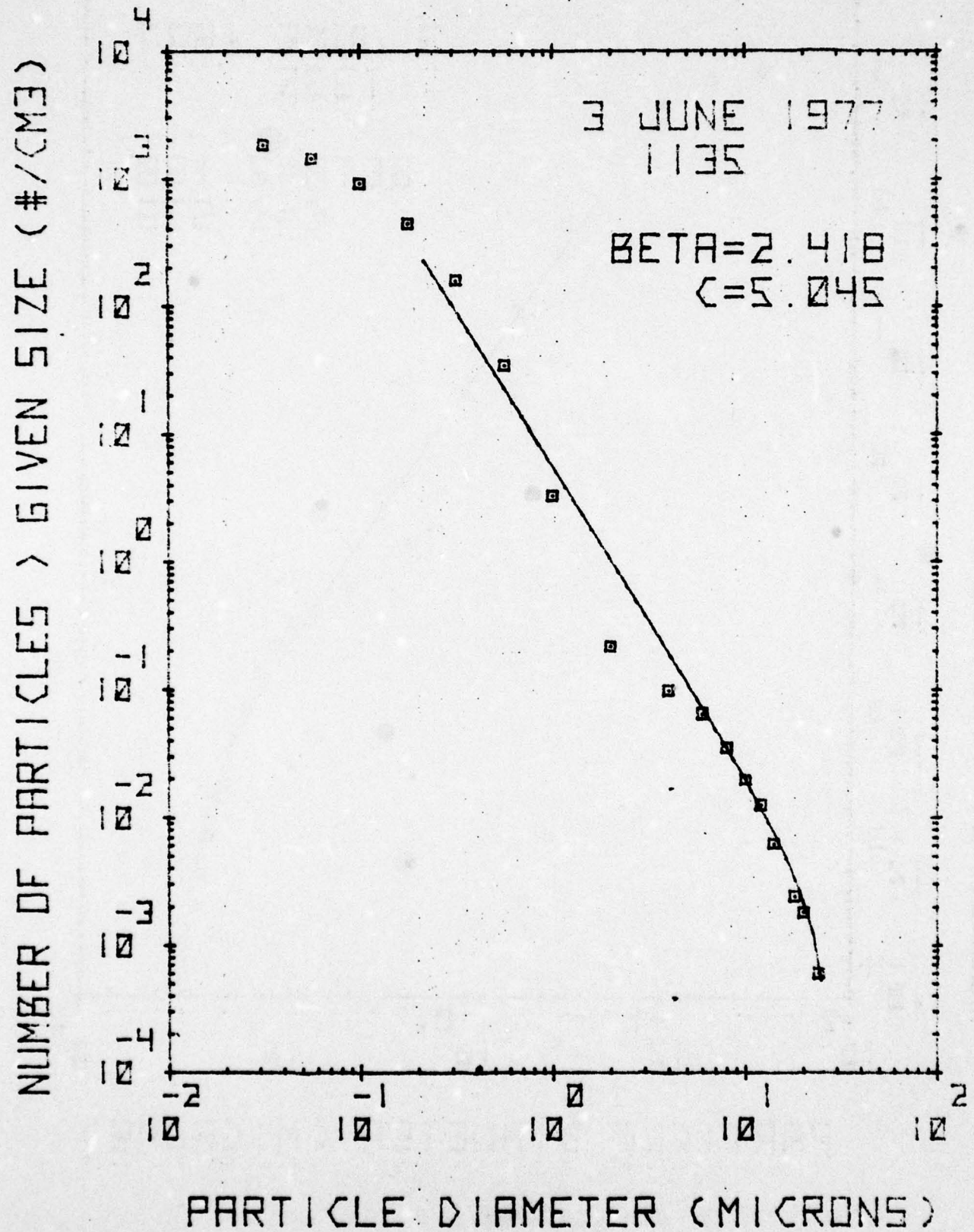
3 JUNE 1977
1135
BETA=2.418
C=5.045
NUMBER OF PARTICLES > GIVEN SIZE (#/CM3)
PARTICLE DIAMETER (MICRONS)

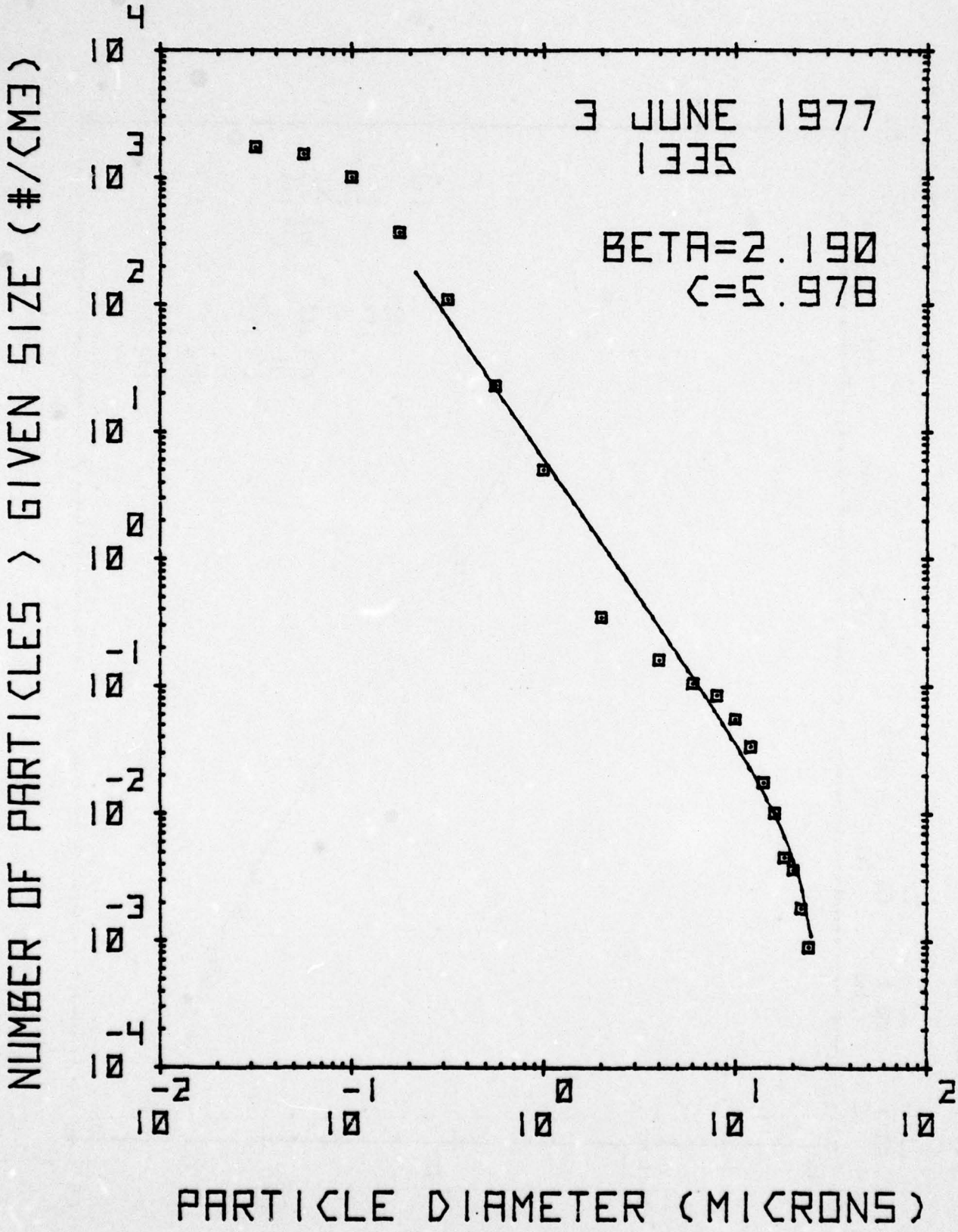
3 JUNE 1977
1335
BETA=2.190
C=5.978
NUMBER OF PARTICLES > GIVEN SIZE (#/CM3)
PARTICLE DIAMETER (MICRONS)

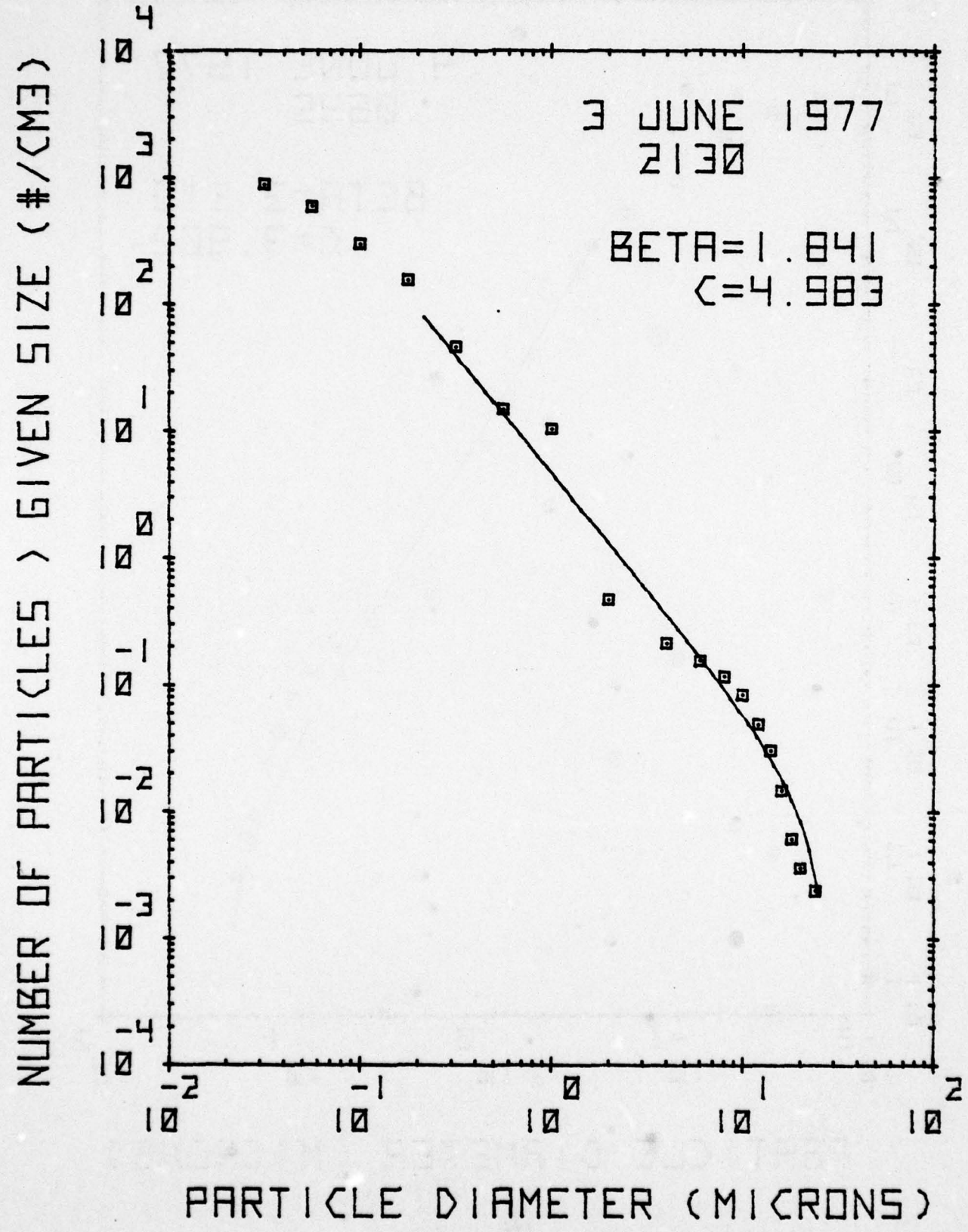
3 JUNE 1977
2130
BETA=1.841
C=4.983
NUMBER OF PARTICLES > GIVEN SIZE (#/CM3)
PARTICLE DIAMETER (MICRONS)
10^4
10^3
10^2
10^1
10^0
10^-1
10^-2
10^-3
10^-4
10^-2
10^-1
10^0
10^1
10^2

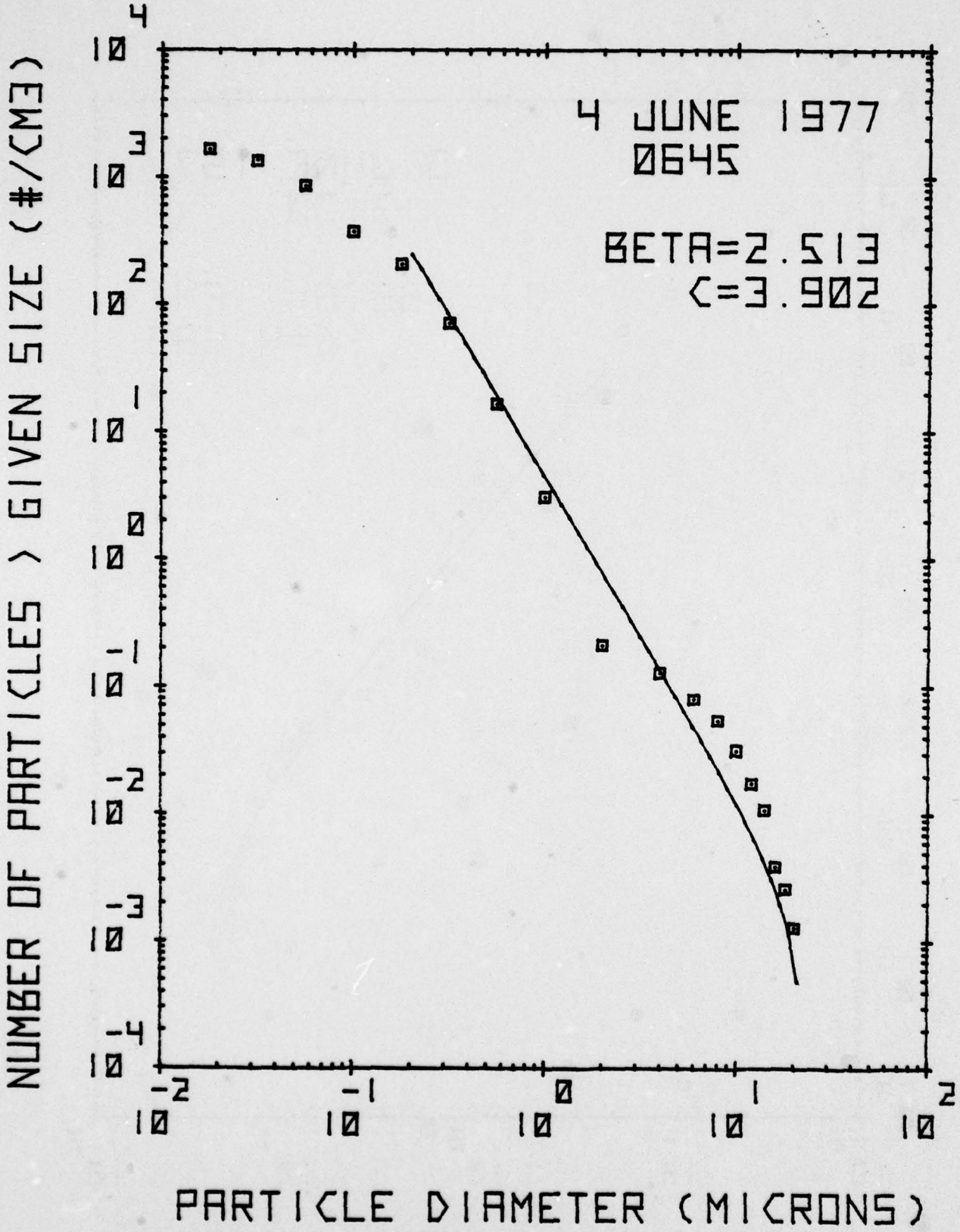
4 JUNE 1977
0645
BETA=2.513
C=3.902
NUMBER OF PARTICLES > GIVEN SIZE (#/CM3)
PARTICLE DIAMETER (MICRONS)

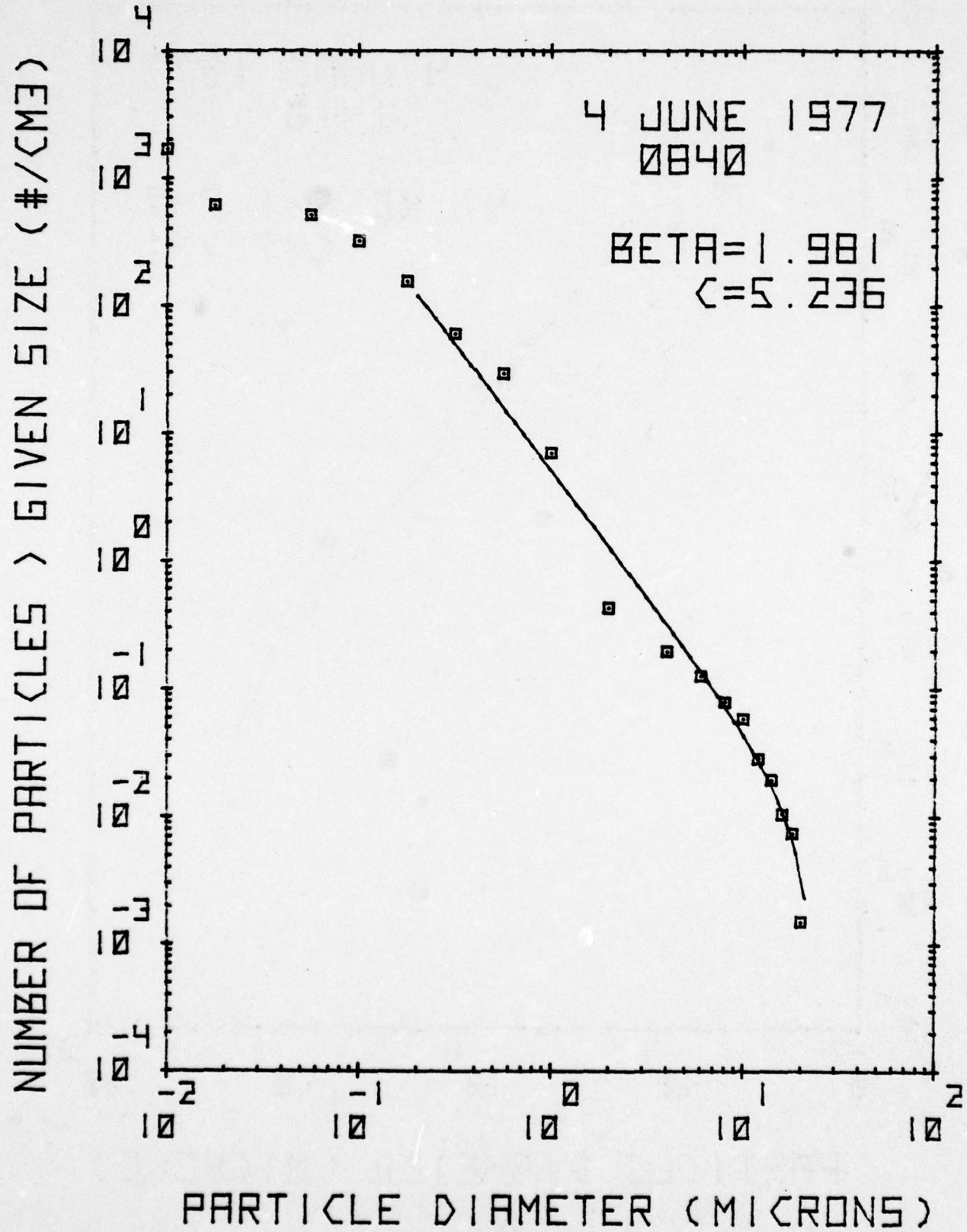
4 JUNE 1977
0840
BETA=1.981
C=5.236
NUMBER OF PARTICLES > GIVEN SIZE (#/CM3)
PARTICLE DIAMETER (MICRONS)

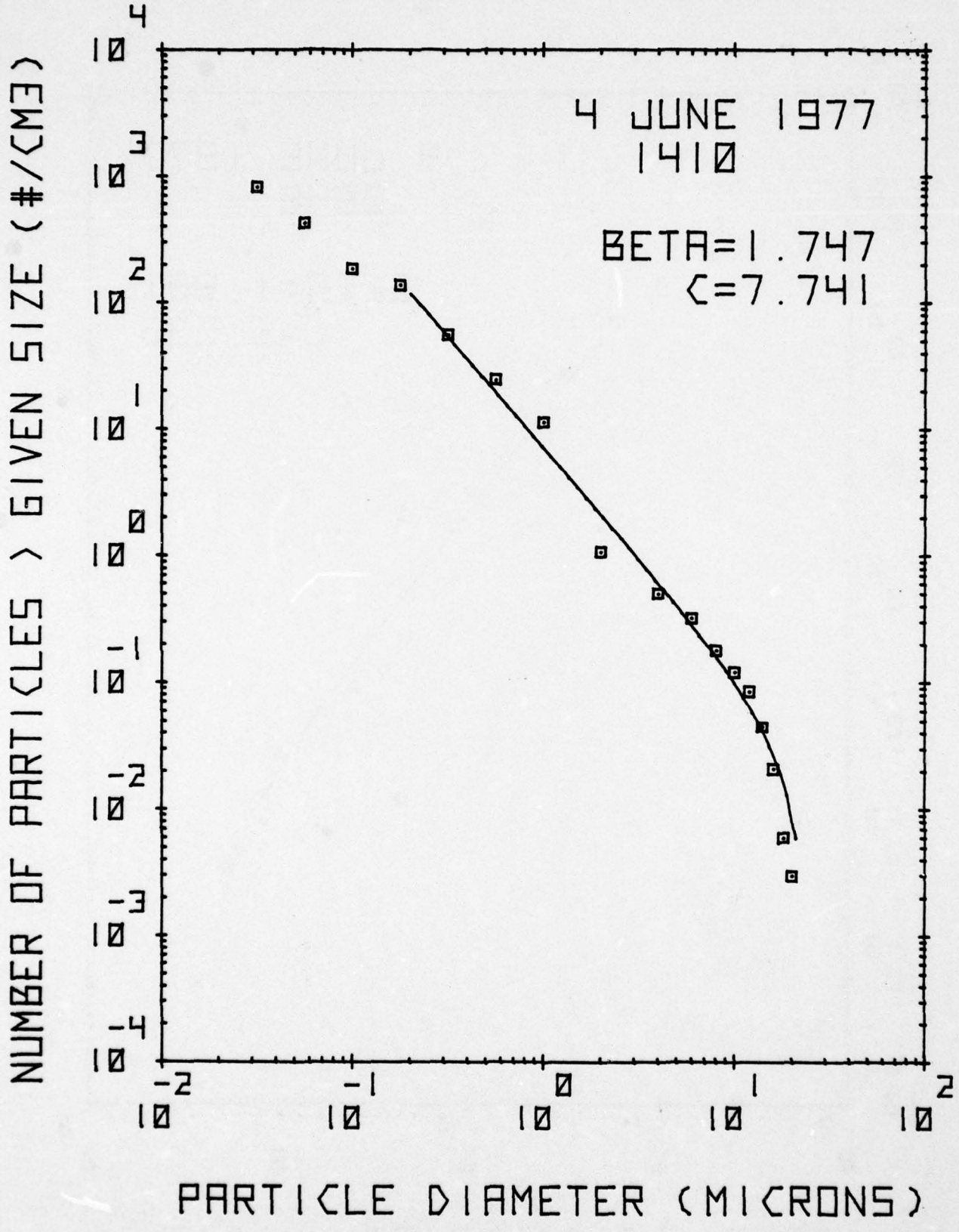
4 JUNE 1977
1410
BETA=1.747
C=7.741
NUMBER OF PARTICLES > GIVEN SIZE (#/CM3)
PARTICLE DIAMETER (MICRONS)
10^4
10^3
10^2
10^1
10^0
10^-1
10^-2
10^-3
10^-4
10^-2
10^-1
10^0
10^1
10^2

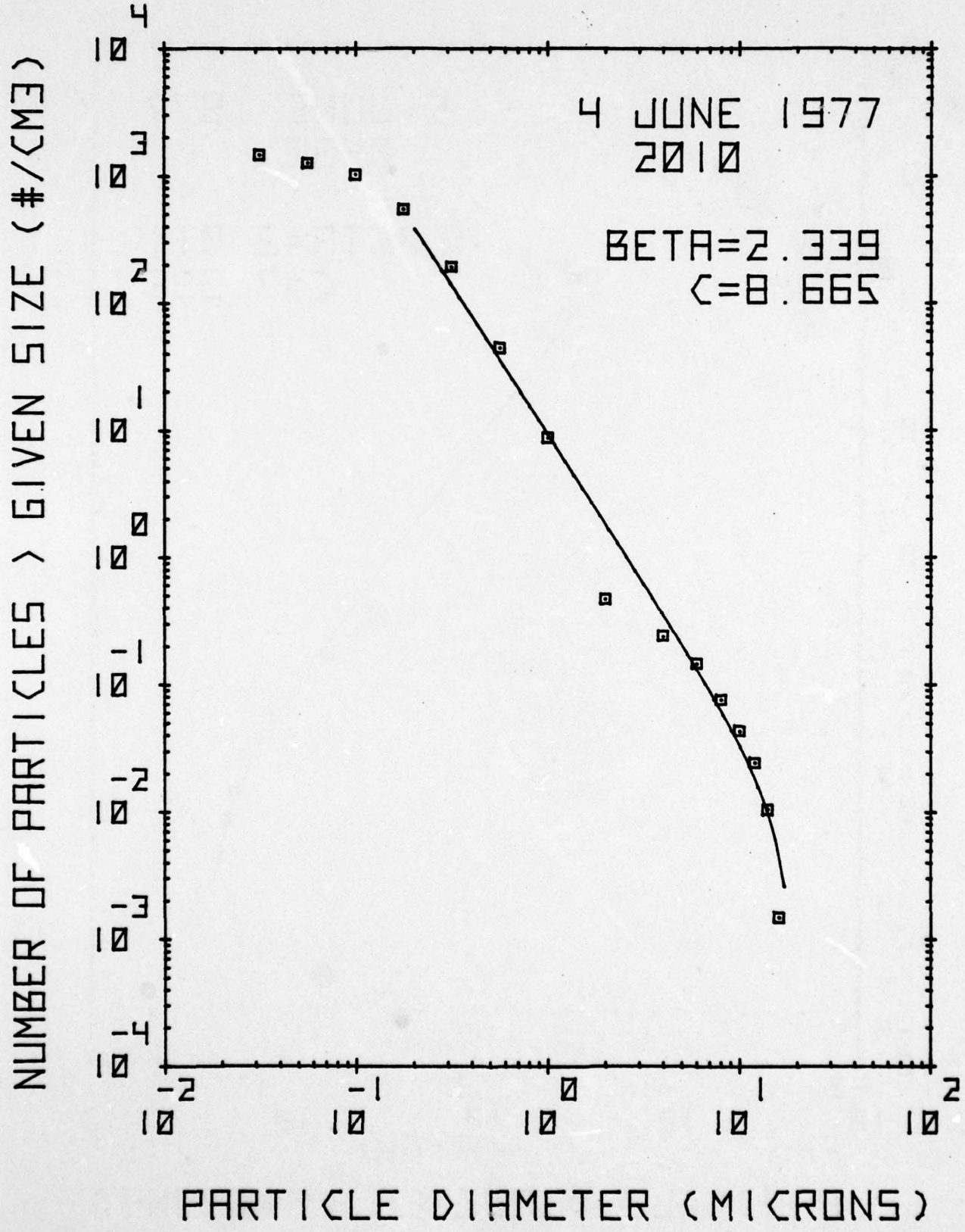
4 JUNE 1977
2010
BETA=2.339
C=8.665
NUMBER OF PARTICLES > GIVEN SIZE (#/CM3)
PARTICLE DIAMETER (MICRONS)
10^4
10^3
10^2
10^1
10^0
10^-1
10^-2
10^-3
10^-4
10^-2
10^-1
10^0
10^1
10^2

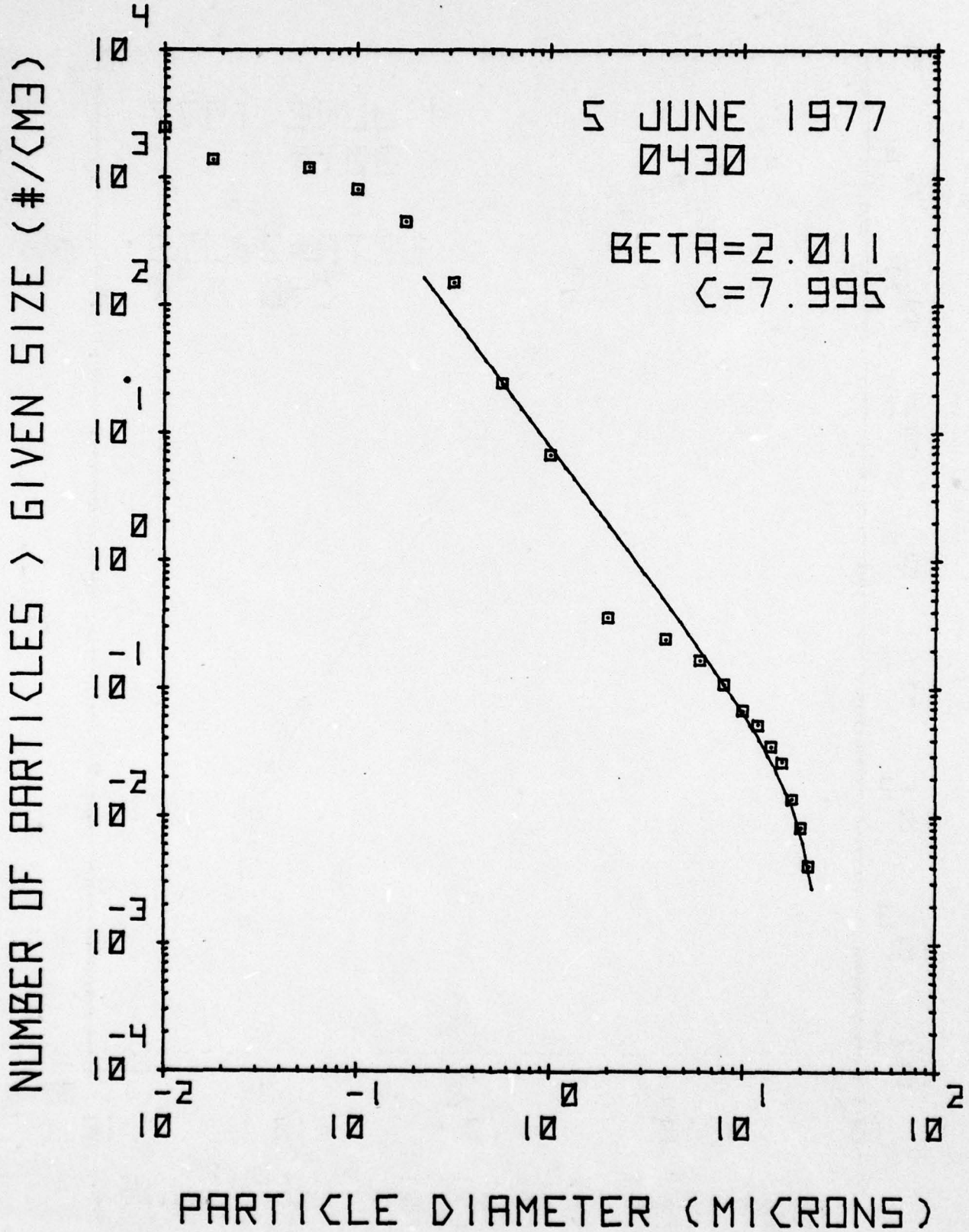
5 JUNE 1977
0430
BETA=2.011
C=7.995
NUMBER OF PARTICLES > GIVEN SIZE (#/CM3)
PARTICLE DIAMETER (MICRONS)
10^4
10^3
10^2
10^1
10^0
10^-1
10^-2
10^-3
10^-4
10^-2
10^-1
10^0
10^1
10^2

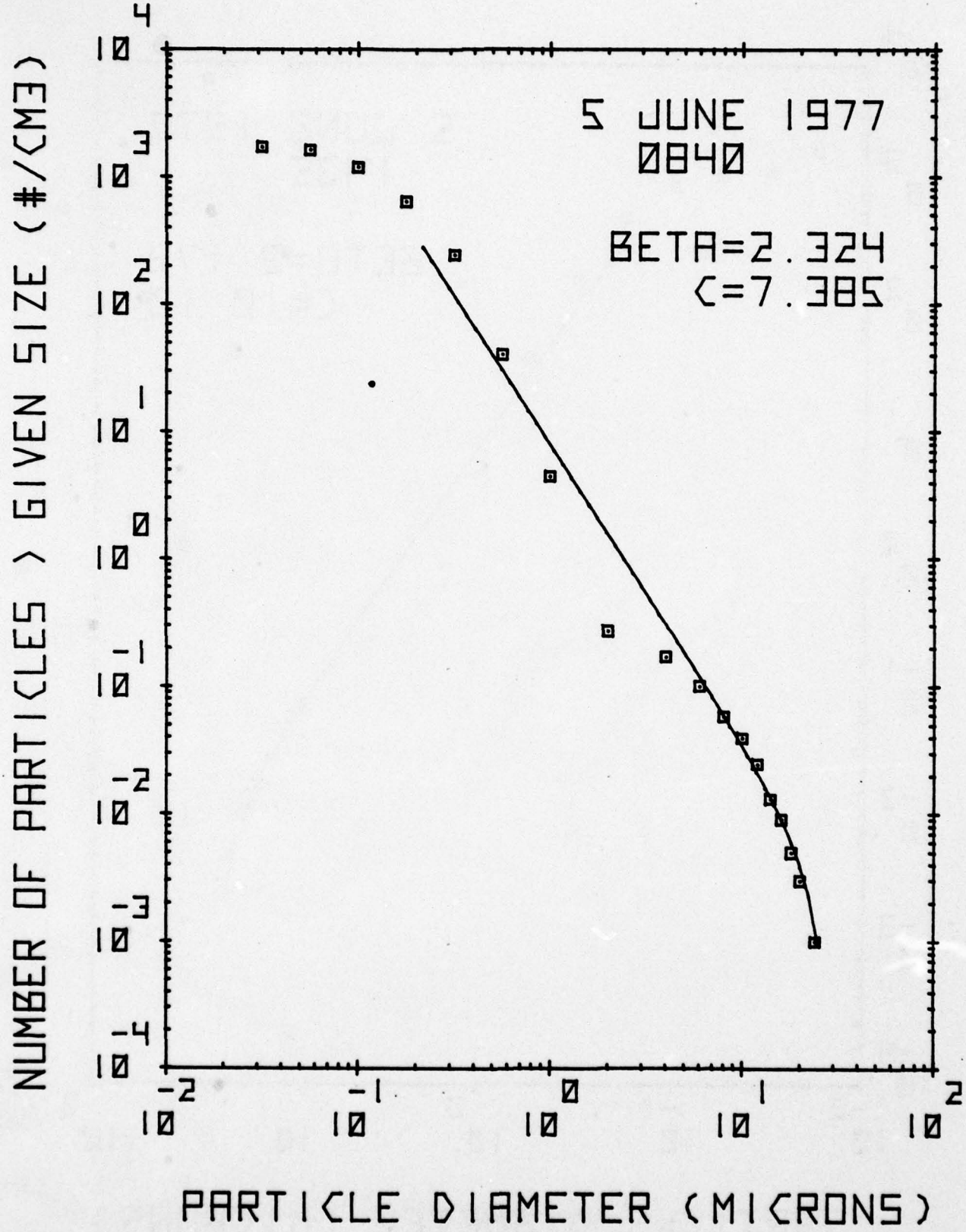
5 JUNE 1977
0840
BETA=2.324
C=7.385
NUMBER OF PARTICLES > GIVEN SIZE (#/CM3)
PARTICLE DIAMETER (MICRONS)

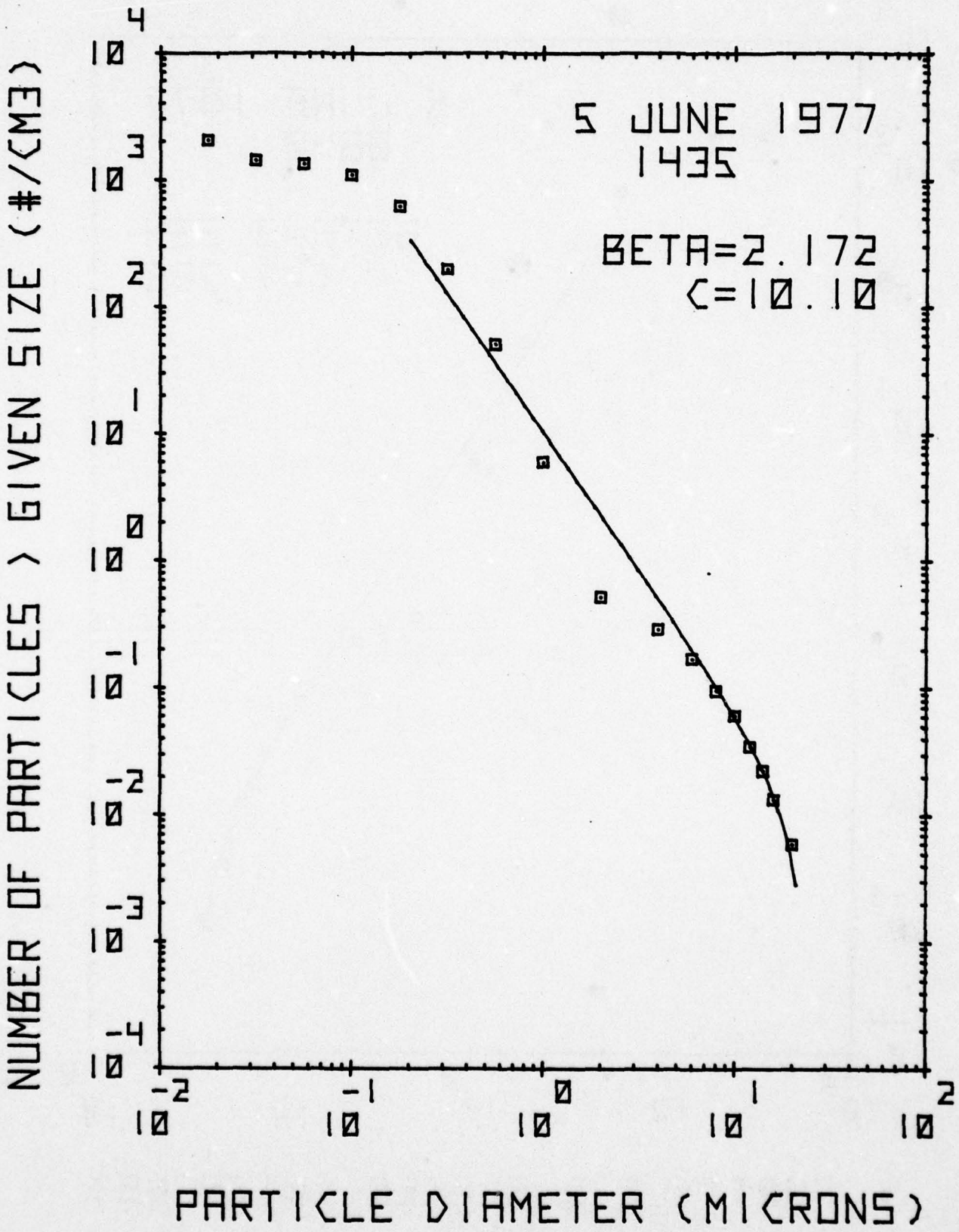
5 JUNE 1977
1435
BETA=2.172
C=10.10
NUMBER OF PARTICLES > GIVEN SIZE (#/CM3)
PARTICLE DIAMETER (MICRONS)

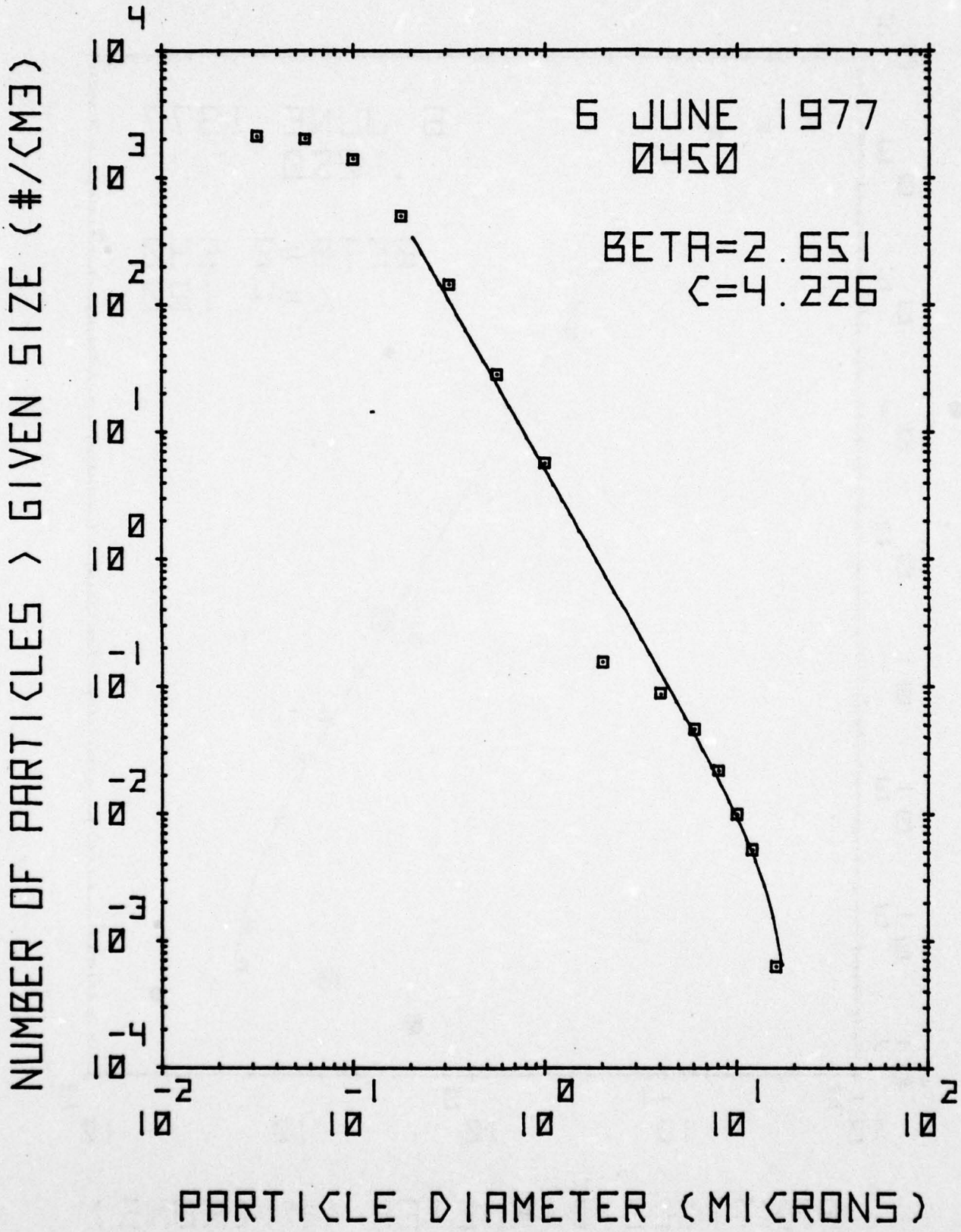
6 JUNE 1977
0450
BETA=2.651
C=4.226
NUMBER OF PARTICLES > GIVEN SIZE (#/CM3)
PARTICLE DIAMETER (MICRONS)

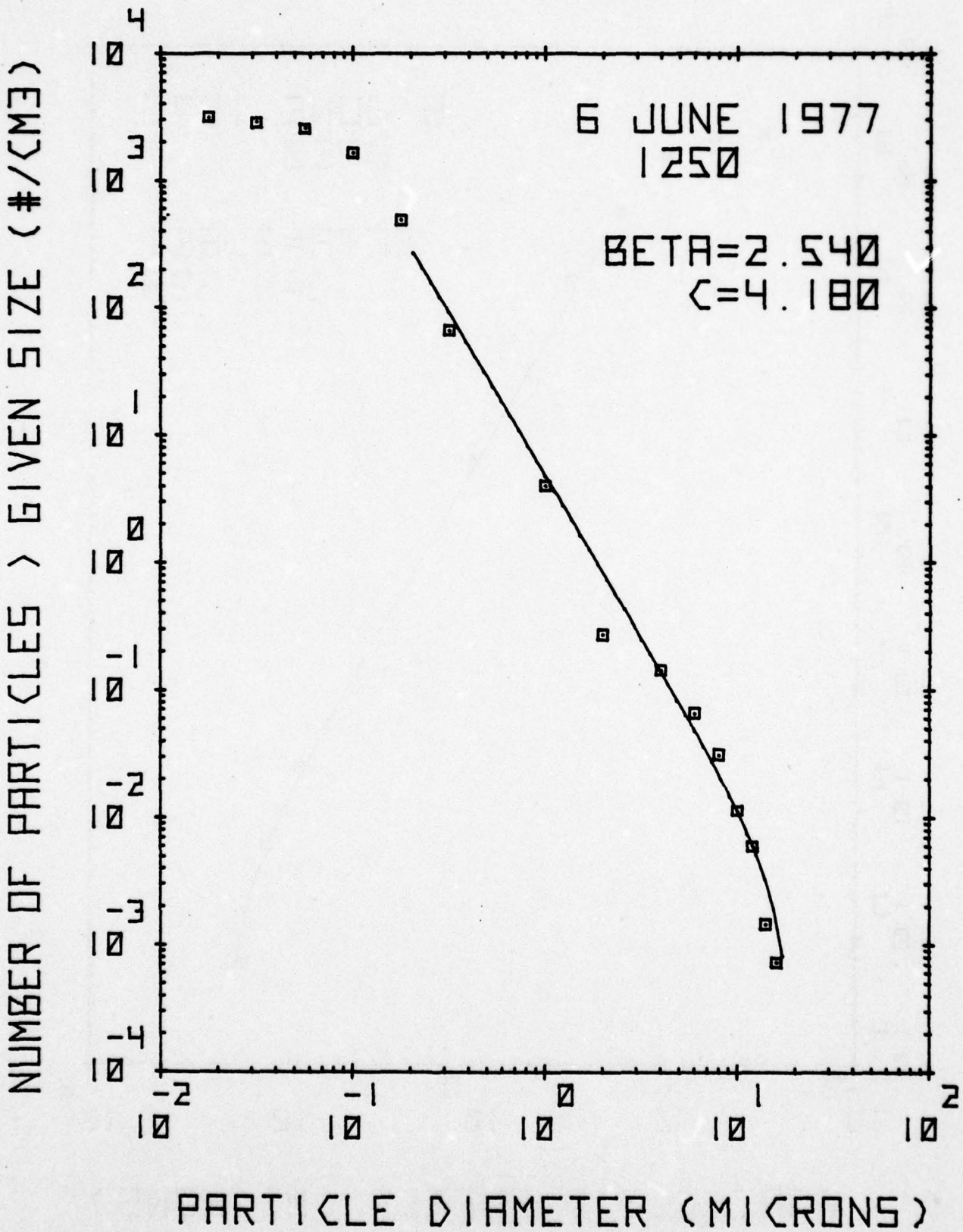
6 JUNE 1977
1250
BETA=2.540
C=4.180
NUMBER OF PARTICLES > GIVEN SIZE (#/CM3)
PARTICLE DIAMETER (MICRONS)
10^4
10^3
10^2
10^1
10^0
10^-1
10^-2
10^-3
10^-4
10^-2
10^-1
10^0
10^1
10^2

Appendix G

PLOTS OF CCN ACTIVITY SPECTRA

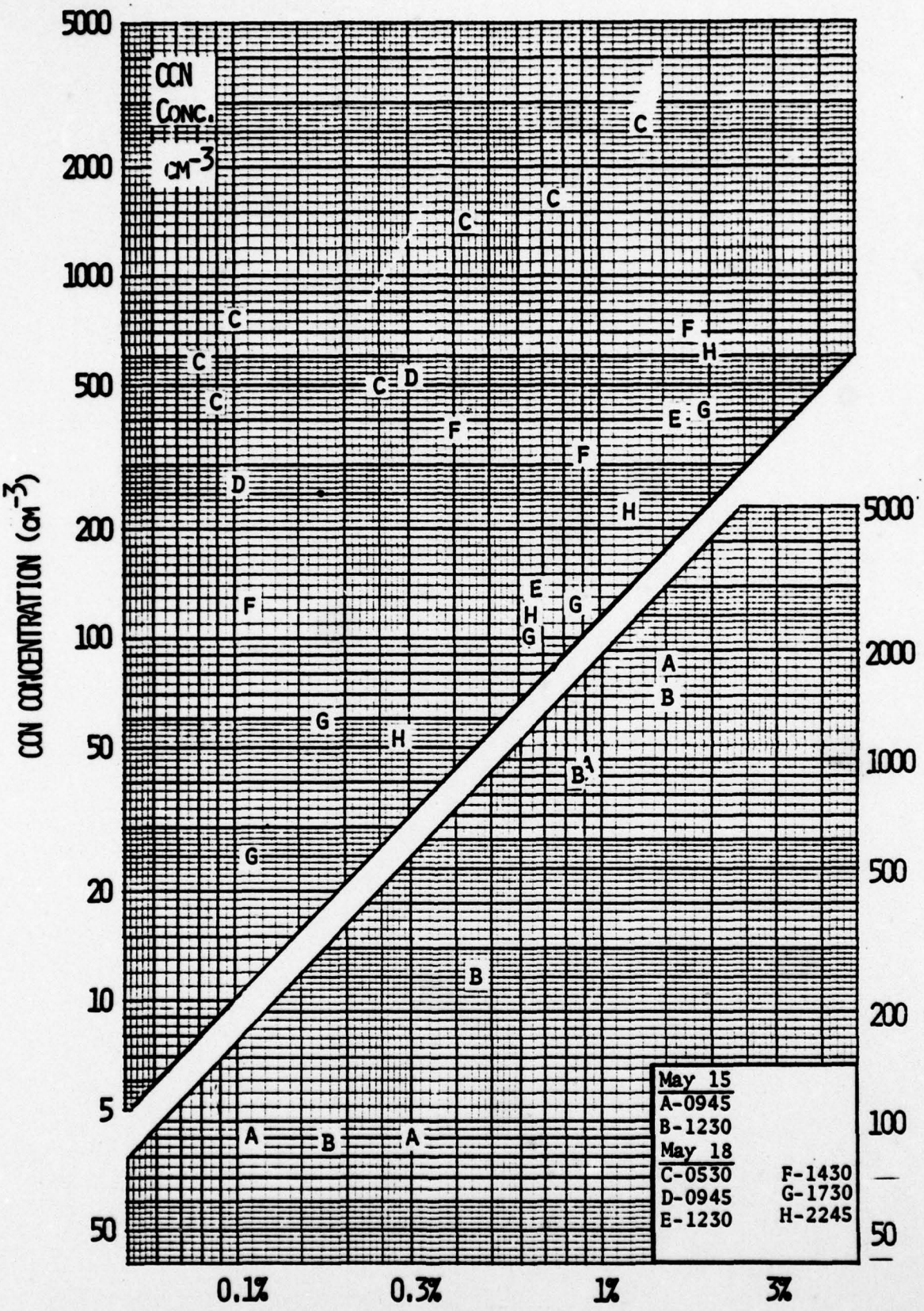

FIGURE : CCN SPECTRA FOR 15 AND 18 MAY, 1977, USNS HAYES

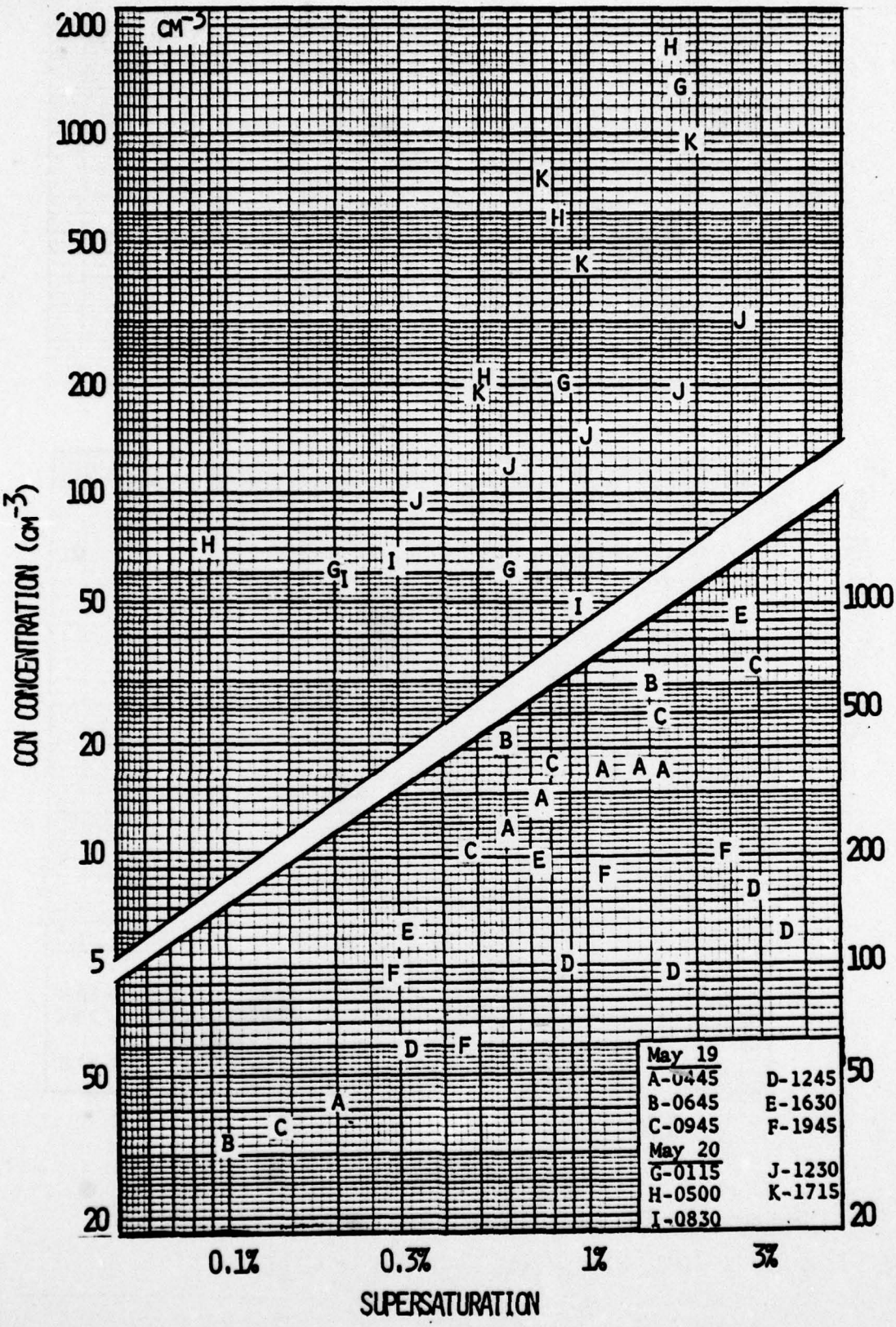

FIGURE : CCN SPECTRA FOR 19 AND 20 MAY, 1977, USNS HAYES

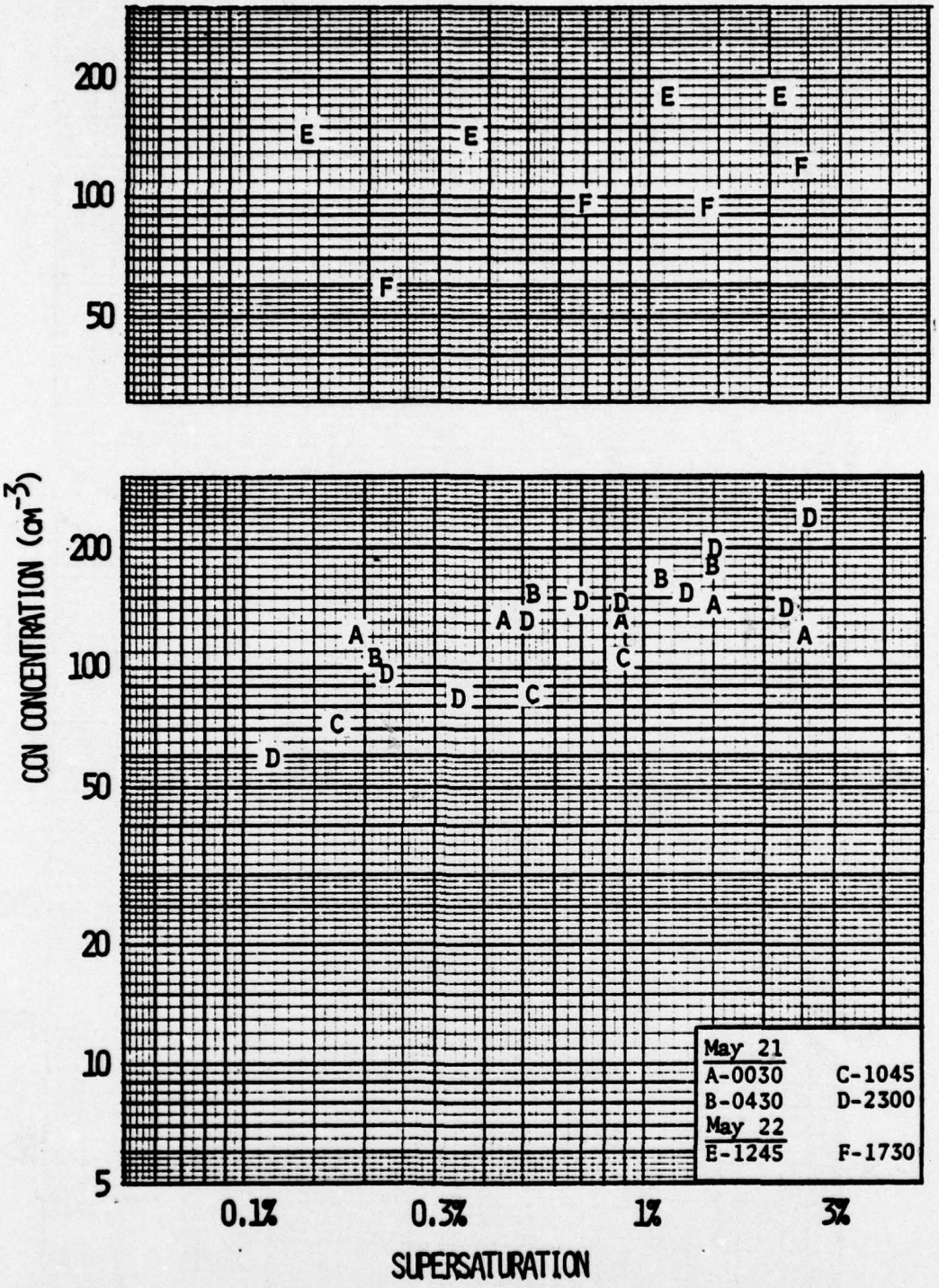

FIGURE : CCN SPECTRA FOR 21 AND 22 MAY, 1977, USNS HAYES

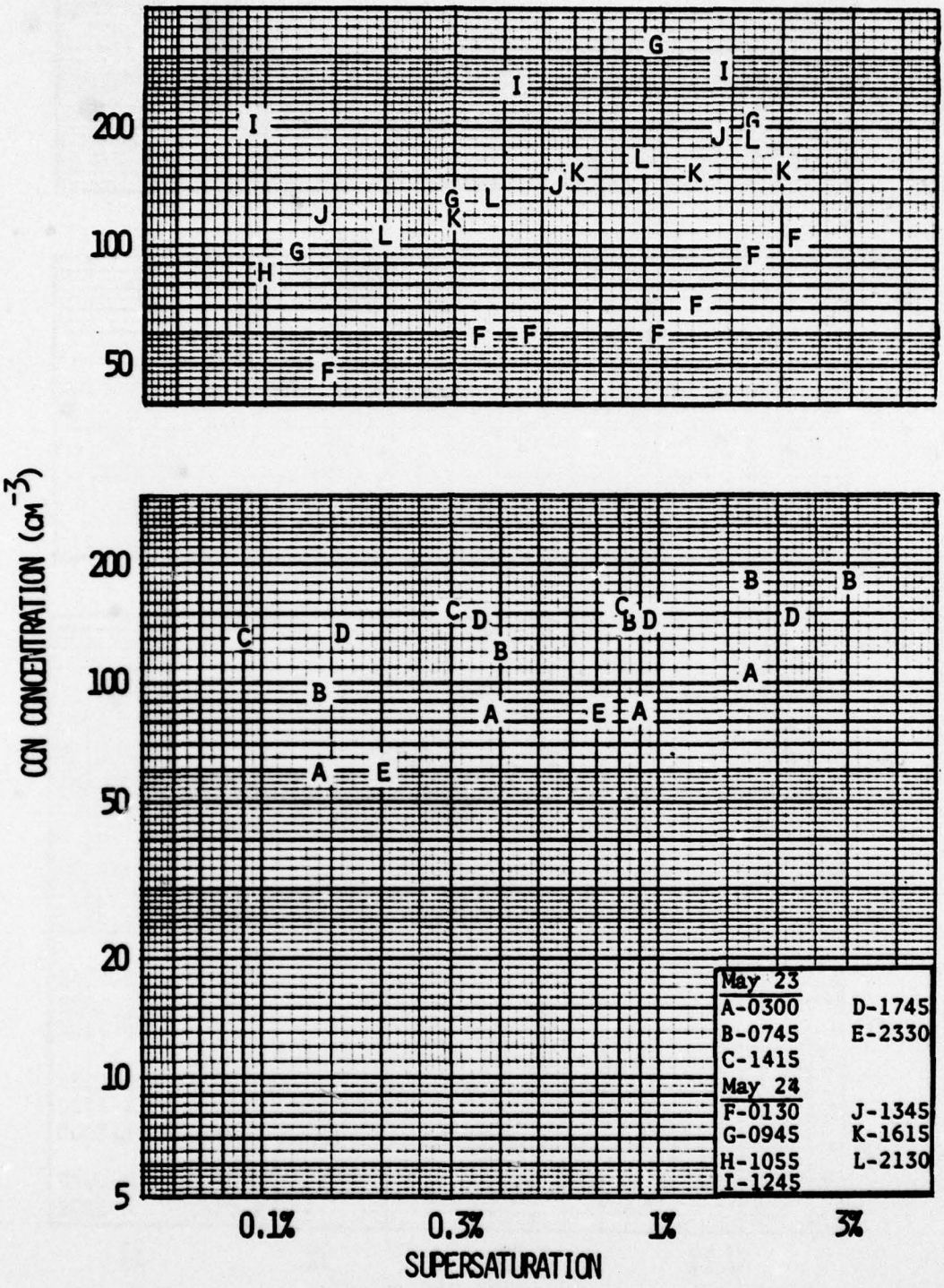

FIGURE : CCN SPECTRA FOR 23 AND 24 MAY, 1977, USNS HAYES

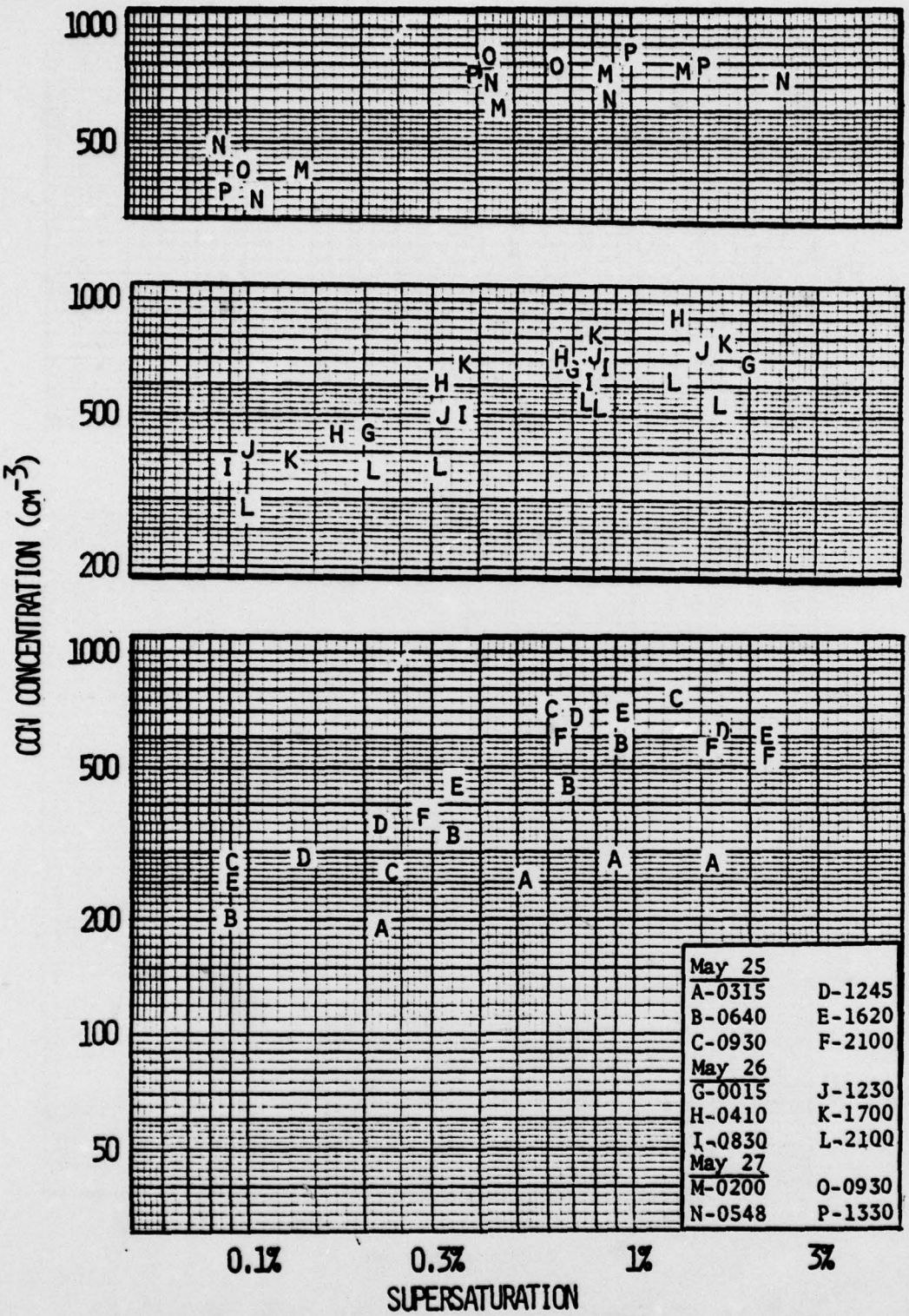

FIGURE : CCN SPECTRA FOR 25, 26, AND 27 MAY, 1977, USNS HAYES

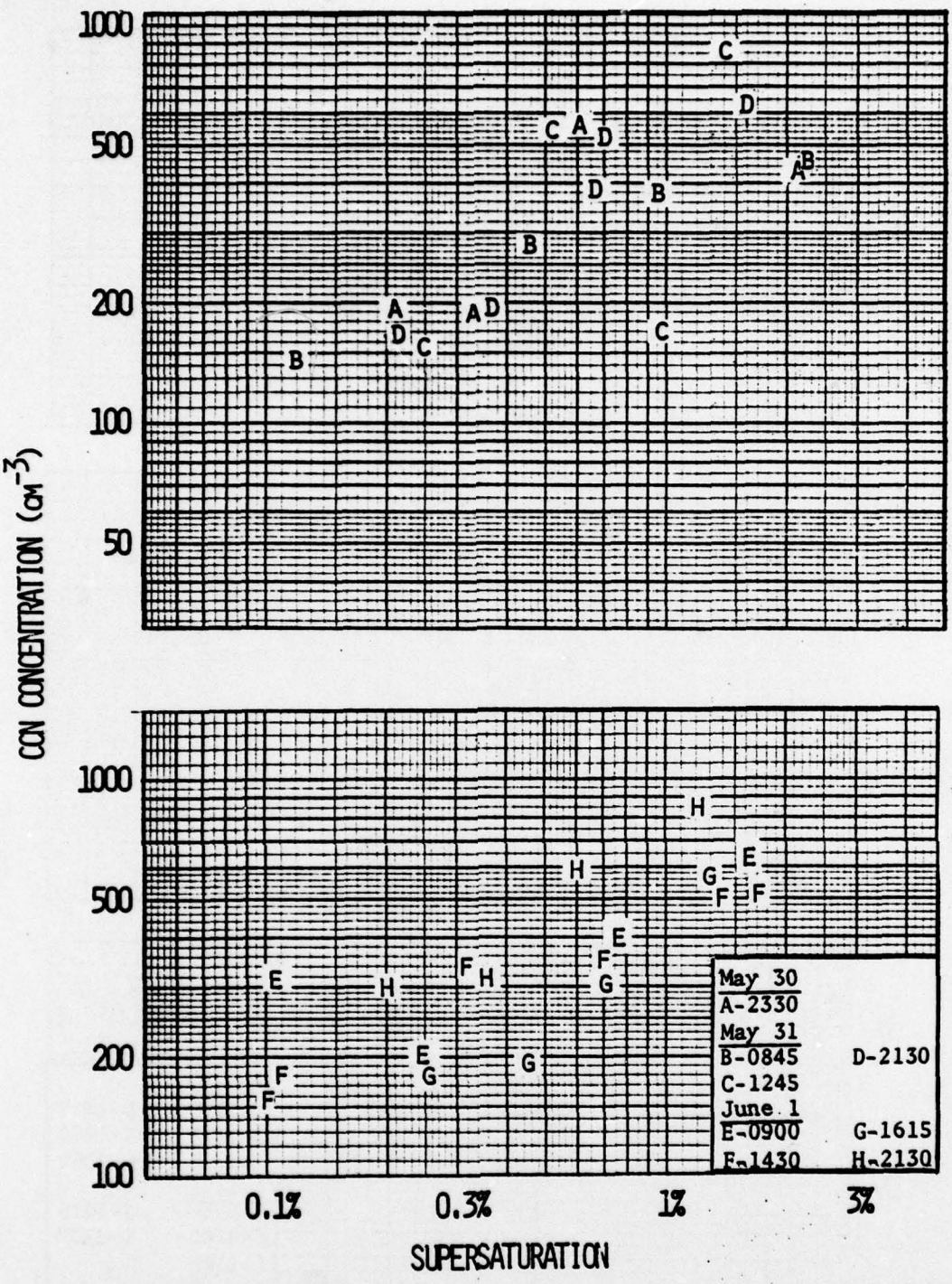

FIGURE : CCN SPECTRA FOR 30, 31 MAY, AND 1 JUNE 1977, USNS HAYES

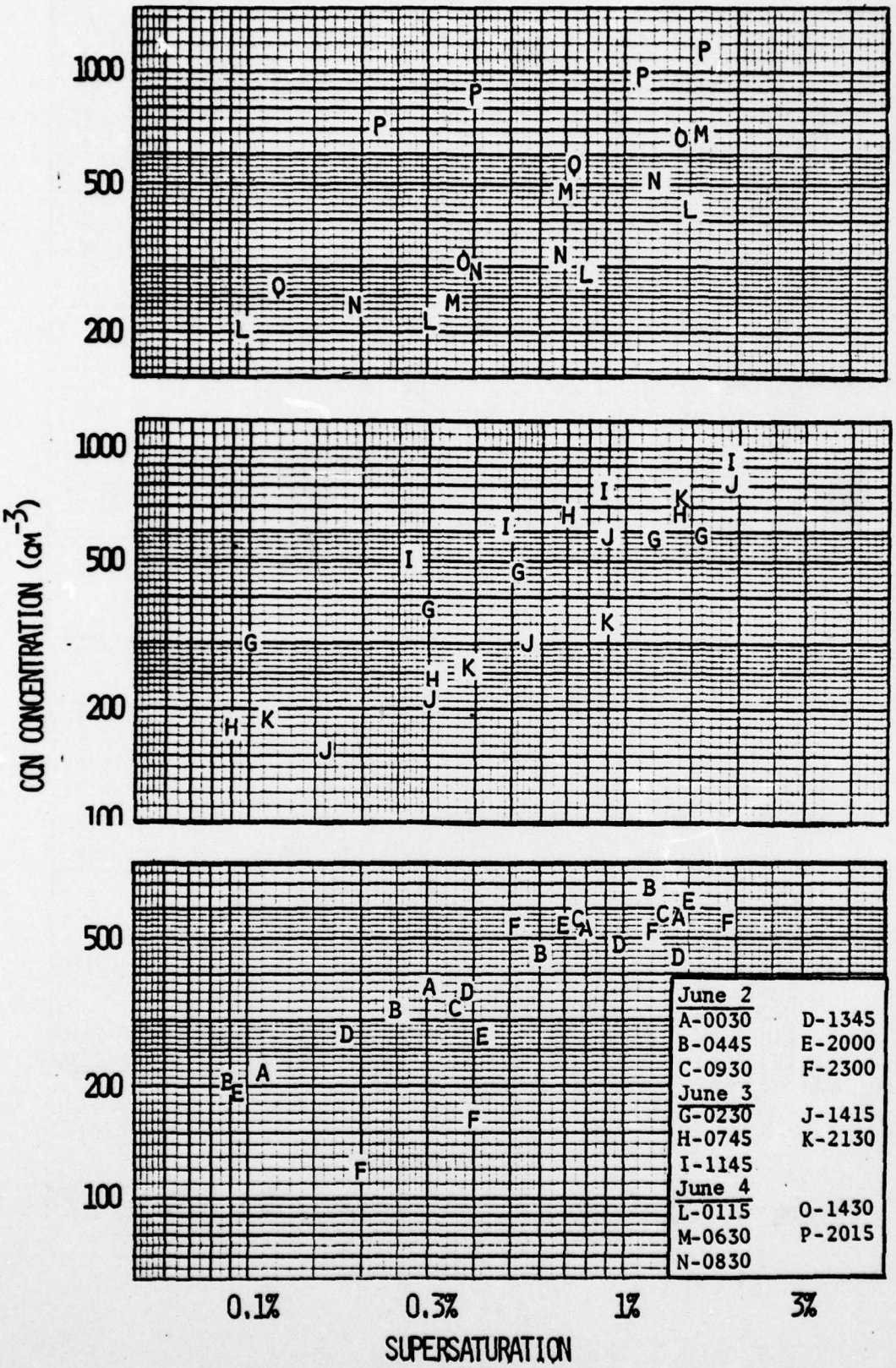

FIGURE : CCN SPECTRA FOR 2, 3, AND 4 JUNE, 1977, USNS HAYES

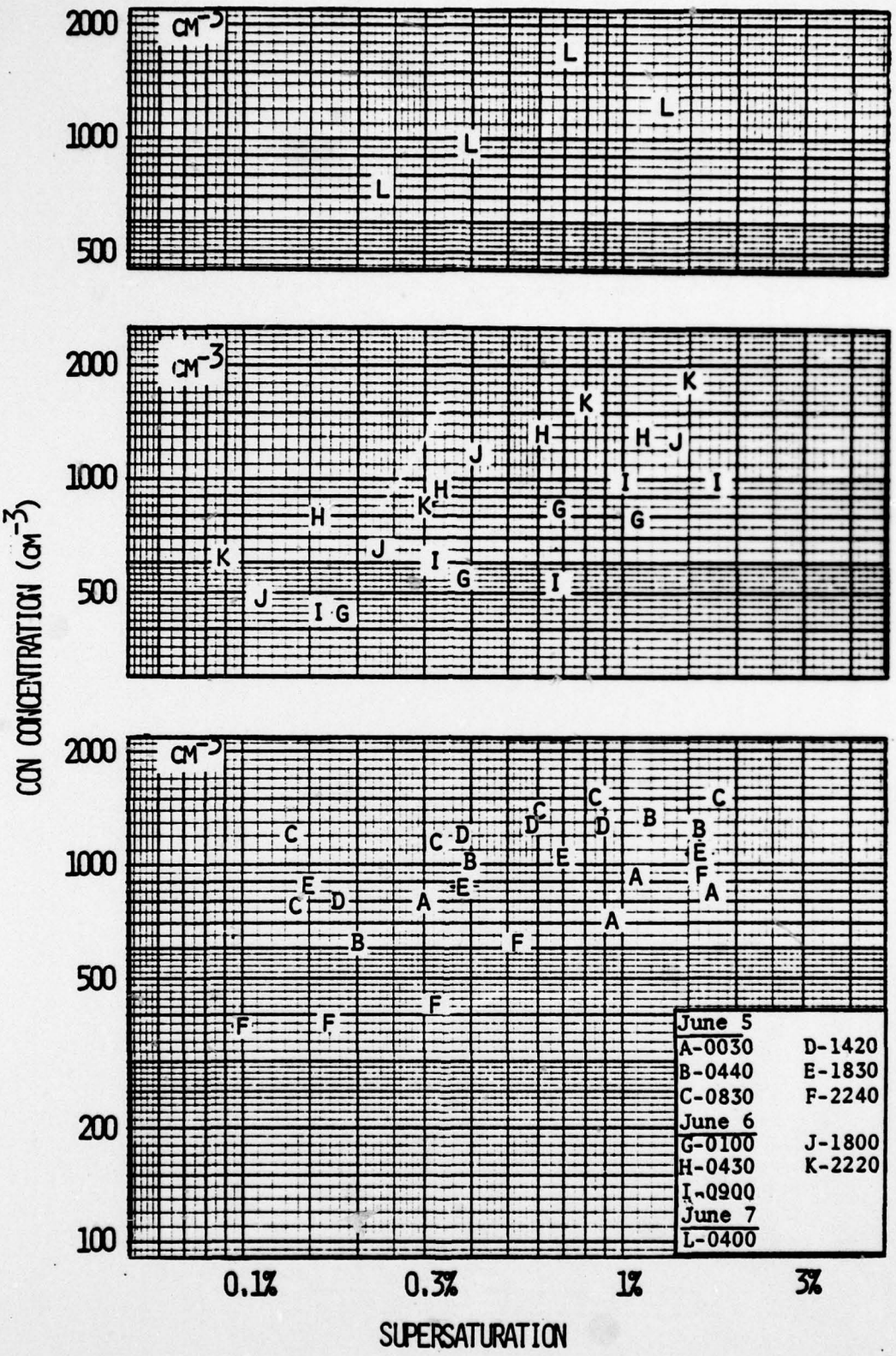

FIGURE : CCN SPECTRA FOR 5, 6, AND 7 JUNE, 1977, USNS HAYES

Appendix H

LOG OF CCN DATA

DATE: 5 15 1977

TIME (GMT)	CCN CONCENTRATIONS AT GIVEN SUPERSATURATIONS 0.2%SS (/CM↑3)	0.5%SS (/CM↑3)	1.0%SS (/CM↑3)
945	180	510	1120
1230	100	365	970

DATE: 5 18 1977

TIME (GMT)	CCN CONCENTRATIONS AT GIVEN SUPERSATURATIONS 0.2%SS (/CM↑3)	0.5%SS (/CM↑3)	1.0%SS (/CM↑3)
530	900	1420	2000
945	410	720	1100
1230	0	105	190
1430	180	320	500
1730	50	115	200
2245	40	95	185

DATE: 5 19 1977

TIME (GMT)	CCN CONCENTRATIONS AT GIVEN SUPERSATURATIONS 0.2%SS (/CM↑3)	0.5%SS (/CM↑3)	1.0%SS (/CM↑3)
445	40	170	450
645	85	330	890
945	60	210	550
1245	45	70	100
1630	95	160	245
1945	80	125	175

DATE: 5 20 1977

TIME (GMT)	CCN CONCENTRATIONS AT GIVEN SUPERSATURATIONS 0.2%SS (/CM↑3)	0.5%SS (/CM↑3)	1.0%SS (/CM↑3)
115	60	65	270
500	115	200	620
830	60	65	0
1230	80	110	145
1715	65	190	450

DATE: 5 21 1977

TIME (GMT)	CCN CONCENTRATIONS AT GIVEN SUPERSATURATIONS 0.2%SS (/CM↑3)	0.5%SS (/CM↑3)	1.0%SS (/CM↑3)
30	120	130	140
430	110	145	175
1045	75	90	105
2230	85	120	160
2315	65	105	150

DATE: 5 22 1977

TIME (GMT)	CCN CONCENTRATIONS AT GIVEN SUPERSATURATIONS 0.2%SS (/CM↑3)	0.5%SS (/CM↑3)	1.0%SS (/CM↑3)
1245	145	160	175
1730	60	80	100

DATE: 5 23 1977

TIME (GMT)	CCN CONCENTRATIONS AT GIVEN SUPERSATURATIONS 0.2%SS (/CM↑3)	0.5%SS (/CM↑3)	1.0%SS (/CM↑3)
300	135	145	150
745	65	80	95
1415	105	125	150
1745	145	155	160
2330	60	75	90

DATE: 5 24 1977

TIME (GMT)	CCN CONCENTRATIONS AT GIVEN SUPERSATURATIONS 0.2%SS (/CM↑3)	0.5%SS (/CM↑3)	1.0%SS (/CM↑3)
130	55	60	65
945	115	150	185
1245	230	250	270
1345	125	150	170
1615	105	140	175
2130	105	140	170

DATE: 5 25 1977

TIME (GMT)	CCN CONCENTRATIONS AT GIVEN SUPERSATURATIONS 0.2%SS (/CM↑3)	0.5%SS (/CM↑3)	1.0%SS (/CM↑3)
320	185	230	270
640	265	400	540
935	270	400	850
1240	340	490	660
1620	360	520	700
2055	300	520	700

DATE: 5 26 1977

TIME (GMT)	CCN CONCENTRATIONS AT GIVEN SUPERSATURATIONS 0.2%SS (/CM↑3)	0.5%SS (/CM↑3)	1.0%SS (/CM↑3)
15	440	560	650
410	475	640	810
830	440	560	670
1235	475	580	675
1700	480	825	1250
2110	350	460	570

DATE: 5 27 1977

TIME (GMT)	CCN CONCENTRATIONS AT GIVEN SUPERSATURATIONS 0.2%SS (/CM↑3)	0.5%SS (/CM↑3)	1.0%SS (/CM↑3)
200	475	540	800
545	490	590	680
930	560	800	1040
1330	510	720	930

DATE: 5 30 1977

TIME (GMT)	CCN CONCENTRATIONS AT GIVEN SUPERSATURATIONS 0.2%SS (/CM↑3)	0.5%SS (/CM↑3)	1.0%SS (/CM↑3)
2330	190	390	1450

DATE: 5 31 1977

TIME (GMT)	CCN CONCENTRATIONS AT GIVEN SUPERSATURATIONS 0.2%SS (/CM↑3)	0.5%SS (/CM↑3)	1.0%SS (/CM↑3)
845	185	280	390
1245	120	380	0
2130	165	290	750

DATE: 6 1 1977

TIME (GMT)	CCN CONCENTRATIONS AT GIVEN SUPERSATURATIONS 0.2%SS (/CM↑3)	0.5%SS (/CM↑3)	1.0%SS (/CM↑3)
900	180	310	470
1430	220	340	470
1615	175	200	440
2130	300	500	750

DATE: 6 2 1977

TIME (GMT)	CCN CONCENTRATIONS AT GIVEN SUPERSATURATIONS 0.2%SS (/CM↑3)	0.5%SS (/CM↑3)	1.0%SS (/CM↑3)
30	290	440	610
445	290	440	610
930	250	400	570
1345	290	360	480
1945	230	280	340
2000	0	510	950
2300	120	190	250

DATE: 6 3 1977

TIME (GMT)	CCN CONCENTRATIONS AT GIVEN SUPERSATURATIONS 0.2%SS (/CM↑3)	0.5%SS (/CM↑3)	1.0%SS (/CM↑3)
230	215	270	670
745	350	450	550
1145	175	280	610
2130	225	290	350

DATE: 6 4 1977

TIME (GMT)	CCN CONCENTRATIONS AT GIVEN SUPERSATURATIONS 0.2%SS (/CM↑3)	0.5%SS (/CM↑3)	1.0%SS (/CM↑3)
115	230	260	350
630	0	420	560
830	245	320	400
1430	290	500	610
2015	690	930	0

DATE: 6 5 1977

TIME (GMT)	CCN CONCENTRATIONS AT GIVEN SUPERSATURATIONS 0.2%SS (/CM↑3)	0.5%SS (/CM↑3)	1.0%SS (/CM↑3)
25	780	810	840
435	620	880	1200
835	900	1270	1620
1425	840	1350	1910
1830	920	980	1020
2240	390	600	870

DATE: 6 6 1977

TIME (GMT)	CCN CONCENTRATIONS AT GIVEN SUPERSATURATIONS 0.2%SS (/CM↑3)	0.5%SS (/CM↑3)	1.0%SS (/CM↑3)
100	460	600	725
430	825	1050	1230
900	480	650	820
1800	620	850	1100
2215	840	1220	1600

DATE: 6 7 1977

TIME (GMT)	CCN CONCENTRATIONS AT GIVEN SUPERSATURATIONS 0.2%SS (/CM↑3)	0.5%SS (/CM↑3)	1.0%SS (/CM↑3)
400	670	1100	1600